STUDIES ON THE INHIBITION OF HUMAN HYPOXIA INDUCIBLE FACTOR (HIF) HYDROXYLASES

A thesis submitted to the Board of the Faculty of Physical Sciences of the University of Oxford in partial fulfilment of the requirements for the degree of Doctor of Philosophy

Kar Kheng Yeoh

Trinity College, Oxford

Hilary Term 2012

"When I was 5 years old, my mother always told me that happiness was the key to life. When I went to school, they asked me what I wanted to be when I grew up. I wrote down 'happy'. They told me I didn't understand the assignment, and I told them they didn't understand life." — John Lennon

Abstract

Kar Kheng Yeoh *Hilary Term 2012*

Studies on the Inhibition of Human Hypoxia Inducible Factor (HIF) Hydroxylases

Hypoxia inducible factor (HIF) is an α/β-heterodimeric transcription factor that regulates cellular responses to hypoxia in metazoans. The activity and stability of the HIF-α subunits are regulated by prolyl and asparaginyl hydroxylation. Human HIF-1α prolyl hydroxylation occurs at Pro402 and Pro564 while asparaginyl hydroxylation occurs at Asn803. Asparaginyl hydroxylation blocks the HIF-1α interaction with the p300/CBP co-activator, thus inhibiting HIF transcriptional activation. Prolyl hydroxylation promotes the HIF-1α interaction with the von Hippel-Lindau (VHL) ubiquitin E3 ligase complex and targets it for proteasomal degradation. HIF prolyl hydroxylation is catalysed by the PHDs (prolyl hydroxylase domain) 1, 2 and 3, whereas asparaginyl hydroxylation is catalysed by FIH (factor inhibiting HIF). Both the PHDs and FIH are Fe(II) and 2-oxoglutarate (2OG) dependent oxygenases, which utilise oxygen as a co-substrate. In hypoxia, the activity of the PHDs and FIH are suppressed, thus enabling HIF-α subunits to form a productive transcriptional complex.

There is widespread interest in developing HIF hydroxylase inhibitors for the treatment of ischemic/hypoxic diseases. The extent to which HIF-1α prolyl and asparaginyl hydroxylation are differentially regulated by chemical reagents is an important question. This thesis describes the development of methods employing immunoblotting and HIF hydroxy-residue specific antibodies to enable the simultaneous measurement of the effects of chemical inhibition at all three HIF-1α hydroxylation sites in cells. The findings reveal that HIF prolyl hydroxylation is substantially more sensitive than asparaginyl hydroxylation to inhibition by iron chelators and transition metal ions, in contrast to predictions from *in vitro* studies. Studies on a range of 2OG analogue inhibitors resulted in the identification of several cell-permeable PHD specific inhibitors as well as an FIH specific inhibitor that is active in cells.

Excessive accumulation of *R*-2-hydroxyglutarate (*R*-2HG) in mutated isocitrate dehydrogenase (IDH)-mediated cancers has led *R*-2HG to be recognised as an 'oncometabolite'. The newly developed antibody assays were used to investigate the effects of cell-permeable 2HG derivatives on the activity of the HIF hydroxylases in cells. This indicated that direct *R*-2HG inhibition of PHDs does not play a role in mutated IDH-mediated tumourgenesis. The PHDs have been proposed to play a general role as metabolic sensors besides their function as intracellular oxygen sensors. The Krebs cycle metabolite 2OG (a co-substrate of HIF hydroxylases) was therefore investigated as a potential regulator of the PHDs. The cell-based results demonstrate that 2OG elevation results in HIF-α induction, a mechanism suggested to be, at least in part, through PHD inhibition as supported by *in vitro* and cell-based results.

This thesis also describes the first attempt to apply a chemical-genetic approach to functional studies of the PHD isoforms. The *in vitro* results demonstrate the feasibility of selective inhibition of PHD2 by employing small-molecule-sensitive PHD2 variants. However, attempts to test this approach in mammalian cells have not been successful to date due to the lack of a suitable cell-system. Work on PHD inhibition then describes the development of a new class of diacylhydrazine-based PHD inhibitors. Findings show that some of these compounds are capable of binding to the PHD2 active site and simultaneously inducing the binding of a second iron to PHD2. The reported PHD inhibitor, aspirin metabolite 2,3-dihydroxybenzoylglycine (DHBG), was unexpectedly found to exhibit a concentration-dependent dichotomous effect on HIF stabilisation and HIF suppression in VHL-competent cells. DHBG and other aspirin metabolites including gentisuric acid (GUA) were subsequently found to suppress HIF-1α and HIF-2α levels in renal carcinoma RCC4 VHL-defective cells, suggesting that therapeutic effects of aspirin in cancers may involve potential regulation of HIF-α activity.

Acknowledgements

Foremost, I would like to extend my heartfelt gratitude to my supervisor Professor Chris Schofield for his continuous support and guidance in my D.Phil research and thesis preparation. I could not have imagined having a better supervisor for my study in Oxford.

A huge proportion of the work presented in this thesis results from an extensive collaboration with Professor Peter Ratcliffe laboratory in the Centre for Cellular and Molecular Physiology (CCMP) at Oxford University. Therefore, I would particularly like to thank Professor Peter Ratcliffe and Professor Chris Pugh for allowing me to work at the laboratory for more than a year.

An enormous appreciation must go to Dr Emily Flashman and Dr Ya-Min Tian, for being fantastic mentors in my molecular and cellular biology works which constitute a major part of my DPhil research. I am very grateful to Andrew M. C. Chan for being a very supportive friend and group member, particularly for his great help in obtaining the AlphaScreen inhibition data and guidance in computing. I would also like to thank Dr Eleanor Williams for her help in the Hsp90 protein preparation and for carrying out the thermal shift assays. Many thanks to Ivanhoe K. H. Leung for carrying out the water-LOSGY experiments.

I would also like to thank Dr Esther Woon, Dr Jasmin Mecinovic, Owen Chang, and Armin Thalhammer for their help in synthesising the various compounds tested in this work. Great thanks then go to Dr Micheal McDonough and Dr Rasheduzzaman Chowdhury for their help in crystallograpic studies.

I would also like to express my appreciation to all the members of Chris Schofield and Peter Ratcliffe Laboratories for their great support in various aspects in the course of my D.Phil study in Oxford. Special thanks go to Professor Terry Lappin, Dr Norma Masson, Dr Ian Clifton, Dr Adam Hardy, Richard Hopkinson, Katherine England, Alexandra East, Duncan Hay, Louise Walport, Matthew Robinson and Wei Shen Aik for their great help in proofreading my thesis.

I had a great time working at Dr Antony Fairbanks Laboratory at the beginning of my D.Phil study. The results of the 6-month work have led to a publication in Carbohydrate Research (2009), of which I am very thankful to Dr Antony Fairbanks (who is now at University of Canterbury, New Zealand) for his supervision and support. Next, I would also like to thank Trinity College and my graduate advisor Professor Gus Hancock for their continuous support.

I would like to thank my family, particularly my parents, for their understandings and immense support all these years. I am also deeply indebted to my spiritual teachers including Sayadaw U Sumana, Ven. Aggacitta, Ashin Tejaniya, Ven. Jutipanyo and Ven. Dhammasami for their Dharma teachings and guidance on mindfulness meditation which have helped me tremendously in every aspect of my life.

My D.Phil study was funded by Ministry of Higher Education of Malaysia and Universiti Sains Malaysia. For this, I would like to express my sincere gratitude to the awarding bodies.

Table of Contents

Chapter 1: Introduction

1.1 The hypoxia signaling pathway……1

1.2 HIF Prolyl Hydroxylases (PHDs)……6

1.2.1 The role of the PHD isoforms……...6

1.2.2 Structural features of the PHDs…….. .6

1.2.3 Substrate Specificities of the PHDs……..8

1.2.4 Alternative substrates of the PHDs……...9

1.2.5 PHDs as oxygen sensors……10

1.2.6 Expression levels of the PHDs……11

1.2.7 Knockout models of the PHDs……...12

1.2.8 Problems associated with genetic approaches to assigning the specific function of the PHDs……...13

1.2.9 PHDs as therapeutic targets……14

1.3 HIF system and cancer cell metabolism……16

1.3.1 2-Oxoglutarate (2OG)……16

1.3.2 PHDs as 2OG and metabolic sensors……17

1.3.3 Isocitrate dehydrogenase (IDH) mutations……19

1.3.4 Other signal transduction pathways ……...20

1.4 Other 2OG Oxygenases as Therapeutic Targets

1.4.1 Collagen prolyl-4-hydroxylase……...22

1.4.2 Histone demethylases ……23

1.5 Aims of the work described in this thesis……...25

Chapter 2: Differential Sensitivities of HIF Prolyl and Asparaginyl Hydroxylation to Chemical Inhibition in Cells

2.1Background and Objectives……26

2.2 Results……27

2.2.1 Validation of HIF hydroxy-residue specific antibodies.....27

2.2.2 Development of HIF hydroxy-residue specific antibody assays.....31

2.2.3 Inhibition of HIF prolyl and asparaginyl hydroxylation by iron chelators, transition metal ions and small molecule inhibitors……..32

2.2.4 Selective inhibition on HIF prolyl and asparaginyl hydroxylation.……40

2.2.5 Evaluation of 8-hydroxyquinolines (8HQs) as HIF hydroxylase inhibitors…...49

2.2.6 4-Hydroxy-2-oxo-1,2-dihydroquinoline glycinamide

analogues (4HQs) as specific HIF prolyl hydroxylase inhibitors…….53
2.3 Discussion……...58
2.4 Conclusions and future directions……...60

Chapter 3: Assessment of the Ability of Oncometabolite 2-Hydroxyglutarate to Inhibit 2-Oxoglutarate Dependent Oxygenases

3.1 Background and Objectives.....62
3.2 Results……64
3.2.1 *R*-2HG is an ineffective inhibitor for HIF prolyl hydroxylases in cells…….64
3.2.2 *R*-/*S*-2HG inhibit histone N^{ϵ}-methyl lysine demethylase JMJD2A in cells……68
3.2.3 *In vitro* biochemical studies……69
3.2.4 2HG binds to the same site as 2OG in FIH and JMJD2A……..71
3.3 Discussion……...73
3.4 Conclusions and future directions……...75

Chapter 4: 2-Oxoglutarate Elevation Stimulates HIF-1α Induction in Cells

4.1 Background and Objectives……76
4.2 Results……78
4.2.1 PHD activity is inhibited by high concentrations of 2OG *in vitro*…….78
4.2.2 Ascorbate is important to maintain stability of PHD2.Fe.2OG complex……...81
4.2.3 2OG ester derivatives are ineffective PHD inhibitors *in vitro* ……..83
4.2.4 Exogenous 2OG stabilises HIF in cells……..86
4.2.5 Evaluation of 2OG dependent inhibition of PHDs in cells…….89
4.2.6 2OG-induced HIF-1α stabilisation is alleviated by ascorbate……92
4.3 Discussion……...94
4.4 Conclusions and future directions……...97

Chapter 5: Towards Selective Inhibition of HIF Prolyl Hydroxylase-2 Isoform

5.1 Background and Objectives……98
5.2 Results and Discussion……100
5.2.1 Generation of the PHD2 variants……..100
5.2.2 The PHD2 variants are active *in vitro*……..104
5.2.3 Kinetic parameters of the PHD2 variants ……107
5.2.4 Selective inhibition of the PHD2 variants by NOG analogues…….. ..111
5.2.5 Selective inhibition of the PHD2 variants by BIQ analogues……..115
5.2.6 The effects of the BIQ analogue inhibition on NODD hydroxylation…….118

5.2.7 Potential combination: L343A-PHD2 variant and D-Ala-BIQ (15)……121
5.2.8 Crystallographic and docking studies……...123
5.2.9 Cell-based studies……126
5.2.9.1 L343A-PHD2 variant is functionally active in the cells……126
5.2.9.2 PHD null cell-system……130
5.3 Conclusions and future directions……132
5.4 Synthesis and Characterisation of the BIQ Analogues……....133

Chapter 6: Dual Action HIF Prolyl-Hydroxylase Inhibitors That Induce Binding of a Second Iron Ion

6.1 Background and Objectives……..148
6.2 Results and Discussion……150
6.2.1 Inhibitor design and synthesis……..150
6.2.1.1 Synthesis of diacylhydrazine fumarate derivatives ……..153
6.2.2 Binding affinities and inhibitory potencies of the diacylhydrazines……154
6.2.2.1 Monocyclic diacylhydrazines……154
6.2.2.2 Bicyclic and tricylic diacylhydrazines……...158
6.2.3 *N*-Oxalylglycine (NOG) competition studies……...161
6.2.4 Docking studies……164
6.2.5 Cell-based studies……166
6.3 Conclusions and future directions……174
6.4 Synthesis and characterisation of the fumarate derivatives…….....176

Chapter 7: Aspirin Metabolites Suppress HIF-α Levels in von Hippel-Lindau (VHL)-Defective Renal Cell Carcinomas

7.1 Introduction……...186
7.1.1 Aspirin and salicylic acid……..186
7.1.2 Aspirin and cancers……...187
7.1.3 Inhibition of cyclooxygenases……..187
7.1.4. Other possible mechanisms……189
7.1.5 Metabolism of aspirin……...189
7.2 Background and Objectives…… 193
7.3 Results and Discussion……194
7.3.1 Aspirin metabolites DHBG and GUA are HIF-1α Inhibitors……...194
7.3.2 Concentration-dependent effects of DHBG and GUA……200

7.3.3 DHBG and GUA are ineffective Hsp90 inhibitors *in vitro*……..202
7.3.4 HIF-1α degradation or modification?.....210
7.3.5 Precursors of DHBG and GUA exhibit HIF-1α suppression……216
7.3.6 Effects of DHBG and GUA on HIF-α mRNA expression……...218
7.3.7 DHBG can regulate multiple potential cancer targets…….....222
7.4 Conclusions and future directions…….224

Chapter 8: Summary……226

Chapter 9: Materials and Methods
9.1 Chemicals……..229
9.2 General methods used in chemical synthesis……229
9.3 Cell-lines……...230
9.4 Protein immunoblotting analyses……..230
9.5 Antibodies……231
9.6 Plasmids and transient transfections……231

9.7 Heat shock protein 90……...231
9.8 Preparation of the PHD2 variants……232
9.7.1 Materials……...232
9.7.2 Generation of PHD2 variant plasmids……..233
9.7.3 Protein expression and fast protein liquid chromatography purification…….237
9.9 AlphaScreen PHD2 hydroxylation assay……..240
9.10 MALDI mass spectrometry PHD2 hydroxylation assay……240

References……242

Appendix……271

Abbreviations

2HG	2-Hydroxyglutarate
2OG	2-Oxoglutarate
2TY	2-Trytone/yeast medium
ARNT	Aryl hydrocarbon receptor nuclear translocator
ASA	Aspirin
bHLH	Basic helix-loop-helix
BIQ	Bicyclic isoquinoline compound
BSA	Bovine serum albumin
CAD	*C*-Terminal transactivation domain
CBP	CREB (cyclic adenosine monophosphate-response element binding protein) binding protein
CHCA	α-Cyano-4-hydroxycinnamic acid
CODD	*C*-Terminal oxygen-dependent degradation domain
COX	Cyclooxgenase
C-P4H	Collagen prolyl-4-hydroxylase
DFO	Desferrioxamine
DHBG	2,3-Dihydroxybenzoylglycine
DMOG	Dimethyloxalylglycine
DNA	Deoxyribonucleic acid
DSBH	Double-strand-β-helix
DTT	Dithiothreitol
EPO	Erythropoeitin
ESI-MS	Electrospray ionisation mass spectrometry
FH	Fumarate hydratase
FIH	Factor inhibiting HIF

GDH	Glutamate dehydrogenase
GUA	Gentisuric acid
Hep3B	Human hepatoma cell-line
HEPES	N-[2-Hydroxyethyl]piperazine-N´-[2-ethanesulfonic acid]
HIF	Hypoxia inducible factor
HRE	Hypoxia response element
IC_{50}	Half-maximal inhibitory concentration
IDH	Isocitrate dehydrogenase
I_KB	Inhibitor of NF_KB
JMJD	Jumonji-C domain containing protein
KDM	Lysyl demethylase
K_m	Michaelis constant
K_i	Inhibition constant
m/z	Mass to charge ratio
MALDI-TOF	Mass assisted laser desorption ionisiation-time-of-flight
MEF	Mouse embryonic fibroblast
mTOR	Mammalian target of rapamycin
MS	Mass spectrometry
NAD	*N*-Terminal transactivation domain
ND	Not determined
NF_KB	Nuclear factor kappaB or Nuclear factor enhancing-kappa-light-chain gene expression in B cells
NMR	Nuclear magnetic resonance
NODD	*N*-Terminal oxygen-dependent degradation domain
NOG	*N*-Oxalylglycine
PAGE	Polyacrylamide gel electrophoresis

PAS	Per-ARNT-Sim
PI3K	Phosphatidylinositol 3-kinase
PCR	Polymerase Chain Reaction
PDB	RCSB Protein Data Bank
PDG	Phosphate-dependent glutaminase
P*fu*	Pyrococcus furiosus
PHD	HIF prolyl hydroxylase or prolyl hydroxylase domain
pVHL	Von Hippel-Lindau tumour suppressor protein
RCC4	Human renal carcinoma VHL-defective cells
RCC4/VHL	RCC4 re-expressing functional VHL
ROS	Reactive oxygen species
rpm	Revolutions per minute
SA	Salicylic acid
SDH	Succinate dehydrogenase
SDS	Sodium dodecylsulphate
siRNA	Small-interfering ribonucleic acid
SUA	Salicyluric acid
TEMED	*N*, *N*, *N′*, *N′*, Tetramethylethylene-diamine
TKO	Triple knockout
Tris	Tris(hydroxymethyl)aminomethane
U	Units
U2OS	Human osteosarcoma cell-line
VEGF	Vascular endothelial growth factor
VHL	von-Hippel-Lindau tumour suppressor

Standard abbreviations for nucleotides, standard amino acids, SI-units/prefixes and chemical elements are used throughout.

Chapter 1: Introduction

1.1 The hypoxia signaling pathway

Hypoxia inducible factor (HIF) is an α/β-heterodimeric transcription factor which upon binding to hypoxia response elements (HREs) activates the cellular responses to hypoxia in mammalian cells. HIF-regulated genes include those that enable erythropoiesis (the production of red blood cells), angiogenesis (the formation of new blood vessels from a pre-existing bed of vessels), and alter energy metabolism.[1-3] A selection of direct transcriptional targets of HIF are shown in **Fig. 1.1**. Many other genes may also be positively or negatively regulated by HIF, as demonstrated by 'genome-wide' gene array and DNA-sequencing analyses.[2, 4-6]

Both HIF-α and HIF-β subunits are constitutively expressed; however levels of the HIF-α (HIF-1α, HIF-2α, and HIF-3α), but not HIF-β, are regulated by cellular oxygen levels. Of the known β-subunits, HIF-1β is the most studied and is also known as the aryl hydrocarbon receptor nuclear translocator (ARNT). The HIF-1α isoform is the most widely expressed of the HIF α-subunits in mammalian tissues and appears to have the most generalised functions. HIF-2α has been reported to have a distinct role in hypoxia-induced expression of erythropoeitin (EPO) in the liver.[7] Mutations of the HIF-2α gene (which result in HIF-2α stabilisation) have been found in patients with familial erythrocytosis.[8, 9] HIF-3α has fewer known functions and is proposed to be a negative regulator of HIF-1α activity.[10, 11]

HIF-α levels are regulated by post-translation modifications. Proline residues within either of the two highly conserved LXXLAP sequence motifs of the HIF-α subunits (Pro402 in the *N*-terminal oxygen-dependent degradation domain (NODD) and Pro564 in the *C*-terminal oxygen-dependent degradation domain (CODD) of the human HIF-1α, **Fig. 1.2**) undergo *trans*-4-hydroxylation. Prolyl hydroxylation enables binding of HIF-α to the von Hippel-Lindau (pVHL) E3 ubiquitin ligase complex, which targets HIF-α for

ubiquitin-mediated proteolytic degradation.[12-14] In addition, HIF-α is also hydroxylated at an asparagine residue (Asn803 in human HIF-1α) in its *C*-terminal transactivation domain (CAD) (**Fig. 1.2**), which prevents its interaction with the co-activator protein p300/CBP (CBP, CREB-binding protein), thus disabling HIF-mediated transcription.[15, 16]

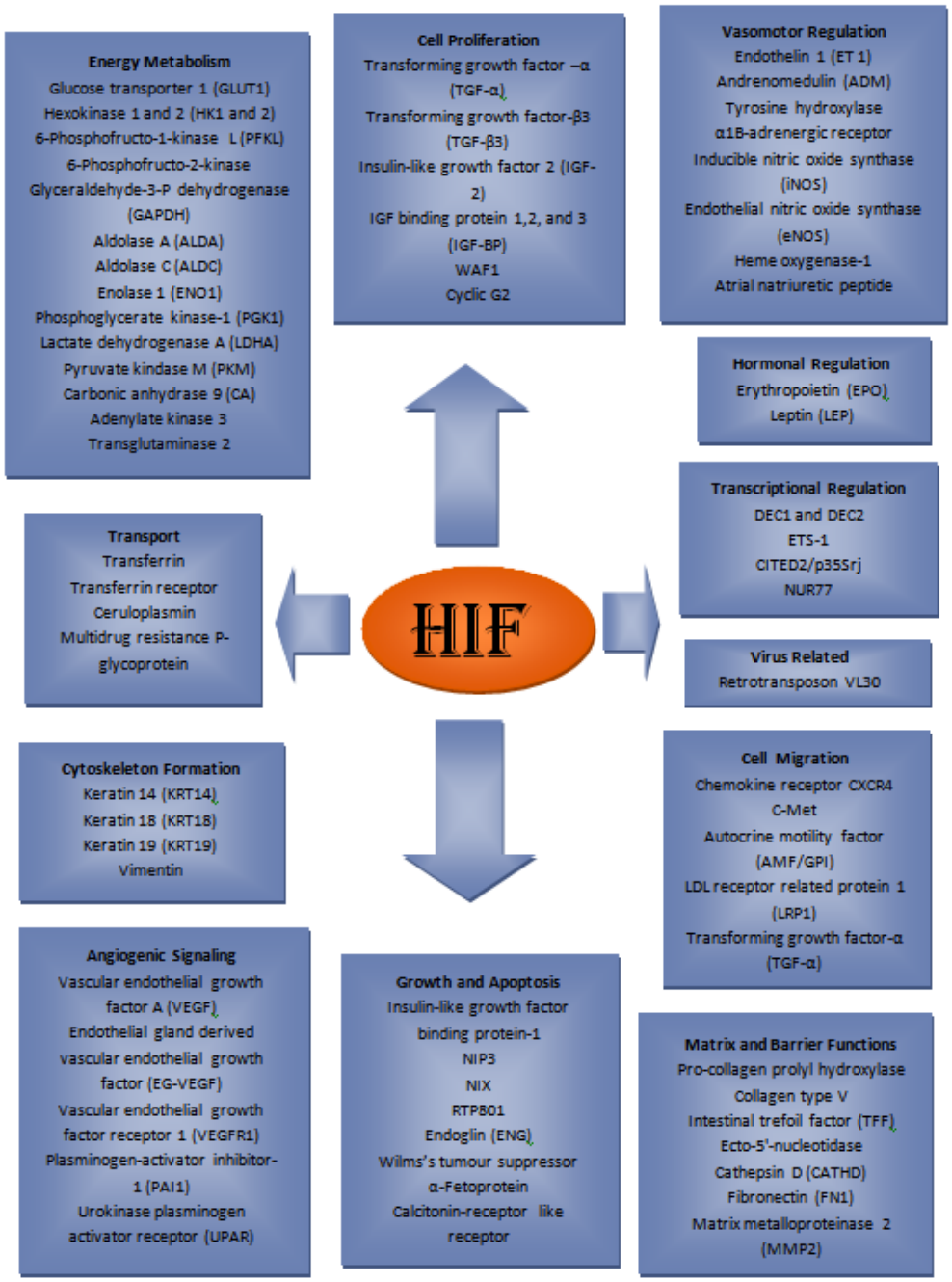


Figure 1.1: Transcriptional targets directly regulated by HIF. Figure adapted from Chowdhury *et al.*[4]

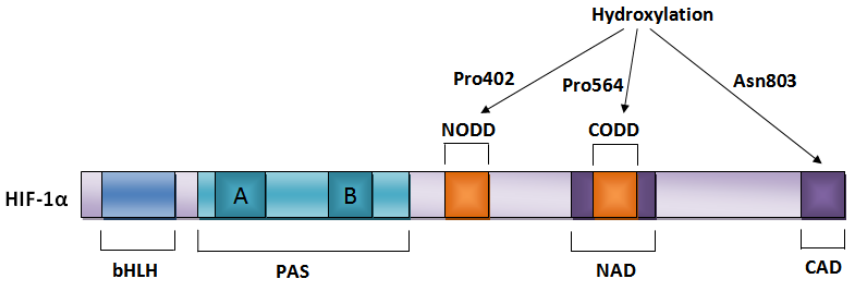


Figure 1.2: The domain structure of human HIF-1α showing the basic helix-loop-helix (bHLH) and PAS (PER-ARNT-SIM) domains which are involved in HIF-β and hypoxia response element (HRE) binding. Also shown are the *N*-terminal oxygen-dependent degradation domain (NODD), *C*-terminal oxygen-dependent degradation domain (CODD), *N*-terminal transactivation domain (NAD) and *C*-terminal transactivation domain (CAD).[2] PER, period circadian protein; ARNT, aryl hydrocarbon receptor nuclear translocator; SIM, single minded protein.

The prolyl and asparaginyl hydroxylation of HIF-α are catalysed by the HIF prolyl hydroxylases (PHDs 1-3) and factor inhibiting HIF (FIH), respectively. The PHDs and FIH are Fe(II) and 2-oxoglutarate (2OG) dependent oxygenases that use 2OG and oxygen as co-substrates and produce hydroxy-proline/asparagine residues, succinate and carbon dioxide as products (**Fig. 1.3**).[16-19] **Fig. 1.4** outlines the proposed consensus mechanism for 2OG oxygenases. Upon binding of an Fe(II) ion, 2OG coordinates the metal in a bidentate manner by displacing two ligating water molecules to form an enzyme.Fe(II).2OG complex. Oxygen binding is then followed by oxidative decarboxylation of 2OG, resulting in generation of succinate and a reactive Fe(IV)=O species. This intermediate then hydroxylates the (HIF-α) peptide substrate, probably by a radical-rebound type reaction.[2, 4, 20]

Their absolute requirement for molecular oxygen as a co-substrate coupled to appropriate kinetic properties, is proposed to enable the HIF hydroxylases to act as cellular oxygen sensors.[21-23] K_m values for oxygen for PHDs and FIH have been reported to be in the range of 65-250 μM.[24-26] At low oxygen availability, the catalytic activity of HIF hydroxylases is reduced, allowing HIF-α to accumulate and dimerise with HIF-β, forming a transcriptionally active complex by binding to HREs in the nucleus. **Fig. 1.5** shows a schematic illustration for the differential regulation of HIF-α by PHD and FIH catalysis in normoxia and hypoxia.[2, 3]

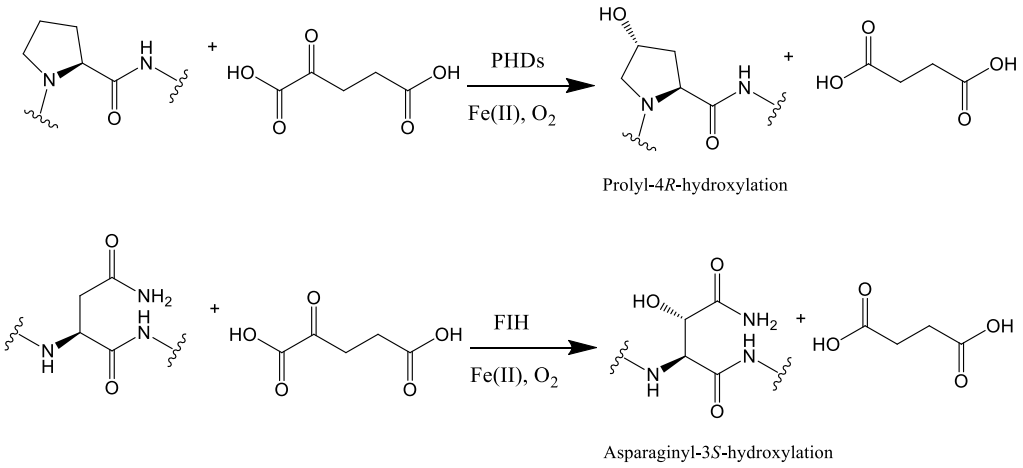


Figure 1.3: Hydroxylation reactions catalysed by HIF prolyl hydroxylases (PHDs) and factor inhibitor HIF (FIH). Both the PHDs and FIH require Fe(II), 2-oxoglutarate (2OG) and oxygen as co-factor/co-substrates and produce hydroxy-proline/asparagine residue, succinate, and carbon dioxide as products.

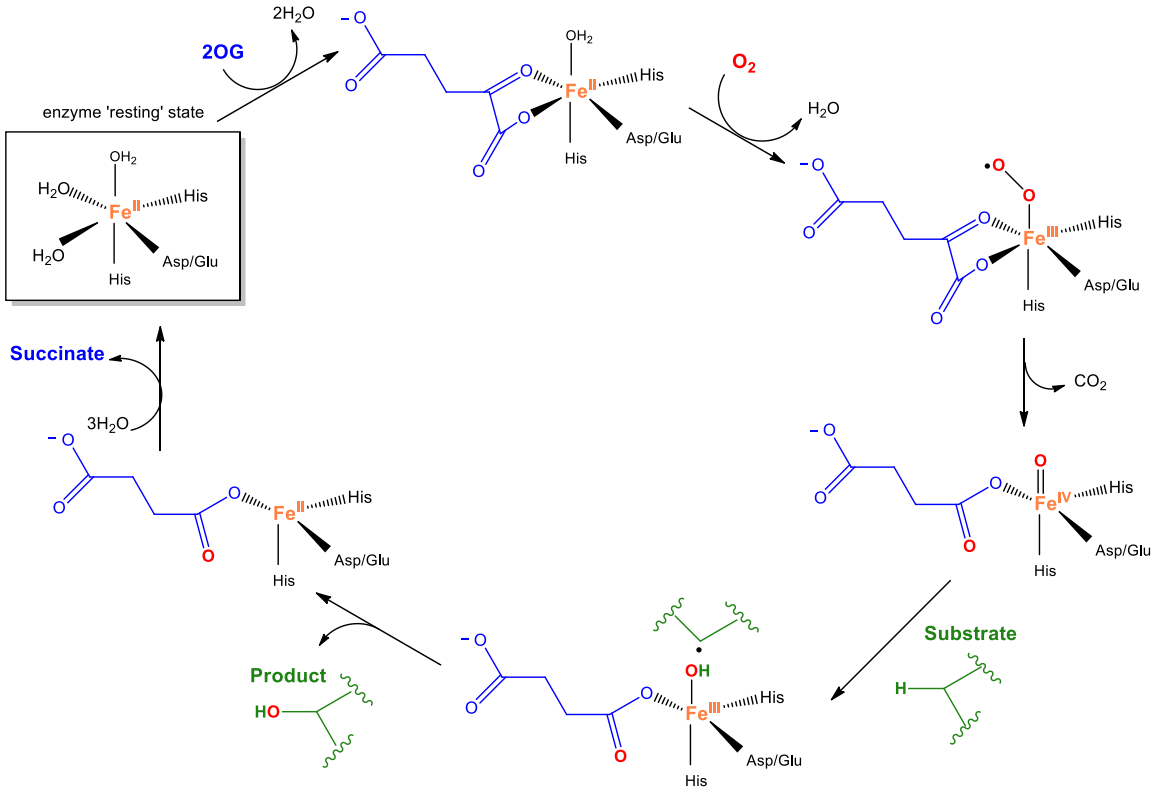


Figure 1.4: Outline mechanism for 2OG and Fe(II) dependent oxgenases.[2, 4, 20] 2OG coordinates the active site Fe(II) ion by replacing two water molecules. Oxygen binding is then followed by attack of oxygen on the oxo-group of the bound 2OG, which undergoes oxidative decarboxylation and resulting in generation of succinate and Fe(IV)=O intermediate. This reactive species then hydroxylates the peptide substrate, probably by a radical mechanism. The hydroxylated substrate and succinate then leave the enzyme active site, leading to regeneration of the enzyme 'resting' state.

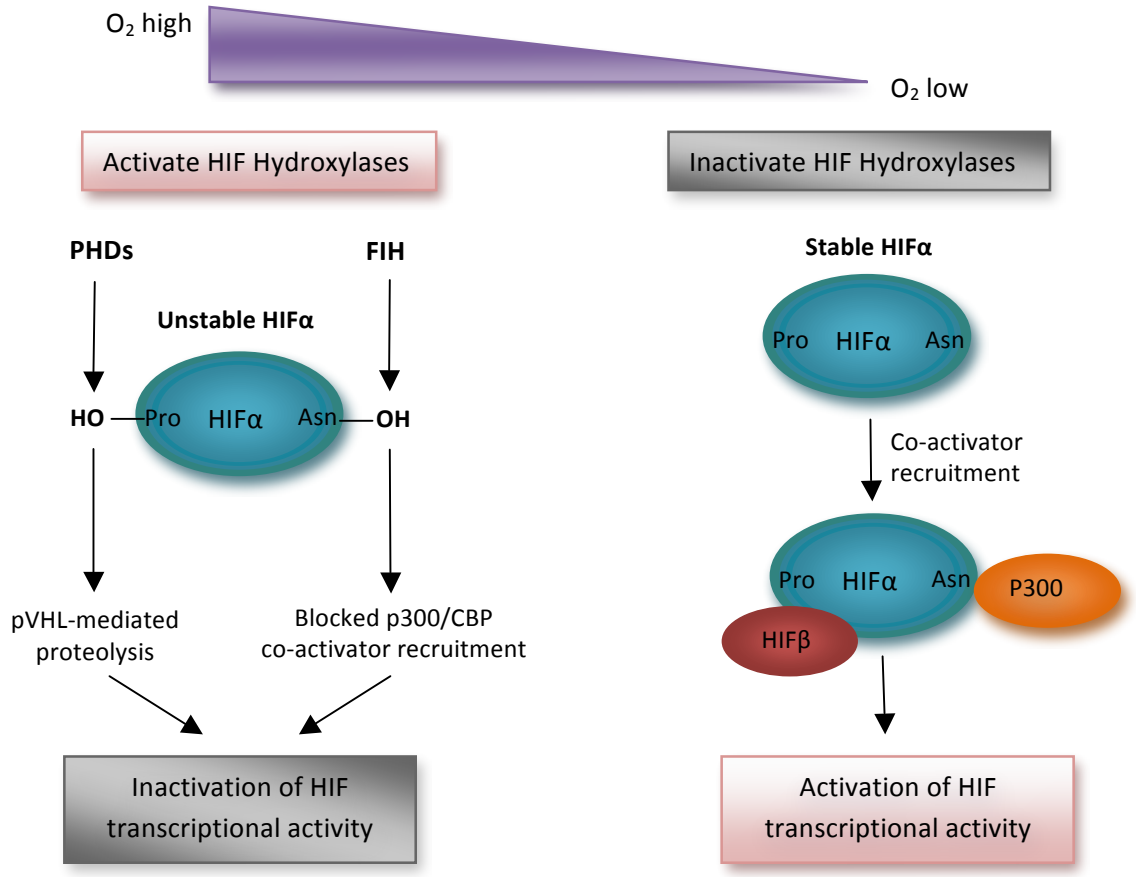


Figure 1.5: HIF-α levels are regulated by prolyl hydroxylase (PHD) and factor inhibiting HIF (FIH) catalysis depending on the cellular oxygen availability. In normoxia, HIF-1α is hydroxylated at one or both proline residues (Pro402/564), then targeted for pVHL-mediated proteasomal degradation. HIF-1α is also hydroxylated at asparagine residue (Asn803) which prevents its interaction with co-activator p300/CBP thus disabling HIF transcription pathway. At low oxygen availability (hypoxia), HIF hydroxylase activity is suppressed thus enabling binding of the dimerised HIF-α/HIF-β complex to hypoxia response elements (HRE), recruitment of the co-activator p300/CBP and activation of HIF transcriptional activity.[4] Figure adapted from Schofield *et al.*[2]

1.2 HIF Prolyl hydroxylases (PHDs)

1.2.1 The role of the PHD isoforms

The human PHD isoforms (PHD1, PHD2, and PHD3) have a sequence identity of ~ 40-60% and are believed to have arisen by gene duplication and divergence.[17, 19, 22, 27, 28] In *Caenorhaditis elegans* and *Drosophila*, the PHDs are represented by a single gene and are reported to have a critical function in HIF-α stabilisation.[17, 19, 28] As yet, the precise function of each PHD isoform in higher organisms remains unclear.

1.2.2 Structural features of the PHDs

Full-length human PHD1, PHD2 and PHD3 have 407, 426, and 239 amino-acid residues, respectively (**Fig. 1.6**). Their *C*-terminal catalytic domains are highly conversed (~55% identity), whereas the *N*-terminal domains are more divergent and have poorly characterised functions. PHD3 has a short *N*-terminus as compared to PHD1 and PHD2.[17, 29, 30] Crystallographic studies have thus far revealed the structure of an *N*-terminally truncated construct of PHD2. **Fig. 1.7** shows a crystal structure of PHD2 in complex with Fe(II) and a bicyclic 2OG analogue (8-iodo bicyclic isoquinoline) (PDB ID 2G19).[31]

Similarly to other Fe(II) and 2OG dependent oxygenases, PHD2 contains a double-stranded β-helix (DSBH) core (jelly roll motif), comprising two β-sheets consisting of eight anti-parallel β-strands (I-VIII) which are arranged to form its catalytic centre. Three α-helices (α1, α2, and α3) pack along the major β-sheet and help to stabilise the DSBH structure.[32] In the crystal structure of PHD2 (PDB ID 2G19) (**Fig 1.7**), the *C*-terminal α-helix (α4) stretches from strand VIII (β10) into the catalytic centre of a neighbouring enzyme.[31-33]

A recent crystal structure of the PHD2 catalytic domain in complex with a truncated form of HIF-1α substrate (a 19-mer fragment of the CODD polypeptide) demonstrated a

dramatic structural change of the PHD2 on binding to the CODD peptide. Coupled to mutagenesis studies, these findings suggest that PHD2 catalysis involves a mobile region (*i.e.* the 'finger-like' β2/β3 loop of residues ~ 237–254) that assists in isolation of the catalytic site and stabilisation of the PHD2.Fe(II).2OG.CODD complex.[34, 35] Interestingly, this mobile β2/β3 loop has also been shown to play an important role in determining the substrate selectivity of the PHDs.[35]

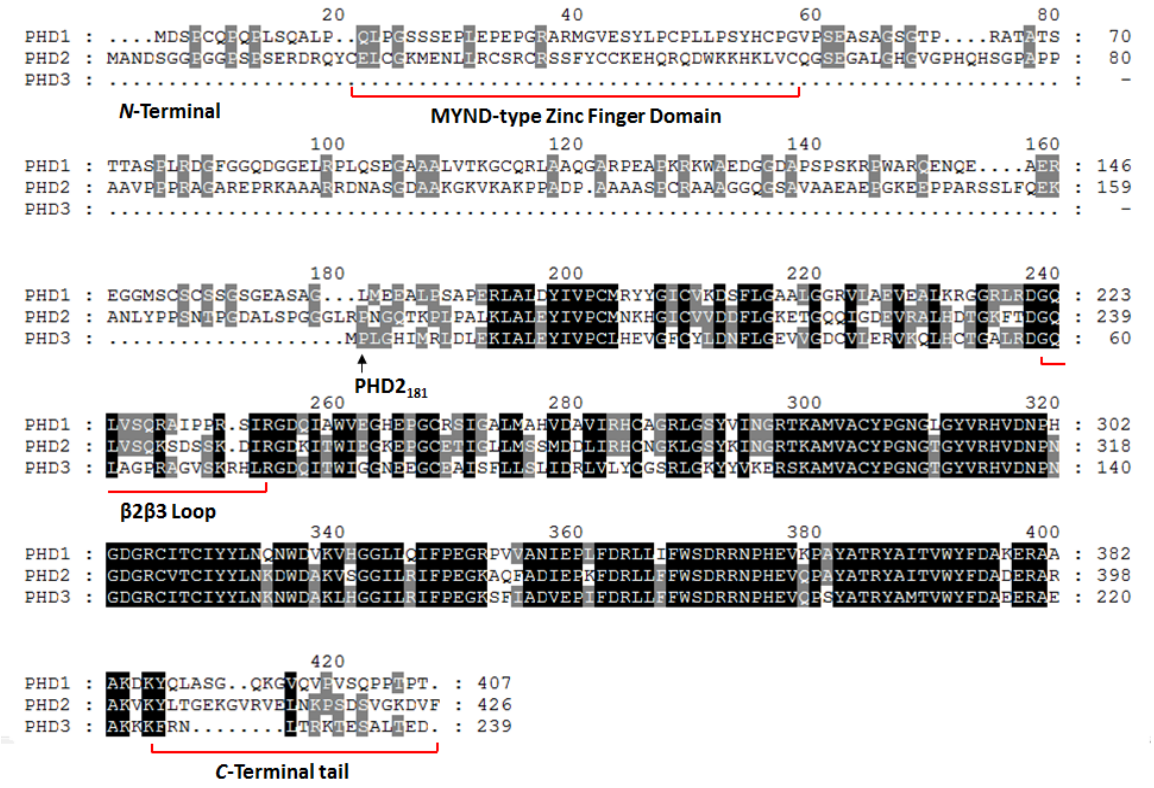


Fig. 1.6: A sequence alignment of human PHDs 1-3.[35] Figure created by using Genedoc software. Black and grey shades represent highly and moderately conserved sequence similarities, respectively.

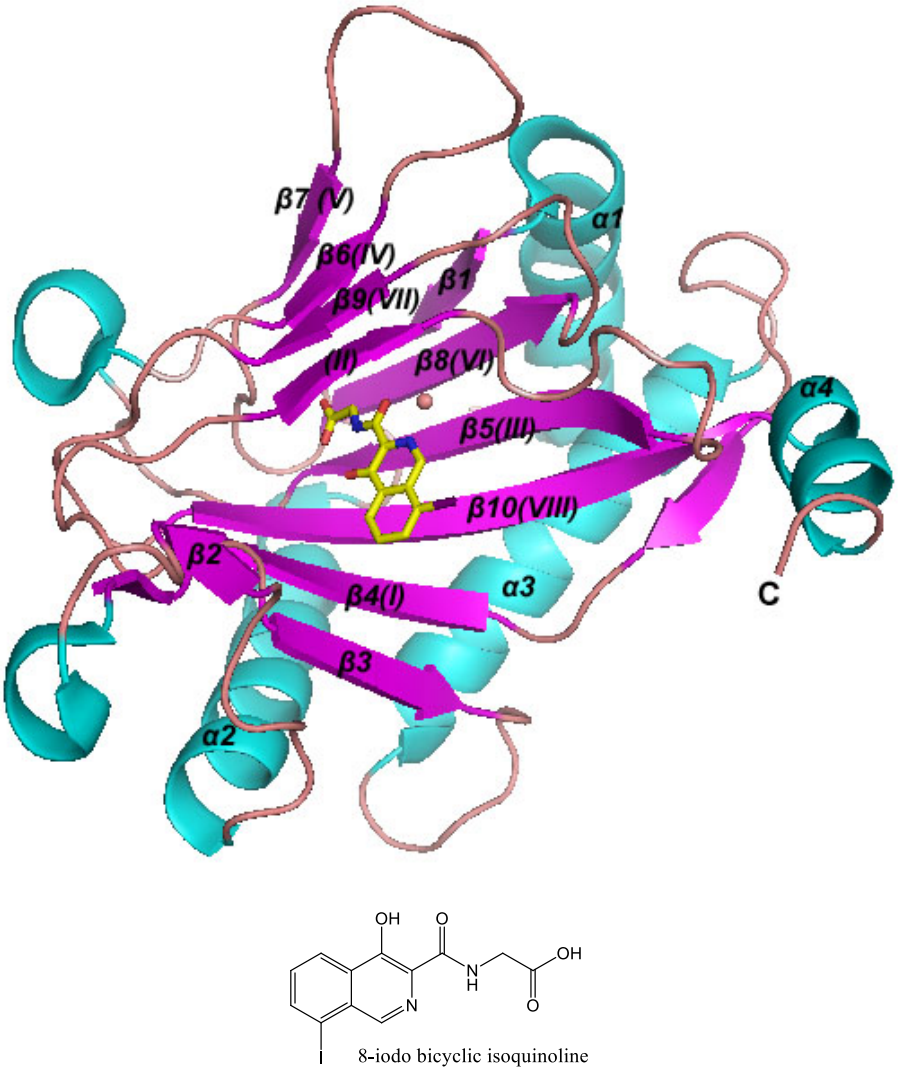


Figure 1.7: Stereoview ribbons representation of the secondary structure of the catalytic domain of PHD2 complexed with 8-iodo bicyclic isoquinoline inhibitor (yellow) and the active site Fe(II) (orange sphere) (PHB ID 2GHT).

1.2.3 Substrate Specificities of the PHDs

The PHDs have different substrate specificities with regards to NODD and CODD hydroxylation. All three PHDs are more active with respect to CODD hydroxylation, whereas unlike for PHD1 and PHD2, PHD3 is only very weakly active with respect to NODD hydroxylation. The reasons for this substrate selectivity are unclear.[13, 36]

Sequence and substitution analyses have revealed that the CODD/NODD selectivity of the PHDs may involve a mobile 'β2/β3 loop' (**Fig. 1.6**).[35] A PHD2 variant in which the β2/β3 loop was replaced with that of PHD3 demonstrated complete selectivity for CODD over a period of 60 min (in competition experiments in the presence of NODD), as observed for wild-type PHD3.[35] CODD was also shown to bind much more strongly to this PHD2/PHD3 chimeric protein than the wild-type PHD2. These results therefore suggest that this flexible β2/β3 loop is a major determinant in conferring selectivity for CODD over NODD.[35]

The PHDs have also been shown to display different specificities for the HIF-α isoforms in cells; PHD2 is relatively more specific for HIF-1α over HIF-2α, and PHD3 is more specific for HIF-2α than HIF-1α.[37, 38] The reasons for these differences are yet to be investigated.

1.2.4 Alternative substrates of the PHDs

Although each of the three PHDs is capable of hydroxylating HIF-α, it remains uncertain whether HIF is the only physiological substrate of all three hydroxylases *in vivo* as HIF-independent functions of the PHDs have also been described. PHD1 and PHD2 have been reported to regulate the transcriptional activity of NFkappaB (NF-$_K$B) by catalysing the hydroxylation of I_KB kinase (IKKβ).[39, 40] This modification was shown to impair phosphorylation of the inhibitory factor I_KBα, resulting in an inactivated NF-$_K$B complex. Under hypoxic conditions (or when activity of PHD1 and PHD2 were suppressed), hydroxylation of IKKβ was inhibited, thus enabling phosphorylation of I_KBα which eventually led to its dissociation from NF-$_K$B and activation of transcriptional responses including those involve the regulation of cell proliferation and cell survival (**Fig. 1.8**).[39-41]

pVHL has been reported to bind specifically to the large subunit of RNA polymerase II in a prolyl hydroxylation-dependent manner. Prolyl hydroxylation of the RNA polymerase

II has been proposed to be catalysed by the PHDs.[42] Furthermore, a recent study describes that the β_2-adrenergic receptor (β_2-AR) is an additional substrate of PHD3. PHD3 is reported to catalyse the prolyl hydroxylation of β_2-AR, which promotes its binding to the pVHL-E3-ligase complex and upon ubiquitination leads to proteasomal degradation in a mechanism similar to HIF-α degradation.[43] PHD3 has also been shown to catalyse the hydroxylation of Pro403 and Pro408 residues in pyruvate kinase M2 (PKM2), a modification which enhances the PKM2 interaction with HIF-1α and promotes HIF-1α transactivation activity and regulates glucose metabolism in cancer cells.[44, 45] However, it is important to note that none of these non-HIF modifications has been confirmed *in vitro* using tandem mass spectrometry (MS/MS) which is used to provide direct evidence of specific amino acid modifications.

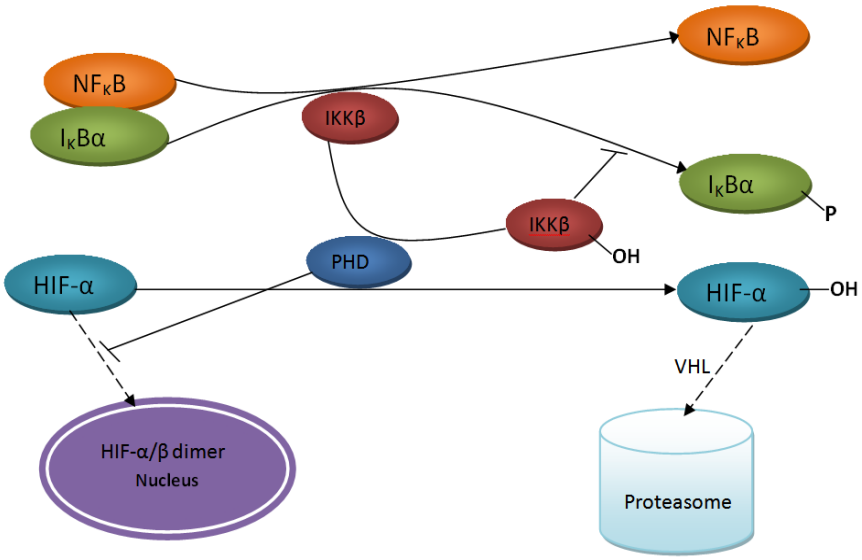


Figure 1.8: The PHDs are proposed to regulate the transcriptional activity of NFkappaB (NF-κB) by catalysing the hydroxylation of IκB kinase (IKKβ). This modification impairs phosphorylation of the inhibitory factor IκBα, resulting in an inactivated NFκB complex. The regulatory role of PHDs in the HIF pathway is also shown. –P and –OH represent phosphorylation and hydroxylation, respectively. Dashed line arrows indicate molecular movement. Lines with short perpendicular lines at the end indicate negative regulation. Figure adapted from Fong *et al.*[29]

1.2.5 PHDs as oxygen sensors

The K_m values of the PHDs 1-3 for oxygen have been reported to be approximately 240 μM,[25, 26] slightly higher than the (atmospheric) dissolved oxygen level (~200 μM) (one study even reported a K_m value for oxygen for PHD2 of 1.7 mM).[46] Furthermore, in transient kinetic studies PHD2 has been shown to react with oxygen at significant slower rate compared to other studies of 2OG oxygenases.[47] These properties (high K_m values and slow reaction rate with oxygen) are proposed to enable the PHDs to act as efficient oxygen sensors.

Interestingly, studies employing small interference RNA (siRNA) have shown that specific 'silencing' of PHD2 mRNA (which eventually leads to reduced PHD2 protein levels) alone in normoxia is sufficient to stabilise HIF-1α, leading to the proposal that PHD2 is the key human oxygen sensor.[22] In contrast, suppression of PHD1 and PHD3 mRNAs had little or no effect on HIF-1α expression in several cell types. They were therefore assumed to have less significant roles in cellular oxygen sensing.[22] These proposals are supported by data indicating that PHD2 has the highest specificity for the primary hydroxylation site of HIF-1α (*i.e.* CODD), and that it represents the ancestral form of the PHD (EGLN, egg-laying-defective nine in *C. elegans*) gene family.[27, 48, 49]

1.2.6 Expression levels of the PHDs

The abundance of PHD enzymes has been argued to be an important factor in HIF regulation.[29, 37] mRNA and protein analyses show the existence of tissue-specific and hypoxia-dependent expression of each PHD.[26, 50-53] The basal level of PHD2 protein has been reported to be far greater than PHD1 and PHD3 levels across a wide range of normoxic cells (even for cells which express relatively low levels of PHD2 mRNA).[37] It is therefore not surprising that suppression of PHD2 in these cells will have a significant effect on HIF regulation. By employing cells which express relatively high levels of PHD1 and PHD3 under different culture conditions, it has been demonstrated that PHD1

and PHD3 enzymes contribute in a non-redundant manner to HIF-α regulation. Overexpression of each PHD was shown to hydroxylate the HIF-α polypeptides and suppress HRE-mediated transcriptional activity.[37]

The PHDs also have distinct patterns of intracellular distribution. Initial studies using PHDs fused with enhanced green fluorescent proteins indicated that PHD1 was exclusively present in the nucleus, PHD2 was primarily located in the cytoplasm, and PHD3 was homogeneously distributed in both.[54] However, subsequent studies using monoclonal antibodies argue that all endogenous PHDs are predominantly located in the cytoplasm.[55] A putative PHD4 which is proposed to be expressed in the endoplasmic reticulum has also been described; however, it has not yet been shown to be active *in vitro*.[51, 56]

1.2.7 Knockout models of the PHDs

Interestingly, while PHD1 and PHD3 homozygous knockout mice apparently survive normally, PHD2 homozygous knockout embryos die at mid-gestation stages due to severe placental and heart defects.[29, 57] Adult PHD1 and PHD3 homozygous knockout mice had no apparent defects, however, PHD1/3 double knockout mice demonstrated moderate erythrocytosis.[38]

Notably, cardiomyocyte-specific PHD2 conditional knockout mice have been found to have protective effects against acute myocardial ischemic injury.[58] A recent report shows that specific inhibition of PHD2 activity in cancer cells results in stimulation of blood vessel formation but paradoxically leads to significant reduction of tumour growth; a phenomenon associated with the antiproliferative activity of the transforming growth factor-β (TGF-β) signaling pathway, which is believed to be HIF-independent. (TGF-β has been shown to display dichotomous activity (*i.e.* tumour suppressor or tumour promoter), an effect known as the 'TGF-β paradox').[59, 60] Specific inhibition of PHD1

(but not PHD2 or PHD3) using siRNA has also been reported to cause neuroprotective effects against oxidative death via a HIF-independent pathway.[61]

Given that each of the PHD enzymes may contribute differentially to specific biological processes and clinical phenotypes, pharmacological inhibition of a particular PHD isoform is proposed to have the potential for selective alterations of the HIF-mediated response or other pathophysiological pathways that may be beneficial in therapeutic applications.[29, 37]

1.2.8 Problems associated with genetic approaches to assigning the specific function of the PHDs

Although genetic approaches employing siRNA and knockout mice models are powerful tools for studying the specific functions of the PHDs in biological systems, the results obtained from these studies do not fully reflect the physiological system. There are some disadvantages of these techniques that must be taken into consideration.

Gradual depletion of the PHD enzyme by siRNA could give rise to unexpected results. The cell might adapt to the change by up- or down-regulating other proteins, and resulting phenotypes could therefore arise from complex mechanism. Furthermore, incomplete depletion of the target protein could lead to false conclusions. It is therefore hard to know whether the observed effect is due to complete ablation of the enzyme, or to a small but crucial amount of the remaining enzyme. It is also unclear whether the observed phenomena are due to the loss of scaffold functions or the catalytic activity of the proteins. Finally, it is possible that the siRNA may have 'off-target' effects, especially when considering transcriptional regulation. Knockout models often produce a lethal embryonic phenotype (as in the case of the PHD2 homozygous knockout mice),[57] resulting in difficulties in obtaining relevant information about adult organisms.[62-64]

Some of the concerns about using genetic approaches might be overcome by applying small-molecule based methods to investigate the function of each PHD isoform. Such an

approach can enable probing of enzyme function in a highly controllable and pharmacologically relevant way. Chemical inhibition of a targeted enzyme does not normally change its protein concentration, therefore avoiding side effects caused by protein loss. Importantly, unlike gene inactivation techniques, drug-like molecules can act quickly and reversibly, enabling them to behave as 'chemical switches' for the studies of signal transduction pathways which can occur on millisecond time scales.

There are of course potential disadvantages to using small-molecule based approaches for determining enzyme function. The relative lack of knowledge about specificity, poor cell-permeability, toxicity and off-target effects can lead to erroneous conclusions. Small-molecules may also be targeted for metabolic alterations *in vivo*, which could substantially modify their activities and toxicities. Small-molecule enzyme inhibition can also inhibit the activities of closely related proteins, so the observed effects may not reflect the functions of the target enzyme.[62, 64, 65] In the case of the PHDs, selective inhibition of each PHD isoform by small-molecule inhibitors is not yet possible, probably because all three PHD isoforms have a highly conserved active site.[19]

1.2.9 PHDs as therapeutic targets

As well as being activated by hypoxia, the HIF-transcriptional pathways can be activated artificially by 'hypoxia mimetic' chemical agents, including the iron chelators desferrioxamine (DFO), 2,2'-dipyridine (DIP), divalent transition metal ions (e.g. Co(II), Ni(II), Zn(II)) and small-molecule inhibitors that are 2-oxoglurate (2OG) analogues. The latter includes dimethyloxalylglycine (DMOG, a prodrug form of *N*-oxalylglycine, a 'generic' inhibitor of 2OG oxygenases).[3, 20, 66, 67] Iron chelators inactivate the HIF hydroxylases by sequestering the active site iron, whereas metal ions compete with the catalytic Fe(II) for binding to the active site metal chelating residues. 2OG analogues suppress PHD/FIH activity by binding to the enzyme active site competitively with 2OG (and possibly oxygen). Some potent inhibitors have also been shown to hinder HIF substrate binding to the active site region.[2, 20, 68, 69]

There is interest in the development of HIF hydroxylase inhibitors (particularly PHD inhibitors) that activate the HIF-mediated responses for the treatment of hypoxic related disorders such anaemia, stroke, ischaemic heart disease, kidney disease and inflammatory bowel disease.[67, 70-74] Prior to the advent of recombinant human erythropoietin (rhEPO) therapy, Co(II) was used as a treatment for anaemia.[74, 75] It was proposed that Co(II) stimulates erythropoietin (EPO) production (a hormone that regulates erythropoisesis (red blood cells production)), at least in part, by inhibiting the HIF hydroxylases.[4] Expression of the EPO gene is dominantly regulated by HIF-α, and thus by the HIF hydroxylases.

Several studies have shown that inhibition of the PHDs increases EPO levels.[38, 76] Several PHD inhibitors are currently being investigated as potential anti-anaemia drugs. Three have progressed to Phase II clinical trials, of which FibroGen's compound FG-2216[77, 78] has been shown to increase haemoglobin production in patients.[74, 76, 79] Interestingly, various Krebs cycle intermediates[80, 81] including oxaloacetate, malate, fumarate and succinate and the aspirin metabolite 2,3-dihydroxybenzoylglycine (DHBG)[82] have been reported to inhibit the PHDs *in vitro*, and some of these metabolites have been shown to activate HIF-1α activity in the cells.

HIF-stabilisation also leads to induction of vascular endothelial growth factor (VEGF) which stimulates the proliferation and migration of endothelial cells (*i.e.* angiogenesis). HIF-mediated angiogenesis plays a role in wound healing[83, 84]. Furthermore, promotion of angiogenesis is thought to be desirable to repair tissue damage caused by cardiovascular and cerebral ischaemic disorders. Ischaemic preconditioning (an experimental technique used to produce repeated short episodes of ischaemia/hypoxic response by restriction of blood (oxygen) supply or in this case by chemical inhibition of the HIF hydroxylases) has been proposed to have a therapeutic protective effect against stroke and myocardial infarction [85-88].

HIF is also known to play a role in tumour progression by supplying oxygen to the hypoxic tumours.[1, 89] Indeed, high levels of HIF are associated with poor clinical outcome.[1, 89] Although some evidence suggest improved oxygenation (via HIF

hydroxylase inhibition) may make tumours more sensitive to radiotherapy and chemotherapy treatments,[20] it must always be considered that pharmacological inhibition of the HIF hydroxylases for treatment of cardiovascular diseases may have unwanted side effects.

1.3 HIF system and cancer cell metabolism

1.3.1 2-Oxoglutarate (2OG)

2OG has been proposed to act as a 'hub-molecule' in cellular metabolism.[90] 2OG is produced by the oxidative decarboxylation of isocitrate catalysed by isocitrate dehydrogenases (IDH1/2) in the Krebs cycle (**Fig. 1.9**). In proliferating/cancer cells, high fluxes of anaplerotic reactions re-feed 2OG into the cycle which is primarily carried out via the glutaminolysis pathway. In this pathway, glutamine is metabolised by phosphate-dependent-glutaminase (PDG) to give glutamate which is then converted to 2OG by glutamate dehydrogenase (GDH).[91, 92] In addition to GDH, glutamate can also be converted to 2OG by the catalytic activities of aminotransferases.[93, 94]

Increased 2OG in the Krebs cycle leads to production of oxaloacetate which in turn reacts with acetyl-CoA to generate citrate for lipid synthesis (**Fig. 1.9**). Lipid synthesis products (*i.e.* fatty acids, cholesterol, and isoprenoids) are used as major membrane building blocks for proliferating/tumour cells.[95, 96] Oxaloacetate and 2OG also supply the intracellular pools of non-essential amino acids to be used for protein and nucleotide synthesis. Therefore, a key role of Krebs cycle intermediates, including 2OG, is to supply a carbon source for macromolecular biosynthesis in proliferating/cancer cells.[91] In addition to glutaminolysis, aerobic glycolysis (a phenomena known as the Warburg effect)[97] is another major anaplerotic pathway that cancer cells use for energy generation and biomass synthesis.[92] In aerobic glycolysis, most glycolytic pyruvate is directed away from mitochondrial oxidative phosphorylation to form lactate, a reaction catalysed by lactate dehydrogenase-A (**Fig. 1.9**).

1.3.2 PHDs as 2OG and metabolic sensors

In normal cells, activation of signal transduction pathways often requires extracellular stimulation (e.g. growth factors). In contrast, tumour cells normally harbour germline mutations that chronically promote these pathways, resulting in an increased metabolic autonomy that is not regulated by normal physiological constraints.[91, 98]

Mutations in the Krebs cycle enzymes succinate dehydrogenase (SDH) and fumarate hydratase (FH) (**Fig. 1.9**) result in elevation of succinate and fumarate. Excessive accumulation of succinate and fumarate in SDH and FH associated tumours are proposed to suppress PHD activity leading to activation of HIF-mediated oncogenic pathways (via stimulation of the tumour progression gene VEGF).[67, 99-102] These proposals are consistent with the *in vitro* results which show that fumarate and succinate can compete with 2OG (a co-substrate of the PHDs) to bind to the active sites of PHDs.[81, 100]

Elevated HIF activity in tumour-associated IDH mutants has also been proposed to arise from reduced PHD activity due to depleted 2OG levels.[103] Consistent with this proposal, artificial increase of the cellular 2OG levels has been demonstrated to reverse HIF-stabilisation in SDH harbouring mutant cell-lines; this is believed to be a result of reactivation of PHD activity.[104] Given that HIF prolyl hydroxylation is apparently sensitive to cellular 2OG fluctuation, it has been proposed that the PHDs may play a more general role as 2OG and metabolic sensors besides their function as intracellular oxygen sensors.[90, 91]

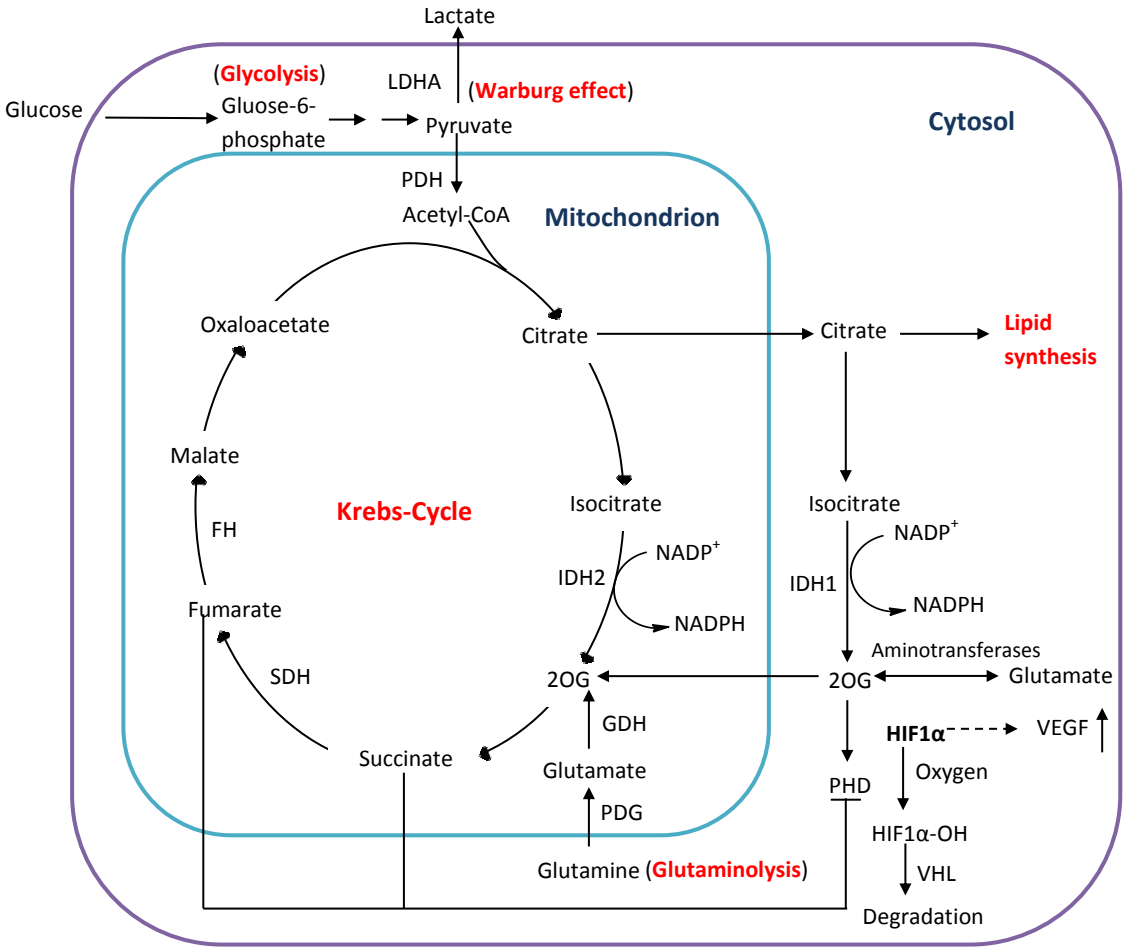


Figure 1.9: In proliferating/cancer cells, anaplerotic reactions replenish 2-oxoglutarate (2OG) into the Krebs cycle via the glutaminolysis pathway catalysed by phosphate-dependent-glutaminase (PDG), and glutamate dehydrogenase (GDH) and transamination reactions catalysed by aminotransferases. Malfunctions of succinate dehydrogenase (SDH), and fumarate hydratase (FH) and isocitrate dehydrogenases (IDH1/2) are associated with upregulation of HIF-mediated tumorigenesis. GDH, glutamate dehydrogenase; PDG, phosphate-dependent glutaminase; LDHA, lactate dehydrogenase-A; PDH, pyruvate dehydrogenase; PHD, HIF prolyl hydroxylases; VEGF, vascular endothelial growth factor; HIF1α-OH, hydroxylated-HIF-1α.

1.3.3 Isocitrate dehydrogenase (IDH) mutations

Heterozygous mutations in either of the two IDH isoforms (IDH1/2) occur in more than 70% of low-grade gliomas (brain tumours) and secondary glioblastoma multiforme (malignant brain tumours).[105-108] The mutations produce single residue substitutions of the substrate-binding arginine-residues (Arg 132 in IDH1; Arg 140 and Arg 172 in IDH2) which abolish IDH catalytic activity for the conversion of isocitrate to 2OG.[103] Furthermore, these forms of mutated IDHs gain a new function for catalysing the reduction of the α-ketone in 2OG to *R*-2-hydroxyglutarate (*R*-2HG or D-2HG).[109-111]

High levels of *R*-2HG (5-35 μmol/g of tumour or approximately 5-35 mM, if assuming tissue density of 1 g/ml) were reported in most IDH1 mutant human gliomas compared to wild-type IDH1 which had 100-fold less *R*-2HG.[109] The excessive accumulation of *R*-2HG in mutated IDH malignant glioblastoma and acute myeloid leukaemia has led *R*-2HG to be reported as an 'oncometabolite'. To date, the mechanism of action of *R*-2HG is unknown. However, it has been argued that the excessive accumulation of *R*-2HG may directly inhibit the PHDs, and is therefore responsible for the increased HIF-1α activity observed in the defective IDH human gliomas;[109] inhibition may occur in a manner similar to fumarate and succinate inhibition of the PHDs. **Fig. 1.10** shows the structural similarities between 2OG, 2HG, fumarate, and succinate (the C-2 carbonyl oxygen atom in 2OG is subsituted with a hydroxyl group in 2HG).

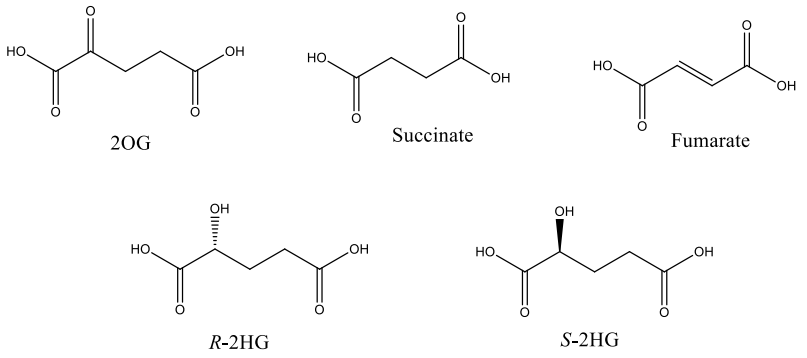


Figure 1.10: Structure similarities between 2-oxoglutarate (2OG), succinate, fumarate and 2-hydroxygularate (2-HG).

1.3.4 Other signal transduction pathways

The PI3K/Akt/mTOR (PI3K, phosphatidylinositol 3-kinase; mTOR, mammalian target of rapamycin) signalling pathway and transcription factors HIF-1α and c-Myc have been associated with metabolism of growth-factor dependent cells and cancer cells (**Fig. 1.11**). Growth factor (e.g. insulin-like growth factor-1 and -2) binding to the surface receptor of PI3K leads to activation of the serine/threonine kinases Akt and mTOR, resulting in higher anaplerotic glucose flux and increased levels of essential amino acids and protein translation which support bioenergetics and biosynthesis in normal or cancer cells.[112-115] High activity of PI3K/Akt/mTOR has also been reported to be a common feature in malignancies which correlate with mutations in tumour suppressor genes including PTEN, TSC1, and TSC2 (**Fig. 1.11**).[113, 116, 117]

Interestingly, stimulation of the PI3K/Akt/mTOR pathway has been found to activate HIF-1α activity.[118-120] HIF-1α transcriptional targets include genes encoding glucose transporter-1 (GLUT1), lactate dehydrogenase-A (LDHA) and pyruvate dehydrogenase kinase-1 (PDK1) which are directly involved in the regulation of glucose metabolism that has been shown to promote tumour growth.[121, 122]

Amplification of Myc family genes (especially the master transcription factor c-Myc) in cancer cells has been associated with stimulation of glucose and glutamine anaplerosis, and *de novo* nucleotide biosynthesis. c-Myc has recently been shown to increase glutaminolysis by activating the expression of glycolytic genes such as LDHA.[123-125] The possible interaction between mTOR-HIF-Myc signalling networks and the involvement of other pathways suggests an additional level of complexity to the currently understood picture of cancer cell metabolism.

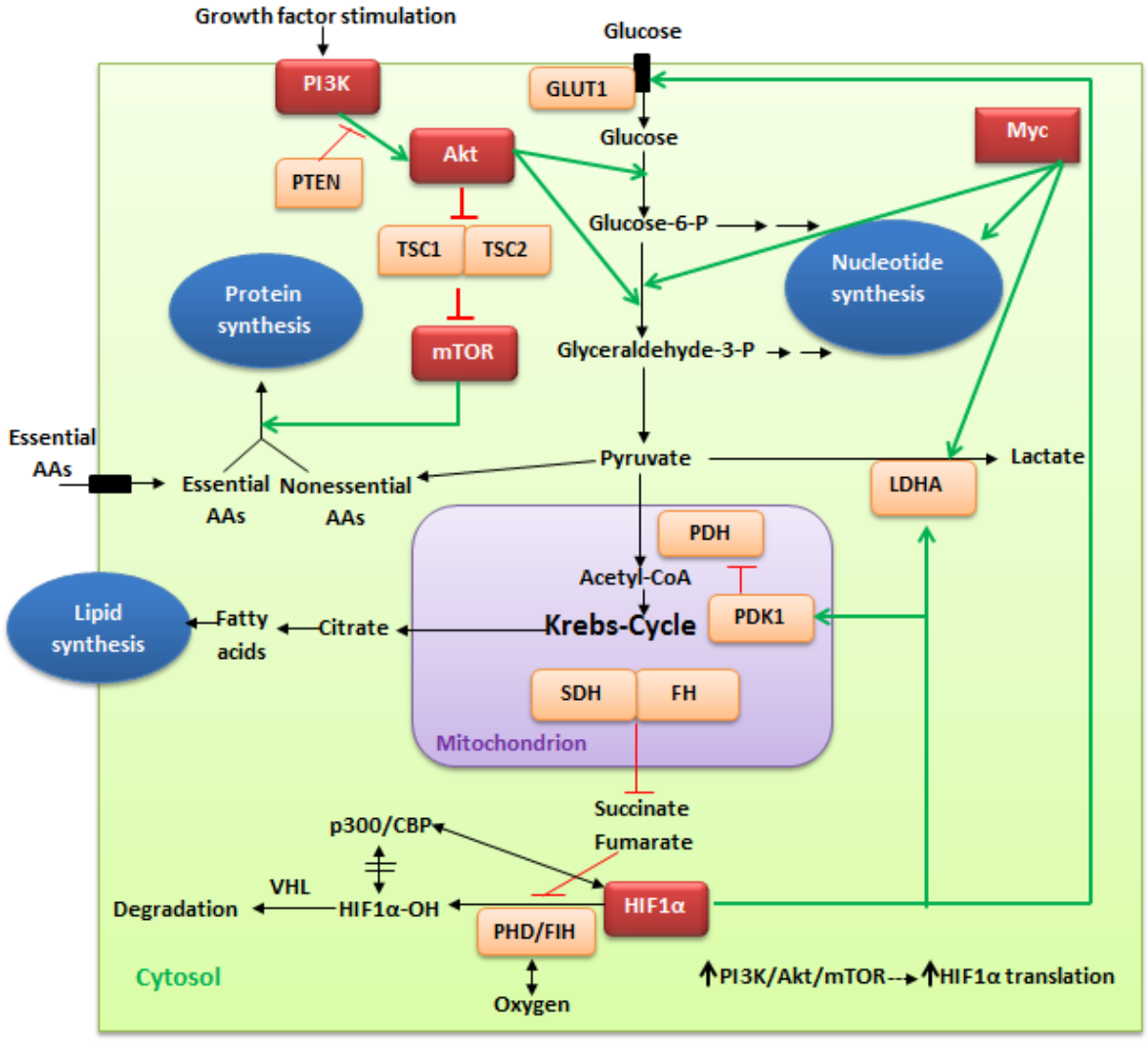


Fig. 1.11: A signal transduction network that regulates cancer cell metabolism. PI3K/Akt/mTOR, HIF-1α, and Myc signaling pathways involved in various aspects of cancer cell metabolism. Binding of a growth factor to the PI3K surface receptor activates the PI3K/Akt/mTOR pathway. Constitutive stimulation of the PI3K/Akt/mTOR system in cancers can result from mutations to the tumour suppressors *PTEN*, *TSC1*, and *TSC2*. Activation of the PI3K/Akt/mTOR pathway leads to increased glucose utilisation and promotes production of essential amino acids and translation. The PI3K/Akt/mTOR pathway has been found to stimulate HIF-1α translation. Elevation of Krebs cycle intermediates succinate and fumarate caused by malfunction of the SDH and FH have also been found to activate HIF transcriptional activity. Upregulation of the HIF system leads to expression of genes which encode for GLUT1, LDHA, and PDK1 which favour glucose uptake and lactate formation. The transcription factor Myc stimulates expression of several metabolic enzymes, including those that enhance anaplerotic glucose and glutamine metabolism and nucleotide biosynthesis, favouring cancer cell proliferation. Abbreviations: PI3K, phosphatidylinositol 3-kinase; PTEN, phosphatase and tensin homolog; TSC, tuberous sclerosis complex; mTOR, mammalian target of rapamycin; glucose-6-P, glucose-6-phosphate; glyceraldehyde-3-P, glyceraldehyde-3-phosphate; LDHA, lactate dehydrogenase-A, PDK1, pyruvate dehydrogenase kinase-1; GLUT1, glucose transporter-1; SDH, succinate dehydrogenase; FH, fumarate hydratase; PHD, HIF prolyl hydroxylases; HIF1α-OH, hydroxylated-HIF-1α. Figure adapted from DeBerardinis *et al.*[91]

1.4 Other 2OG oxygenases as therapeutic targets

1.4.1 Collagen prolyl-4-hydroxylase

Collagens are a family of extracellular matrix proteins that are a major component of connective tissues and are responsible for maintaining structural integrity.[126] Pathological fibrosis of an organ or tissue is characterised by excessive accumulation of fibrous tissue.[127] Kidney fibrosis is commonly associated with renal disease; whilst liver fibrosis often occurs in response to chronic inflammation as a result of alcohol abuse or liver infections.[127] Pharmacological intervention to prevent fibrosis progression is therefore desirable.

Mature fibrillar collagens exist as large, uninterrupted triple helices supercoiled around a common axis. The stability of these three constituent collagen strands (triple helices) substantially depends on 4-hydroxylation of the proline residues in the repeating X-Y-Gly-motif, where X is proline residue, and Y is proline or lysine residue.[126, 128] Prolyl-4-hydroxylation is catalysed by the 2OG dependent collagen prolyl-4-hydroxylase (C-P4H) and has been shown to occur exclusively at the Y position.[129] Other collagen modifications that help to maintain its function include prolyl hydroxylation at the C-3 position and lysyl hydroxylation at the C-5 position (**Fig. 1.12**).[129, 130]

Suppression of the collagen prolyl-4-hydroxylation was shown to lead to significant decreases in its structural stability, impairs its ability to interact with other components of the extracellular matrix, and targets the collagen for proteolytic degradation.[128, 129] Therefore, C-P4H is a potential therapeutic target. Extensive medicinal chemistry efforts have been undertaken to develop C-P4H small-molecule inhibitors; some of which have progressed to clinical trials. However, to date no drugs targeting C-P4H have been approved for clinical use.[20, 126]

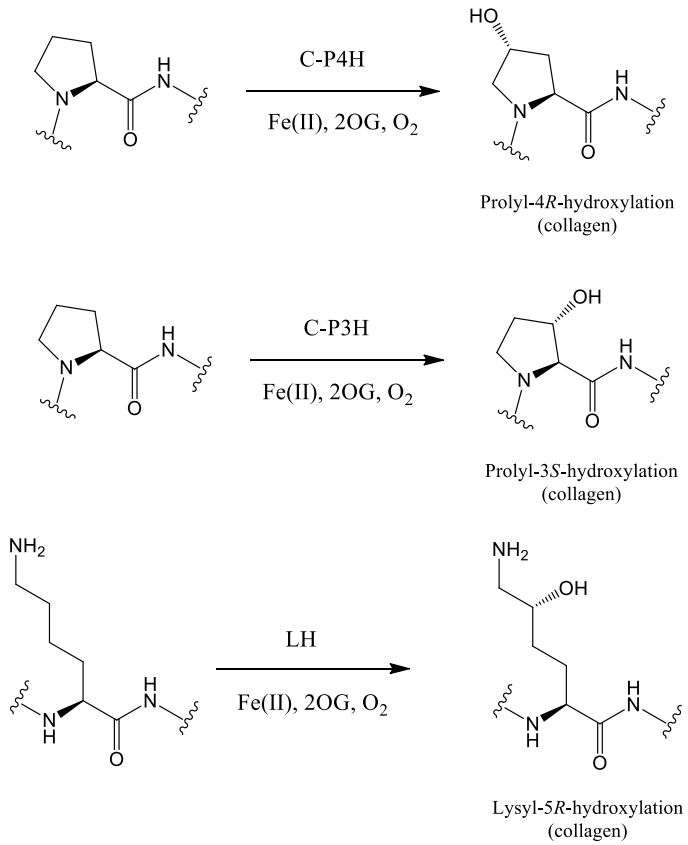


Figure 1.12: Hydroxylation of proline and lysine residues in collagen. The post-translational protein modifications are catalysed by collagen prolyl-4-hydroxylase (C-P4H), prolyl-3-hydroxylase (C-P3H), and lysyl hydroxylase (LH)/PLOD.

1.4.2 Histone demethylases

DNA is packaged into chromatin by formation of nucleosomes. Nucleosomes consist of eight histones (4 pairs: H2A, H2B, H3 and H4), which are short (100-150 amino acids), basic globular proteins that package DNA. Post-translational modifications (including acetylation, methylation, among others) of the amino acid residues in the *N*-terminal tails of histone proteins have been shown to contribute to regulation of transcription.[20]

Histone lysyl demethylases remove methyl groups from N^{ε}-methyl lysines on the histone tails. The first 2OG and Fe(II) dependent oxygenase to be identified as a histone demethylase was FBXL11 (F-box, leucine rich repeat protein 11) (in 2006).[131] FBXL11

is a H3K36me2 demethylase (i.e targeting the N^{ε}-dimethyllysine of Lys36 of human histone H3).[131, 132] Demethylases that act on H3K4, H3K9, H3K27, and H3K36 residues have subsequently been identified. Most of these 2OG dependent enzymes (e.g. JARID1A-D, JMJD2A-E and JMJD3) were reported to contain the JmJC (Jumonji-C) domain which is required for their catalytic activity and can catalyse the N^{ε}-demethylation of all three possible methylation states of N^{ε}-methyl lysine residues (**Fig. 1.13**).[20, 133]

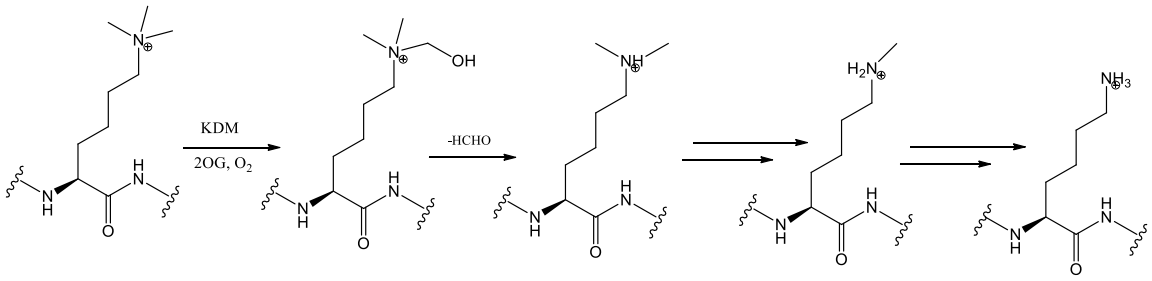


Figure 1.13: The JmJC subfamily 2OG dependent histone lysyl demethylases (KDM) catalyse the N^{ε}-demethylation of all three N^{ε}-methylated forms of histone lysine residues.

The biological roles and potential contributions of individual histone demethylases to diseases have yet to be fully deciphered, although there is evidence to suggest that they may be attractive potential targets for cancer therapy. For example, the histone H3K4me3 demethylase, JARID1A (Jumonji, AT rich interactive domain 1A) is upregulated in gastric cancer; genetic inhibition of its expression leads to senescence.[134] JARID1B is overexpressed in both prostate and cancer cells and believed to promote tumour cell proliferation by repressing negative regulators of cell growth.[135, 136] JMJD2 (Jumonji-C domain-containing 2) H3K9me3 demethylases have been associated with androgen receptor dependent transcription genes, including prostate specific antigen. Consistent with this role, high levels of JMJD2A-C are expressed in prostate cancers.[137, 138] The JMJD2 demethylases are also activated in esophageal squamous cell carcinomas, suppression of their activities by siRNA has been shown to reduce cancer proliferation.[138] In recent years, there has been increasing effort towards developing selective histone demethylase inhibitors, both as chemical probes for functional assignment, and as potential drug targets for therapeutic applications.[20, 139]

1.5 Aims of the work described in this thesis

Pharmacological activation of the HIF transcriptional response could be of significant therapeutic importance (**Section 1.2.9**). However, there is currently no biological data available for the selectivities of the potential HIF hydroxylase inhibitors against the HIF prolyl and asparaginyl hydroxylases. In work described in this thesis, I aimed to develop a cell-based method to enable simultaneous measurement of the effects of chemical inhibition on all three HIF hydroxylation sites (*i.e.* CODD, NODD, CAD). This method can then be further applied to investigate HIF hydroxylase inhibition, including the hypothesis of *R*-2HG mediated HIF response (**Section 1.3.3**), and the evaluation of the specificities of a series of novel and known HIF hydroxylase inhibitors. Given the problems associated with the current approaches used for functional assignment of individual PHDs (**Section 1.2.7**), my work also aimed to develop a new approach which may enable selective inhibition of a modified form of PHD2 in cells. Specific aims of the research described in this thesis included:

1) Development of a HIF hydroxy-residue specific antibody assay to enable direct analysis of the differential modulations of HIF prolyl and asparaginyl hydroxylation by chemical inhibitors in cells.
2) Evaluation of the specificities of HIF hydroxylase inhibitors in cells using the HIF hydroxy-residue specific antibody assay developed in (1).
3) Testing the hypothesis that the oncometabolite *R*-2HG inhibits the HIF hydroxylases using the hydroxy-residue specific antibody assay developed in (1).
4) Investigating the possibility of 2OG mediated HIF stabilisation in cells.
5) Development and evaluation of a 'chemical-genetic' approach that may enable selective inhibition of PHD isoforms.
6) Development and characterisation of a new class of dual-action HIF prolyl hydroxylase inhibitors that induce the binding of a second iron at the enzyme active site.
7) Evaluation of aspirin metabolites as HIF-α inhibitors in cells (a separate introduction of this work is given in **Chapter 7**).

Chapter 2: Differential Sensitivities of HIF Prolyl and Asparaginyl Hydroxylation to Chemical Inhibition in Cells

2.1 Background and Objectives

As described in **Chapter 1**, HIF-mediated transcriptional signalling plays a central role in directing cellular responses to hypoxia. Pharmacological activation of the hypoxic response by HIF hydroxylase inhibitors is a potential therapeutic target for a wide range of disorders including aneamia, stroke, and ischeamic heart disease.[72, 74, 88, 140] However, it is important to note that any pharmacological application involving upregulation of specific genes targeted by the HIF-system will have to take into account the regulation of hundreds of other genes.[20] The extent to which HIF prolyl and asparaginyl hydroxylation are differentially modulated by chemical agents is therefore important for the understanding of potential regulation of the HIF transcriptional response. The two prolyl hydroxylation sites in HIF-1α (Pro402 and Pro564) are regulated differentially at different oxygen tensions,[141] however to date there have been no reports of the differential regulation of HIF prolyl and asparaginyl hydroxylation sites by chemical intervention in cellular systems.

This chapter describes the development of methods which employ highly specific hydroxy-residue antibodies and immunoblotting (Western blotting) to monitor the regulation of hydroxylation states at all three human HIF-1α hydroxylation sites by different chemical reagents including iron chelators, transition metal ions, and small-molecule inhibitors. These cell-based assays were successfully used to identify several selective inhibitors of the HIF hydroxylases. The work in this chapter was carried out in collaboration with Dr Y-M Tian at Centre for Cellular and Molecular Physiology, University of Oxford. Part of the work in this chapter has been published in *Journal of Biological Chemistry* (2011).[142]

2.2 Results

2.2.1 Validation of HIF hydroxy-residue specific antibodies

Three antibody preparations were used in this work. An anti-HIF-1α hydroxy-Pro402 (Hyp402) antibody was developed in collaboration with Millipore Biosciences; an anti-HIF-1α hydroxy-Pro564 (Hyp564) (clone-D43B5) antibody was purchased from New England Biolabs and an anti-HIF-1α hydroxy-Asn803 (HyAsn803) antibody work was a gift from Dr S. H. Lee.[143]

The specificities of the HIF-1α (Hyp402 and Hyp564 and Asn803) antibodies were first evaluated using different hydroxylated HIF-α species. A series of HIF-α polypeptides, including wild-type or those which contained alanine or glycine mutations at each of the prolyl and asparaginyl hydroxylation sites were prepared as GAL4-HIF-α fusion proteins using an *in vitro* transcription/translation (IVTT) system (Promega).[13, 37, 142] Plasmids expressing GAL4/HIF-1α residues 28–826 (wild-type or Pro402, Pro564, and Asn803 mutants), or GAL4/wild-type HIF-2α residues 19–870 were constructed from the pcDNA3 vector using standard recombinant methods. In the IVTT system, the labelled HIF-α proteins were expressed in reticulocyte lysates, in the presence or absence of an iron chelator (desferrioxamine (DFO)) or an Fe(II) supplement ($FeCl_2$)[66] to inhibit or promote HIF prolyl and asparaginyl hydroxylation, respectively. The lysates were then assayed in immunoblotting studies using the hydroxy-specific antibodies.

In the presence of DFO (100 μM), the Hyp402, Hyp564 and HyAsn803 antibodies showed little or no binding, however, in the presence of Fe(II) (100 μM), a strong band corresponding to the target hydroxylated HIF-1α was apparent in the immunoblots, suggesting that each of these antibodies is highly specific for the hydroxylated forms of HIF-1α (**Fig. 2.1 A**; compare lanes 1 and 2). These antibodies also displayed high specificities for HIF-1α compared with HIF-2α (**Fig. 2.1 A**; compare lanes 2 and 3), demonstrating that they are both sequence and hydroxylation status specific.[142]

Substitution of the HIF-1α residue targeted for hydroxylation with an alanine or glycine residue at each of the HIF-1α hydroxylation sites (*i.e.* Pro402Ala, Pro564Gly, and Asn803Ala) ablated detection by the relevant antibody, showing that the hydroxy-residue antibodies were highly specific to each site; anti-Hyp402 did not react against Hyp564 and *vice versa* (**Fig. 2.1 A**; compare lanes 4, 5, and 6). A series of small-interfering RNA (siRNA) experiments were also carried out in human renal carcinoma VHL-defective cells (referred to here as RCC4 cells) to investigate the specificities of these antibodies for endogenous HIF-1α and HIF-2α. The results (**Fig. 2.1 B**) further supported the proposed high specificities of the HIF hydroxy-residue antibodies for HIF-1α and specific hydroxylation sites in cells.[142]

Mass spectrometry (MS) was further employed to verify the specificities of the antibodies for the hydroxylated forms of HIF-1α in cells. HIF-1α polypeptides were expressed in cells at a level that enabled direct analysis of hydroxylation by MS. Aliquots of the cell extracts were then analysed in parallel by hydroxy-residue specific immunoblotting. Cells were treated with either DMOG (a cell-permeable inhibitor of 2OG oxygenases used to inhibit HIF hydroxylation) or with MG132 (a proteasome inhibitor that causes accumulation of hydroxylated HIF-1α) under normoxic conditions.[144, 145] Neighbouring methionine residues (Met561 and Met568) were substituted with alanines to simplify the semi-quantitative analysis of Hyp564 by MS (*i.e.* to avoid redundancy in mass shifts due to adventitious methionine oxidation to the sulfoxide form).[13] The resulting MS spectra and immunoblots of a typical set of experiments are shown in **Fig. 2.2**. Comparison of immunoblotting results with MS analysis confirmed that each antibody demonstrated a high degree of specificity to each HIF hydroxylated epitope.[142]

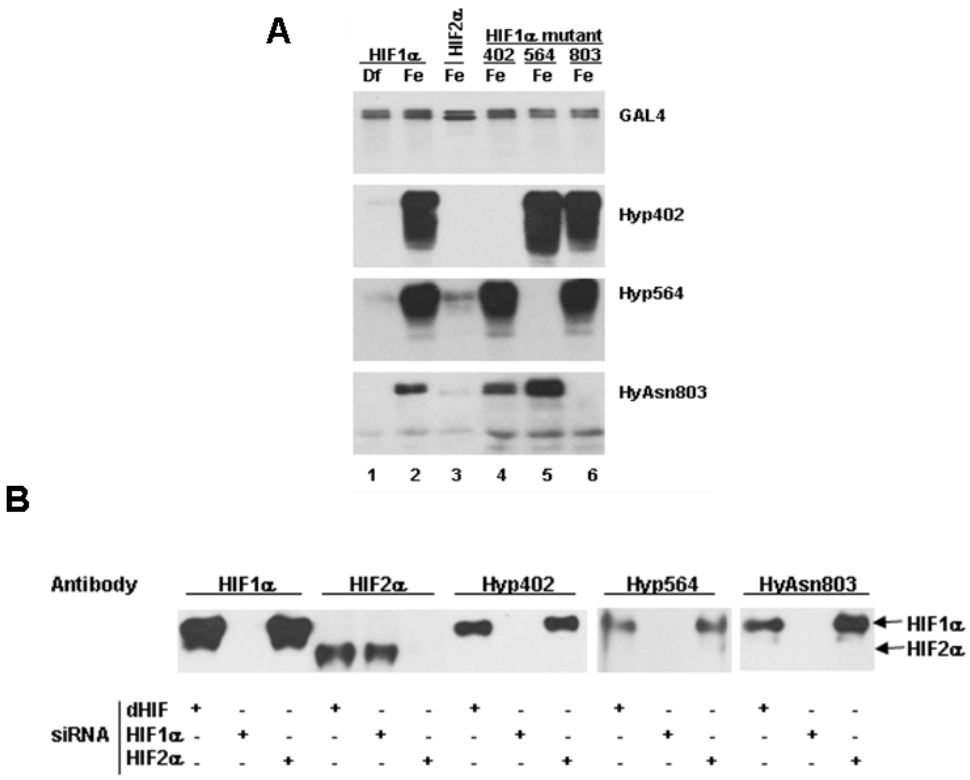


Figure 2.1 (A) Reactivities of hydroxy-residue specific anti-HIF1α antibodies. Immunoblots demonstrating the specificities of hydroxy-Pro402 (Hyp402), hydroxy-Pro564 (Hyp564) and hydroxy-Asn803 (HyAsn803) antibodies for these hydroxylated residues in human HIF-1α. HIF-1α (residues 28-826) (wild-type and mutant P402A, P564G or N803A) and HIF-2α (residues 19-870) polypeptides were produced as GAL4 fusions in IVTT reactions in the presence of DFO (Df) or ferrous chloride (Fe). Anti-GAL4 signals provide an internal control for normalisation. (**B)** The specificities of hydroxy-residue specific antibodies for endogenous HIF-1α in cells. RCC4 cells were treated with siRNAs against human HIF-1α or HIF-2α or a control (dHIF, *Drosophila* SIMA). Immunoblots were probed with the indicated antibodies. In the siRNA experiments, RCC4 cells were seeded at 40% confluence in antibiotic-free medium for 16 h prior to transfection with siRNAs directed against *Drosophila* SIMA (dHIF)[22], human HIF-1α or HIF-2α[146]. Oligofectamine was used for transfection of 20 nm siRNA duplex twice at 24 h intervals. Cells were harvested 24 h after the second transfection. (Data obtained from Dr Y-M Tian).[142]

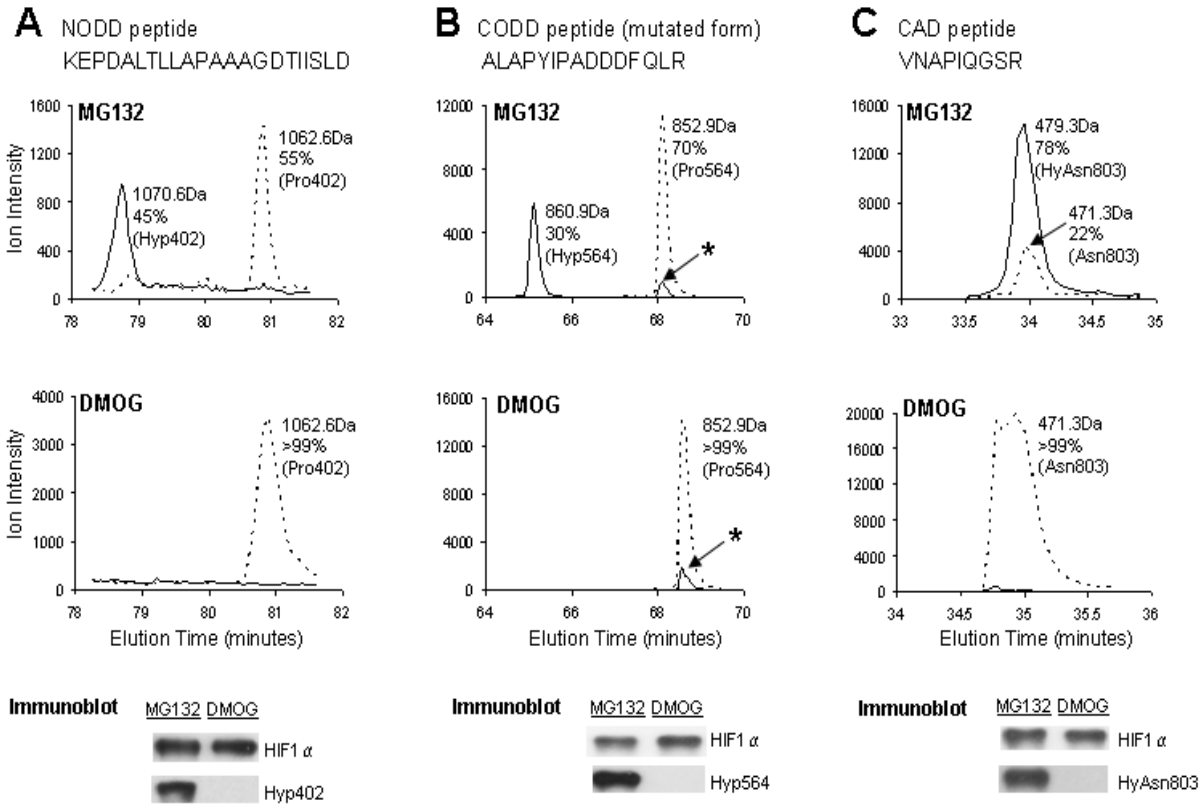


Figure 2.2 Validation of hydroxy-residue specific antibody performance by MS. (**A), (B), and (C)** show data for sites in HIF-1α NODD, CODD and CAD sequences, respectively. Cells expressing doxycycline-inducible PK-tagged wild-type or mutant (M561A+M568A) HIF-1α were induced with doxycycline (1μg/ml) in the presence of 1 mM DMOG for 24 h, or 25 μM MG132 for the last 4 h. For MS analysis, the PK IP (immunoprecipitation) was followed by in-gel digestion. The resulting peptides were analysed by MS. The $[M+2H]^{2+}$ precursor ions corresponding to the unhydroxylated and hydroxylated peptides are given together with chromatographic output (extracted ion counts) at these masses. Percentage hydroxylation was calculated from peak areas. * indicates other likely non HIF-1α derived ions with a similar mass to the hydroxylated CODD peptide. Aliquots of the IP samples were immunoblotted with the hydroxy-residue specific or pan-HIF-1α antibodies as indicated (data obtained from Dr Y-M Tian).[142]

2.2.2 Development of HIF hydroxy-residue specific antibody assays

By employing the HIF hydroxy-residue specific antibodies and RCC4 cells, it was possible to directly compare changes in prolyl *versus* asparaginyl hydroxylation by probing using immunoblotting. Prolyl hydroxylated HIF-1α is targeted by the pVHL-E3 ligase complex for proteasomal degradation,[12-14, 142] thus confounding comparison of prolyl and asparaginyl hydroxylation in VHL competent cells. In VHL deficient RCC4 cells, however, the proteasomal pathway is disabled and HIF-1α is stabilised,[12] therefore allowing for simultaneous measurement of prolyl and asparaginyl hydroxylation in HIF-1α.

Under normoxic conditions, both HIF prolyl and asparaginyl hydroxylation in RCC4 cells have been shown to proceed efficiently and are estimated to be close to completion at all three sites (*i.e.* Pro402, Pro564 and Asn803).[142] The half-life of HIF-1α in RCC4 cells has been estimated to be in the region of 60 min; therefore treatment of the cells with chemical reagents for more than 4 h is expected to be sufficient to allow HIF hydroxylation to achieve a new steady state.[142]

The general protocols of the newly developed HIF hydroxy-residue specific antibody assays are as follows: RCC4 cells were cultured in DMEM (Dulbecco's Modified Eagle Medium) supplemented with 10% fetal calf serum, 2 mM L-glutamine, 50 U/mL of penicillin and 50 μg/mL of streptomycin. Cells were seeded at 40-60% confluence 12-16 h prior to reagent treatments at 70-100% cell confluency in a 12-well plate. The chemical reagents were then exposed to the cells for 5 h, and cells were lysed using an urea/SDS buffer (6.7 M urea, 10 mM Tris-Cl (pH 6.8), 10% glycerol, and 1% SDS (sodium dodecyl sulphate)) supplemented with 1 mM dithiotreitol and 1 mM protease inhibitor. The extracts were resolved by SDS-polyacrylamide gel electrophoresis, electroblotted onto a polyvinylidene fluoride membrane (Millipore), and probed with the primary antibodies (1:1000 dilution) followed by horseradish peroxidase (HRP)-conjugated secondary antibodies (1:1000 dilution). SuperSignal Chemiluminescent Substrates (Pierce) were used to visualise immunoreactive species. In the immunoblotting analyses, HIF-1α signals provide an internal control for normalisation.[142]

2.2.3 Inhibition of HIF prolyl and asparaginyl hydroxylation by iron chelators, transition metal ions and small-molecule inhibitors

Several supposedly non-specific inhibitors of the HIF hydroxylases, including the iron chelators desferrioxamine (DFO) and 2,2'-dipyridine (DIP), cobaltous ions (Co(II)) and dimethyloxalylglycine (DMOG) (the cell-permeable prodrug form of *N*-oxalylgylcine (NOG), a non-reactive 2OG analogue) have been commonly employed as "hypoxia mimetics" in the studies of HIF system.[3, 66, 67] On the other hand, the transition metal ions Mn(II), Ni(II), and Zn(II) and the small-molecule inhibitors, 4-oxo-1,4-dihydro-1,10-phenanthroline-3-carboxylic acid (DPCA/FG0041), 3,4-dihydroxybenzoic acid (DHBA), pyridine-2,4-dicarboxylic acid (2,4-PDCA) and pyridine-2,5-dicarboxylic acids (2,5-PDCA) (**Fig. 2.3**) have also been commonly used as HIF hydroxylase inhibitors.[24, 66, 68, 147]

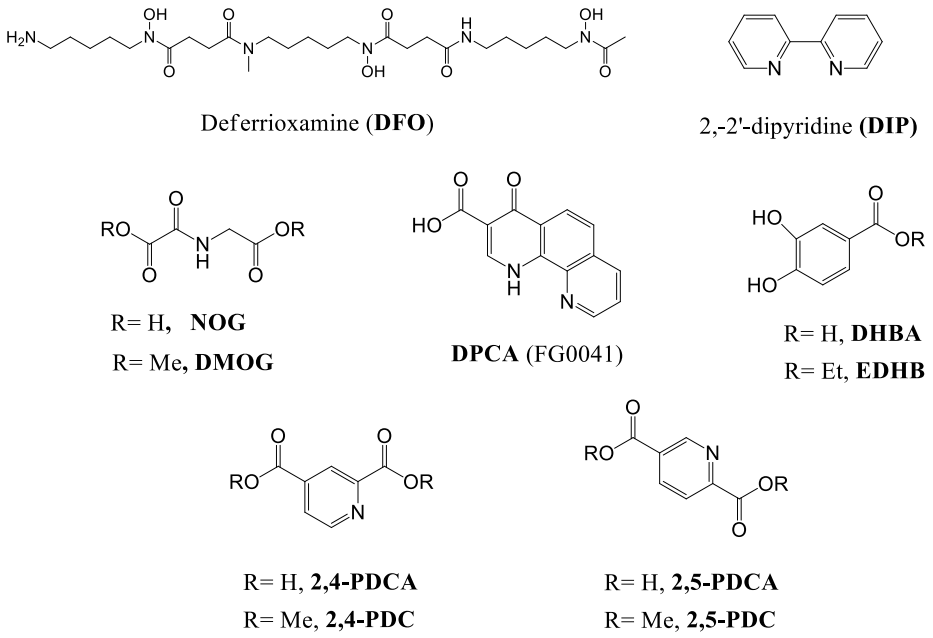
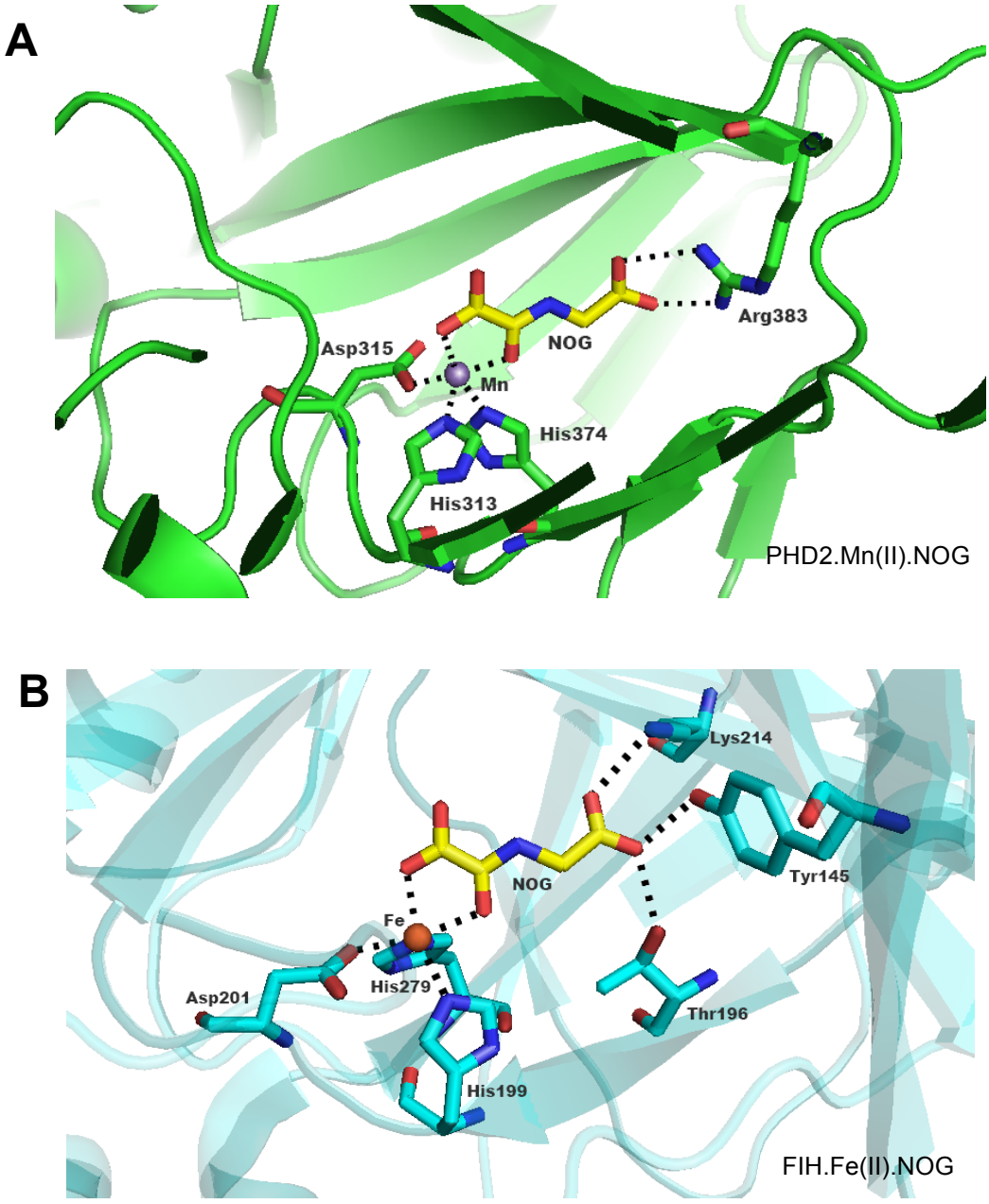
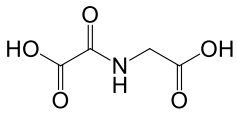


Figure 2.3: Iron chelators and small-molecule inhibitors.

The iron chelators such as DFO were expected to inhibit HIF hydroxylase activity by removing the iron away from the active site, whereas metal ions were expected to suppress enzyme activity by competition with the cellular iron pool.[2, 66, 148] Small-molecule inhibitors largely inhibit by competing with the co-substrate 2OG for binding at the active site.[20] NOG, DPCA, DHBA, 2,4-PDC, and 2,5-PDC were initially developed as collagen prolyl-4-hydroxylase (C-P4H) (see **Section 1.4.1**) inhibitors but were later found to inhibit a wide range of other human 2OG oxygenases including the PHDs, FIH and histone demethylases (e.g. JMJD2A and JMJD2E), likely all via 2OG competition.[18, 20, 24, 26, 139, 147, 149] Spectroscopic and crystallographic studies show that the generic non-reactive 2OG analogue inhibitor NOG, binds in the 2OG oxygenase active site and chelates the active site metal in a bidentate manner.[20, 32, 34, 150] Views from the crystal structures of PHD2 (PDB ID 3HQR) and FIH (PDB ID 1H2K) in complex with NOG are shown as representative examples in **Fig. 2.4.**

The reported inhibition data (half-maximal inhibitory concentration (IC_{50}) or inhibition constant (K_i) values) for the metal ions Co(II), Mn(II), Ni(II), and Zn(II) and small-molecule inhibitors NOG, DPCA, DHB, 2,4-PDCA, and 2,5-PDCA against purified HIF hydroxyxlases (PHDs 1-3 and FIH) are summarised in **Table 2.1** and **Table 2.2** (see below for discussion). Most C-P4H inhibitors that were previously reported to be active in cells were methyl/ethyl ester prodrug forms of the *in vitro* inhibitors.[149, 151, 152] For instance, DMOG, has been extensively used in cell culture and animal models to inhibit HIF hydroxylases.[84, 153-155] For this reason, the ester forms of the above mentioned inhibitors (*i.e.* DMOG, EDHB, 2,4-PDC and 2,5-PDC, **Fig. 2.3**) were used in the subsequent cell-based experiments.





N-Oxalylglycine (**NOG**)

Figure 2.4: Views derived from crystal structures of PHD2 (green, **A**) (PDB ID 3HQR) and FIH (cyan, **B**) (PDB ID 1H2K) in the presence of NOG and the active site metal. Only important active site residues are shown. Dashed lines represent coordination or hydrogen bonds.

	DFO	Co(II)	Mn(II)	Ni(II)	Zn(II)
PHDs 1-3	(PHD3) 10 μM[66]	9-100 μM [66]	>1000 μM[66]	120-1000 μM[66]	4-130 μM[66]
PHD2	~50% inhibition at 10-1000 μM[66]	48 μM[68]	21 μM[68]	185 μM[68]	9 μM[68]
FIH	8 μM[66]	(1 μM)[66]	(10 μM)[66]	(4 μM)[66]	(0.5 μM)[66]
C-P4H	-	14 μM[66]	>500 μM[66]	37 μM[66]	(0.6 μM)[66]

Table 2.1: Reported IC_{50} or K_i (in parentheses) values for the iron chelator desferrioxamine (DFO) and divalent transition metal ions Co(II), Mn(II), Ni(II), and Zn(II) against PHDs and FIH.

	NOG	DPCA	DHBA	2,4-PDCA	2,5-PDCA
K_i (PHDs 1-3)	8-50 μM[24]	10-30 μM[26]	>300 μM[24]	7-40 μM[24]	>300 μM[24]
K_i (FIH)	2 μM[24]	60 μM[147]	10 μM[24]	30 μM[24]	50 μM[24]
K_i (C-P4H)	1.9 μM[156]	2 μM[18]	5 μM[156]	2 μM[156]	0.8 μM[156]

Table 2.2: Reported K_i values for the small-molecule inhibitors NOG, DPCA, DHB, 2,4-PDCA, and 2,5-PDCA against PHDs and FIH. NOG, *N*-oxalylgylcine; DPCA, 4-oxo-1,4-dihydro-1,10-phenanthroline-3-carboxylic acid , DHBA, 3,4-dihydroxybenzoic acid; 2,4-PDCA, pyridine-2,4-dicarboxylic acid; 2,5-PDCA, pyridine-2,5-dicarboxylic acid.

Once the antibody detection method had been validated, the specificities of DMOG, DFO, DIP, and Co(II) for the different hydroxylation sites of HIF-1α were first tested in the HIF hydroxy-specific antibody assays in RCC4 cells. Surprisingly, results from the HIF hydroxy-residue specific antibody assays reveal considerable specificities for DMOG, iron chelators and Co(II) in their responses to HIF prolyl and asparaginyl hydroxylation in cells. DMOG was demonstrated to suppress asparaginyl hydroxylation more than prolyl hydroxylation (**Fig. 2.5 A**, lanes 2 and 3), whereas the opposite was true for Co(II), which inhibited prolyl hydroxylation but not asparaginyl hydroxylation (**Fig. 2.5 B**, lanes 3-5). However, iron chelators DFO and DIP (at 100 μM) were observed to suppress both hydroxylation, even though prolyl hydroxylation was more susceptible to inhibition by DFO and DIP than asparaginyl hydroxylation (**Fig. 2.5 A** lane 5 and **Fig. 2.5 B** lane 6) in RCC4 cells. These findings thus suggest these chemical agents might be expected to have

substantially different effects on the asparaginyl hydroxylation states of HIF-1α protein that is stabilised in VHL-competent cells.

To test the above proposal, RCC4 re-expressing functional VHL (RCC4/VHL) cells were then treated with the HIF hydroxylase inhibitors. The level of asparaginyl hydroxylation in the inhibitor-induced HIF was then compared to the total HIF level (**Fig. 2. 5 C** and **E)**. Surprisingly, all the tested transition metals (at 300 μM) stabilised HIF-1α protein (with the potencies Co(II) > Ni(II) ≈ Zn(II) > Mn(II)) that remained strongly hydroxylated on Asn803 (>70% hydroxylation) in VHL-competent cells (**Fig. 2.5 C**). These observations were further confirmed with the assays using RCC4 cells (**Fig. 2.5 D**) which showed that the transition metals substantially suppressed Pro564 hydroxylation at high dosages; however, Asn803 hydroxylation was mainly unaffected.

In contrast with the results with transition metals, the iron chelators DFO and DIP were shown to have different concentration-dependent effects on asparaginyl hydroxylation; with DIP but not DFO suppressing asparaginyl hydroxylation at a high dosage (*i.e.* 100 μM) (**Fig. 2.5 E**) in the VHL-competent cells. Similarly, exposure of RCC4/VHL cells to small-molecule inhibitors (DMOG, DPCA, and EDHB) also demonstrated strikingly different effects on the HIF-1α hydroxylation sites. DMOG and DPCA restricted asparaginyl hydroxylation strongly, whereas EDHB had no apparent effect on asparaginyl hydroxylation state even at high concentrations. 2,4-PDC and 2,5-PDC only weakly upregulated HIF in RCC4/VHL cells (**Fig. 2.5 F)** and showed no apparent inhibition of both prolyl and asparaginyl hydroxylation in RCC4 cells (**Fig. 2.5 G**).

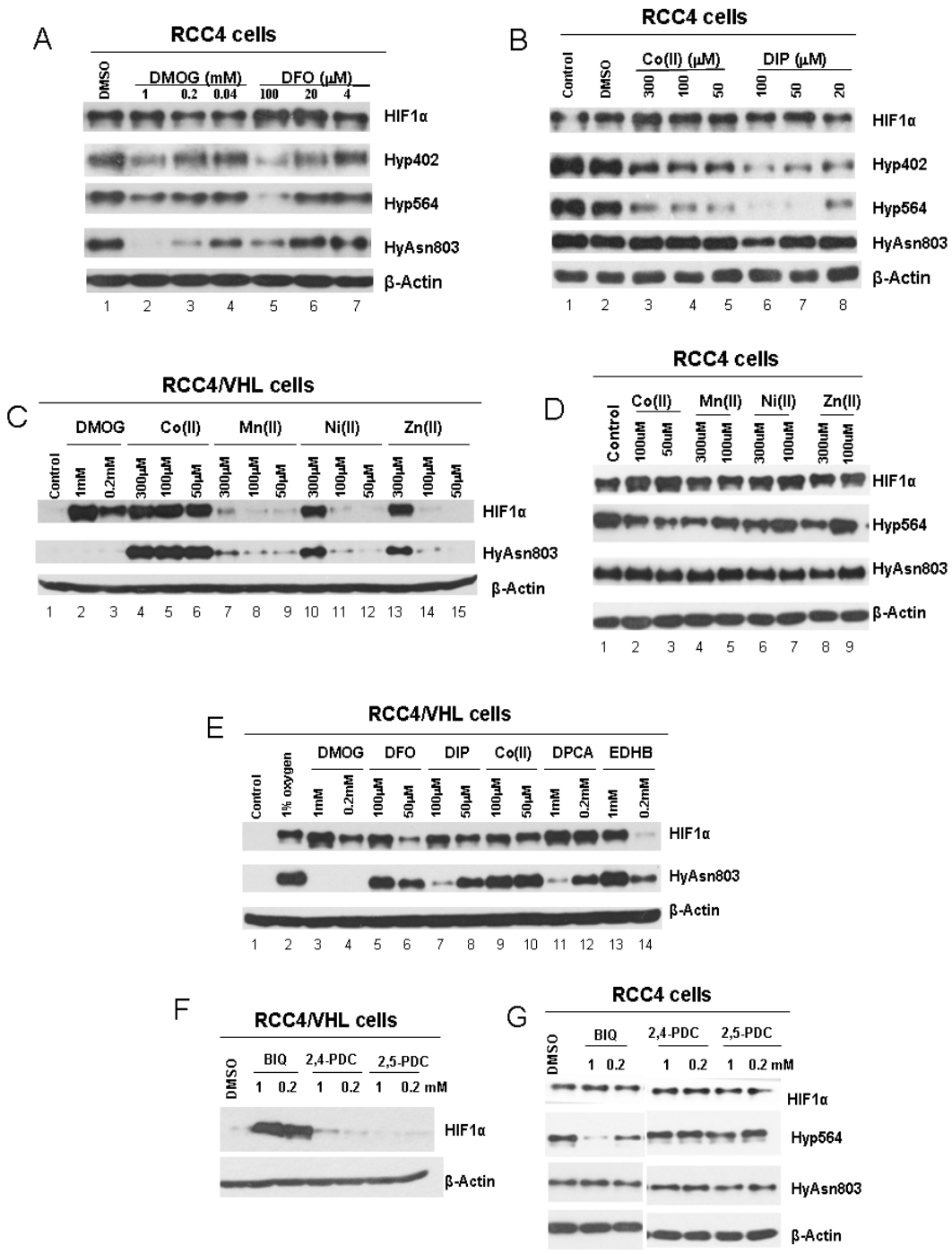


Figure 2.5: Differential inhibition of HIF prolyl and asparaginyl hydroxylation by HIF hydroxylase inhibitors. (**A, B, D**, **G**) RCC4 cells. (**C, E**, **F)** RCC4/VHL cells. The cells were treated with different transition metal ions (Co(II), Mn(II), Ni(II), or Zn(II)), iron chelators (desferrioxamine (DFO), and 2,2'-dipyridine (DIP) and small-molecule inhibitors (DMOG, DPCA, and EDHB, 2,4-PDC and 2,5-PDC) (see **Fig. 2.3** for structures) at indicated concentrations for 5 h. Immunoblots probed with indicated antibodies. Controls were treated with 0-2% DMSO in accordance with the diluent used for the test substance. HIF-1α signals provide an internal control for normalization. DMOG was prepared as 100 mM stock solution in PBS (phosphate buffered saline); other compounds were prepared as 100 mM stock solutions in DMSO and added to cells at 1% DMSO.

These findings on the differential sensitivities of prolyl and asparaginyl hydroxylation to the divalent metals ions and iron chelators in cells are very different from their effects in the *in vitro* studies (**Table 2.1**).[66, 68] PHDs are less susceptible to metal ion inhibition than FIH *in vitro* (**Table 2.1**), at least under the tested conditions. However, the opposite was observed in cells (**Fig. 2.5 C-D**). Purified PHDs 1-3 were reported to bind Fe(II) very tightly *in vitro* with a binding constant of << 1 μM (for PHD2) and K_m values for Fe(II) in the range 0.03-0.1 μM for PHDs 1-3. They are also much less sensitive to inhibition by DFO and metal ions compared to FIH (**Table 2.1**) (K_m value for Fe(II) for FIH is 0.5 μM).[24, 33, 66, 157] However, in this current work, the reverse was observed; iron chelators suppressed prolyl hydroxylation more than asparaginyl hydroxylation in both the RCC4 and RCC4/VHL cells (**Fig. 2.5 A-C**).

The reasons for these contrasting observations on the effects of transition metals and iron chelators on HIF hydroxylation between *in vitro* and cell-based results are not clear. This may reflect the complexity of the *in vivo* system, however the findings do strongly suggest that other mechanism(s) of inhibition might be involved other than the facile exchange of active site iron of the HIF hydroxylases with a chelatable iron pool. The lack of inhibition of asparaginyl hydroxylation by transition metals under the standard assay conditions may be due to tight binding of catalytic bound iron in FIH in cells. Furthermore, Fe(II) binding in HIF hydroxylases is reversible[30] (the enzymatic activity of HIF hydroxylases is dependent on cellular Fe(II) levels), thus how iron is delivered and maintained at the PHD and FIH enzyme active sites might affect its susceptibility to iron chelation or inhibition by metal ions.

It has been reported that Co(II) prevents degradation of HIF-α, at least in part, by inhibiting the interaction between pVHL and hydroxylated HIF-α.[158] There is also evidence that Co(II) suppresses prolyl hydroxylation of HIF-2α by binding to a conserved region in the oxygen-dependent degradation (ODD) domain/VHL-binding domain of HIF-2α.[158] Furthermore, exposure of cells to Co(II) and Ni(II) causes depletion in intracellular ascorbate level.[159] As ascorbate is an important co-factor (at least *in vitro*)

for PHD, but not FIH activity, this could offer a possible reason as to why asparaginyl hydroxylation is less susceptible to inhibition by metal ions.

Some, but not all of the small-molecule inhibitors tested showed similar inhibitory potencies in cells relative to *in vitro* studies. Consistent with the reported *in vitro* results, which showed partial selectivity over asparaginyl hydroxylation (**Table 2.2**), DMOG at 1 mM significantly inhibited asparaginyl hydroxylation and moderately suppressed HIF prolyl hydroxylation (Pro402 and Pro564) in RCC4 cells (**Fig 2.5 A**). Furthermore, HIF-1α stabilised by DMOG in VHL-competent cells was also not hydroxylated at Asn803 (**Fig. 2.5 E**). DPCA, which was found to inhibit PHD and FIH *in vitro* (**Table 2.2**),[26, 147] showed a similar inhibitory pattern in cells (**Fig. 2.5 E**).

EDHB was found to stabilise HIF at high dosage, but did not inhibit HIF asparaginyl hydroxylation (**Fig. 2.5 E**) in VHL-competent cells. These observations contrast with the *in vitro* findings for the corresponding acid, DHBA (K_i values for FIH = 10 μM; PHDs 1-3 = > 300 μM) (**Table 2.2**).[66] However, 2,4-PDC which has recently been shown to inhibit histone demethylase activity in cells (JMJD2E, IC_{50} 1.4 μM),[139] had no apparent effect on HIF prolyl and asparaginyl hydroxylation (**Fig. 2.5 F** and **G**); even though its corresponding acid 2,4-PDCA is a potent inhibitor for PHD and FIH *in vitro* (**Table 2.2**). The reasons for these differences are unclear.

Given that the above agents (*i.e.* iron chelators, divalent metal ions, DMOG, DPCA, and EDHB) mimic hypoxia, and also that they have been shown to inhibit a range of other 2OG oxygenases, it may be that these inhibitors are unsuitable for clinical applications, because the complexity of non-HIF off-target effects would be a major concern. Extensive efforts in medicinal chemistry have been directed towards the development of specific HIF hydroxylase inhibitors (particularly for the PHDs) by leading pharmaceutical companies and academic research groups.[74, 160, 161] However, very little selectivity data has been reported for these compounds.

2.2.4 Selective inhibition of HIF prolyl and asparaginyl hydroxylation

Having observed diversified inhibitory potencies of the aforementioned agents, studies then focused upon investigating the cellular specificities of a number of other HIF hydroxylase inhibitors. Previous *in vitro* studies on recombinant PHD2 and FIH have shown that it is feasible to selectively inhibit the HIF hydroxylases by varying the amino acid side chain of *N*-oxalyl amino acid derivatives, with L-amino acids preferentially inhibiting PHD2, and D-amino acids preferentially inhibiting FIH.[161]

Several bicyclic isoquinoline (BIQ) and *N*-oxalyl amino acid derivatives (**Fig. 2.6** and **2.7,** respectively) were therefore synthesised and tested in the antibody assays to enable the studies of the specificities of these inhibitors against PHDs and FIH in cells (the chemical synthesis and characterisation of the BIQ derivatives (**1-7**) are reported in **Chapter 5**. *N*-Oxalylglycine (NOG) derivatives (**8-16**) were synthesized by M. Tilliet).[161]

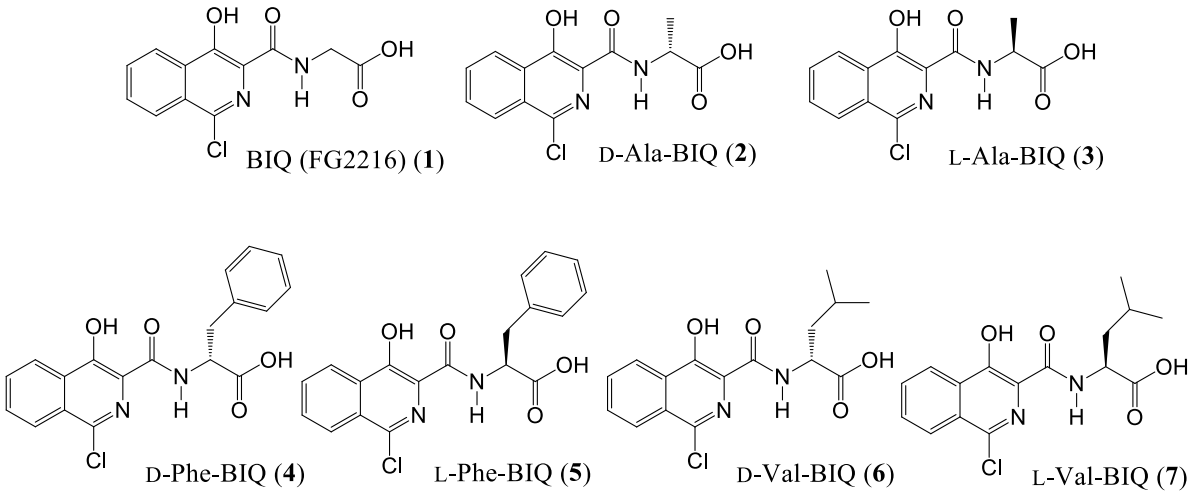


Figure 2.6 Bicyclic isoquinoline (BIQ) derivatives tested as potential HIF hydroxylase inhibitors.

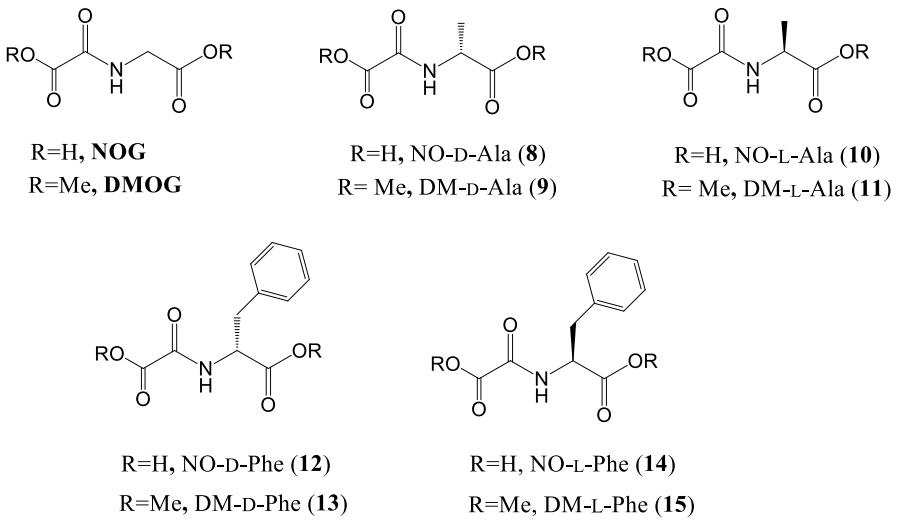


Figure 2.7: *N*-Oxalyl amino acid derivatives tested as potential HIF hydroxylase inhibitors. The dimethyl esters were tested in the cell-based experiments.

BIQ (**1**) has been reported to be FibroGen's first clinical candidate, FG-2216, which is currently under Phase II clinical trials for the treatment of anaemia.[74, 77] FG-2216 is shown to bind similarly to its analogue 8-iodo-bicyclic isoquinoline in the active site of PHD2.[31, 162] **Fig. 2.8** shows two different views of the PHD2 crystal structure in complex with BIQ (**1**) superimposed with the 8-iodo bicylic inhibitor complex.[31, 162] The crystal structure reveals that the nitrogen atom in the aromatic ring and the amide carbonyl oxygen of BIQ (**1**) chelate the active site iron in a bidentate manner. The active site metal coordinates in an octahedral fashion with the inhibitor, His313, Asp315, His374, and a water molecule making up the ligands. The carboxylic acid in the glycinamide group occupies the 2OG binding pocket, and is positioned to form a salt bridge with Arg383, and the 3-hydroxyl group in the isoquinoline moiety hydrogen bonds with the nearby Tyr303 residue in the PHD2 active site (**Fig. 2.8**).[31, 162] In addition to competition with 2OG, the bicyclic isoquinoline inhibitors block the conformational change in PHD2 that is required for HIF-substrate binding,[34] therefore making them 'dual-action' PHD inhibitors (a crystal structure of PHD2 in complex with L-Ala-BIQ (**3**) was later solved and will be described in **Chapter 5**).

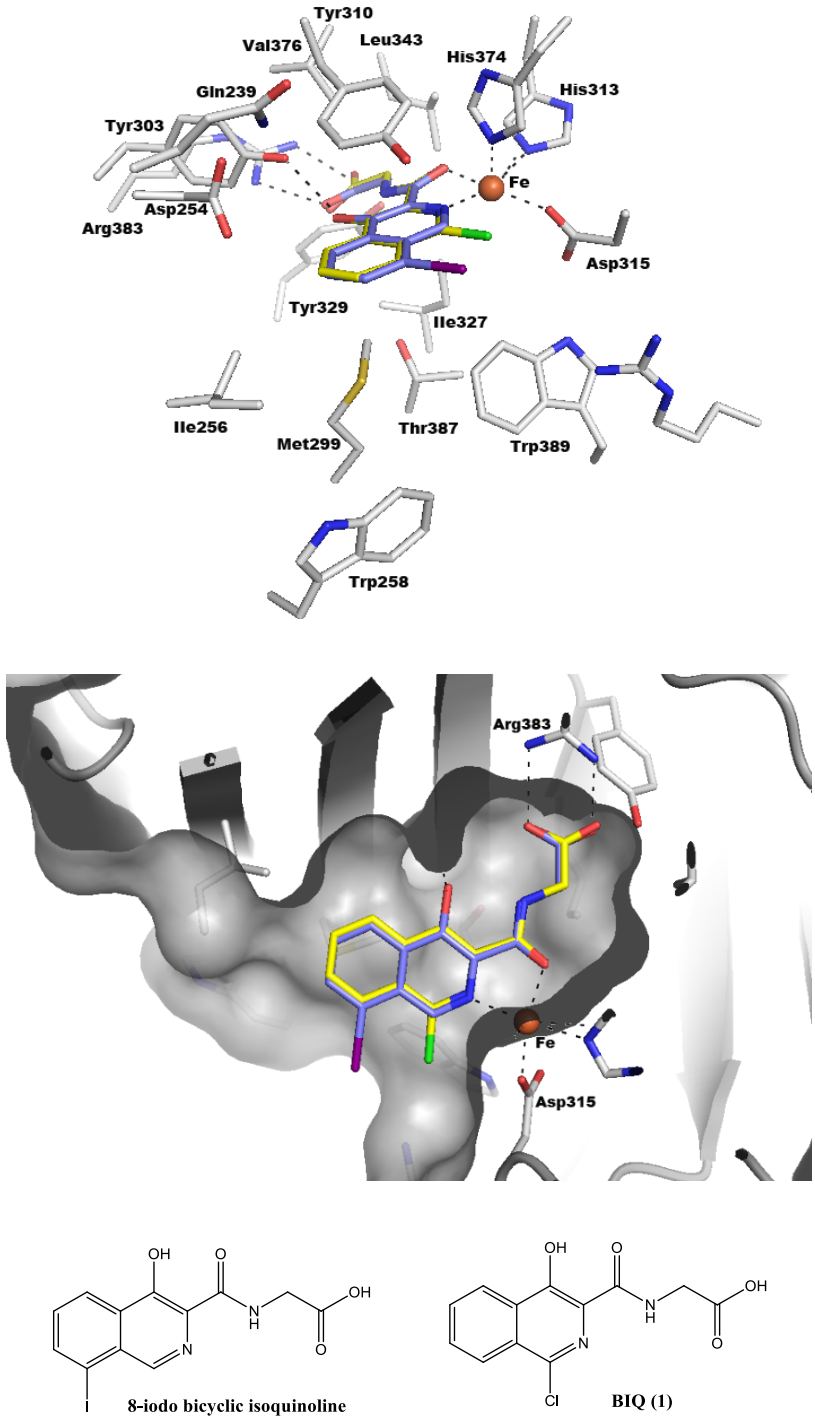


Figure 2.8: Presentations of two different views of crystal structures of PHD2 in complex with 8-iodo bicyclic inhibitor (blue) superimposed with BIQ (yellow). BIQ chelates the active site iron and binds in the 2OG binding site by forming a salt bridge with Arg383, while its 3-hydroxyl group hydrogen bond with Tyr303. The entrance of the PHD2 active site is relatively narrow and 'slot-shaped'. (PDB ID 2G19) (PDB ID 2HBT).[31, 162]

The IC_{50} values of the BIQ and NOG derivatives (**1-15**, **Fig. 2.6** and **Fig. 2.7**) were first obtained employing an *in vitro* assay for PHD2 activity using an amplified luminescent proximity homogeneous assay (ALPHA, hereafter referred to as the AlphaScreen PHD2 hydroxylation assay). The AlphaSreen PHD2 hydroxylation assay uses a monoclonal HIF-1α hydroxy-Pro564 specific antibody (Hyp564) to detect the hydroxylation of a biotinylated CODD peptide (HIF-1α residues 556-574), catalysed by recombinant PHD2. Using an AlpaScreen immunoglobulin G (IgG) detection kit (PerkinElmer) containing streptavidin-conjugated donor beads and protein A-conjugated acceptor beads,[163] the interaction of the Hyp564 antibody with the hydroxylated CODD peptide can be detected (**Fig. 2.9**). Standard reaction mixtures consisted of the compound (in < 2% DMSO final concentration), 1 nM of PHD2, 20 μM of Fe(II), 200 μM of ascorbate, 60 nM of biotinylated CODD peptide and 2 μM of 2OG. The IC_{50} values for the BIQ and NOG derivatives (free acids) against PHD2 obtained from the AlphaScreen hydroxylation assay are shown in **Table 2.3** and **Table 2.4** (experiments were carried out together with Andrew M. C. Chan). Reported inhibitory data are shown for comparison.

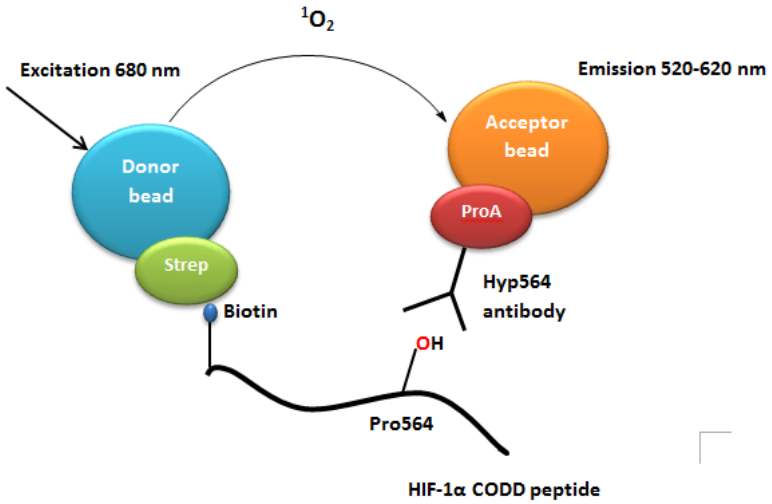


Figure 2.9: AlphaScreen PHD2 hydroxylation assay setup. In AlphaScreen assays, laser excitation (680 nm) of a photosensitiser within the "donor bead" results in the conversion of ambient oxygen to an excited O_2 singlet oxygen ($^1O_2$). If an "acceptor bead" (containing thioxene derivative) is within ~200 nm, energy transfer occurs, generating a luminescent signal at 520-620 nm. In the absence of an acceptor bead, singlet oxygen returns to its ground state and no signal is detected.[163, 164] Both donor and acceptor beads can be conjugated to biomolecules. In the PHD2 hydroxylation assay, the streptavidin-coated donor and protein-A-coated acceptor pair was used to detect the hydroxylation of the biotinylated CODD peptide by employing the HIF-1α hydroxy-Pro564 (Hyp564) specific antibody.

Compounds	BIQ (**1**)	**2**	**3**	**4**	**5**	**6**	**7**
IC_{50} (PHD2)	1.4 μM (73 nM)[165]	> 300 μM (230 μM)[165]	1.1 μM (0.512 μM)[165]	> 300 μM	> 300 μM	> 300 μM	> 300 μM

Table 2.3: IC_{50} values for the bicyclic isoquinoline derivatives (**1-7**, **Fig. 2.6**) against purified PHD2 obtained from an AlphaScreen PHD2 hydroxylation assay. Reported IC_{50} values for BIQ **1-3** (in parentheses)[165] obtained from a time resolved fluorescence resonance energy transfer (FRET) turnover assay are shown for comparison. The variations in absolute IC_{50} values may reflect differences in assay conditions used in the assays.

	NOG (DMOG)	**8 (9)**	**10 (11)**	**12 (13)**	**14 (15)**
PHD2	4.6 μM (K_i 8 μM)[26]	>300 μM (Does not inhibit)[161]	9.5 μM (Inhibits)[161]	> 300 μM (Does not inhibit)[161]	> 300 μM (Does not inhibit)[161]
FIH	(K_i 2 μM) [24]	(Inhibits) [161]	(Inhibits) [161]	(K_i 83 μM)[161]	(Does not inhibit)[161]

Table 2.4: IC_{50} values for the NOG derivatives (**1-7**, **Fig. 2.6**) against purified PHD2 obtained from an AlphaScreen PHD2 hydroxylation assay. Reported inhibitor data or K_i values (in parentheses) for NOG derivatives (tested at 1 mM)[161] against purified FIH and PHD2 are shown for comparison. Compound numbers in parentheses indicate the corresponding dimethyl esters tested in the cell-based experiments.

The HIF hydroxy-residue specific antibody assays were then employed to investigate the specificities of the BIQ and NOG derivatives on HIF hydroxylase inhibition in RCC4 cells. Similarly to the *in vitro* data (**Table 2.3**), the cell-based results show that BIQ (**1**) and L-Ala-BIQ (**3**) (IC_{50} values of 1.4 , and 1.1 μM, respectively) strongly suppress HIF prolyl hydroxylation at both Pro402, and Pro564 sites in RCC4 cells. Furthermore, their inhibitory activities are shown to be highly specific for prolyl over asparaginyl hydroxylation (**Fig. 2.10 A**). These observations were further confirmed in the assays using RCC4/VHL cells. In contrast to DMOG-induced HIF-1α, in which asparaginyl hydroxylation was almost completely inhibited, both the BIQ (**1**) and L-Ala-BIQ (**3**)-induced HIF-1α were strongly hydroxylated at Asn803 (**Fig. 2.10 B**).

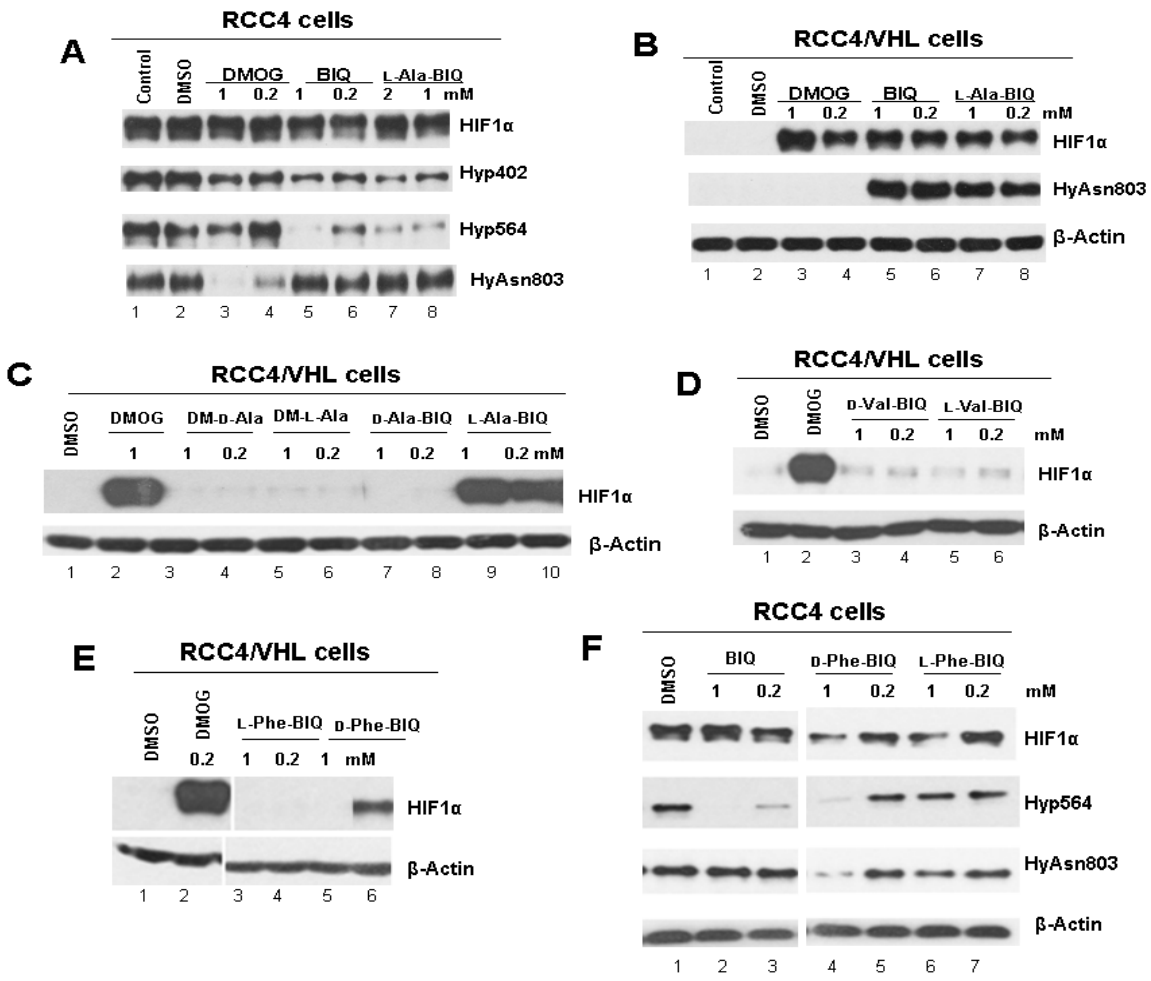


Figure 2.10: BIQ (**1**) and L-Ala-BIQ (**3**) demonstrate selective inhibition against HIF prolyl hydroxylation. (**A**) and (**F**), RCC4 cells. (**B**-**E**) RCC4/VHL cells. Cells were treated with the bicyclic isoquinoline (BIQ) or the *N*-oxalyl amino acid derivatives at the indicated concentrations for 5 h. DMOG was prepared as 100 mM stock in PBS solution; other compounds were prepared as100 mM stock solutions in DMSO and added to cells at 0% or 1% DMSO. Controls were treated with 0-1% DMSO in accordance with the diluent used for the test substance. Unless otherwise stated, DMOG was used as a positive control at 1 mM. 'Control' means untreated cell-sample.

As expected, D-Ala-BIQ (**2**), D-Val-BIQ (**6**), and L-Val-BIQ (**7**) did not stabilise HIF-1α (**Fig. 2.10 C-D**), in line with the *in vitro* results which indicate that they are weak PHD inhibitors (**Table 2.3**). Surprisingly, despite its D-amino acid side chain and bulky aromatic ring (which was expected to hinder its binding to PHD active site), D-Phe-BIQ (**4**) (IC_{50} for PHD2 >300 μM), was observed to weakly upregulate HIF-1α in RCC4/VHL cells at high dosage (**Fig. 2.10 E**). D-Phe-BIQ (**4**) was also shown to inhibit HIF prolyl and asparaginyl hydroxylation to a certain extent in RCC4 cells (**Fig. 2.10 F**). However,

some morphological changes were observed when cells were treated with **4** at high concentrations which indicate compound toxicity in cells. It seems likely that the binding mode of D-Phe-BIQ (**4**) to PHD2 is different from its analogues including BIQ (**1**). Consistent with the *in vitro* data, DM-D-Ala (**9**) did not upregulate HIF-1α. However, unlike L-Ala-BIQ (**3**), its *N*-oxalyl counterpart, DM-L-Ala (**11**) did not stabilise HIF-1α in RCC4/VHL cells (**Fig. 2.10 C**), contrast with the *in vitro* observations which show that NO-L-Ala (**10**) (its free acid) (IC_{50} 9.5 μM) is a potent PHD inhibitor.[161] It is possible that compound **11** might be less cell-permeable compare to DMOG.

Previous efforts to develop specific FIH inhibitors have shown that the 2OG competitive inhibitor *N*-oxalyl-D-phenylalanine (NO-D-Phe, **12**) (K_i value of 83 μM for FIH), together with other *N*-oxalyl-D-amino acid derivatives (e.g. alanine (**8**), leucine and valine) selectively inhibits FIH over PHD2.[161] A crystal structure of FIH in complex with NO-D-Phe (**12**) reveals that the phenyl ring of the **12** in the FIH active site causes a slight distortion in the octahedral-coordination of the ligands to iron (apart from the inhibitor, the other ligands comprise two histidines, an aspartic acid and a water molecule) (**Fig. 2.11**) and is likely to hinder oxygen and HIF-substrate binding.[161]

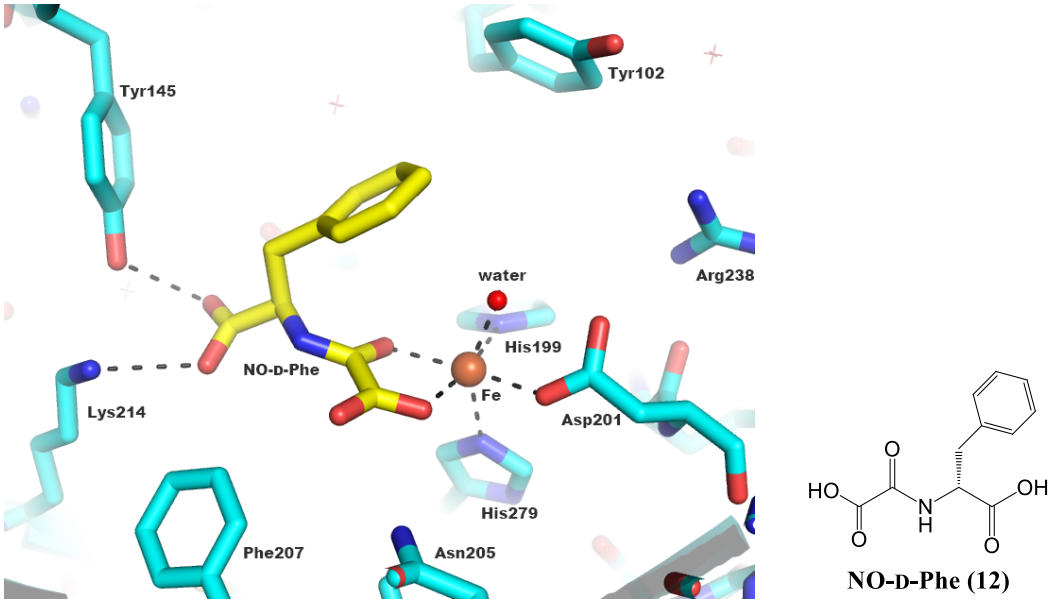


Figure 2.11: View from a crystal structure of NO-D-Phe (**12**) in complex with FIH and Fe(II) (only selected amino acid residues are shown (PDB ID 1YCI). The phenyl ring of NO-**D**-Phe (**12**) causes a slight distortion in the octahedral-coordination of the ligands to the active site Fe(II).

Whether NO-D-Phe (**12**) can selectively inhibit HIF-asparaginyl hydroxylation in cells was next examined. For comparison, NO-D-Phe (**12**) and its L-enantiomer (**14**), together with their potential cell-permeable esterified derivatives (DM-D-Phe (**13**) and DM-L-Phe (**15**), (see **Fig. 2.7** for structures)) were tested in the cell-based antibody assays. RCC4 cells were treated with both the esters and free acids; the results are shown in **Fig. 2.12**. The NO-D-Phe (**12**) and DM-D-Phe (**13**) were shown to specifically suppress HIF asparaginyl hydroxylation over prolyl hydroxylation in RCC4 cells at high dosage (**Fig. 2.12 A**). However, the L-enantiomers (**14**, and **15**) did not. The free acid **12** is a less potent inhibitor, suggesting that the dimethyl ester may be more cell-penetrating.

When DM-D-Phe (**13**) was tested in RCC4/VHL cells, it did not upregulate HIF, thus further confirming that it does not inhibit the PHDs (**Fig. 2.12 B**). In addition, DM-D-Phe (**13**) was also found to substantially inhibit HIF asparaginyl hydroxylation in both hypoxic- and Co(II)-stabilised HIF-1α (**Fig. 2.12 C** and **D**), although to a lesser extent in the latter. DM-D-Phe (**13**) seems to be, so far, the first cell-permeable selective FIH inhibitor that has been reported. Although there has been little selectivity data available for other 2OG oxygenases, initial *in vitro* screening showed that NO-D-Phe (**12**) is not a potent inhibitor for collagen prolyl-4-hydroxylase (C-PH4) and histone lysine demethylase (JMJD2E).[20, 166]

Furthermore, in addition to HIF, FIH also catalyses asparaginyl hydroxylation in a wide range of ankyrin repeat domain (ARD) proteins that play roles in the inflammatory response, cell-cyle regulation, and development. ARD proteins are expressed in relatively high abundance across a wide range of cells; some of these, such as the Notch-1 receptor, were found to compete with HIF-1α *in vitro*. However, the significance of ARD hydroxylation *in vivo* remains unclear.[4, 167-171] Therefore, the specific cell-permeable inhibitor DM-D-Phe (**13**) could be useful for further functional assignment work for FIH.

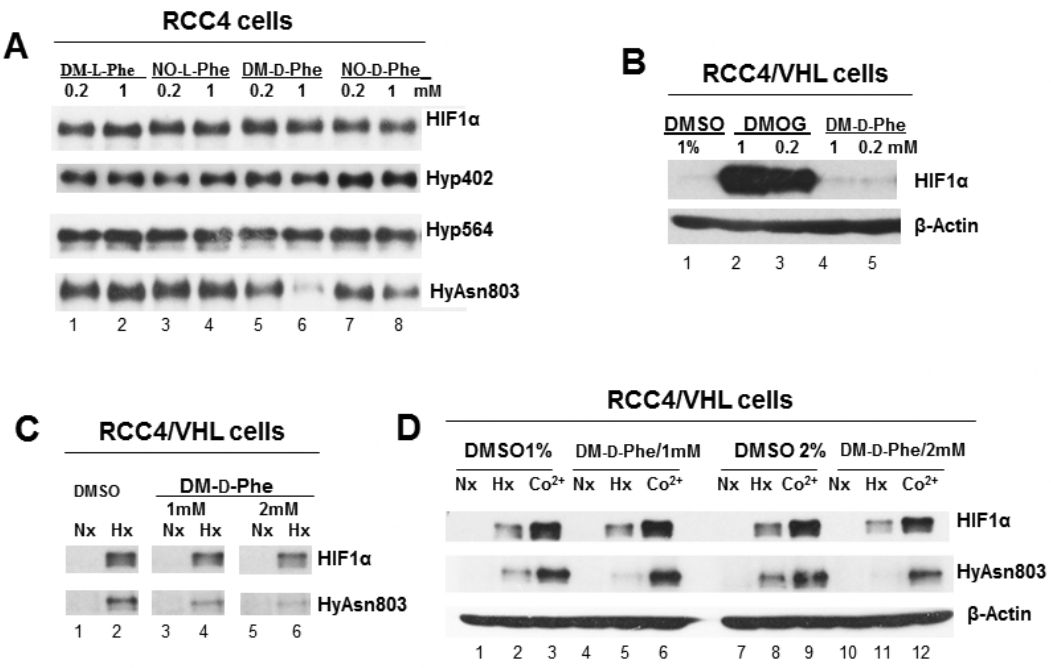


Figure 2.12: Selective chemical inhibition of HIF asparaginyl hydroxylation by DM-D-Phe (13). (**A**) RCC4 cells were treated with inhibitors at indicated concentrations for 5 h. Immunoblots show inhibition on Asn803 hydroxylation by DM-D-Phe (**13**) and NO-D-Phe (**12**). (**B**) DM-D-Phe (**13**) did not upregulate HIF-1α in RCC4/VHL cells (5 h). (**C**) Asparaginyl hydroxylation was strongly suppressed in the DM-D-Phe (**13**) treated RCC4/VHL cells (5 h) exposed to hypoxia (1% oxygen, last 2 h). (**D**) DM-D-Phe (**13**) substantially inhibited asparaginyl hydroxylation in the hypoxia- and Co(II)- induced HIF-1α in RCC4/VHL cells (5 h).

2.2.5 Evaluation of 8-hydroxyquinolines (8HQ) as HIF hydroxylase inhibitors

A series of C-5 and C-7 substituted 8-hydroxyquinoline (8HQ) derivatives have previously been reported as histone demethylase (JMJD2E)[139] and HIF prolyl hydroxylase[162] inhibitors, respectively. The C-7 substituted 8HQs were developed by Procter and Gamble Pharmaceuticals Inc. as potential anti-anaemia drugs.[162] Using a VEGF ELISA assay as an indirect measure of PHD inhibition in cells (VEGF is a downstream biomarker for HIF-1α stabilization), 8HQs **16** and **17** were identified as relatively potent PHD inhibitors (having EC_{50} values of 0.58 μM and 0.62 μM, respectively).[162] Reported docking studies of 8HQ **16** with PHD2[162] predicted that the compound binds in a different mode when compared to NOG and BIQ (in which both form a salt bridge with Arg383, see above). The 8HQ **16** distal phenyl group is predicted to position in a way that allows it to interact with Arg322 (*i.e.* cation-π interaction) close to the entrance of the active site (**Fig. 2.13**).[162]

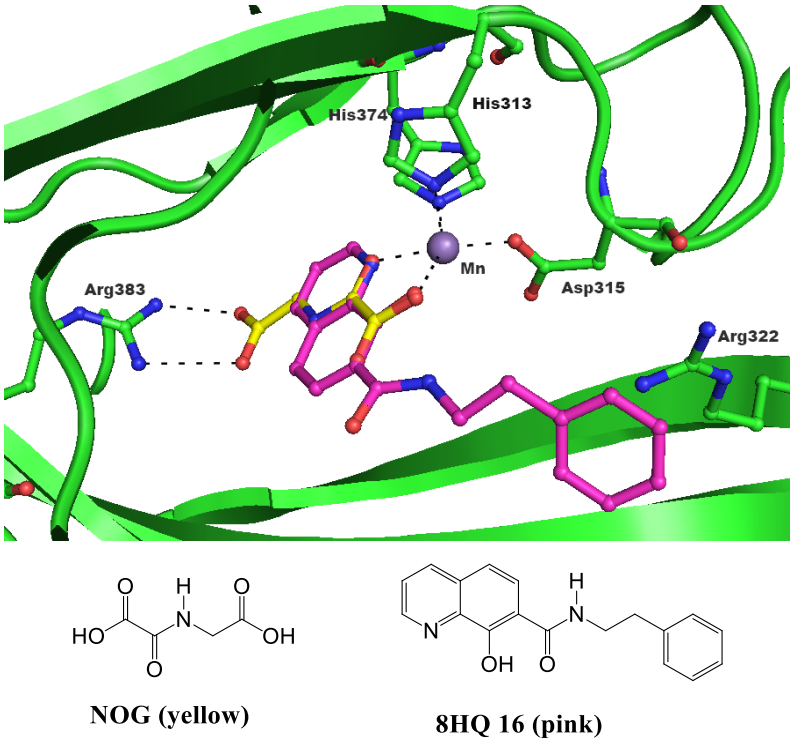


Figure 2.13: Reported docking studies suggested 8HQ **16** binds in a different binding mode when compared to NOG in the PHD2 active site.[162] This figure was created by docking 8HQ **16** into a crystal structure of PHD2 in complex with NOG (with the assistance of Dr M. McDonough) (PDB ID 3HQR) (see also **Fig. 2.4 A**).

Several C-5 substituted 8HQs have also been reported as non-specific inhibitors for the histone demethylase JMJD2E, PHD2 and FIH *in vitro*.[139] 5-Carboxy-8HQ (**22**) was reported to be a JMJD2E inhibitor, with an IC_{50} value of 86.5 μM.[139] To date, there have been no specific biological inhibition data available for the HIF hydroxylases with these compounds. Thus, a number of reported and novel 8HQs (**19-21** and **23-25**) (see **Fig. 2.14** for structures) were synthesised and evaluated as HIF hydroxylase inhibitors using the cell-based antibody assays. The 8HQs **16-19** were prepared by Owen K-H Chang; other 8HQ derivatives (except **22** which was from Sigma) were synthesised by Dr Esther C. Y. Woon. IC_{50} values for 8HQs were obtained from the AlphaScreen PHD2 hydroxylation assay (by Andrew M. C. Chan) or from the literature. The inhibitory data of the 8HQs are shown in **Table 2.5**.

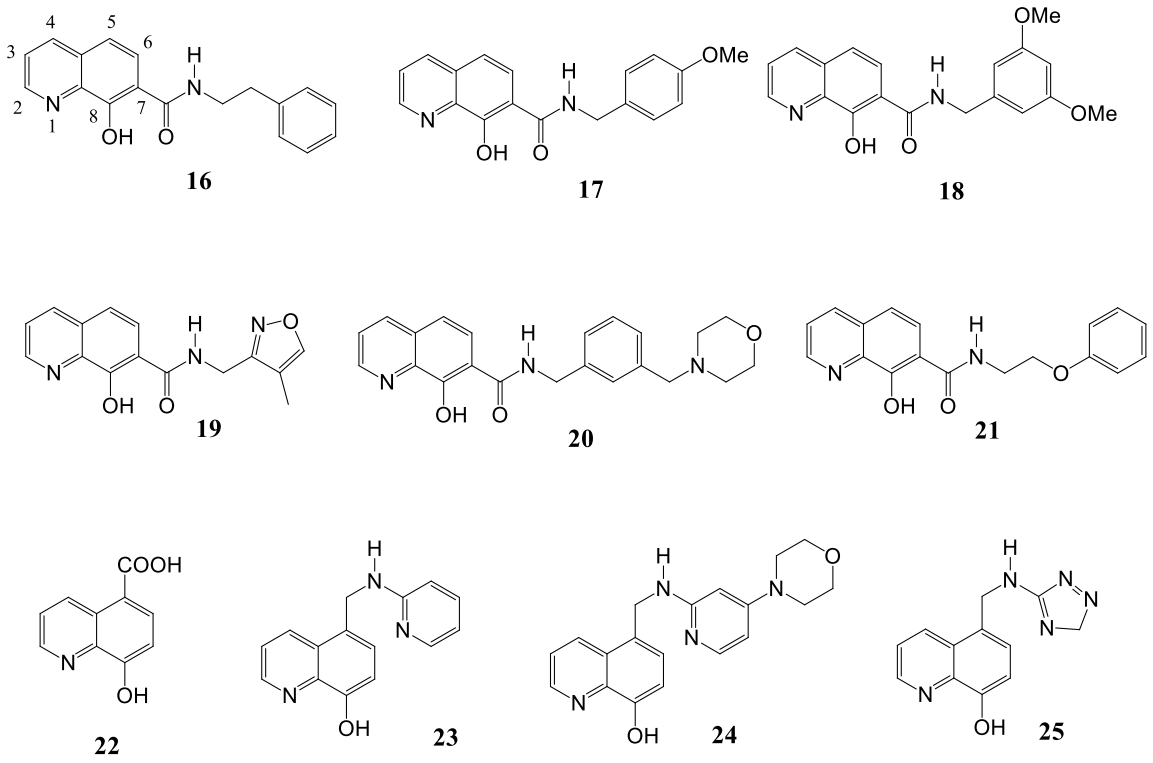


Figure 2.14: C-5 and C-7 substituted 8-hydroxyquinoline analogues evaluated as HIF hydroxylase inhibitors.

	16	17	18	19	20
IC_{50} (PHD2)	7.2 μM[162]	4.6 μM[162]	7.4 μM[162]	> 300 μM	> 300 μM

	21	22	23	24	25
IC_{50} (PHD2)	131.6 μM	> 300 μM	> 300 μM	25.3 μM	27.8 μM

Table 2.5: IC_{50} values for the 8-hydroxyquinoline (8HQ) derivatives against PHD2.

Despite their varying inhibitory potencies as shown from the *in vitro* PHD2 assays (**Table 2.5**), all the tested 8HQs (**16-25**) substantially stabilised HIF-1α in the VHL-competent cells (**Fig. 2.15 A** and **B**). However, they were later shown also to inhibit HIF asparaginyl hydroxylation (**Fig. 2.15 C-E**) with C-7 substituted 8HQs (**16-21**) preferentially inhibiting prolyl hydroxylation over asparaginyl hydroxylation (**Fig. 2.15 C-D**); and C-5 substituted 8HQs preferentially inhibiting asparaginyl hydroxylation over prolyl hydroxylation (**Fig. 2.15 E**).

C-7 Substituted 8HQs **17** and **18** with electron donating (methoxy) group(s) at the phenyl ring were shown to be slightly more potent than 8HQ **16** in cells (**Fig. 2.15 C**), even though they exhibit similar potencies *in vitro* (**Table 2.5**).[162] Interestingly, 8HQs **19** and **20** (IC_{50} values > 300 μM) which displayed weaker inhibitory potencies than **21** (IC_{50} 131.6 μM) *in vitro*, exhibit greater potencies in cells (**Fig. 2.15 D**). In contrast, 8HQ **24** which is a more potent PHD inhibitor *in vitro* (PHD2 IC_{50} 25.3 μM) only moderately inhibited prolyl hydroxylation in cells. The reasons for the differences between the observations *in vitro* and in cells are unclear; it may be due to the different cell-permeability of the compounds. However, 8HQ **25** (PHD2 IC_{50} 27.8 μM) with an amino-triazole side chain (which may be expected to have low cell permeability) was found to be the most potent PHD inhibitor among the tested C-5 substituted 8HQs in cells (**Fig. 2.15 E**).

Overall, the cell-based results indicate that the C-5 and C-7 substituted 8HQs (**16-25**) displayed partial selectivities against HIF hydroxylase inhibition. It could be anticipated that other C-5 and C-7 substituted 8-hydroxyquinoline analouges are likely to inhibit both HIF hydroxylases and possibly other 2OG dependent oxygenases. Thus, they may not be

ideal templates for the design of specific HIF prolyl or asparaginyl hydroxylase inhibitiors.

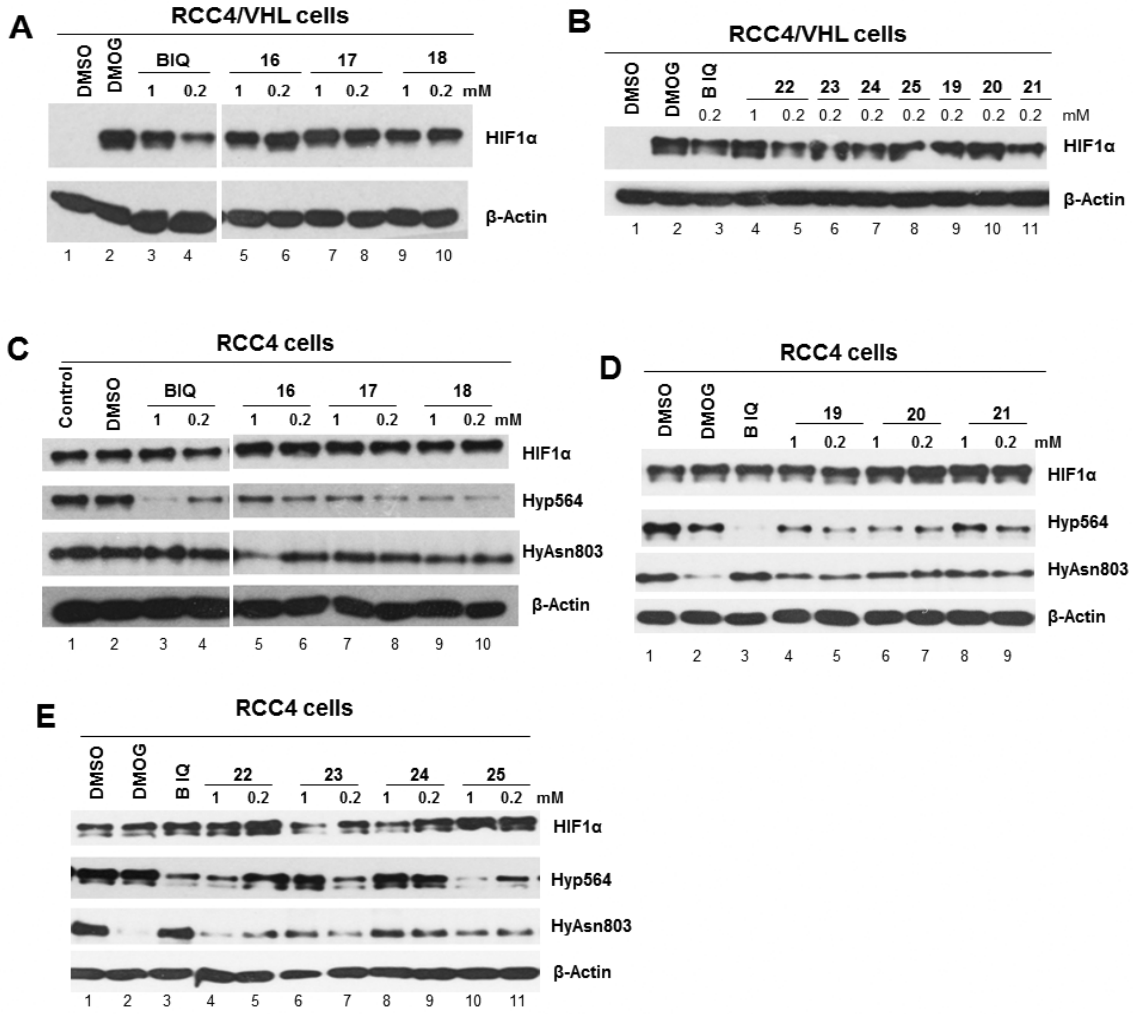


Figure 2.15: Most of the tested 8-hydroxyquinoline (8HQ) derivatives displayed partial selectivies against HIF prolyl hydroxylation over asparaginyl hydroxylation. (**A-B**) RCC4/VHL cells; **C**-**E** RCC4 cells. Cells were treated with the 8HQs at indicated concentrations for 5 h. Immunoblots were probed with the indicated antibodies. Unless otherwise stated, DMOG and BIQ (**1**) at 1 mM were used as positive controls.

2.2.6 4-Hydroxy-2-oxo-1,2-dihydroquinoline glycinamide analogues (4HQs) as specific HIF prolyl hydroxylase inhibitors

A series of 4-hydroxy-2-oxo-1,2-dihydroquinoline glycinamide analogues (referred to here as 4HQs) and other closely related glycinamide derivatives (e.g. pyridinone and pyrimidone moiety) have been developed by GlaxoSmithKline and Amgen as PHD inhibitors for the treatment of anaemia and ischeamia related diseases (**Figure 2.16** shows examples of these inhibitors).[74] These PHD inhibitors have reported PHD3 IC_{50} values of < 1 μM and EC_{50} values of < 20 μM.[74] It has also been shown that substitution on the N1 with a benzyl or alkyl group and substitution on C6 and C7 with electron withdrawing groups such as bromo and fluoro were preferred.[74] However, selectivity data of these 4HQ inhibitors (**Fig. 2.16**) has not been reported. Therefore, investigations were attempted to determine the selectivities of the 4HQ inhibitors employing the HIF hydroxy-residue specific antibody assays.

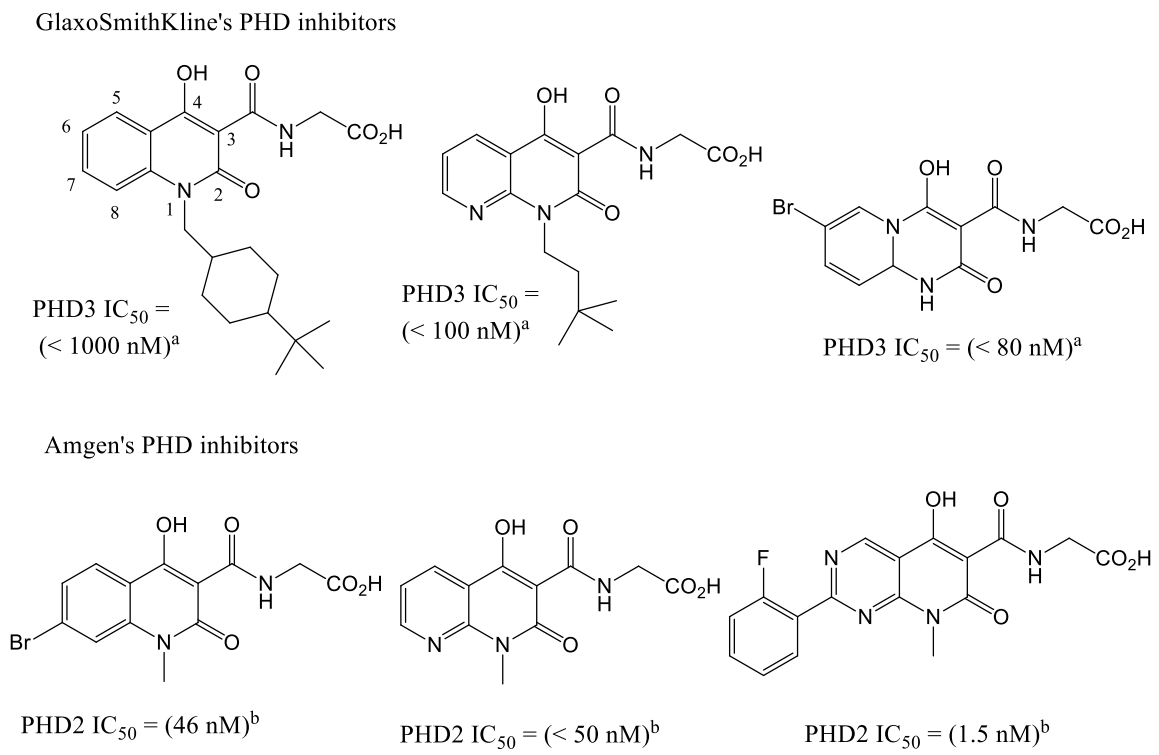


Figure 2.16: GlaxoSmithKline and Amgen's glycinamide-based PHD inhibitors. a – Refs.[172-174] b - Refs.[175-177].

A series of 4HQs (**26-31**, **Fig. 2.17**) were synthesised (by Dr J. Candela) and tested in the *in vitro* and cell-based assays. IC_{50} values for the 4HQ derivatives (**26-31**) against PHD2 (**Table 2.6**) were determined using the AlphaScreen PHD2 hydroxylation assay (by Andrew M. C. Chan). The *in vivo* inhibitory potencies and specificities of these 4HQs were then compared with the proposed clinical candidate BIQ (**1**) (IC_{50} 73 nM)[165] and bicyclic naphthalenylsulfone (BNS), a potent PHD inhibitor (PHD2 IC_{50} 27 nM) developed by Amgen.[178]

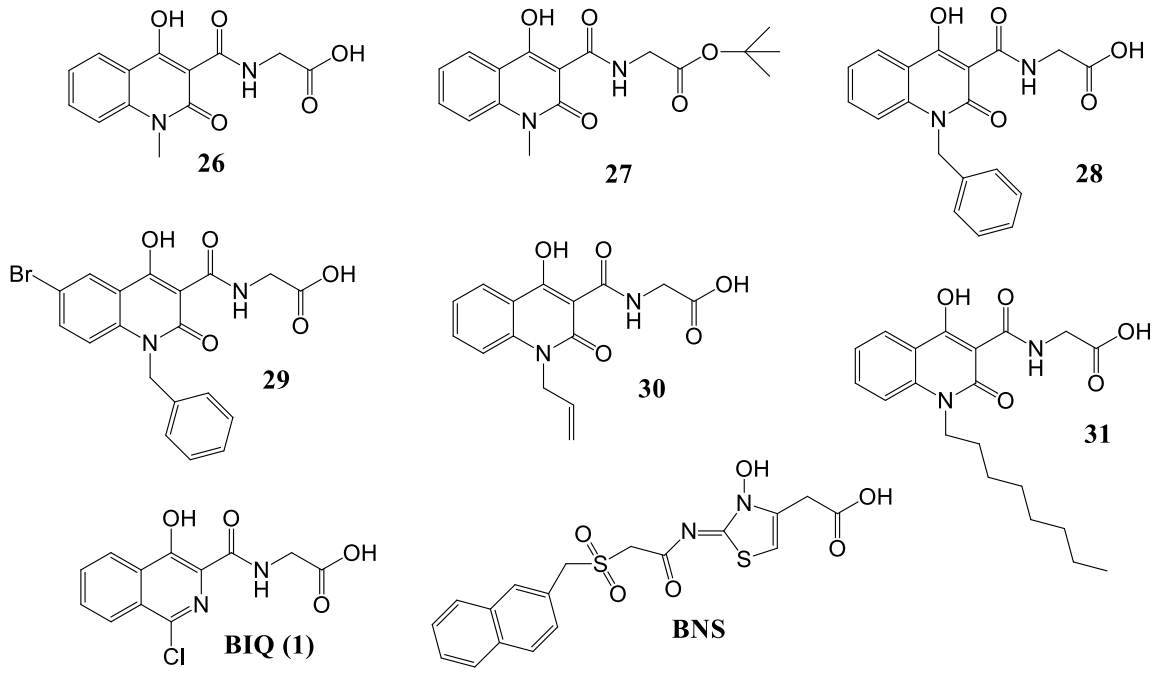


Figure 2.17: Structures of the 4-hydroxy-2-oxo-1,2-dihydroquinoline glycinamide analogues (4HQs), bicyclic isoquinoline (BIQ) and bicyclic naphthalenylsulfone (BNS) tested in the cell-based experiments.

	26	**27**	**28**	**29**	**30**	**31**	**BIQ (1)**	**BNS**
IC_{50} (PHD2)	22 nM	>300 μM	11 nM	44 nM	1200 nM	48 nM	73 nM[165]	27 nM[178]

Table 2.6: IC_{50} values for the 4HQs (**26-31**), bicyclic isoquinoline (BIQ) and bicyclic naphthalenylsulfone (BNS) against PHD2.

Given the structural similarities between the 4HQs and BIQ (**1**), they can be predicted to bind in a similar manner as BIQ (**1**) does, *i.e.* the 4HQ 2-oxo-group and amide carbonyl oxygen would probably chelate the active site iron, and the carboxylate group in the glycinamide side chain would form hydrogen bond with the Arg383 residue, while the 4-hydroxyl group would interact with Tyr303 (see also **Fig. 2.9**). However, two possible iron coordination/binding modes have been predicted for BNS (**Fig. 2.18**).[178] Modelling studies indicate that salt bridge formation is possible between the carboxylate moiety of the BNS and Arg383 (a key binding element in the 2OG binding site) for both the two putative iron binding modes.[178]

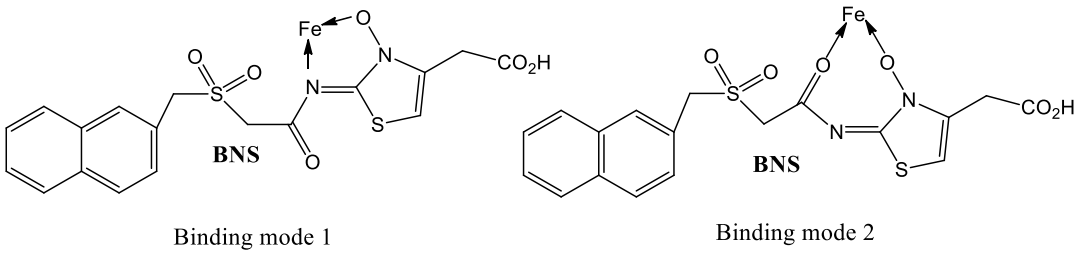


Figure 2.18: Two putative iron binding modes for BNS in the PHD active site.[178]

The 4HQs (**26-31**) were first tested in the HIF hydroxy-residue specific antibody assay in RCC4 cells (**Fig. 2.19 A** and **B**). Consistent with the *in vitro* data, all 4HQs except **27** (with PHD2 IC_{50} values ranging from 10-1200 nM) (**Table 2.6**) significantly inhibited HIF prolyl hydroxylation at 250 μM. The bulky *tert*-butyl group in **27** (PHD2 IC_{50} > 300 μM) is expected to hinder its binding to the PHD2 active site (*in vitro*) or prevents it from penetrating into the cells, rendering the compound an ineffective PHD inhibitor. The results also demonstrate that the 4HQs (**26**, **28-31**) and BNS are highly selective against HIF prolyl hydroxylation over asparaginyl hydroxylation. Compounds **28**, **29**, and BNS are more potent than BIQ (**1**) in the tested cells (**Fig. 2.19 B**, compare lanes 3, 7, 9, 13).

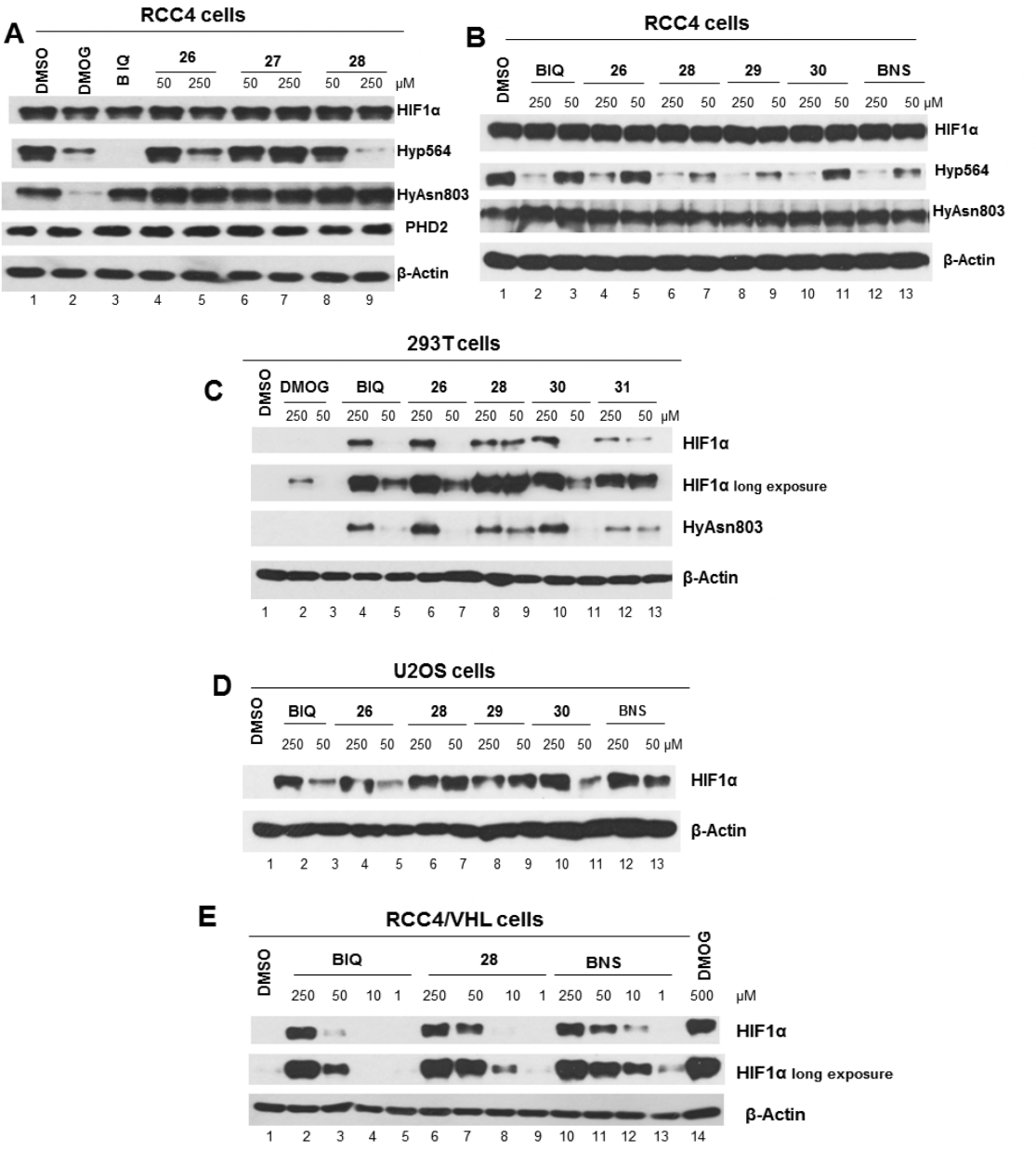


Figure 2.19: Selective inhibition of HIF prolyl hydroxylation demonstrated by the 4-hydroxy-2-oxo-1,2-dihydroquinoline glycinamide analogues (4-HQs). (**A**-**B**) RCC4 cells. (**C**-**E**) VHL-competent cells as indicated, 293T (human embryonic kidney cell line); U2OS (human osteosarcoma cell line), and RCC4/VHL. Cells were treated with various 4HQ inhibitors at indicated concentrations for 5 h. Immunoblots (**A)** and (**B**) show 4HQs selectively inhibit Pro564 hydroxylation over Asn803 hydroxylation. (**C**) shows asparaginyl hydroxylation in the 4HQs stabilised HIF-1α was not suppressed by the inhibitors. (**D**) shows 4HQs upregulate HIF-1α in U2OS cells. (**E)** The potency of HIF-stabilisation by 4HQ **28** was compared with BIQ and BNS.

When VHL-competent human embryonic kidney 293T cells, human bone osteosarcoma U2OS cells and RCC4/VHL cells were treated with the 4HQs, they effectively stabilised HIF-1α as expected (**Fig. 2.19 C-E**). Their selective inhibition of HIF prolyl over asparaginyl hydroxylation was again demonstrated in VHL competent cells. Similar to BIQ (**1**), it was shown that asparaginyl hydroxylation in the 4HQ-induced HIF-1α was not suppressed by the 4HQs (**Fig. 2.19 C**, compare immunoblot signals of HyAsn803 to total HIF-1α), therefore indicating specific inhibition of the HIF prolyl hydroxylases.

The level of HIF-1α protein stabilised by 4HQ treated cells was also found to be many fold higher than DMOG-induced HIF at the same concentration (**Fig. 2.19 C**, HIF-1α long exposure immunoblot, compare lanes 2, 6, 8, 10), suggesting the 4HQ glycinamide derivatives are potent hydroxylase inhibitors, in keeping with the *in vitro* results which show they inhibit at an nanomolar range (**Table 2.7**). The cell-based assays reveal that **28** and **29** are potent inhibitors (with *in vitro* PHD2 IC_{50} values of 11 nM and 44 nM respectively) among the tested 4HQs, showing that a phenyl substituent in *N*-1 is preferred. The phenyl substituent is expected to promote hydrophobic interaction between the compound and the active site residues. However, *N*-alkyl substituted 4HQs (e.g. *N*-methyl (**26**) *N*-allyl (**30**) and *N*-octyl (**31**); with IC_{50} values 22 nM, 1200 nM, and 48 nM respectively) showed slightly lower potencies in cells (**Fig. 2.19 B-D**).

The potency of **28** was then compared to two other potent HIF prolyl hydroxylase inhibitors, BIQ **(1)** and BNS in RCC4/VHL cells. At concentrations lower than 250 μM, **28** appeared to upregulate HIF-1α to a higher level when compared to BIQ (**1**) (**Fig. 2.19 E**, compare lanes 3 and 7); but to a lower level than BNS (compare lane 8 and 12). Thus, the potencies of these specific HIF prolyl hydroxylase inhibitors in cells can be ranked in the order of BNS > **28** > BIQ (**1**).

2.3 Discussion

The work described in this chapter enabled a comparative analysis of different modes of chemical inhibition of HIF-1α hydroxylation sites using hydroxy-residue specific antibodies. It is worth noting that although the use of RCC4 (VHL-defective) cells was necessary to enable direct comparison of the effects of chemical intervention on prolyl and asparaginyl hydroxylation, activation of the HIF transcriptional response in these cells also leads to constitutive expression of two of the HIF prolyl hydroxylases (PHD2 and PHD3), which are themselves HIF-target genes.[17, 179] In contrast, FIH expression is unlikely to be affected by the VHL status.[142] Therefore, it is suggested that VHL-competent cells which express relatively lower levels of endogenous PHD2 and PHD3 could more effectively reflect the differential sensitivities of HIF prolyl and asparaginyl hydroxylation to chemical intervention.

Striking differences were observed in cells among inhibitors that are often regarded as being non-specific hydroxylase inhibitors *in vitro* and which are commonly applied to cells as hypoxia mimetics. It is important to note that the effects may vary in different types of cells/tissues. However, at least in the tested cell types, the generic 2OG analogue DMOG was found to be more effective at suppressing HIF asparaginyl hydroxylation than HIF prolyl hydroxylation. In contrast, at concentrations that had marked effects on HIF prolyl hydroxylation, iron chelators were much less effective, and transition metals ions such as Co(II) and the small-molecule inhibitor EDHB, were almost completely ineffective in inhibiting HIF asparaginyl hydroxylation in cells, contrary to the *in vitro* findings.

Desferrioxamine (DFO), Co(II), Ni(II), and Mn(II) were reported to be effective inhibitors for recombinant FIH, but almost ineffective against the PHDs 1-3 (purified from insect cells), reflecting the weaker Fe(II) binding of HIF asparaginyl hydroxylase *in vitro*.[66] It seems likely that the apparent resistance of FIH to inhibition by iron chelators and metal ions observed in cells suggests a more complex mechanism than facile exchange of the metal ions with a labile cellular pool, one speculation being the presence

of additional binding/transport proteins in the exchange/delivery processes.[30] These findings further suggest that PHD and FIH might have different physiological roles in responses to changes in intracellular iron in regulating the HIF-system.

Interestingly, in a separate study, HIF-1α Asn803 hydroxylation was also found to be substantially more resistant to hypoxia and chronic hypoxia than Pro402 and Pro564 hydroxylation. Asparaginyl hydroxylation was shown to remain at 50~90% in different VHL-competent cells exposed to 1% oxygen and in the region of 40% in VHL-defective cells exposed to severe hypoxia (0.1%). In addition, the hydroxylation was found to persist in human tumour tissues.[142]

Although asparaginyl hydroxylation in the *C*-terminal transactivation domain (CAD) of HIF-α has been shown to inhibit HIF transcriptional activity (*i.e.* via preventing the interaction between HIF-α and co-activator p300/CBP, see **Chapter 1** (**Fig. 1.5)**), it may not be the case for all HIF-target genes and in all cellular contexts. HIF-mediated responses are clearly activated in VHL-deficient cells and in some well-oxygenated tumours, in which HIF asparaginyl (and prolyl) hydroxylation remained at a high level.[144, 180] Despite the high levels of HIF-1α asparaginyl hydroxylation observed in the Co(II)- and specific PHD inhibitor- (e.g. BIQ (**1**)) treated cells in this study; both treatments have previously been reported to significantly induce EPO (and other HIF-target genes) which is dominantly regulated by the HIF pathway.[20, 79] Therefore, it is possible that HIF-target genes could be activated by a second transactivation domain in the N-terminal (NAD), as HIF-1α variants lacking the CAD have also been shown to upregulate certain HIF-targets.[180, 181] This speculation is supported by a recent report which shows that besides interacting with HIF-α CAD, the coactivator p300/CBP can also directly interact with NAD mediates the transactivation function.[182]

Suppression or over-expression of FIH, which alters HIF asparaginyl hydroxylation in both directions have reciprocal effects on the expression of a range of HIF-transcriptional genes.[183] An important question raised by these findings is to what extent HIF asparaginyl and prolyl hydroxylation need to be inhibited to yield a therapeutic HIF-response. Therefore, the identification of specific cell-permeable FIH and PHD small-

molecule based inhibitors within this study should assist in guiding attempts to pharmacologically modulate the hypoxia pathway. However, it is worth noting that the HIF-transcriptional response may potentially involve contributions from oxygenases other than the HIF hydroxylases.[184-186] Indeed, it may be that the relatively non-specific inhibitors may better mimic the natural hypoxic response.

Although this study has focused mainly on HIF-1α, it is worth noting that chemical inhibition of the HIF hydroxylases may also have different effects on the regulation of other HIF-α isoforms. Small interfering RNA (siRNA) targeting each PHD has demonstrated differential effects on HIF-1α and HIF-2α activation. Suppression of PHD1 and PHD3 were found to have greater influence on HIF-2α than HIF-1α, whereas the converse was observed for PHD2.[37] Therefore, the potential contributions of other HIF-α isoforms in the HIF-mediated response cannot be excluded when considering the therapeutic intervention approaches.

2.4 Conclusions and future directions

The studies described in this chapter comprise the first direct analysis of the differential modulation of HIF prolyl and asparaginyl hydroxylation by chemical inhibition in cells. Hydroxy-residue specific antibodies, whose performance was validated by MS, were used to analyse hydroxylation levels at each of the three known sites of hydroxylation in human HIF-1α (Pro402, Pro564, and Asn803). The findings reveal major differences in the regulation of HIF prolyl and asparaginyl hydroxylation and their sensitivities to supposedly nonspecific hypoxia mimic inhibitors. Whereas these substances induced HIF by inhibition of prolyl hydroxylation, they have highly variable effects on asparaginyl hydroxylation.

Employing the newly developed HIF hydroxy-residue specific antibody assays, the current work has taken the first steps to provide biological selectivity data of previously developed and novel HIF hydroxylase inhibitors, which has resulted in the identification of several specific cell-permeable PHD inhibitors (BIQ (**1**), L-Ala-BIQ (**3**), 4HQs (**28**-**30**) and BNS), and one specific FIH inhibitor (DM-D-Phe (**13**)). The results clearly demonstrate that high specificity could be achieved in inhibiting each of the HIF hydroxylases by these small-molecule based inhibitors in cells.

Despite being a sensitive method for the studies of HIF-α protein modification, the HIF hydroxylase cell-based antibody assays that employ immunoblotting techniques can be technically demanding, time consuming and labour intensive; therefore, it is normally not suitable for high throughput screening. Nevertheless, the current work should provide a foundation for the development of high throughput screening methods such as enzyme-linked immunosorbent assay (ELISA) employing the hydroxy-residue specific antibodies. Other future studies may involve:

i) Quantitative analysis (densitometry or other measurements) of the extent of inhibition by the chemical inhibitors in cells.

ii) More detailed kinetic studies, such as the determination of EC_{50} values of the HIF hydroxylase inhibitors in cells.

iii) Selectivity studies of the specific PHD and FIH inhibitors over other 2OG oxygenases including the functionally related collagen prolyl-4-hydroxylase and the recently indentified tumour-associated chromatin modifying enzymes, the histone demethylases.[187, 188 189]

iv) Microarray analysis of the potential differential effects of the specific HIF hydroxylase inhibitors on modulating HIF-target gene expressions.

Chapter 3: Assessment of the Ability of Oncometabolite 2-Hydroxyglutarate to Inhibit 2-Oxoglutarate Dependent Oxygenases

3.1 Background and Objectives

Increased HIF-1α activity in defective isocitrate dehydrogenase (IDH) gliomas has been proposed as a direct result of competitive inhibition of PHD activity caused by excessive accumulation of *R*-2-hydroxyglutarate (*R*-2HG) in the tumour growth environment.[109] However, no experimental evidence has yet been shown to support this hypothesis (see also **Introduction** in **Section 1.3.3**).

It was envisaged that the newly developed HIF hydroxy-residue specific antibody assays described in **Chapter 2** would enable direct measurement of potential inhibitory effects of elevated 2HG on all the three HIF hydroxylation sites (*i.e.* Pro402 in NODD, Pro564 in CODD, and Asn803 in CAD). This would provide an ideal tool for probing the mechanism of action of the oncometabolite *R*-2HG on the HIF system. This chapter describes the use of this assay to test the hypothesis of 2HG inhibition of the HIF hydroxylases.

There are approximately sixty human 2OG dependent oxygenases.[190] Many of these 2OG oxygenases have reported K_m values for 2OG close to its reported physiological concentrations.[32, 190, 191] This makes them potentially susceptible to fluctuation of intracellular 2HG[192] and suggests that inhibition by 2HG may be pathophysiologically relevant.[108, 193] Given the high concentrations of *R*-2HG (approximately 5-35 mM) in the IDH-associated tumours (tumours with wild-type IDH1 have 100-fold less *R*-2HG),[109] it was hypothesised that 2HG may also inhibit other 2OG oxygenases.

Among the 2OG oxygenases, the chromatin-modifying histone demethylases have recently been associated with oncogenesis.[187, 188] The effects of 2HG elevation on both histone demethylases (*i.e.* JMJD2A, JMJD2C, and FBXL11) and HIF hydroxylases (*i.e.* PHD and FIH) were therefore investigated using different biochemical and structural analyses. The work in this chapter was carried out in collaboration with Dr R. Chowdhury, Dr L. Hillringhaus, Dr N. R. Rose, and Dr A. Kuwamura and has been reported in *EMBO* Reports (2011).[184]

3.2 Results

3.2.1 *R*-2HG is an ineffective inhibitor for HIF prolyl hydroxylases in cells

Potential inhibitory effects of 2HG on the activities of the PHDs and FIH were first examined using the HIF hydroxy-residue specific antibody assays described in **Chapter 2.** Cell-penetrating 2HG analogues - dimethyl *R*-2HG and dimethyl *S*-2HG (hereafter *R*/*S*-2HG) (prepared by Dr Esther C. Y. Woon) (**Fig. 3.1**) were used as an exogenous source of 2HG in the cell-based experiments. The dimethyl 2HG esters were first tested using RCC4 VHL-defective cells (*i.e.* RCC4 cells) by incubation (4 h) at a range of concentrations (0.1-100 mM) (**Fig. 3.2 A-B**). Cells were harvested and extracts were analysed by immunoblotting, employing the HIF hydroxy-residue specific antibodies. Dimethyloxalylglycine (DMOG), a cell-penetrating derivative of *N*-oxalylglycine (NOG) (a 'generic' 2OG oxygenase inhibitor) and/or the specific PHD inhibitor bicyclic isoquinoline compound (BIQ) were used as positive controls (**Fig. 3.1**).

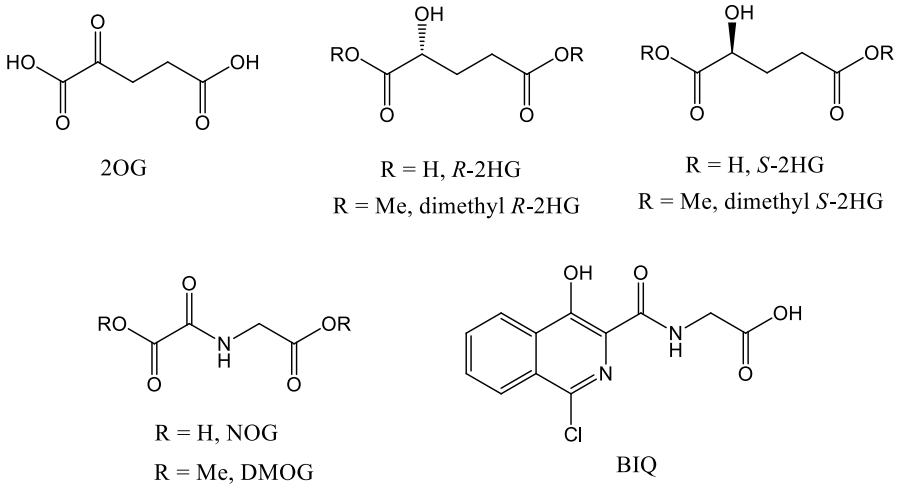


Figure 3.1: Structures of the cell-permeable 2-hydroxyglutarate (2HG) analogues, dimethyloxylglycine (DMOG) and the bicyclic isoquinoline inhibitor (BIQ) used in the cell-based experiments.

A potent HIF hydroxylase inhibitor normally displays suppression of HIF hydroxylation at 0.1-1 mM (see **Chapter 2**), however, the *R*/*S*-2HG did not show any inhibition at low concentrations (**Fig 3.2 A**). When exposed to higher concentrations (> 50 mM), the 2HGs were found to be cytotoxic (observed from morphological changes/detachment of cells) (**Fig. 3.2 B**). However, inhibition of asparaginyl hydroxylation was observed in both the *R*- and *S*-2HG treated cells at multiple additions (10 mM x 8 at 30 min intervals). Prolyl hydroxylation was weakly suppressed by the 2-HG enantiomers under these assay conditions (**Fig. 3.2 B,** lanes 6 and 11). Multiple additions (10 mM x 8 at 30 min intervals) were therefore considered as the optimum testing conditions.

Further assays were carried out in triplicate and the extent of suppression by *R*- and *S*-2HG on each HIF hydroxylation site were measured and analysed by densitometry of the immunoblot signals. Representative immunoblots and quantification data of the 2HG treated samples (8 x 10 mM additions, at 30 min intervals) are shown in **Fig. 3.2 C** and **D**. The results show that both *R*- and *S*-2HG inhibit HIF asparaginyl hydroxylation more than 50%, whereas *S*- but not *R*-2HG shows modest inhibition of prolyl hydroxylation (~ 30%) at this high dose exposure (**Fig. 3.2 D**).

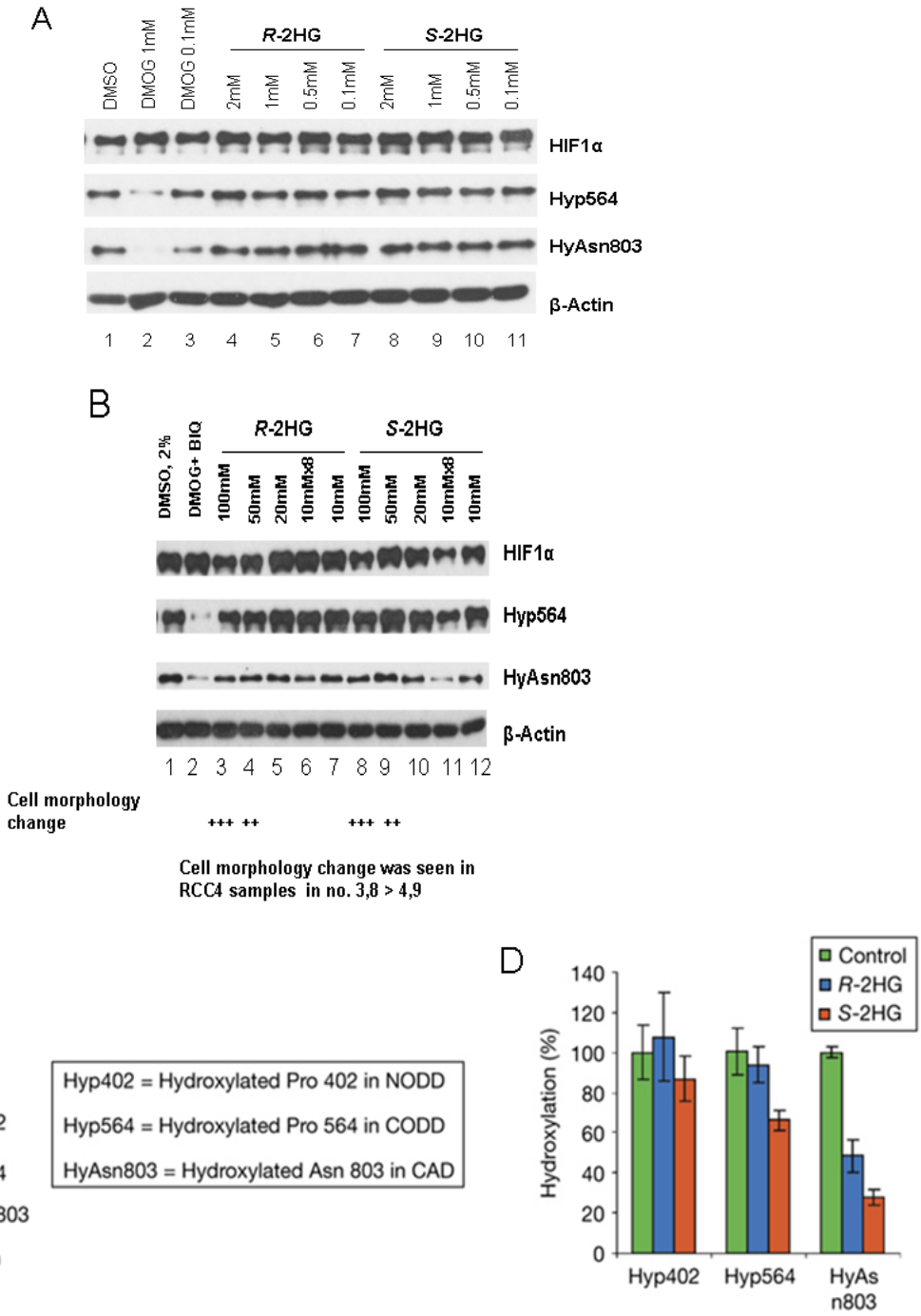


Figure 3.2: Inhibition of HIF prolyl hydroxylation and asparaginyl hydroxylation by *R*- and *S*-2HG in RCC4 cells. (**A**) and (**B**) Immunoblots of protein extracts from RCC4 cells (renal cell carcinoma) treated for 4 h with different doses of *R*- and *S*-2HG compared to a DMSO-treated negative control and DMOG or DMOG + BIQ positive controls (1 mM). (**C**) Representative immunoblots of the *R*- and *S*-2HG treated (10 mM × 8) samples. *R*-and *S*-2HG were tested in their dimethyl ester forms. Signals of total HIF-1α and hydroxylated NODD (Hyp402), CODD (Hyp564) and CAD (HyAsn803) were analysed. (**D**) Quantification of data from (**C**) and two other independent experiments (data not shown) by densitometry; band intensities were normalized to HIF-1α signals. Vertical bars represent standard errors ($n > 3$).

These results suggest that *R*-2HG, the enantiomer over-produced by IDH1 mutants,[109] did not effectively inhibit the HIF prolyl hydroxylation and would therefore likely be relatively ineffective in upregulating HIF-1α. To test this directly, *R*-/*S*-2HG dimethyl esters were applied to various VHL-competent cells including RCC4 re-expressing functional VHL (RCC4/VHL), human hepatoma Hep3B cells and breast cancer MCF7 cells either at a single dose (20 mM) or multiple additions (8 x 10 mM additions, at 30 min intervals). Neither dose of *R*-2HG induced HIF-1α. Modest HIF-1α induction was observed with *S*-2HG treated cells (see **Fig. 3.3 A,** lanes 6, 10, 11, and 14**)**, consistent with the previous results which showed *S*-2HG modestly inhibited HIF prolyl hydroxylation in RCC4 cells (**Fig. 3.2 C** and **D**). Minimal HIF-2α accumulation was also observed in some samples (**Fig 3.3 A,** lanes 10 and 11). Since HIF asparaginyl hydroxylation is more 2HG-sensitive than prolyl hydroxylation (based on the assay in RCC4 cells), the HIF-1α induced by *S*-2HG was therefore anticipated not to be hydroxylated at Asn803. It was subsequently confirmed that this was the case (**Fig 3.3 B)**.

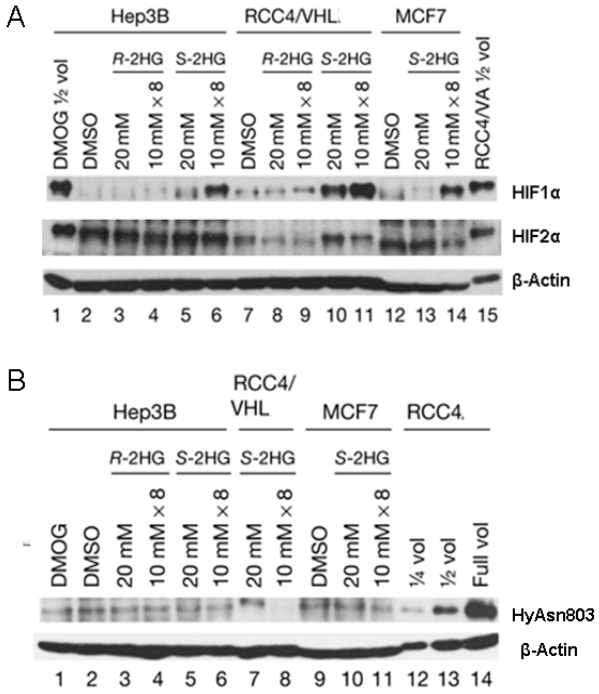


Figure 3.3: (**A**) Effect of *R*-/*S*-2HG on HIF-1α protein levels in Hep3B (human hepatoma cell line), RCC4/VHL (renal cell carcinoma re-expressing functional VHL) and MCF7 (breast cancer cells). (**B**) Immunoblot analyses of HIF1α asparaginyl hydroxylation of selected samples from (**A**). RCC4 VHL-defective protein extracts were used as positive controls for the HIF-1α/HIF-2α immunoblots in (**A**) and HyAsn803 immunoblots (lane 12-14) in (**B**).

3.2.2 *R*-/*S*-2HG inhibit histone N^{ϵ}-methyl lysine demethylase JMJD2A in cells

Evidence from epigenetic studies has started to change our view of cancer, which was previously thought primarily be a genetic disorder (*i.e.* resulting from mutation in DNA sequence). Chromatin modifications as a result of post-translational alterations to histones (*i.e.* acetylation, methylation, or demethlyation) have recently been associated with cancer progression in different types of tumours.[187, 188189] Therefore, the effects of 2HG on histone N^{ϵ}-methyl lysine demethylase JMJD2A activity in cells were next investigated using an immunofluorescence assay (carried out by Dr L. Hillringhaus). *R*-/*S*-2HG dimethyl esters were added (5 mM or 10-mM x 8 additions, at 30 min intervals) to Hela cells transfected with JMJD2A expressing plasmid. DMOG (2.5mM) was used as a positive control and for comparison (**Fig. 3.4 A**). Surprisingly, both 2HG enantiomers were found to inhibit JMJD2A in a dose-dependent manner (**Fig. 3.4 B**), with *R*-2HG demonstrating slightly more potent inhibition (data analysed by Dr L. Hillringhaus).[184]

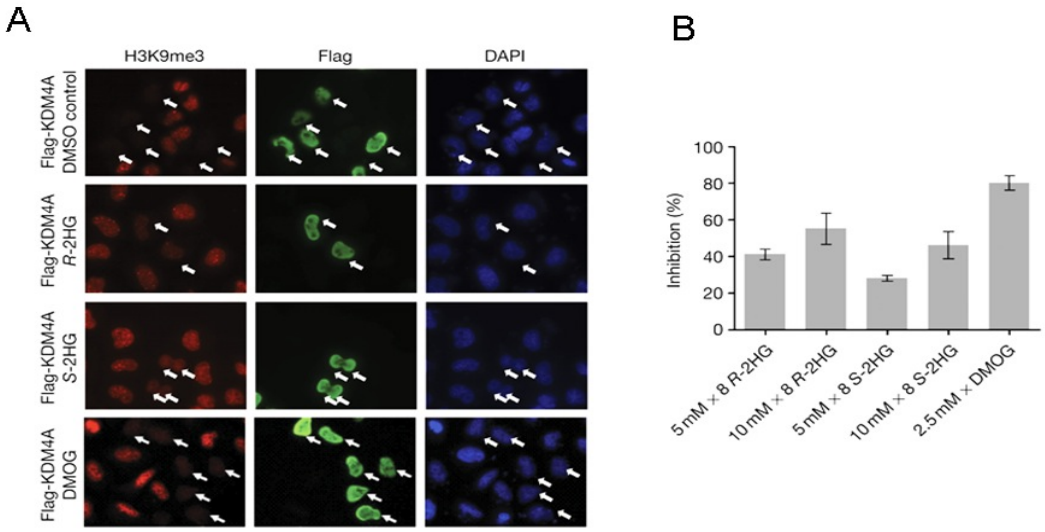


Figure 3.4: Inhibition of JMJD2A (KDM4A) activity revealed the immunofluorescence assay. *N*-terminally Flag-tagged JMJD2A protein was overexpressed in Hela cells. Results with DMOG are shown as comparison. (**A**) Indirect immunofluorescence analyses using antibodies against $H3K9me_3$ (left panels) or Flag (middle panels) were used to analyse the inhibition of ectopically expressed JMJD2A. DAPI (4′,6-diamidino-2-phenylindole) staining (right panels) indicates location of nuclei. Rows represent control (0.5% DMSO), *R*-/*S*-2HG- and DMOG-treated cells. White arrows in the left and right panels indicate nuclei in which JMJD2A is overexpressed. Higher levels of $H3K9me_3$ were detected in both *R*- and *S*-2HG and DMOG treated cells, indicating inhibition of JMJD2A, whereas the DMSO control shows only a level of $H3K9me_3$ in nuclei in which JMJD2A is overexpressed. (**B**) Percentage inhibition of JMJD2A activity, using addition of doses of *R*- and *S*-2HG in their dimethyl ester forms (5 or 10 mM × 8); error bars represent standard error (n >50) (Data obtained from Dr L. Hillringhaus).[184]

3.2.3 *In vitro* biochemical studies

Following these cell-based assays, the potential inhibitory effects of *R*- and *S*-2HG on HIF prolyl (PHD2) and asparaginyl (FIH) hydroxylase and a wider range of human histone lysine demethylases (JMJD2A, JMJD2C and FBXL11/JHDM1A) were further studied using *in vitro* biochemical methods. *In vitro* assays for PHD2 and FIH activities were carried out using matrix-assisted laser desorption/ionization mass spectroscopy (MALDI MS) hydroxylation assays.[81, 166, 184] In the MALDI MS assays, hydroxylation of CODD (HIF-1α residues 556-574) and CAD (HIF-1α residues 786-826) peptides were monitored by an observation of a +16 Da mass shift in the mass spectra.[194]

Inhibition of JMJD2A, JMJD2C, and FBXL11 was assessed using a formaldehyde dehydrogenase (FDH) coupled assay.[166, 195] **Fig. 3.5** shows the general mechanism of histone lysine demethylation catalysed by the 2OG dependent demethylases in which the reaction products include demethylated lysine residues and formaldehyde. In the FDH coupled assay, formaldehyde release was monitored by its oxidation to form formate, a reaction catalysed by FDH that concomitantly produces NADH which was measured by fluorescence spectroscopy.[166, 195] The biochemical assays were conducted using a 2OG (co-substrate) concentration at or close to the 2OG K_m values for the individual enzymes and the assay conditions are shown in **Appendix 1**. The half-maximal inhibitory concentration (IC_{50}) values of *R*- and *S*-2HG for the HIF hydroxylases and histone demthylases are shown in **Table 3.1**. The biochemical assays were carried out by Dr N. Rose and Dr A. Kawamura.

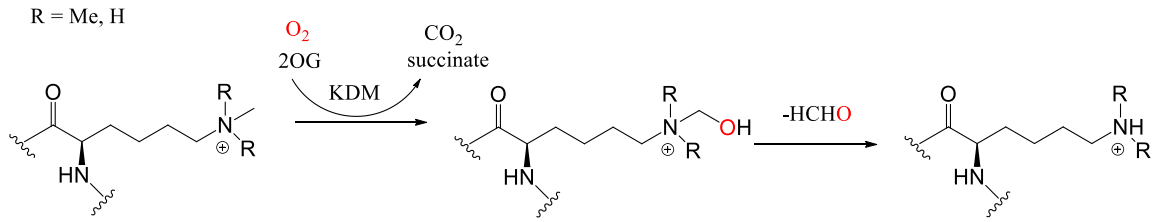


Figure 3.5: General mechanism of lysine demethylation catalysed by 2OG and Fe(II) dependent histone lysyl demethlyases (KDM). 2OG and oxygen are co-substrates, reaction products include demethylated lysine residues, formaldehyde (HCHO), carbon dioxide and succinate.

Enzyme	IC_{50} ± s.e.m. (μM)		
	R-2HG	*S*-2HG	NOG
FIH	1500 ± 400*	189 ± 34	46 ± 8
PHD2	7300 ± 3300*	419 ± 150	0.8 ± 0.2
JMJD2A	24 ± 2 (17 ± 4)	26 ± 3 (33 ± 5)	17 ± 2 (20 ± 3)
JMJD2C	79 ± 7	97 ± 24	14 ± 3
FBXL11	106 ± 22	48 ± 15	252 ± 50

Table3.1: The IC_{50} values of *R*- and *S*-2HG for the HIF hydroxylases (PHD2 and FIH) and histone demethylases (JMJD2A, JMJD2C, and FBXL11). Italicised IC_{50} values in parentheses were determined at 10-fold higher Fe(II) concentration than the standard assay conditions. All assays were performed in triplicate. IC_{50} values of *N*-oxalylglycine (NOG) were shown for comparison. *Partial dose–response curves (Data obtained from Dr N. R. Rose and Dr A. Kawamura).[184]

Interestingly, *R*-/*S*-2HG demonstrated a wide range of IC_{50} values ranging from approximately 25 μM to more than 7 mM for the tested 2OG oxygenases (**Table 3.1**). Consistent with the HIF hydroxy-residue specific antibody assay results (**Fig. 3.2** and **3.3**), *R*-2HG was shown to be an ineffective inhibitor for PHD with a notably high IC_{50} value at approximately 7 mM. On the other hand, *R*-2HG displayed moderate inhibition on FIH with an IC_{50} value of approximately 1.5 mM. In both cases, *S*-2HG was a more potent inhibitor (**Table 3.1**). The *in vitro* findings are therefore consistent with the observations in cells.

Both *R*- and *S*-2HG effectively inhibit JMJD2A, for which the IC_{50} values (24 and 26 μM respectively) were close to that observed for NOG (17 μM) (**Table 3.1**). The findings are in keeping with the JMJD2A cell-based results in which both the 2HG enantiomers show similar inhibitory potencies. However, much higher concentrations of 2HG were needed to see the inhibitory effect in cells (see **Fig 3.4 B**). In addition, *R*-/*S*-2HG also substantially inhibited the activities of two other histone demethylases JMJD2C and FBXL11 with IC_{50} values ranging from 50 -100 μM. In the case of FBXL11, 2HG was more potent than the generic 2OG oxygenase inhibitor NOG (IC_{50} > 250 μM). To rule out a possible iron chelating effect by 2HG, assays (for JMJD2A) were next carried out using higher (10-fold) iron concentrations (**Table 3.1**, IC_{50} values in parentheses). The lack of

substantial increase in the JMJD2A IC_{50} values indicates that the mode of inhibition by *R*-/*S*-2HG is not predominantly iron sequestration.

In conclusion, both *R*- and *S*-HG were found to be more potent inhibitors of the tested histone demethylases than the HIF hydroxylases. The highest potency was observed against JMJD2A. Furthermore, both *in vitro* and cell-based studies show no evidence of PHD inhibition by the tumour derived *R*-2HG. However, caution must be taken when comparing IC_{50} values determined with different assay conditions for the 2OG oxygenases.

3.2.4 2HG binds to the same site as 2OG in FIH and JMJD2A

Structural analysis was then carried out (by Dr R. Chowdhury) to investigate the mechanistic actions of R-/S-2HG inhibition in human 2OG oxygenases. FIH or JMJD2A was co-crystallized with 10 equivalents of *R*- and *S*-2HG by vapor diffusion and the crystals were cryo-cooled as previously described.[196] The crystal structures of FIH and JMJD2A with *R*- or *S*-2HG were then solved. The JMJD2A.2HG structures were co-crystallised with a histone H3K36me3 substrate fragment, which bound similarly to previously reported structures.[184, 195, 197, 198]

Both enantiomers were shown to bind bidentately to the catalytic site iron or surrogate nickel (**Fig. 3.6**) in FIH and JMJD2A. Similarly to 2OG and NOG,[196, 198] they coordinate the metal with the 2-hydroxyl group *trans* to $D201^{FIH}$/$E190^{JMJD2A}$ and one oxygen of the C1-carboxylate *trans* to $H199^{FIH}$/$H188^{JMJD2A}$ (**Fig. 3.5 A, B, D** and **E**). The other oxygen atom of the 2HG C1-carboxylate is positioned to form a hydrogen bond with $N205^{FIH}$ (**Fig. 3.5 A** and **B**) or $S288^{JMJD2A}$ (**Fig. 3.6 D** and **E**); whereas the 2HG C5-carboxylate is positioned to form a hydrogen bond to $K214^{FIH}$, $Y145^{FIH}$ and $T196^{FIH}$ (**Fig 3.6 A** and **B**) and to $K206^{JMJD2A}$ and $Y132^{JMJD2A}$ (**Fig. 3.6 D** and **E**) (data analysed by Dr R. Chowdhury).[184]

Overall, the crystallographic analyses demonstrate that as have been observed for the crystal structures of FIH and JMD2A in complex with succinate (**Fig. 3.6 C and F**),[81] both *R*- and *S*-2HG occupy the same catalytic site as 2OG in FIH and JMJD2A, indicating that 2HG has the potential to compete with 2OG for binding.[184]

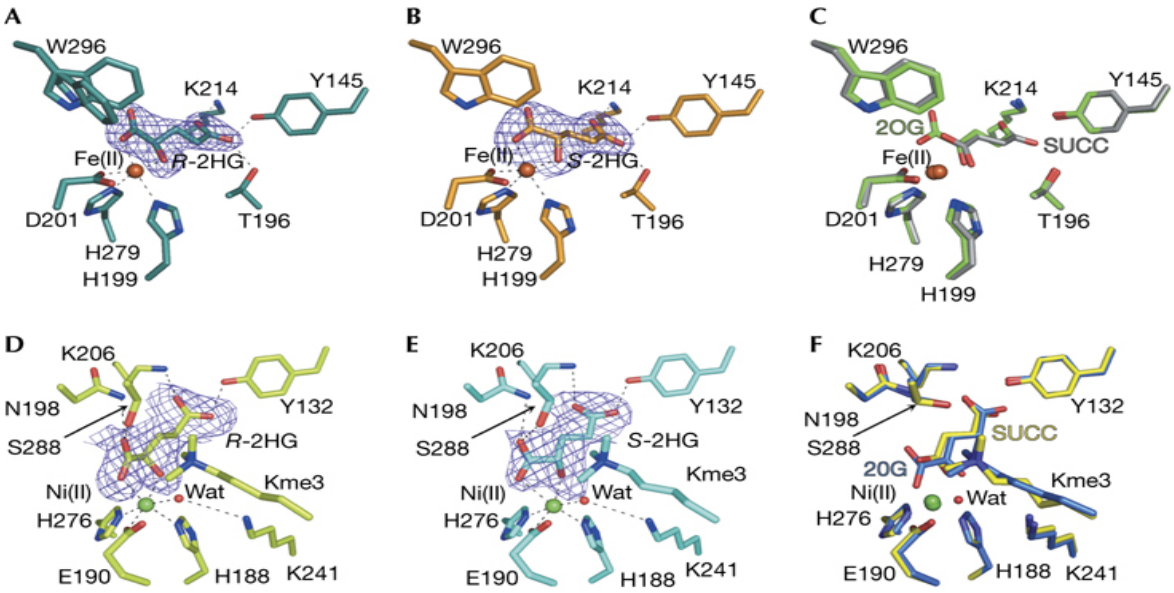


Fig. 3.6: Crystal structures of FIH and JMJD2A in complex with *R*- and *S*-2HG indicate binding of 2HG to the 2OG binding site. FIH/JMJD2A folds were similar to those reported. Dotted lines indicate apparent hydrogen bonds and polar interactions. (**A**) View of the FIH.Fe(II).*R*-2HG complex (2.1 Å) . (**B**) FIH.Fe(II).*S*-2HG complex (2.3 Å). (**C**) Overlay of views from structures of FIH in complex with 2OG or succinate. (**D**) View from the active site of the JMJD2A.Ni(II).*R*-2HG.H3K36me3 structure; Kme3=N^{ε}-trimethylated lysine substrate residue; Ni(II) substitute for Fe(II) (2.0 Å). (**E**) JMJD2A.Ni(II).*S*-2HG.H3K36me3 structure (2.3 Å). (**F**) Overlay of views from structures of JMJD2A in complex with 2OG or succinate. Resolution (Å) was shown in parentheses. (Data obtained from Dr R. Chowdhury).[184]

3.3 Discussion

By employing cellular, biochemical and structural studies, the work in this chapter describes investigation on 2HG inhibition of 2OG dependent HIF hydroxylases and histone demethylases. Board concordance between the cell-based and *in vitro* results was observed. Because IDH mutations produce only *R*-2HG (not *S*-2HG),[109, 111] its inhibition is thus of more pathological relevance. However, for most of the human 2OG oxygenases tested *in vitro* and in cells, *R*-2HG is significantly less potent than *S*-2HG.

The HIF hydroxy-residue specific antibody assays indicated that HIF prolyl hydroxylation (*i.e.* Pro402 and Pro564) were poorly inhibited by high concentrations of *R*-2HG in VHL-defective RCC4 cells (**Fig. 3.2**). Consistent with this, *R*-2HG was also ineffective in stimulating HIF-1α in VHL competent cells (**Fig. 3.3**). These cell-based results were further supported by the *in vitro* biochemical data which confirmed *R*-2HG was an ineffective inhibitor for recombinant PHD2. Therefore, the high HIF activity observed in IDH-associated tumours is most probably not a direct result of competitive inhibition of *R*-2HG on PHDs.

Increased HIF activity in IDH-associated gliomas and IDH1 knockdown cells has been proposed to be caused by intracellular 2OG depletion due to the defective function of the IDH (mutant) in conversion of isocitrate to 2OG.[103, 192] It is possible that the depleted 2OG levels might synergize with *R*-2HG, inactivating HIF prolyl hydroxylases (or other 2OG oxygenases) and upregulating HIF by an unknown mechanism.[184] *R*-2HG in turn might potentially regulate HIF transcriptional activity by suppressing the FIH activity as elevated *R*-2HG was shown to suppress HIF aspraginyl hydroxylation in cells (**Fig. 3.2**). The potential effect of *R*-2HG mediated FIH inhibition could be further investigated in IDH mutant cell-lines.

Notably, both *R*- and *S*-2HG were shown to inhibit the histone N^{ε}-methyl lysine demethylase JMJD2A at potencies similar to NOG (a 2OG competitive inhibitor) (IC_{50} values ~ 20 μM) (**Table 3.1**). Defective JmjC histone demethylase genes have been correlated with multiple myeloma (a type of cancer arising from plasma cells in bone

marrow), glioblastoma multiforme (malignant primary brain tumour) and several other cancers.[199-201] Given the structural similarity of JMJD2A to some other JmjC family histone demethylases, it is possible that *R*-2HG will inhibit other demethylases. A recent study by Xu *et al.*[192]supports this proposal; the investigators reported that 2HG inhibits several histone demethylases including *C. elegans* histone demethylase CeKDM7A and human histone demethylases FBXL11 and KDM5B/JARID1B, with the *S*-enantiomer being the more potent inhibitor, consistent with the findings in this chapter.

The reported cell-based studies employing addition of exogenous 2HG (octyl-2HG, a cell-permeable 2HG derivative) or overexpression of the mutated $IDH1^{R132H}$ gene (both increase cellular *R*-2HG), demonstrated substantial inhibition on multiple human histone demethylase activities (e.g. H3K4me3, H3K9me2, H3K27me2, H3K79me2).[192] Together, these findings suggest the candidacy of histone demethylases as potential targets for 2HG-mediated tumourgenic progression. However, they by no means exclude other 2OG oxygenases or other mechanisms of 2HG-associated oncogenesis.[184] The elevated *R*-2HG levels (> 10 mM) that have been observed in malignant brain tumours and leukaemias,[109-111, 192] might be sufficient to inhibit even the less-susceptible 2OG oxygenases.[184]

Finally, excessive accumulation of *D(R)*-2HG or *L(S)*-2HG as a result of germline mutations in mitochondrial *D/L*-2HG dehydrogenases which catalyse the reversible reaction of 2OG from 2HG has been associated to a rare neurometabolic disorder, 2-HG aciduria[202-205]. Therefore, the findings of 2HG-dependent inhibition of 2OG dependent oxygenenases (*i.e.* FIH and histone demethylases) in this chapter also suggest their candidacies as potential therapeutic targets for 2HG aciduria therapy.

3.4 Conclusions and future directions

Overall, the findings in this chapter argue against HIF upregulation through the direct action of *R*-2HG inhibition on PHDs being a major factor in IDH1/2-mediated tumuorgenesis. However, excessive accumulation of *R*-2HG in IDH-associated gliomas might potentially regulate HIF transcriptional activity by inhibiting FIH. Notably, 2HG inhibition was found to regulate the activities of 2OG-dependent chromatin-modifying histone lysine demethylases, therefore suggesting oncogenic pathways mediated by 2HG elevation might involve epigenetic chromatin alterations. Future studies may involve direct analysis of the activities of histone demethylases and FIH using IDH1/2 mutant cell models.[103, 192]

Chapter 4: 2-Oxoglutarate Elevation Stimulates HIF-1α Induction in Cells

4.1 Background and Objectives

Krebs cycle intermediates, including 2-oxoglutarate (2OG), act both as carbon sources for macromolecular and small-molecule biosynthesis and energy sources for proliferating/tumour cells. 2OG is replenished into the Krebs cycle primarily through the glutaminolysis pathway (see **Introduction** in **Section 1.3.1)**. Due to a high flux of glutaminolysis being a common feature in tumour cells;[91, 92, 206] fluctuation of intracellular 2OG levels relative to normal cells can therefore be expected.

Glycolytic and Krebs cycle intermediates including pyruvate, oxaloacetate, malate, fumarate and succinate have been reported to inhibit the HIF prolyl hydroxylases (PHDs 1-3) *in vitro*.[80, 81, 100] Accumulation of some of these metabolites has also been reported to upregulate HIF-1α activity in cells.[80, 100, 102, 207] The PHDs have been reported to have high affinities for 2OG. Binding constant for 2OG for purified PHD2 is < 2 μM[157] and K_m values for 2OG for purified PHDs 1-3 are < 1 - 12 μM).[100, 208] (K_m values for 2OG of 55-60 μM have been reported for PHDs 1-3 obtained from soluble cell extracts).[26] Recombinant PHD2 can also be copurified with endogenous levels of 2OG.[157] Given the high affinities of PHDs for 2OG, it was considered possible that the PHDs may also be susceptible to 2OG fluctuation (*i.e.* their activities regulated by 2OG levels) in the tumour growth environment.

Although an elevated level of 2OG has not been commonly associated with oncogenesis, a 2.3-fold increase in urinary 2OG has been reported in a human gastric cancer mouse model.[209] High levels of plasma and urinary 2OG have also been associated with DOOR (deafness, onycho-osteodystrophy, and mental retardation) syndrome, a rare genetic disease resulting from a defective 2OG dehydrogenase complex which inefficiently catalyses the conversion of 2OG to succinyl-coA in the Krebs cycle.[210, 211] On the other hand, relatively high cellular 2OG concentrations (0.6 – 2.7 mM) have been reported in

healthy human liver and brain tissues[208, 212, 213] Given that the physiological 2OG levels in certain human tissues and cancer cells are well above the reported K_m values for PHDs 1-3 (<1-12 uM),[100, 208] the feasibility of a 2OG-mediated HIF transcriptional response may therefore be pathophysiologically relevant.

In this study, the potential 2OG inhibition of PHDs in cells was investigated. Using cellular and biochemical assays, the work described in this chapter demonstrates that HIF-1α can be upregulated by elevated 2OG levels in some cells, possibly as a result of substrate (2OG) inhibition of the PHDs. The work in this chapter was carried out in collaboration with Dr Y-M Tian, Andrew M. C. Chan, and Dr E. Flashman.

4.2 Results

4.2.1 PHD activity is inhibited by high concentrations of 2OG *in vitro*

High concentrations of the 2OG co-substrate have been reported to inhibit various 2OG-dependent oxygenases *in vitro*; including deacetoxycephalosporin C synthase,[214] thymine-7-hydroxylase,[215] DNA demethylase AlkB,[216] HIF prolyl hydroxylases,[80] and histone demethylases JMJD2A and FBXL11 (Schofield laboratory, unpublished data).

In the *in vitro* assays using cell lysate as a PHD source and a HIF-1α fusion protein (prepared using an *in vitro* transcription/translation system) as substrate, *Pan et al.*[80] demonstrated that when 2OG (5 mM) was added together with ascorbate (5 mM), HIF prolyl hydroxlation was increased by approximately 30%. However, when added alone, 2OG (0.1 mM and 1 mM) was found to suppress the prolyl hydroxylation by about 6%.[80] The investigators also showed that an addition of 3 mM 2OG reversed the inhibitory effect of 1 mM succinate on HIF prolyl hydroxylation, however, similar treatment further increased the inhibitory effects (6-14%) of 1 mM fumarate and 1 mM malate on HIF prolyl hydroxylation.[80] The reasons for these differences are unclear.

Ascorbate is normally used as a stimulant in assays for PHD activity.[26, 80, 157] Although ascorbate has been reported to increase the initial rate and promote activity of the recombinant PHDs, its contributions *in vivo* remain unclear.[26, 194] However, a recent *in vivo* study employing ascorbate-deprived *L*-gulonolactone oxidase knockout ($Gulo^{-/-}$) mice and ascorbate-free culture media showed that ascorbate is dispensable for cellular oxygen sensing *in vivo*.[217]

To study the hypothesis that 2OG may inhibit PHD activity, experiments were first carried out using the AlphaScreen PHD2 hydroxylation assay described in **Chapter 2** (**Section 2.2.4.1)**. 2OG was titrated exponentially from 0.1 nM to 100 mM into a reaction mixture which contained PHD2 (1 nM), Fe(II) (20 μM), and 19-mer biotinylated-CODD peptide (60 μM), in the presence or absence of ascorbate (200 μM) (experiments were performed by Andrew M. C. Chan).

The AlphaScreen results show that PHD2 activity was significantly inhibited at high 2OG concentrations (**Fig. 4.1 A**). In the absence of ascorbate, PHD2 reached its maximal activity at 10 μM 2OG, and the activity was substantially suppressed at higher concentrations (> 100 μM). On the other hand, higher doses (>1 mM) of 2OG were required for 2OG inhibition to take place in the presence of 200 μM ascorbate, possibly due to increased enzyme activity (**Fig. 4.1 A**).

Given the effects seen with 200 μM ascorbate, further assays were carried out with mixed concentrations of 2OG at 20 mM and 100 mM and titration of ascorbate into the reaction mixtures. Addition of ascorbate at 0.1-0.3 mM was found to effectively reverse the 2OG-mediated PHD2 inhibition as observed by increasing hydroxylation activity of the CODD peptide. However, at high concentrations (> 1mM), ascorbate was found to suppress PHD activity under the standard assay conditions (**Fig. 4.1 B**).

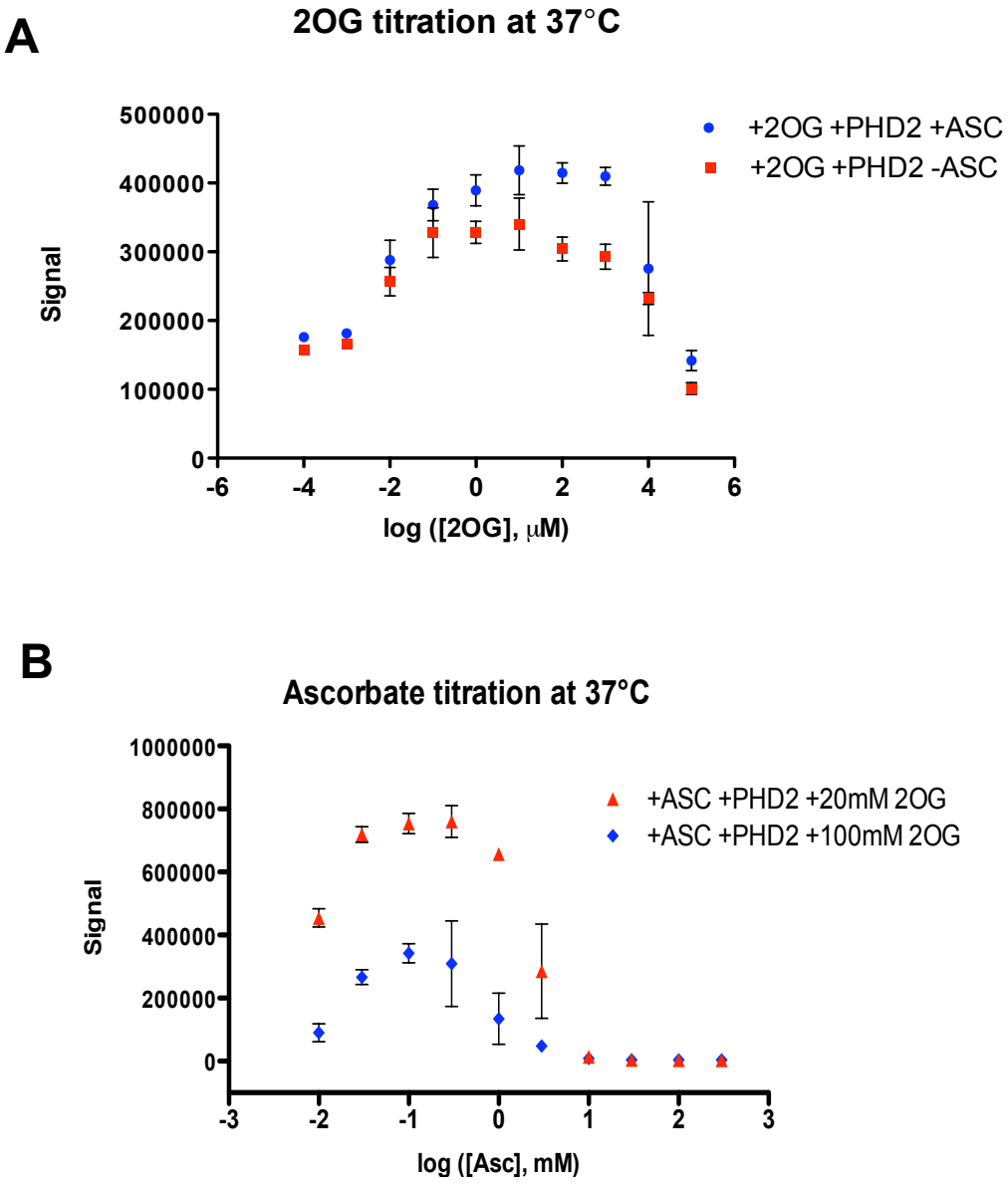


Figure 4.1: Inhibition of PHD2 by 2OG. (**A**) PHD2 activity was inhibited at increased 2OG concentrations. 2OG was titrated exponentially at concentrations: 0.1 nM, 1 nM, 10 nM, 100 nM, 1 μM, 10 μM, 100 μM, 1 mM, 10 mM, and 100 mM. The reaction mixtures contained PHD2 (1nM), Fe(II) (20 μM), biotinylated-CODD peptide (60 nM), in the presence or absence of ascorbate (200 μM). The reaction mixtures were incubated at 37°C for 10 min. (**B**) 2OG inhibition is reversed to some degree by ascorbate. Ascorbate was titrated (no ascorbate, 0.1 mM, 0.3 mM, 1 mM, 3 mM, 10 mM, 30 mM, 100 mM, 300 mM and 1 M) to the reaction mixtures which contained PHD2 (1nM), Fe(II) (20 μM), biotinylated-CODD peptide (60 nM), and 2OG (20 or 100 mM) and incubated at 37°C for 10 min. (Data obtained from Andrew M. C. Chan).

4.2.2 Ascorbate is important to maintain stability of PHD2.Fe.2OG complex *in vitro*

The effects of ascorbate on 2OG mediated inhibition of PHD2 were further investigated using two different biochemical assays: (i) matrix-assisted laser desorption/ionization mass spectrometry (MALDI MS) hydroxylation assay, and (ii) ultraviolet (UV) absorbance assay (experiments were carried out by Dr E. Flashman).

In the MALDI MS hydroxylation assay, PHD2 activity was measured by monitoring the hydroxylation of a 19-mer CODD (residues 556-574) peptide as observed by an addition of a +16 Da mass shift in the mass spectrum.[194] Mixtures containing recombinant PHD2, Fe(II), and 2OG were pre-incubated at room temperature for 0, 15, 30, 45, 60 min in the presence or absence of ascorbate. The incubation was then followed by the addition of the CODD peptide and a subsequent standard 5 min hydroxylation assay. Where ascorbate had not been added in the incubation, it was introduced to the assay mixture at this point. Interestingly, pre-incubation of the PHD2.Fe.2OG mixture in the absence of ascorbate was shown to substantially inactivate the enzyme over the period of 1 h, contrary to the observation that the PHD2.Fe.2OG.ascorbate mixtures retained optimal activity after 1 hr. The inactivation cannot be reversed by the later addition of ascorbate (**Fig. 4.2 A**).

In the UV absorbance assays, the stability of the PHD2.Fe.2OG complex was monitored by UV absorbance at 250-800 nm (wavelength). Interestingly, in the absence of ascorbate, the broad increase in absorbance over the whole spectrum indicates precipitation of the PHD2.Fe.2OG complex over the period of 1 h (compare **Fig. 4.2 B** and **C**). In contrast, the UV absorbance was shown to persist over the 1 h incubation when the reaction mixture contained ascorbate. Precipitation of the PHD2.Fe.2OG complex could possibly be the reason for the inactivation observed in the MALDI MS hydroxylation assay. However, this *in vitro* observation might not be relevant in the *in vivo* system.

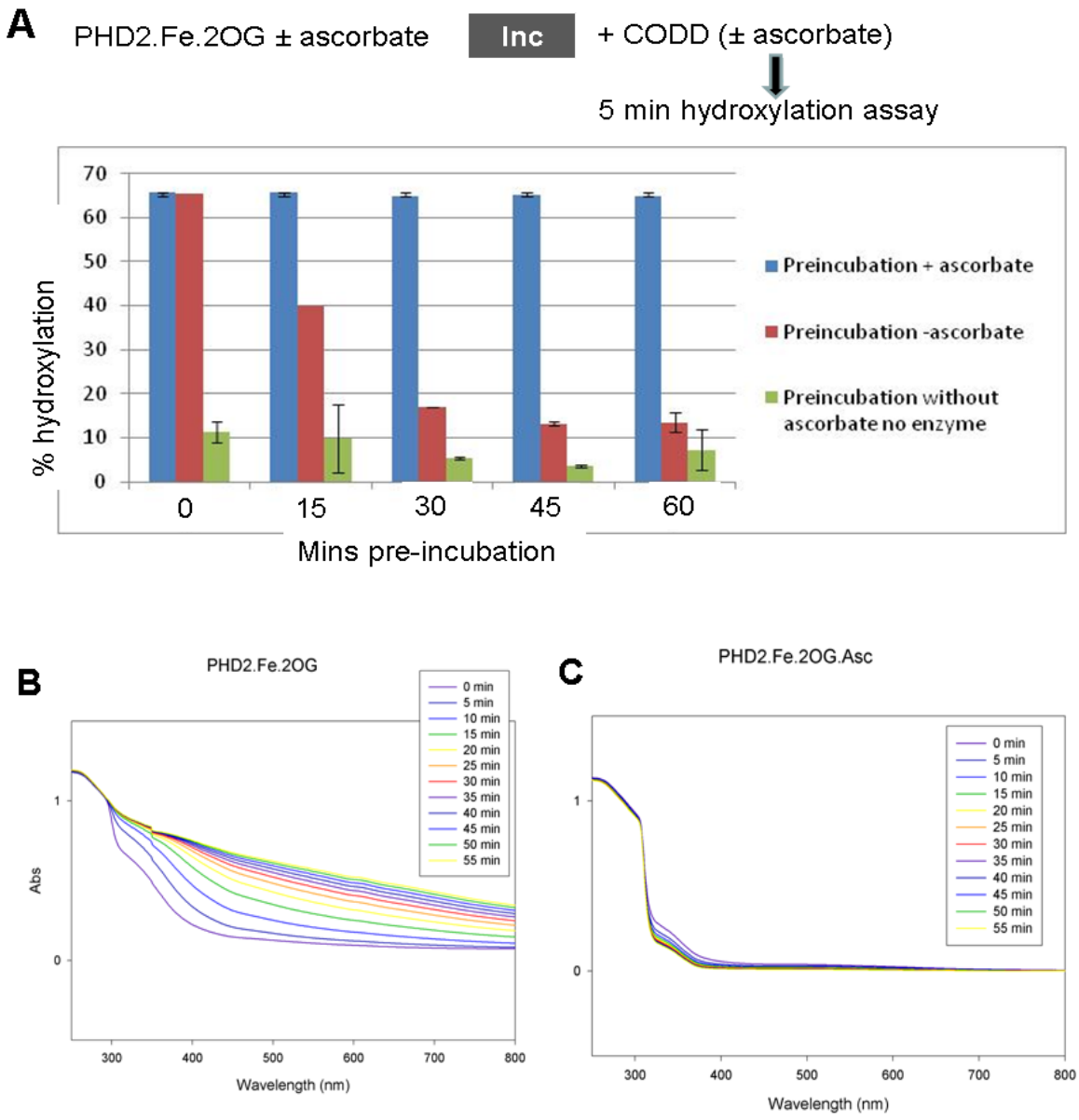


Figure 4.2: Ascorbate is important to maintain the activity and stability of PHD2.Fe.2OG complex. (**A**) The MALDI MS hydroxylation assay for PHD2 activity suggests inactivation of PHD2.Fe.2OG complex in the absence of ascorbate. (Assay conditions: PHD2 = 4 μM, Fe(II) = 50 μM, CODD peptides = 100 μM, 2OG = 300 μM, ascorbate = 4 mM) (**B**) UV absorbance time course experiments indicate the PHD2.Fe.2OG complex forms precipitation over time in the absence of ascorbate. (**C**) Ascorbate was clearly shown to protect against the precipitation of the PHD2.Fe.2OG complex. Assay conditions: PHD2 = 100 μM, Fe(II) = 1.25 mM, 2OG = 7.5 mM, ascorbate = 100 mM; replicating the ratios used in (**A**). (Data obtained from Dr E. Flashman)

4.2.3 2OG ester derivatives are ineffective PHD inhibitors *in vitro*

The *in vitro* results described above demonstrate that PHD2 can be inhibited by high concentrations of 2OG in the presence or absence of ascorbate. This was then further investigated in cells. 2OG is a hydrophilic molecule, therefore it cannot efficiently penetrate the cell membrane and achieve sufficiently high intracellular concentrations.[104] Therefore, a series of potential cell-penetrating mono- and di-esters 2OG derivatives were synthesised (**Fig. 4.3**, compounds were prepared by Armin Thalhammer). Among these 2OG analogues, dimethyl-2OG (DM-2OG),[102, 218-221] octyl-2OG (MO-2OG), and 3-trifluoromethylbenzyl-2OG (MTF-2OG)[104] have previously been reported as precursors of 2OG in cell-based studies.

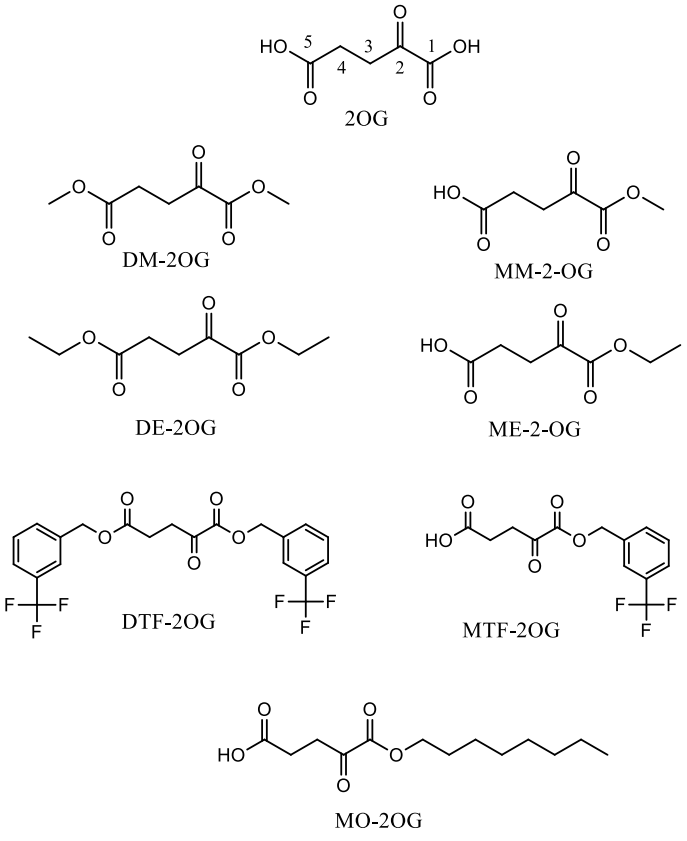


Figure 4.3: (**A**) Structures of the 2-oxoglutarate (2OG) ester derivatives tested in the cell-based assays; dimethyl-2OG (DM-2OG), monomethyl-2-OG (MM-2OG), diethyl-2OG (DE-2OG), monoethyl-2OG (ME-2OG), di-(3-trifluoromethylbenzyl)-2OG (DTF-2OG), 3-trifluoromethylbenzyl-2OG (MTF-2OG), and octyl-2OG (MO-2OG).

To exclude the possibility of direct PHD inhibition by the 2OG esters, their inhibitory potencies were first tested *in vitro* using the AlphaScreen PHD2 hydroxylation assay (by Andrew M. C. Chan). The results demonstrated no inhibition of recombinant PHD2 activity by the 2OG ester derivatives; except for DTF-proctecting 2OG which may lead to weak inhibition (**Fig. 4.4**).

2OG is expected to bind to PHD2 in a bidentate manner by chelating the active site iron, in a similar (but not necessarily identical) manner to the unreactive 2OG analogue *N*-oxalylglycine (NOG) (**Fig. 4.5**).[34] A crystal structure of PHD2 in complex with NOG (see **Section 2.2.3**, **Fig. 2.4**) suggests that the C-1 carboxylate and C-2 oxo groups of 2OG coordinate the iron whereas the C-5 carboxylate oxygens of 2OG are positioned to form a salt bridge with the nearby Arg383 residue in the PHD2 active site[34]. In these 2OG ester analogues, C-1 or/and C-5 oxygen atoms were used in the formation of mono- or di-ester bonds which caused the oxygen atom to be more electropositive, therefore likely preventing or hindering the salt bridge formation or iron coordination. Structural studies also indicate that the 2OG binding pocket in the PHD2 is relatively narrow and small,[31] thus steric factors might also prevent the binding of these 2OG esters to PHD2.

Interestingly, incubation of PHD2 with the C-1 mono-esters MM-2OG, ME-2OG and MTF-2OG resulted in higher enzyme activity compared to (no compound) controls. This may be a result of non-enzymatic (or enzymatic) hydrolysis of the C-1 alkyl-esters leading to increased 2OG (substrate) concentration and enhanced enzyme activity. This view is supported by a previous study which showed that C-1 mono-methyl and mono-ethyl esters of *N*-oxalylglycine (NOG) were hydrolysed to form NOG in reaction mixtures, therefore forming a PHD2.Fe.NOG complex which was detected by non-denaturing mass spectrometry.[222] However, no complex was formed when C-5 mono-methyl NOG was incubated with PHD2.[222]

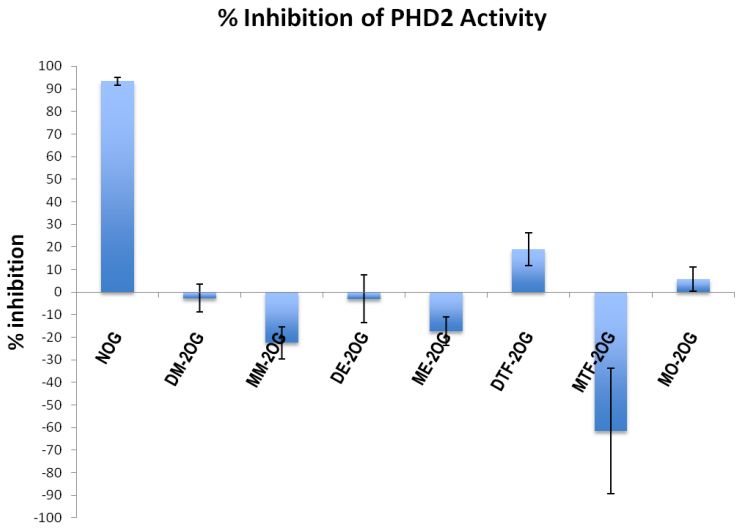


Figure 4.4: 2OG ester derivatives did not inhibit PHD2 *in vitro*. Assay conditions: DM-2OG (1 mM), MM-2OG (1 mM), DE-2OG (1 mM), ME-2OG (1 mM), DTF-2OG (50 µM), MTF-2OG (1 mM), MO-2OG (1 mM), NOG (20µM) was used as positive control for comparison. AlphaScreen PHD2 assay conditions: PHD2 (1 nM), Fe^{2+} (20µM), and COOD peptides (60 µM). (Data obtained from Andrew M. C. Chan)

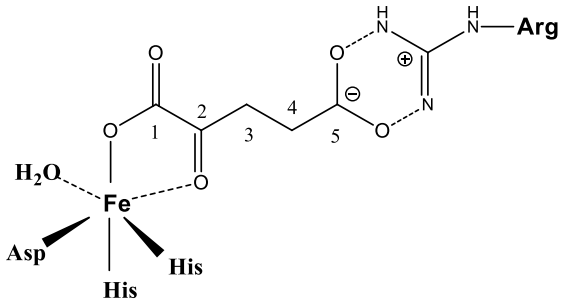


Figure 4.5: Proposed outline binding mode of 2OG in the PHD active site.[34]

4.2.4 Exogenous 2OG stabilises HIF in cells

It was proposed that if elevated 2OG levels could lead to PHD inhibition in cells, increased HIF-1α activity might be detected. To test this hypothesis, RCC4 re-expressing functional VHL (RCC4/VHL) cells were incubated with the 2OG ester derivatives at 2 and 10 mM. After 4 h, extracts were prepared and analysed by immunoblotting. The immunoblots are shown in **Fig. 4.6 A** and **B**. Surprisingly, DM-2OG, but not the other 2OG ester derivatives, was shown to substantially upregulate HIF-1α in cells (**Fig. 4.6 A** lanes 2 and 3). DM-2OG was also shown to induce HIF-1α in a concentration-dependent manner (**Fig. 4.6 A** lanes 2, 3). Weak HIF-1α induction was observed for diethyl-2OG (DE-2OG) and monoethyl-2OG (ME-2OG) treated cells. Some morphological changes/cell-detachment were observed in the DE-2OG, MTF-2OG, DTF-2OG and MO-2OG treated cells, indicating that the compounds may be toxic (possibly due to their acylating potential).

When the cells were exposed to increased concentrations of methanol (the 2OG dimethyl ester hydrolysis product), no HIF-1α upregulation was observed (**Fig. 4.6 C**), arguing against the possibility of HIF-1α stabilisation by the ester hydrolysis product. DM-2OG was therefore selected as a candidate cell-penetrating 2OG analogue in subsequent cell-based experiments. In the cells, DM-2OG can be cleaved to produce either, or both of, C-1 or C-5 mono-methyl 2OG, and subsequently 2OG, by the activity of esterases in the cell cytosol.[218] Previous *in vitro* studies and structural analyses suggest that the C-1 and C-5 mono-methyl 2OG esters are probably ineffective as PHD inhibitors (see above).

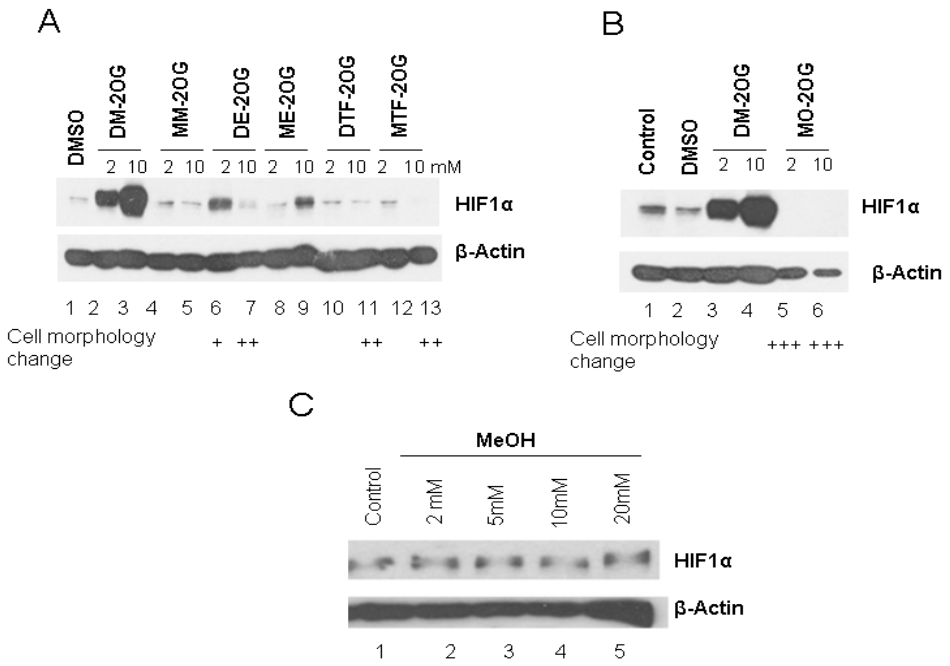


Figure 4.6: 2OG elevation leads to HIF-1α upregulation in cells. (**A**-**B**) 2OG ester analogues were incubated with RCC4/VHL cells for 4 h; the resulting cell extracts were probed with HIF-1α antibody. (2OG analogues were prepared as 20 mM and 1 M stock solutions in DMSO and added to cells at 1% DMSO) (**C**) Ester hydrolysis product methanol (MeOH) did not upregulate HIF-1α in RCC4/VHL cells.

High concentrations of exogenous succinate, fumarate and *S*-2-hydroxyglutarate (*S*-2HG) (**Chapter 3**) have also been shown to upregulate HIF-1α in cells.[100, 104, 192] Therefore, the HIF induction potency of DM-2OG was next compared with dimethyl succinate (DM-Succ), dimethyl fumarate (DM-Fuma) and dimethyl *S*-2HG (DM-*S*-HG). Surprisingly, in all cases, HIF stabilisation by DM-2OG elevation was significantly higher (> 5 fold) than that with DM-Fuma, DM-Succ, or DM-*S*-2HG treated cells (**Fig. 4.7 A** and **B**), suggesting that application of 2OG derivatives is as potent a method as, if not stronger, than addition of fumarate or succinate, at HIF-1α stabilisation, at least in the tested cell-types.

Interestingly, exogenously applied 2OG (using MO-2OG at 1-3 mM[104] or DM-2OG at 2 mM[102]) has been reported to alleviate HIF-1α levels and restore the PHD enzyme activity of succinate- or fumarate-mediated PHD inhibition in cells.[102, 104] Pharmacological elevation of intracellular 2OG has therefore been proposed as a potential therapeutic target for dysfunctional Krebs cycle associated tumorigenesis.[104] However, the current

work shows that at these concentrations (2 mM or higher), exogenous 2OG (*i.e.* DM-2OG) can in fact upregulate HIF (MO-2OG at 2 mM was shown to be cytotoxic under the standard assay conditions in this study, **Fig. 4.6 B**), at least in the tested cell-lines. Therefore, the dose-dependent effects of 2OG on HIF-1α levels should be taken into consideration in any therapeutic approaches involving application of 2OG derivatives aimed at elevated 2OG levels in cells. It is also worth noting that physiological concentrations of 2OG in certain human tissues/cells (e.g. brain) are well above 2 mM.[208]

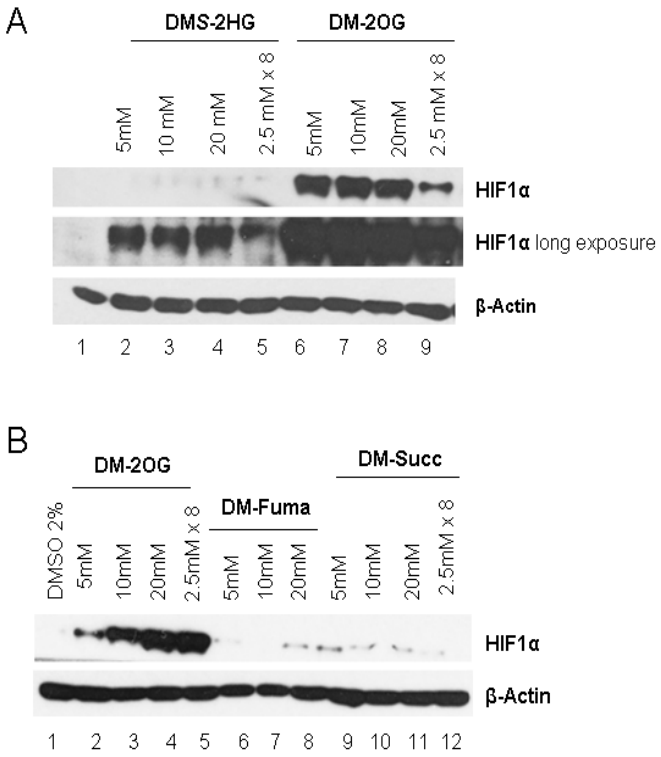


Figure 4.7: (**A-B**) HIF-1α accumulation induced by dimethyl-2-oxoglutarate (DM-2OG) in comparison to dimethyl *S*-2-hydroxyglutarate (DM-*S*-2-HG), dimethyl fumarate (DM-Fuma) and dimethyl succinate (DM-Succ). RCC4/VHL cells were treated with the compounds at the indicated concentrations at single or multiple additions (2.5 mM x 8, at 30 min intervals) for 4 h.

4.2.5 Evaluation of 2OG dependent inhibition of PHDs in cells

To investigate whether the increase in HIF-1α protein levels caused by 2OG elevation could be a result of inhibition of HIF hydroxylases, RCC4/VHL cells were exposed to DM-2OG in the presence of the proteasome inhibitor MG132. RCC4-VHL defective cells (RCC4 cells) were also treated with DM-2OG (**Fig. 4.8 A-B**). Proteasomal-inhibited or VHL-deficient cells have constitutive HIF-1α as a result of defective ubiquitin-proteasome dependent proteolysis pathways.[223] By employing hydroxy-residue specific antibodies, the potential 2OG-dependent inhibition on Pro402 (NODD), Pro564 (CODD) and Asn803 (CAD)-hydroxylation could then be measured simultaneously (**Chapter 2**).

As expected, immunoblots of the MG132 treated cells demonstrate high levels of HIF-1α and HIF-2α, and the HIF-1α hydroxylation sites (Pro402, Pro564, and Asn803) were also hydroxylated (**Fig. 4.8 A**, lane 2). Interestingly, in the presence of DM-2OG, HIF prolyl hydroxylation (*i.e.* Pro402 and Pro564) were substantially inhibited, whereas asparaginyl hydroxylation remained almost unaffected (**Fig. 4.8 A**, lanes 3 and 4), clearly demonstrating selectivity in the effects of 2OG addition (compare with DM-*S*-2HG-mediated HIF-1α stabilisation in which HIF-1α was substantially inhibited on both prolyl and asparaginyl hydroxylation; **Chapter 3, Fig. 3.4**). The presence of slower-mobility species (higher molecular weight protein) is a common feature in HIF-1α immunoblots[223] (believed to be ubiquitinated HIF-1α). The detection of a lower level of the slower-mobility species in DM-2OG treated cells (**Fig. 4.8 A** right, long exposure film, compare lanes 2 and 4) is consistent with the observed decrease in prolyl hydroxylation.

In contrast, however, the results from DM-2OG treated RCC4 cells did not demonstrate any convincing inhibition of prolyl hydroxylation or asparaginyl hydroxylation (**Fig. 4.8 B**, there is perhaps some weak evidence for inhibition of Pro564 hydroxylation at 20 mM DM-2OG; compare lanes and 4 to lane 1). The lack of substantial inhibition by DM-2OG observed in RCC4 cells may be a result of the elevated HIF prolyl hydroxylase activity in these cells. In RCC4 cells, HIF-1α is constitutively activated, and PHD2 and PHD3 are present in high abundance relative to other VHL competent cell lines.[223, 224] PHD2 and PHD3 are themselves transcriptional targets of HIF-1α and are significantly upregulated

by hypoxia.[17, 179] However, in RCC4 cells, no further induction of PHD2 and PHD3 protein levels was observed under hypoxia.[142, 224] It has also been reported that HIF-1α hydroxylation in RCC4 cells is close or almost close to completion in normoxia.[142] As a result, 2OG (substrate) inhibition on HIF hydroxylation might not be conveniently demonstrated in these VHL-defective cells.

It was considered that addition of low concentrations of 2OG may activate PHD activity, whereas high concentrations of 2OG may inhibit the hydroxylase activity. The work therefore investigated whether DM-2OG could potentially reverse the effect of DMOG-induced HIF-1α in human embryonic kidney 293T cells. DM-2OG at lower concentrations (1 mM) was shown to modestly decrease the inhibitor-induced HIF-1α level (**Fig. 4.8 C**, lane 3). On the other hand, at high concentrations (5 and 10 mM), DM-2OG was demonstrated to induce HIF-1α in 293T cells showing that the HIF-stabilisation by elevated 2OG is not cell-type dependent. The level of DM-2OG-induced HIF-1α at 10 mM was shown to be similar to DMOG-stabilised HIF-1α at 0.5 mM (**Fig. 4.8 C**, compare lanes 2, and 7).

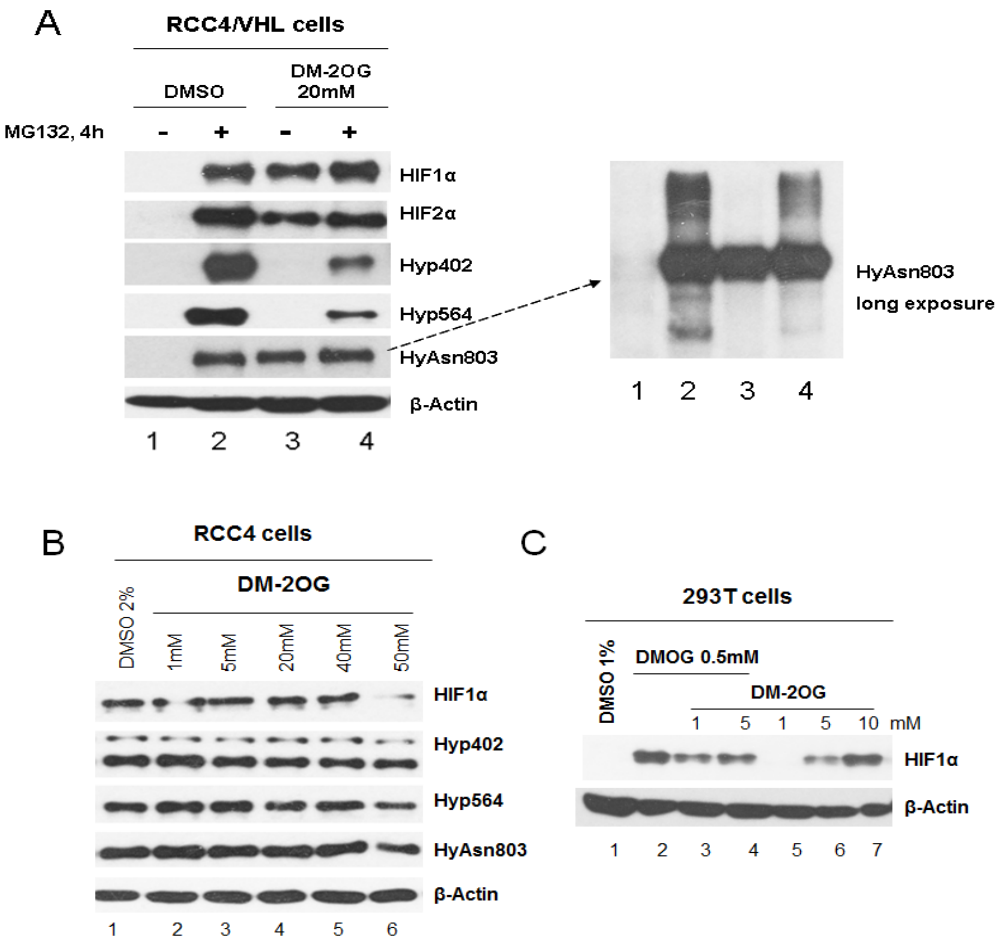


Figure 4.8: (**A**) RCC4/VHL cells were exposed to DM-2OG for 5 h; MG132 was added in the last 4 h. Pro402- and Pro564-hydroxylation were substantially inhibited in the DM-2OG treated cells, in the presence and absence of proteosome inhibitor MG132. (**B**) Increased concentrations of DM-2OG were added to RCC4 cells for 5 h. No significant inhibition on HIF prolyl and asparaginyl hydroxylation was observed, DM-2OG was found to be cytotoxic at concentrations > 50mM. (**C**) DM-2OG was shown to modestly decrease the DMOG-induced HIF-1α levels in human embryonic kidney 293T cells. 293T cells were first exposed to DMOG (0.5 mM, 5 h), DM-2OG was added for the last 4 h.

4.2.6 2OG-induced HIF-1α stabilisation is alleviated by ascorbate

The *in vitro* findings demonstrate that 2OG mediated PHD2 inhibition could be reversed by the addition of ascorbate (**Fig. 4.1**). Ascorbate (as a reducing agent) has been proposed to promote PHD activity by maintaining and replenishing Fe(II) in the enzyme active site.[225] Therefore, the potential effects of ascorbate on the stability of 2OG-induced HIF-1α in cells were further examined.

Human osteosarcoma U2OS cells were first exposed to DMOG controls and DM-2OG at different concentrations in the presence or absence of ascorbate. The DMOG/DM-2OG treatment increased HIF-1α levels and these were strikingly suppressed in the presence of ascorbate (1 mM) (**Fig. 4.9 A**). Ascorbate was also shown to be more effective in alleviating the DMOG-induced HIF levels compared to the addition of DM-2OG (**Fig. 4.9 A**, lanes 3, 4 and 9). Similar observations were also demonstrated in RCC4/VHL cells exposed to DM-2OG, DMOG, and BIQ (a specific PHD inhibitor, see **Chapter 2**) in the presence of ascorbate, however the ascorbate alleviation effect was slightly weaker in the BIQ treated cells (**Fig. 4.9 B**).

The ability of ascorbate to prevent the induction of HIF-1α by DM-2OG in cells may be due to increased PHD activity mediated by the presence of ascorbate. To study this, RCC4 cells were exposed to DMOG, BIQ, and DM-2OG in the presence or absence of ascorbate. As expected, in the absence of ascorbate, DMOG modestly suppressed HIF prolyl hydroxylation, and BIQ strongly restricted PHD activity in RCC4 cells. DM-2OG was again found to have no apparent effect on the prolyl hydroxylation status in RCC4 cells. Interestingly, in the presence of ascorbate, the prolyl hydroxylation status of the inhibitor-treated cells (especially in the case of BIQ) was modestly increased (**Fig. 4.9 C**, compare lanes 5 and 11), which is an indication of increased PHD activity. However, it is worth noting that the concentration of ascorbate tested in the cell-based experiments (*i.e.* 1 mM) is well above the reported K_m values for ascorbate for PHDs 1-3 (140-180 μM)[26] and the reported physiologically relevent levels of ascorbate (~ 25-50 μM).[225]

In conclusion, the combined findings from the *in vitro* and cell-based studies show that ascorbate can alleviate the 2OG-mediated elevation of HIF-1α levels in cells, possibly by promoting PHD activity in cells. Cellular ascorbate concentration may therefore be a determinant factor in potential regulation of PHD activity by 2OG fluctuation in cells. However, it should be noted that the role of ascorbate in PHD catalysis and the HIF system is unclear, with the available evidence being that it is not essential.

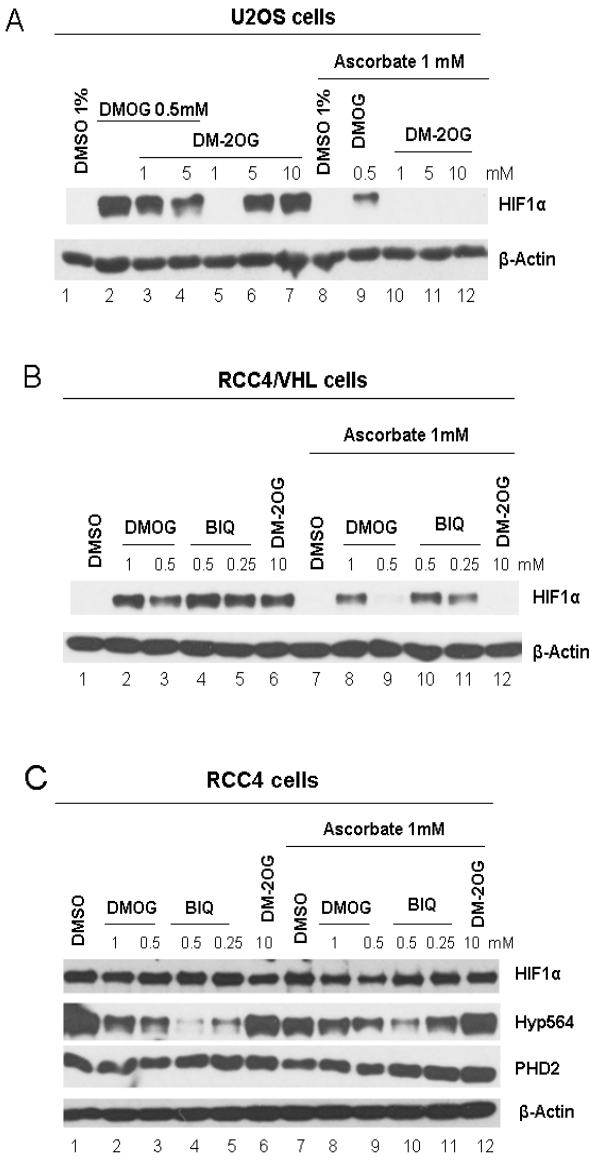


Figure 4.9: The effect of ascorbate on PHD inhibitor- and 2OG-mediated HIF induction. (**A-B**) Ascorbate alleviated 2OG-induced HIF stabilisation in U2OS and RCC4/VHL cells. (**C**) Ascorbate increased PHD activity in RCC4 cells as shown by Hyp564 immunoblot. Cells were exposed to DMOG, BIQ, and DM-2OG in the presence or absence of ascorbate at indicated concentrations for 4 h.

4.3 Discussion

The combined *in vitro* and cell-based results provide evidence that high 2OG levels can inhibit both recombinant PHD2 and endogenous PHD activity in cells. 2OG elevation (> 2 mM) substantially upregulates HIF-1α (and HIF-2α) in VHL-competent cells. Further elevated 2OG levels were shown to significantly suppress the HIF-1α prolyl hydroxylation (but not the asparaginyl hydroxylation) in the proteasome inhibitor treated cells, showing a higher degree of selectivity for PHD over FIH. This finding is supported by the *in vitro* findings which show purified recombinant PHD2 has a high affinity for the 2OG co-substrate.[157]

However, the cell-based studies employing (VHL-defective) RCC4 cells did not support the proposal of 2OG inhibition of PHDs. No apparent suppression on HIF prolyl hydroxylation was observed in the DM-2OG treated RCC4 cells. It can be argued that PHD enzyme abundance is an important determinant factor in the case of 2OG inhibition. As previously discussed, PHD2 and PHD3 are themselves positively regulated by HIF-1α,[17, 223] constitutive activation of HIF-1α in RCC4 is expected to result in higher rates of catalysis (PHDs 1-3 specific activities are approximately 20 mol/mol/min).[226] It is possible that the exogenously applied 2OG (co-substrate of the PHDs) may be effectively turned over by the PHDs (or other HIF regulated 2OG oxygenases present in RCC4 cells), resulting in little or no suppression of HIF-1α prolyl hydroxylation in these VHL-defective cells.

Other cellular mechanisms of 2OG-mediated PHD inhibition/HIF stabilisation are also possible. It is possible that the artificial increase in intracellular 2OG level may promote the production of the downstream Krebs cycle intermediates (**Fig. 4.10**) or other related metabolites. Given that high concentrations of succinate, fumarate, malate, oxaloacetate, and pyruvate have been shown to inhibit the PHDs *in vitro* and upregulate HIF-1α in cells,[80, 81, 100, 102, 207] the observed 2OG-mediated HIF stabilisation in VHL-competent cells may be the result of the collective effects of these downstream metabolites (especially succinate (PHD2 IC_{50} 85 μM)[165] and fumarate (PHD2 IC_{50} 19 μM)[165]). This proposal is

supported by a previous report which demonstrated that addition of 2OG (3 mM) increased the inhibitory effects of fumarate and malate on HIF prolyl hydroxylation, in an *in vitro* experiment using cell-lysate as PHD source[80].

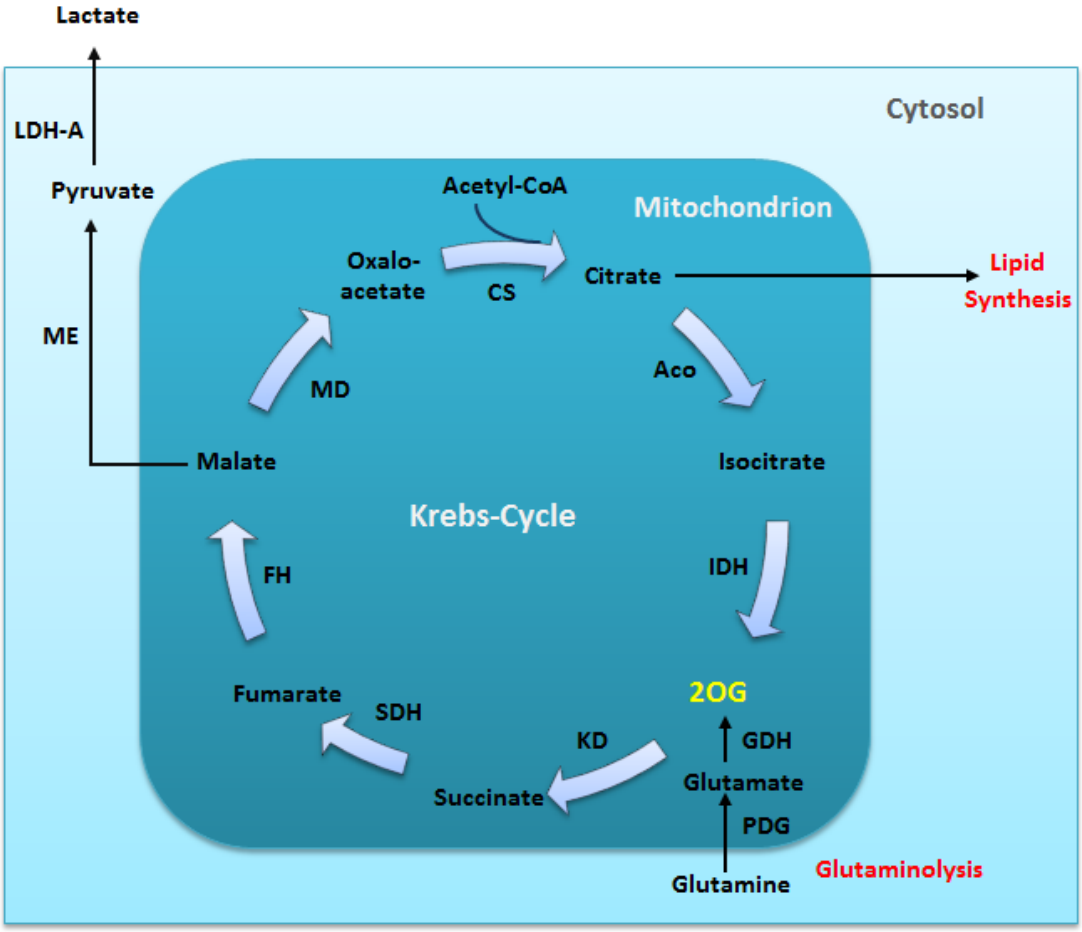


Figure 4.10: Elevation of the intracellular 2OG level is expected to result in increased downstream metabolic intermediates including succinate, fumarate, malate, oxaloacetate and pyruvate which have all been shown to inhibit HIF prolylhydroxylases. Aco, aconitase; IDH, isocitrate dehydrogenase; KD, α-ketoglutarate dehydrogenase; SDH, succinate dehydrogenase; FH, fumarate hydratase; MD, malate dehydrogenase; CS, citrate synthase; ME, malic enzyme; LDH-A, lactate dehydrogenase-A; GDH, glutamate dehydrogenase, PDG, phosphate-dependent glutaminase.

The work in this chapter indicates that HIF-1α levels induced by exogenous 2OG are in fact many times higher than those stabilised by cell-penetrating derivatives of fumarate and succinate (**Fig. 4.7 B**). The reason for this is unclear. One possibility is that it is due to the differing cell-permeability of the 2OG, fumarate, and succinate ester derivatives.

Beside the PHDs, there are many other enzymes which employ 2OG as substrate/co-substrate (e.g. 2OG dehydrogenases, 2OG decarboxylases and other 2OG dependent oxygenases).[20, 227, 228] It is therefore possible that 2OG inhibition of these other 2OG-dependent enzymes may be affecting the HIF-pathway. It is worth noting that physiological concentrations of 2OG (K_i value of 0.32 mM) have been reported to competitively inhibit the purified rat liver phosphoenolpyruvate carboxykinase (PEPCK) that catalyses the conversion of oxaloacetate to phosphoenolpyruvate in gluconeogenesis.[229]

Other pathways can influence HIF-1α induction. Stimulation of endothelin-1 (a 21-amino-acid vasoconstrictor peptide that is involved in regulation of blood pressure) has been shown to stabilise HIF-1α by suppressing PHD2 mRNA and protein levels.[230] Growth factors such as insulin, insulin-like growth factor-1 and -2, and heregulin have also been proposed to activate HIF-mediated responses through the PI3K/Akt/mTOR pathways (see **Introduction** in **Section 1.3.4**) by stimulating HIF-1α translation/protein synthesis.[1, 231, 232] (Interestingly, DM-2OG was also reported to stimulate insulin secretion from β-cells in isolated pancreatic islets).[219, 220] The possible involvement of these pathways in 2OG-mediated PHD inhibition/HIF stabilisation needs further investigation.

4.4 Conclusions and future directions

In conclusion, the research in this chapter shows that, when present at high concentrations, cellular 2OG can negatively regulate PHD activity and stimulate HIF-1α activity in various VHL-competent cells. The *in vitro* results suggest that inhibition of the PHD is a possible mechanism; however, it is unclear if this is the case in cells. In addition, the findings also suggest that ascorbate availability and PHD enzyme abundance in the cellular environment are potential determinants for 2OG-mediated PHD inhibition/HIF stabilisation.

To further investigate if 2OG-mediated HIF-stabilisation is indeed a direct effect of PHD inhibition, future studies may involve quantitative measurement of 2OG cellular levels and the changes in the concentrations of downstream metabolites after compound treatments by employing spectroscopic methods. Experiments could be carried out to investigate the potential effects of 2OG elevation on both the mRNA and protein expression of PHDs, HIF-1α and other HIF-α target genes.

Chapter 5: Towards Selective Inhibition of Variant of the HIF Prolyl Hydroxylase-2 Isoform

5.1 Background and Objectives

By combining protein engineering and small-molecule based methods, Shokat and co-workers have developed a 'chemical-genetic approach' in their studies on the roles of a range of kinases including tyrosine and serine/threonine kinases SAD-1 (synapses of amphids defective-1) and CDK-1 (cyclin-dependent kinase Cdc28).[233-238] In these studies, active site variants of kinases are engineered by substituting naturally occurring residues with smaller residues (typically glycine or alanine) in order to create unique binding pockets that could be selectively inhibited by chemically modified bulkier analogues that did not inhibit the wild-type enzyme. This strategy has been applied in yeast, *C. elegans*, mammalian cell lines, and mice.[233-238]

The chemical-genetic approach enables functional studies which allow the variant enzyme be inhibited selectively. Their initial work employed substitution of the Ile338 residue in the ATP binding site of v-Src tryrosine kinase with glycine. This newly created pocket conferred unique inhibitory-sensitivity to chemically modified analogues of PP1, a Src-family selective inhibitor.[239-242] The corresponding 'gate-keeper' residues (*i.e.* Ile 338 in v-Src) for other protein kinases including SAD-1 were later identified and equivalent mutations were introduced. In this way, a series of kinase-active analogue-sensitive alleles of protein kinases were systematically generated and functionally characterised.[233, 235, 236, 243, 244]

In a demonstration of the 'chemical-genetic' approach, the activity of the SAD-1 kinase was shown to be important for neuronal polarization and synapse formation.[236] This approach has been proposed to have potential for identifying proteins involved in a wide range of human diseases and which may therefore be targets for drug development.[64, 245-248]

Inspired by these studies, it was proposed to apply this strategy in functional studies of human PHD isoforms. By combining molecular biology (protein design) and a small-molecule based method (chemical design), the aims of the project were to design and synthesise specific small-molecule inhibitors which do not inhibit wild-type PHD2, but do inhibit PHD2 variants with specially engineered mutations of targeted amino acid residues (**Fig. 5.1**). This chapter demonstrates the feasibility of specific inhibition of the PHD2 variants by the designed inhibitors *in vitro*, and reports an attempt to test this system in mammalian cells.

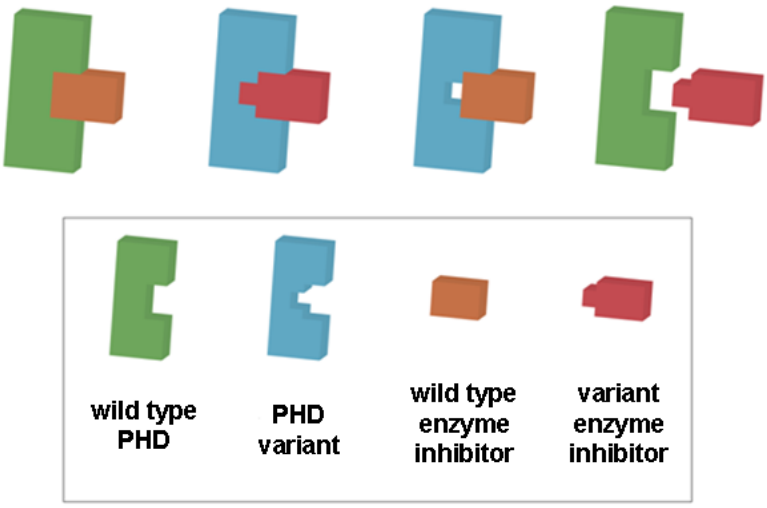


Figure 5.1: Schematic presentation of the 'bump-pocket' approach employed in this work. The wild-type enzyme inhibitor inhibits both the wild-type and variant enzyme but the variant enzyme inhibitor 'bumps' into the wild-type enzyme and preferentially inhibits the variant enzyme.

5.2 Results and Discussion

5.2.1 Generation of the PHD2 variants

PHD2 has been identified as the most important isoform of the human PHDs in hypoxia response under normoxic conditions,[22] and was therefore chosen as the subject of investigation in this study. It was hoped that specific inhibition of PHD2 may reveal information about its specific function. A crucial consideration for the success of this research is the choice of PHD2 active site residues for site directed mutagenesis;[249] one reason is that the PHD2 variants should retain similar activity to the wild-type enzyme. Four potentially variable residues in the active site of wild-type PHD2 (WT-PHD2) were initially selected for single point substitutions. The relatively large side chains of these residues, Ile327, Leu343, Phe366, and Val376, were substituted for smaller side chains. For example, Ile327 was substituted for alanine, thus creating a new 'hole' in the active site. Four single point PHD2 variants were created, produced in *E. coli*, and purified; they were I327A-, L343A-, F366L-, and V376A-PHD2. **Fig. 5.2** shows the active site residues chosen for substitution. Crystallographic analyses suggest that these residues may play a structural role at the active site, but they do not directly bind to substrates or iron,[31, 34] therefore it was considered possible that this alteration might not directly affect the function of the PHD2 variants.

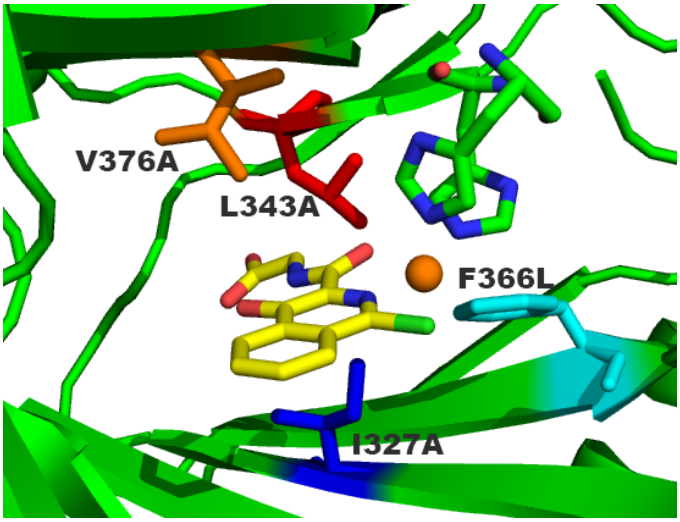


Figure 5.2: View from crystal structure of PHD2 in complex with Fe(II) and bicyclic isoquinoline (**BIQ**) inhibitor (PDB ID 3HQU) showing the active site residues selected for single point mutations (highlighted).

Pre-designed primers were used to generate the point mutations encoding for I327A, L343A, F366L, and V376A variants in a pET-28a(+) *phd2(181-426)* plasmid (previously generated by Dr K. Hewitson)[31] using the site-directed mutagenesis Polymerase Chain Reaction (PCR) method (Stratagene). The corresponding plasmids were transformed into *E. coli* BL21 (DE3) competent cells. Expression trials were carried out to determine the conditions under which the greatest soluble production of the variants could be achieved. The results showed that the highest soluble expression for all the four variant proteins was obtained when bacteria were grown at 15°C for 20 h, following induction with 0.5 mM IPTG (isopropyl β-D-1-thiogalactopyranoside). Sodium dodecyl sulphate polyacrylamide gel electrophoresis (SDS-PAGE) gels of the expression trials of L343A-PHD2 are shown in **Fig. 5.3** as representative examples.

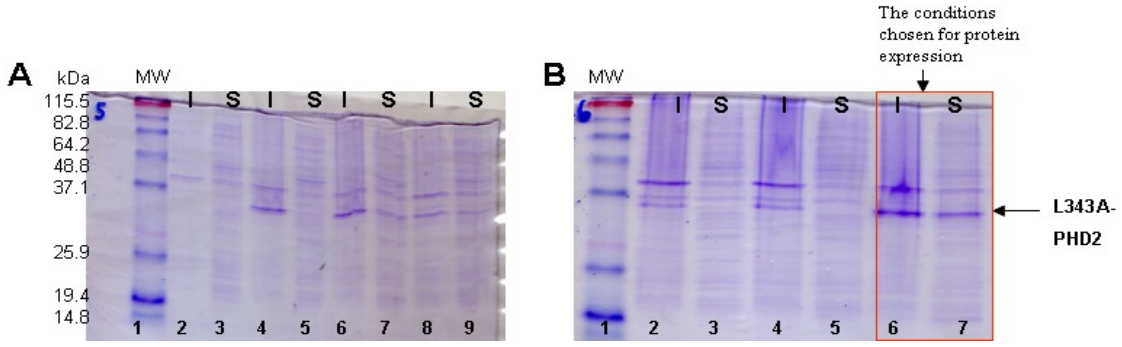


Figure 5.3: SDS-PAGE gels showing protein expression trials of L343A-PHD2. **(A)** Lane 1: Marker; Lanes 2 and 3: Controls (uninduced sample); Lane 4 and 5: 37°C, 3 h; Lanes 7 and 8: 28°C, 3 h; Lane 8 and 9: 15°C, 3 h. **(B)** Lane 1: Marker; Lanes 2 and 3: 37°C, 20 h; Lane 4 and 5: 28°C, 20 h; Lane 6 and 7: 15°C, 20 h. I = Insoluble phase, S= Soluble phase. Temperature and time shown are following 0.5 mM IPTG induction.

Following the expression trials, large scale protein purifications were carried out. Ion exchange chromatography was then used for initial purification of the PHD2 variants. WT-PHD2$_{181-426}$ has a calculated isoelectric point (pI) of 8.46,[157] the variants are expected to have a similar value, as there is no change in charge relative to WT-PHD2. The purifications were carried out in pH 5.8 buffers, in which the proteins have an overall positive charge. The column used contained cross-linked beaded agarose with sulfopropyl (sulfonic acid) functional groups (negatively charged) attached, which bind positively charged proteins via electrostatic interactions.[250] A gradient of NaCl was then run over the column to elute proteins. Na^+ ion exchange with the positively charged

protein causes its release from the column, allowing it to be collected by fractionation. SDS-PAGE analysis was then used to determine fractions containing the highest levels of pure PHD2; these were then combined and concentrated. **Fig. 5.4** shows the fractions containing the highest levels of I327A-PHD2 and L343A-PHD2. The pET-28a(+) vector in which the PHD2 variants were cloned contained 6 consecutive histidine residues, known as a His_6 tag at the *N*-terminus.[25] The His-tag was removed by cleavage with the protease thrombin.

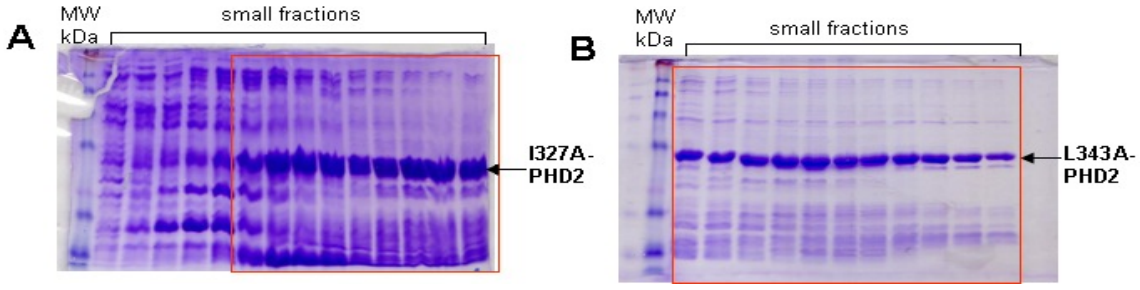


Figure 5.4: SDS-PAGE gels showing fractions containing highest levels of protein **(A)** I327A-PHD2 and **(B)** L343A-PHD2 after cation exchange chromatography. Fractions in red boxes were combined and concentrated.

Gel filtration chromatography was then carried out to further purify the proteins, including removal of thrombin. Concentrated fractions containing a PHD2 variant were loaded onto a gel filtration column containing cross-linked dextran and agarose. The principle of gel filtration is that protein particles of different sizes will elute through the stationary phase at different rates. Small protein molecules flow at a lower rate, as a large volume is available to them, while larger protein molecules flow at a faster rate and therefore are eluted in earlier fractions.[251] Protein fractions of highest purity were further identified by UV/Vis spectroscopy and SDS-PAGE analysis. They were then combined, concentrated and buffer exchanged into 50 mM Tris pH 7.5. In this manner, I327A-PHD2, 8 mg; L343A-PHD2, 7 mg; F366L-PHD2, 11 mg, and V376A-PHD2, 18 mg were prepared with approximately 90% purity. The proteins were then stored at -80^{o}C in small aliquots and used for future tests. **Fig. 5.5** shows the selected gel filtration fractions of the PHD2 variants.

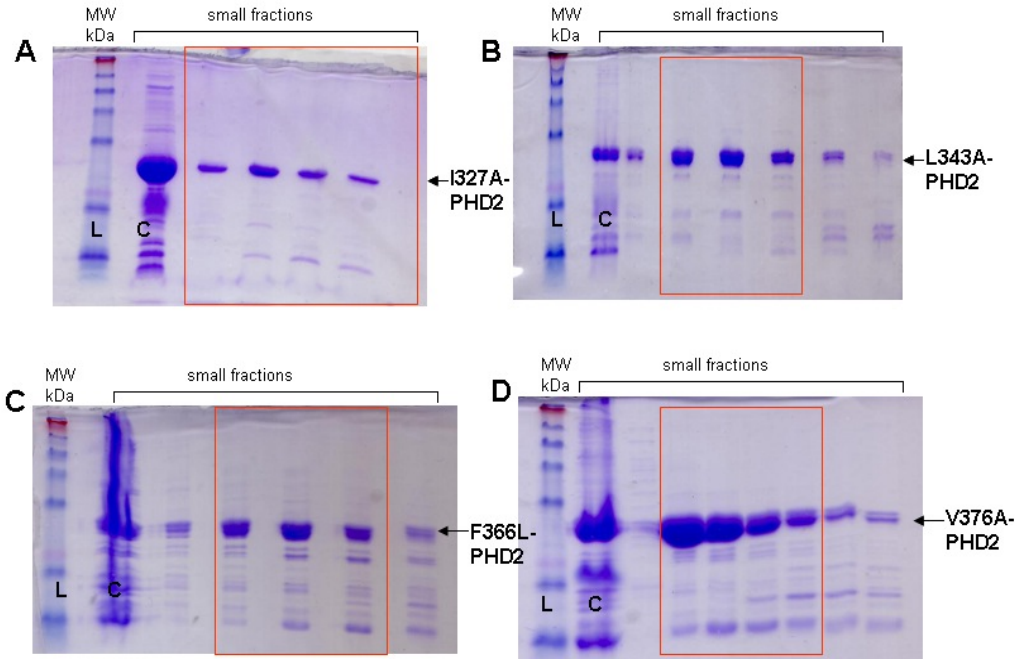


Figure 5.5: SDS-PAGE gel analyses of fractions from gel filtration column purifications of **(A)** I327A-PHD2, **(B)** L343A-PHD2, **(C)** F366L-PHD2, and **(D)** V376A-PHD2. L: Marker ladder; C: Control, partially pure protein applied to column. (Purified fraction proteins in red boxes were combined and concentrated).

5.2.2 The PHD2 variants are active *in vitro*

The enzymatic activities of the PHD2 variants were then compared with the WT-PHD2 (previously expressed and purified by Dr E. Flashman) using an *in vitro* hydroxylation assay. The WT-PHD2 and PHD2 variants used in this study were the *N*-terminally truncated constructs comprising residues 181-426. (Note: PHD1 and PHD3 are difficult to produce in *E. coli* probably due to solubility problems. However, tagged recombinant PHD1 and PHD3 have been successfully expressed in insect cells).[49] The truncated construct of PHD2 does not contain the *N*-terminal MYND-containing region (MYND: Myeloid translocation protein 8, Nervy, and DEAF1: deformed epidermal autoregulatory factor-1))-type zinc finger domain. However, loss of the *N*-terminal domain has not been proven to have deleterious effect on the hydroxylation activity of PHD2.[157]

PHD2 has been reported to have relatively high selectivity both *in vitro* and *in vivo* for CODD (Pro564) hydroxylation than NODD (Pro402) hydroxylation,[13, 30, 36, 142] this work therefore began by focusing on hydroxylation of CODD. The activities of the four PHD2 variants (I327A-, L343A-, F366L-, and V376A-PHD2) were compared with WT-PHD2 by carrying out activity assays that monitored a 19-mer CODD (HIF-1α residues 556-574) peptide substrate hydroxylation using matrix-assisted laser desorption/ionization mass spectrometry (MALDI MS) (hereafter MALDI MS PHD2 hydroxylation assay).[194] The CODD hydroxylation was detected by an observation of a +16 Da mass shift in the mass spectrum. It has previously been identified that the shortest effective CODD substrates for the PHDs are 17-mer peptides,[26] thus the 19-mer peptide used in the *in vitro* PHD2 assays in this work should be sufficient for the catalytic reactions.

The assays were first carried out for 10 min at 37^{o}C using 4 μM PHD2, 100 μM CODD, 300 μM 2OG, 4 mM ascorbate and 50 μM Fe(II). The MALDI MS spectra of the products (**Fig. 5.6 B**) showed that the F366L variant was inactive, with no CODD hydroxylation being observed. Although the F366 residue is expected to have no direct contribution to the catalytic Fe(II) or substrate binding,[31, 34] the phenylalanine residue at this position might contribute to the stability of the enzyme. The other three PHD2

variants all catalysed hydroxylation of the CODD substrate (non-hydroxylated CODD ~ 2247 Da, hydroxylated CODD ~ 2263 Da), as compared to the negative control without enzyme (**Fig. 5.6 A**).

In the initial MALDI MS PHD2 hydroxylation assays (using 4 μM of enzymes), the activities of L343A-PHD2 and V376A-PHD2 were observed to be comparable to WT-PHD2, with I327A-PHD2 being slightly less active. To investigate whether the reaction conditions were not limiting, further assays were carried out to compare the degree of hydroxylation of CODD at different enzyme concentrations. **Fig. 5.6 C** shows that under the standard conditions, WT-PHD2 and all the tested variants (with the exception of F366L) at 4 μM hydroxylated CODD to ~ 50-70%. When the enzyme concentration was reduced to 2 μM, there were significant decreases in CODD hydroxylation levels catalyzed by I327A- and V376A-PHD2 variants. However, the CODD hydroxylation levels catalysed by WT-PHD2 and L343A-PHD2 remained at ~~ 50-70%. When the concentration of the enzyme was further reduced to 1 μM. At 0.5 μM, all the activities of PHD2 variants were markedly reduced to less than 10% of original activity, whereas the activity of WT-PHD2 also significantly reduced, but to a lesser extend (~30% of original activity).

It was also observed that a small percentage (5-8%) of 'CODD hydroxylation' is always present in the negative controls (without enzyme), these + 16 Da peaks are likely due to methionine residue oxidation (the CODD peptide contains two methionine residues corresponding to Met561 and Met568 in wild-type HIF).[13, 194] All the CODD hydroxylation data shown have been normalised to the negative controls.

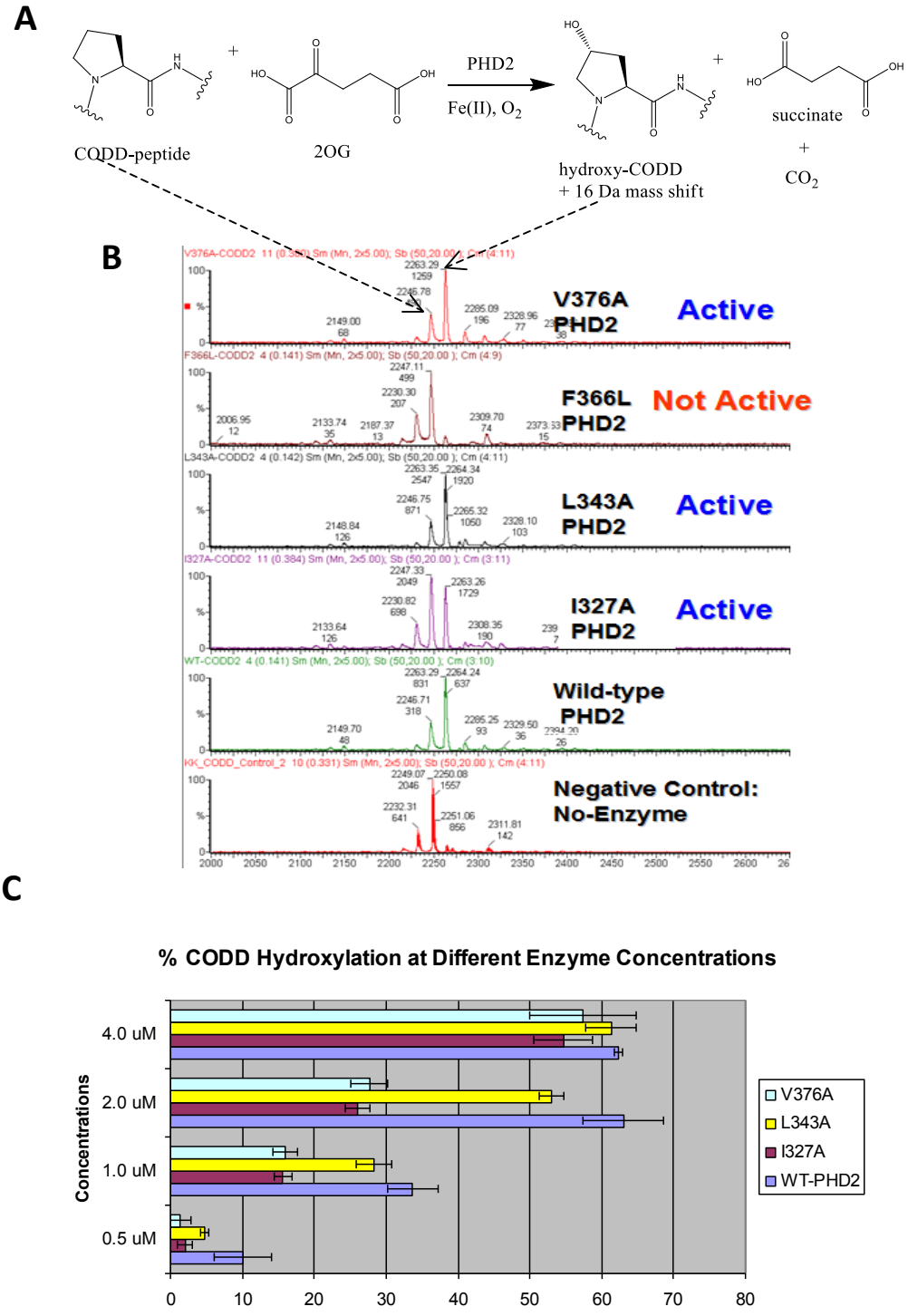


Figure 5.6: (**A)** Scheme showing hydroxylation reaction catalysed by PHD enzyme. (**B**) The representative MALDI MS spectra show hydroxylation of a CODD 19-mer peptide substrate by wild-type PHD2 (WT-PHD2) and the PHD2 variants (I327A-, L343A-, and F366L-, and V376A-PHD2) (at 4 μM enzyme concentration). (**B)** Hydroxylation activities of the PHD2 variants compared with WT PHD2 at different enzyme concentrations. The MALDI MS PHD2 hydroxylation assays were carried out for 10 min at 37°C at the indicated enzyme concentrations, in the presence of CODD (100 μM), 2OG (300 μM), ascorbate (4mM), and Fe(II) (50 μM). Values have been normalized to negative controls (no enzyme). Error bars represent standard deviations, n > 3)

5.2.3 Kinetic parameters of the PHD2 variants

Further studies were carried out to determine the kinetic parameters of the I327A-, L343A- and V376A-PHD2 variants compared to the WT-PHD2 using the previously described MALDI MS PHD2 hydroxylation assays. Time course experiments were carried out under the standard conditions (**Fig. 5.7**). Two sets of kinetic parameters (**Table 5.1**) were obtained measuring initial velocity for WT-PHD2 and the PHD2 variants at varying 2OG or CODD substrate concentrations. The corresponding Michaelis-Menten curves for the kinetic experiments are shown in **Figure 5.8** and **5.9**.

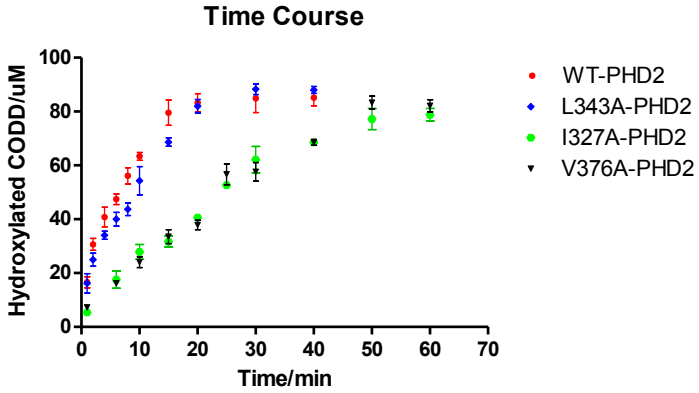


Figure 5.7: Amount of CODD hydroxylation (μM) over time as catalysed by WT-PHD2, L3343A-, I327A-, and V376A-PHD2 variants. The MALDI MS PHD2 hydroxylation assays were carried out at 2 μM enzyme, 100 μM CODD, 300 μM 2OG, 4 mM ascorbic acid, and 50 μM Fe(II). Error bars represent standard deviations, n = 3.

Enzyme	Substrate	Reaction time (min)	K_m (μM)	V_{max} (μMs^{-1})	k_{cat} (s^{-1})	k_{cat}/K_m (M^{-1}s^{-1})
WT-PHD2	2OG	5	15.5 (± 2.9)	0.094 (± 0.005)	0.047 (± 0.003)	3.03 (± 1.0) x 10^3
L343A-PHD2	2OG	5	18.2 (± 2.4)	0.068 (± 0.002)	0.034 (± 0.001)	1.87 (± 0.4) x 10^3
I327A-PHD2	2OG	10	16.0 (± 2.7)	0.037 (± 0.002)	0.019 (± 0.001)	1.19 (± 0.4) x 10^3
V376A-PHD2	2OG	10	13.0 (± 1.8)	0.050 (± 0.002)	0.025 (± 0.001)	1.92 (± 0.6) x 10^3

Enzyme	Substrate	Reaction time (min)	K_m (μM)	V_{max} (μMs^{-1})	k_{cat} (s^{-1})	k_{cat}/K_m (M^{-1}s^{-1})
WT-PHD2	CODD	1.5	21.1 (± 4.6)	0.106 (± 0.009)	0.053 (± 0.005)	2.51(± 1.0) x 10^3
L343A-PHD2	CODD	1.5	23.3 (± 5.0)	0.092 (± 0.008)	0.046 (± 0.004)	1.97 (±0.8) x 10^3
I327A-PHD2	CODD	4	20.0 (± 2.5)	0.040 (± 0.002)	0.020 (± 0.001)	1.00 (± 0.4) x 10^3
V376A-PHD2	CODD	4	20.8 (± 3.7)	0.049 (± 0.003)	0.025 (± 0.002)	1.20 (± 0.5) x 10^3

Table 5.1: Kinetic parameters obtained measuring initial velocity for WT-PHD2 and the PHD2 variants at varying 2OG (top) or CODD (bottom) substrate concentrations. n = 3, values in parentheses represent standard errors.

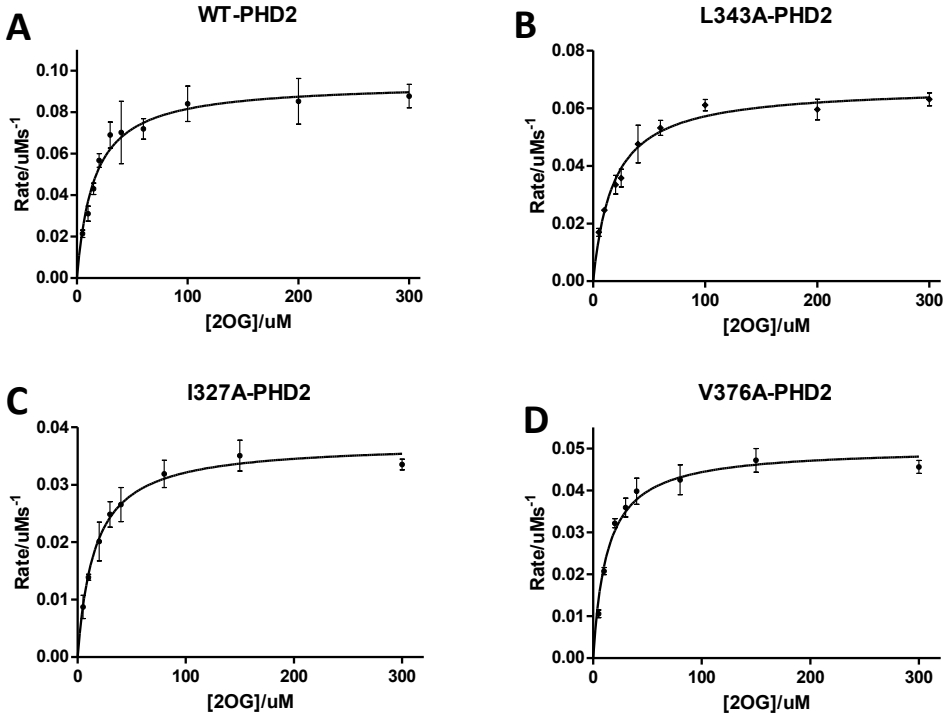


Figure 5.8: Michaelis-Menten curves for the kinetic experiments carried out using 2 µM PHD2 (wild-type or variants), 100 µM CODD, 4 mM ascorbate, 50 µM Fe(II) at 2OG concentrations ranging from 0-300 µM. Error bars represent standard deviations, n = 3.

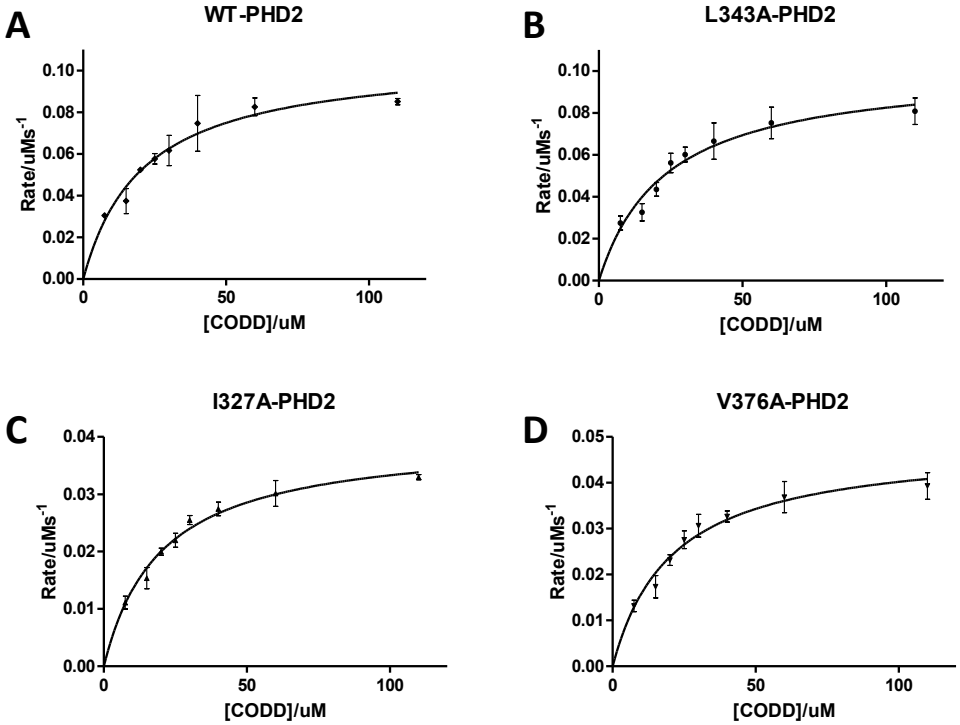


Figure 5.9: Michaelis-Menten curves for the kinetic experiments carried out using 2 µM PHD2 (wild-type or variants), 300 µM 2OG, 4 mM ascorbate, 50 µM Fe(II) at CODD concentrations ranging from 0-110 µM. Error bars represent standard deviations, n = 3.

The kinetic assays measuring initial velocity at varying substrate concentrations gave a K_m value for 2OG of 15.5 μM for WT-PHD2, whilst K_m values for 2OG of 18.2 μM, 16.0 μM, and 13.0 μM, respectively, were obtained for L343A-, I327A-, and V376A-PHD2. These results show that the PHD2 variants have 2OG K_m values similar to WT-PHD2 and within the error ranges (**Table 5.1**). Similar K_m values for CODD were also observed for WT-PHD2 (21.1 μM) and the PHD2 variants (20.0 – 23.3 μM) (**Table 5.1**). Previously, a wide range of 2OG K_m values (< 1 – 60 μM)[25, 26, 100, 208] and CODD K_m values (2- 80 μM)[25, 26, 35] have been reported for PHD2 obtained from purified proteins or crude cell lysates. The 2OG and CODD K_m values for PHD2 obtained in this study are within the reported ranges. The variations inμ K_m values may reflect differences in assay conditions used to determine the kinetic parameters. **Table 5.2** compares some of the reported 2OG and CODD K_m values for PHD2 obtained from different assays.

Assays	PHD2	K_m for 2OG	K_m for CODD
MALDI MS	Purified $PHD2_{181-426}$	15.5 (± 2.9) μM	21.1 (± 4.6) μM
2OG turnover[26, 35]	Purified $PHD2_{181-426}$	N.D.	36.7 (± 9.0) μM[35]
Oxygen consumption[25]	Purified $PHD2_{181-426}$	55.0 (± 11.0) μM[25]	21.6 (± 7.0) μM[25]
2OG turnover	soluble cell extract	10 μM[26]	7 μM[26]
pVHL capture[208, 226]	Purified $PHD2_{1-426}$	0.4 μM[208]	N.D.

Table 5.2: Comparisons of the 2OG and CODD K_m values for PHD2 obtained in this study (using MALDI MS assays) with the reported K_m values. N. D., not determined.

Broad concordance between the V_{max} values (and thus k_{cat} values; $k_{cat} = V_{max}/[E]_0$, where $[E]_0$ = 2μM) for WT-PHD2 and the PHD2 variants was also observed in the kinetic experiments using varying 2OG or CODD substrate concentrations (**Table 5.1**). Substitutions of the active site residues with smaller amino acid side chains in I327A-PHD2 and V376A-PHD2 variants were shown to result in an approximately two-fold decrease in k_{cat} values for both 2OG and CODD compared to WT-PHD2 (**Table 5.1**) (*i.e.* an ~ 50% decrease in the number of substrate molecules converted to product per enzyme molecule per second). However, small differences were observed for the k_{cat} values for 2OG and CODD for L343A-PHD2 (0.034 μM and 0.046 μM, respectively) in comparison to WT-PHD2 (0.047 μM and 0.053 μM, respectively). L343A-PHD2 also

exhibits the highest catalytic efficiency (as shown in the k_{cat}/k_m values for 2OG, and CODD, **Table 5.1**) of the PHD2 variants tested.

In summary, the MALDI MS results demonstrate that L343A-PHD2 shows the closest kinetic paramenters to WT-PHD2. (L343A-PHD2 was later shown to catalyse NODD hydroxylation to a similar degree as WT-PHD2 (**see Section 5.2.6**)). Because it is important to select a variant with catalytic activity as close as possible to the wild-type enzyme, the L343A-PHD2 variant was selected as the preferred candidate for subsequent studies.

5.2.4 Selective inhibition of the PHD2 variants by NOG analogues

McDonough *et al.* have previously tested a series of amino acid side chain *N*-oxalylglycine (NOG) analogues as PHD inhibitors[161] (NOG is a generic non-reactive 2OG analogue inhibitor for most of the 2OG oxygenases).[20] The investigators found that PHD inhibition was markedly decreased as the size of the amino acid side chains increased. It was considered that some of these NOG analogues may be potential candidates for this study, as the analogues with larger substituents may 'bump' into the residues present in the active site of WT-PHD2; however they may complement 'pockets' engineered into the active site of the L343A-PHD2 variant as shown in the schematic presentation in **Fig. 5.1**. A series of NOG analogues (**Fig. 5.10**, compounds **1**-**13**) (prepared by M. Tilliet (**1**-**11**)[161]and Dr Esther C. Y. Woon (**12**-**13**)) were initially tested in the PHD2 variant models to investigate the feasibility of applying the proposed 'bump-pocket' approach to selectively inhibit PHD2.

The potential inhibitory effects of these NOG analogues (**1**-**13**) on the catalytic activities of the PHD2 variants (*i.e.* I327A-, L343A-, and V376A-PHD2) were compared with WT-PHD2 using MALDI MS PHD2 hydroxylation assays. The concentrations of the inhibitors and 2OG co-substrate were kept constant at 300 μM, while the concentrations of the enzymes were varied when necessary. Other assay conditions comprised Fe(II) (50 μM), CODD substrate (100 μM), and ascorbate (4 mM). The reaction mixtures were incubated at 37^{o}C for 10 min. **Fig. 5.11** shows the percentage of inhibition of CODD hydroxylation catalysed by the WT-PHD2 and the PHD2 variants in the presence of the NOG analogue inhibitors (values were normalised by comparison to the no inhibitor control which was set as 0% inhibition).

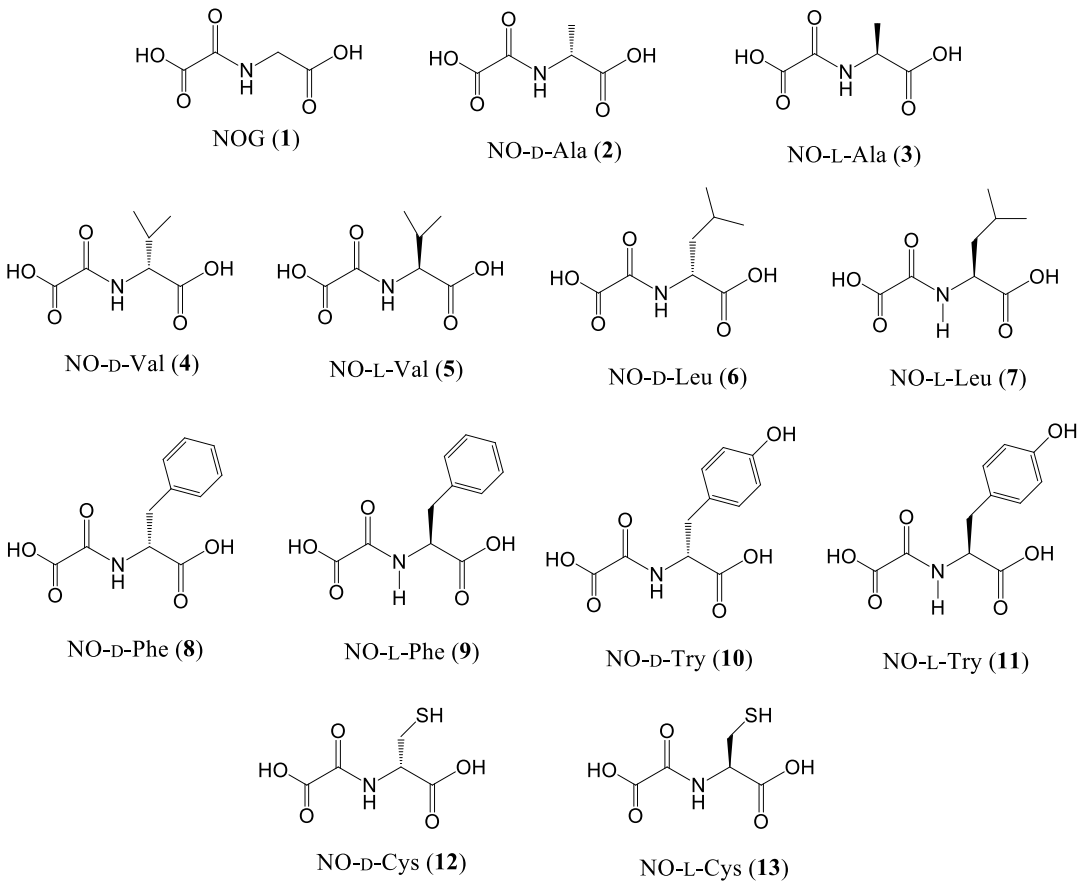


Figure 5.10: *N*-Oxalylglycine (NOG) analogues tested in the *in vitro* MALDI MS PHD2 hydroxylation assays.

Consistent with the previous results obtained using a 2OG turnover assay,[161] NOG **1** and NO-L-Ala **3** were shown to substantially inhibit WT-PHD2 activity (>90% inhibition); other amino acid side chain analogues demonstrated weak inhibitory potencies (ranging from 0-30% inhibition) as their size increased (**Fig. 5.11 A**). (NOG **1** and NO-L-Ala **3** have also been previously reported to inhibit the collagen prolyl-4-hydroxylase (C-P4H).)[252, 253] Notably, NO-D-Ala **2** is a weak inhibitor for WT-PHD2, clearly demonstrating the D/L stereoselectivity on WT-PHD2 inhibition, consistent with previous work.[161]

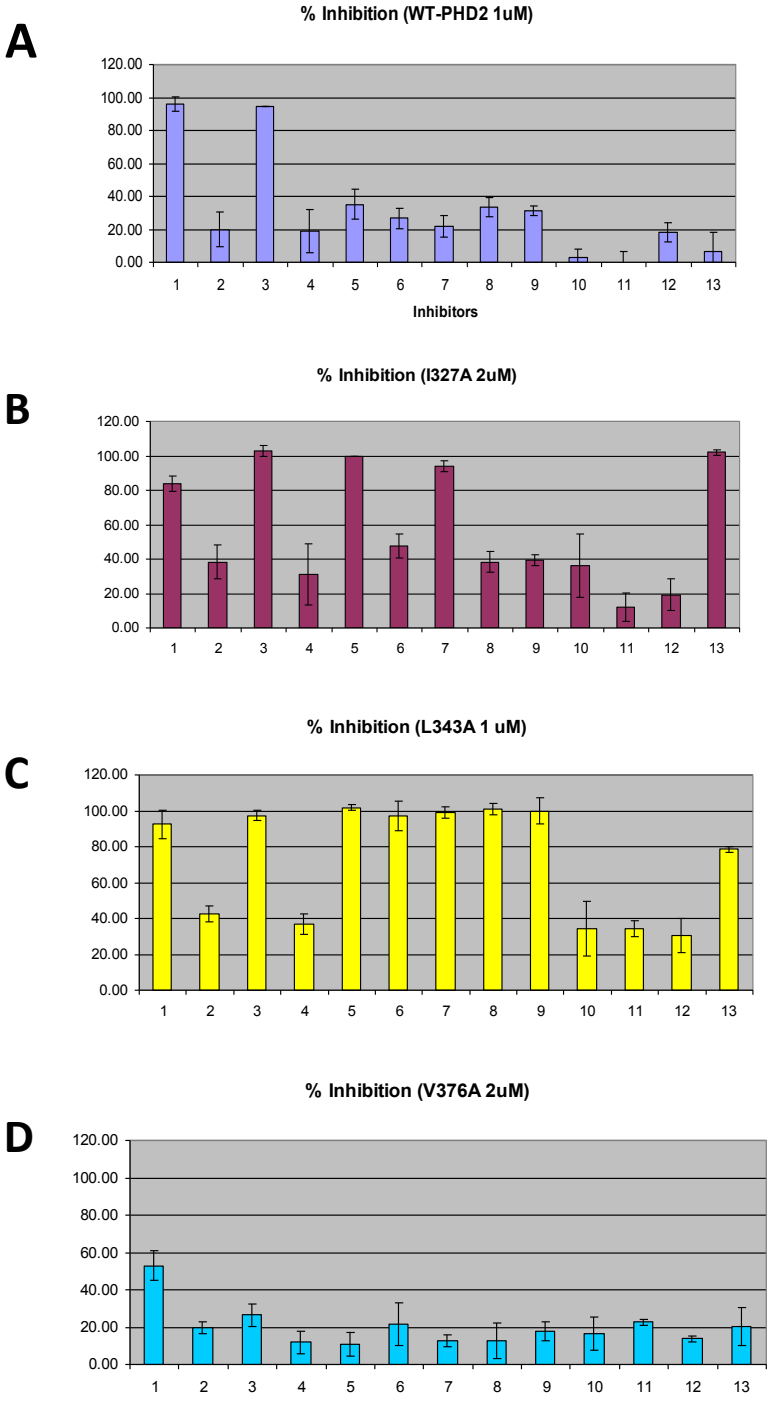


Figure 5.11: Percentage inhibition of CODD hydroxylation catalysed by (**A**) WT-PHD2 (1 μM), (**B**) I327A-PHD2 (2 μM), (**C**) L343A-PHD2 (1 μM) and (**D**) V376A-PHD2 (2 μM) in the presence of *N*-oxalylglycine (NOG) analogue inhibitors (**1-13**, **Fig 5.10**). The MALDI MS PHD2 hydroxylation assays were carried out for 10 min at 37°C at indicated enzyme concentrations. The reaction mixture comprised of PHD2 enzyme, CODD (100 μM), 2OG (300 μM), Fe(II) (50 μM), inhibitor (300 μM), and ascorbate (4mM). Values are normalised to negative controls (no enzyme). Error bars represent standard deviations, $n > 3$.

NOG **1** and NO-L-Ala **3** were also shown to substantially inhibit the PHD2 variants including I327A-PHD2 and L343A-PHD2 (**Fig. 5.11 B** and **C**). In contrast, the *N*-oxalyl Val, Leu, and Cys L-enantiomers (*i.e.* **5**, **7**, and **13**, respectively) which are weak inhibitors for WT-PHD2, were shown to substantially inhibit the I327A-variant (>90% inhibition) (**Fig. 5.11 B**). The NOG analogues **5-9** were shown to preferentially suppress the activity of L343A variant (>90% inhibition) (**Fig. 5.11 C**) over the WT-PHD2 (**Fig. 5.11 A**). The results suggest that the bulkier NOG analogues can bind to the newly created pocket in the active site of the alanine substituted PHD2 variants, probably as a result of reduced steric constraints. Interestingly, the V376A variant was shown to be less susceptible to inhibition by the NOG analogues (**1-13**). This result suggests that Val376 may be important for hydrophobic interaction with the NOG analogues.

The NOG analogue inhibition data clearly demonstrate the feasibility of selective inhibition of the PHD2 variants over the WT-PHD2; however, these compounds may not be suitable for functional studies of the PHD isoenzymes as they may potentially inhibit other 2OG oxygenases. Several D/L-amino acid analogues including **2-8** and **10** were shown to inhibit HIF asparaginyl hydroxylase FIH[161], and histone demethylases (e.g. JMJD2A and JMJD2E) (Schofield lab unpublished results). Therefore, the next aim of the project was to develop more potent variant-sensitive analogue inhibitors employing the bicyclic isoquinoline (BIQ)[77] as a template for inhibitor design.

5.2.5 Selective inhibition of the PHD2 variants by the BIQ analogues

BIQ **14** (IC_{50} 73 nM)[165](**Fig. 5.13**) is a more potent and more specific PHD2 inhibitor than NOG (IC_{50} 18.5 μM)[165]. BIQ was previously shown to selectively inhibit the HIF prolyl hydroxylation and has no apparent effect on HIF asparaginyl hydroxylation in cells (**Section 2.2.4**)[142]. The isoquinoline moiety in BIQ has been proposed to contribute to the stability of the PHD2[165] and to block the conformation change in PHD2 which is required for HIF-substrate binding.[34] BIQ analogues were therefore expected to be more potent candidates for the variant-sensitive inhibitors. The inhibition data described above demonstrates that NOG analogues with D/L-alanine, valine, and phenylalanine amino acid side chains could potentially inhibit the PHD2 variants, therefore a series of BIQ analogue inhibitors with these amino acid substituents (**14-20**, **Fig. 5.13 A**) were synthesised. **Fig. 5.12** describes the reaction steps and reagents used in the synthesis.

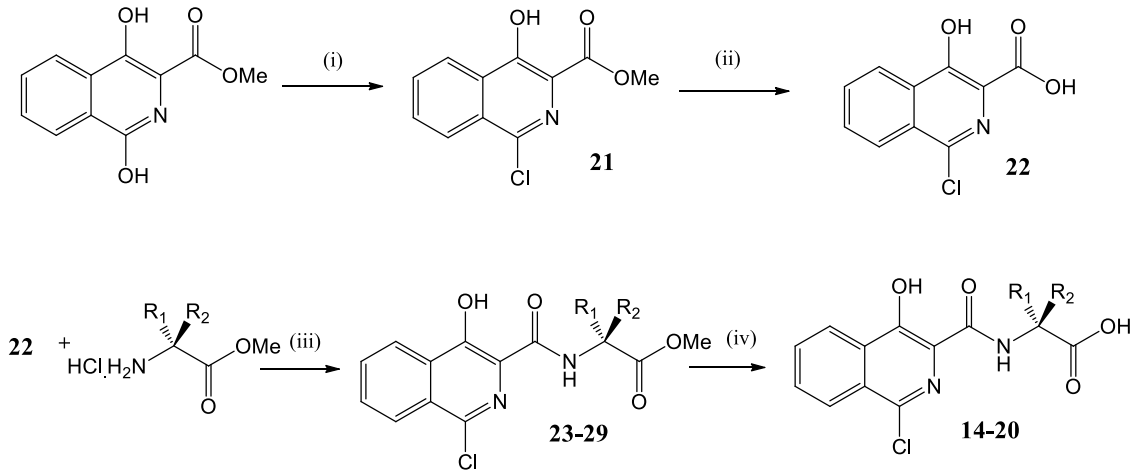


Figure 5.12: Schematic presentation of the reaction steps in the synthesis of BIQ analogue inhibitors**.** Reagents and conditions: (i) $POCl_3$, reflux, 2h; **21**, 98%; (ii) EtOH: NaOH 1:1, reflux, 2h; **22**, 90%; (iii) benzotriazole-1-yl-oxytripyrrolidinophosphonium hexafluorophosphate (PyBOP), Et_3N, CH_2Cl_2, r.t, 20h; **23**, 75%; **24**, 67%; **25**, 59%; **26**, 66%; **27**, 59%; **28**, 50%; **29**, 55% (iv) MeOH: NaOH 1:1, r.t, 2h; **14**, 94%; **15**, 98%; **16**, 93%; **17**, 95%, **18**, 92%; **19**, 88%; **20,** 94%.

The inhibitory potencies of these newly designed BIQ analogues against WT-PHD2 and the PHD2 variants were then investigated. The BIQ analogues (**14-20**) were tested in the previously described MALDI MS PHD2 hydroxylation assays under the standard conditions and the results are shown in **Fig. 5.13 B**.

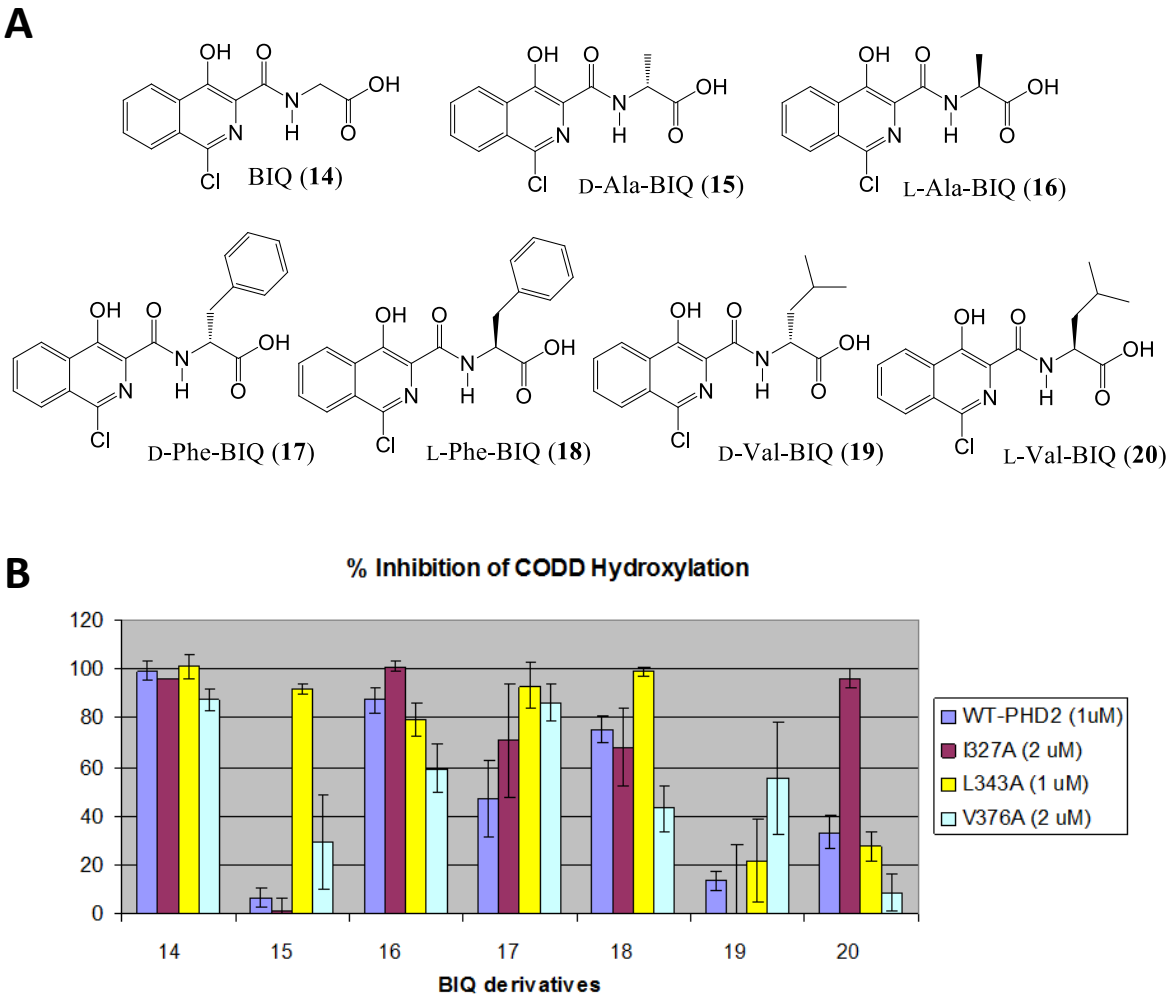


Figure 5.13: (**A**) Bicyclic isoquinoline (BIQ) analogue inhibitors. (**B**) Percentage inhibition of CODD hydroxylation catalysed by WT-PHD2 and PHD2 variants in the presence of BIQ analogue inhibitors (**14-20**). The MALDI MS PHD2 hydroxylation assays were carried out for 10 min at 37°C at indicated enzyme concentrations. The reaction mixture comprised of PHD2 enzyme, CODD (100 µM), 2OG (300 µM), Fe(II) (50 µM), inhibitor (300 µM), and ascorbate (4mM). Values are normalised by comparison to negative controls (no enzyme). Error bars represent standard deviations, n > 3.

The BIQ analogues were shown to inhibit CODD hydroxylation catalysed by WT-PHD2 with a range of different potencies (**Fig. 5.13 B**). BIQ **14** substantially inhibited WT-PHD2 activity (>90% inhibition), as did L-Ala-BIQ **16** (~90% inhibition). In contrast, the D-enantiomer **15** appeared to have no apparent effect on WT-PHD2 activity. Consistent with the results of the N-oxalyl derivatives, the D/L-Phe analogues (**17** and **18**) displayed modest inhibition of WT-PHD2 (40-70% inhibition), despite having a bulky aromatic side chain which was anticipated to preclude binding to the wild-type enzyme active site. The inhibition could at least in part be due to iron chelation in solution (in the absence of enzyme, **17** and **18** formed coloured solutions with Fe(II) in reaction mixtures). The D/L-Val analogues (**19** and **20**) were poor inhibitors for WT-PHD2, possibly due to steric clash of the valine side chains with residues in the WT-PHD2 active site.

Interestingly results were obtained for the BIQ analogues on the PHD2 variants over the WT-PHD2 (**Fig. 5.13 B**). L-Ala-BIQ **16** was shown to substantially inhibit WT-PHD2 and all the PHD2 variants, in a manner similar to BIQ **14.** L-Ala-BIQ **16** was determined to be a potent PHD2 inhibitor with an IC_{50} value of 1.1 μM (**Section 2.2.4**). A crystal structure of PHD2 in complex with **16** has also been solved (**Section 5.2.8**).

Notably, when Leu343 in the PHD2 active site was substituted with alanine (a smaller amino acid residue, thus creating a 'pocket' in the active site), the activity of the variant (*i.e.* L343A-PHD2) decreased significantly in the presence of D-Ala-BIQ **15**, *i.e.* D-Ala-BIQ **15** is capable of inhibiting the activity of L343A-PHD2, but does not inhibit the WT-PHD2. The D-Ala analogue **15** was also shown to moderately inhibit the V376A variant (**Fig. 5.13 B**). It is therefore anticipated that the alanine side chain of the D-enantiomer **15** clashes with the Leu343 and/or Val376 residue in the WT-PHD2 2OG binding pocket, therefore hindering **15** binding to WT-PHD2.[161] In the L343A and V376A variants, there is more space for **15** to bind. Subsequent structural and docking studies support this proposal (see **Section 5.2.8**).

The differential inhibition of PHD2 variant over WT-PHD2 was also displayed in I327A-PHD2 inhibition. L-Val-BIQ **20**, which is a moderate inhibitor of WT-PHD2 (< 30%

inhibition), was shown to substantially suppress the hydroxylation catalysed by I327A-PHD2 (> 90%), in contrast to its D-enantiomer **19** which did not have any apparent effect on the activities of either the I327A-PHD2 or WT-PHD2 (**Fig. 5.13 B**).

The enantiomeric pair D-Phe-BIQ **17** and L-Phe-BIQ **18** were found to inhibit the activities of the PHD2 variants to a greater extent than the WT-PHD2 (**Fig. 5.13 B**). Given that **17** and **18** also inhibit WT-PHD2, they are not suitable candidates for the variant-sensitive inhibitors. On the other hand, the BIQ analogues were also shown to be better inhibitors of V376A variant compared to the NOG analogues under the standard conditions (compare **Fig. 5.11 D** and **Fig. 5.13 B**). However, most of the BIQ analogue inhibitors suppressed the WT-PHD2 and the V376A-PHD2 activities with similar potencies, indicating that V376A-PHD2 is not a suitable candidate for an analogue-sensitive variant.

5.2.6 The effects of the BIQ analogue inhibition on NODD hydroxylation

Because HIF-1α has two prolyl hydroxylation sites (*i.e.* NODD (Pro402) and CODD (Pro564),[12-14] the effects of the BIQ analogue inhibitors on NODD hydroxylation were then examined. MALDI MS PHD2 hydroxylation assay conditions were similar to those described above, except CODD peptide was replaced with NODD (HIF-1α residues 395-413) in the assays and all enzymes were tested at 4 μM.

First the ability of the variants to catalyse NODD hydroxylation was examined. WT-PHD2 and the PHD2 variants were previously shown to hydroxylate CODD to around 60-70% at 4 μM (**Fig. 5.6 B**). Interestingly, whilst WT-PHD2 and L343A-PHD2 were shown to catalyse hydroxylation of NODD to ~70%, the I327A and V376 variants only catalysed hydroxylation of NODD to 20-30% (**Fig. 5.14 A**). These observations indicate that the Ile327 and Val376 residues in the PHD2 active site may have distinct roles in NODD substrate binding/hydroxylation.

The BIQ analogue inhibitors were then introduced to the assays to determine whether they could inhibit NODD hydroxylation in addition to CODD hydroxylation. The results show similar inhibitory patterns for NODD hydroxylation by the WT-PHD2 and the PHD2 variants in comparison to CODD hydroxylation, perhaps with the exception of V376A variant (compare **Fig. 5.13 B** and **Fig. 5.14 B**). NODD hydroxylation catalysed by V376A-PHD2 was shown to be most susceptible to BIQ analogue inhibition. With the exception of L-Val-BIQ **7**, all the BIQ analogues (**14**-**20**) were shown to substantially inhibit NODD hydroxylation (>80% inhibition) catalyzed by V376A-PHD2 (**Fig. 5.14 B**).

Consistent with the inhibition data of CODD hydroxylation, BIQ **14** and L-Ala-BIQ **16** were shown to be non-selective inhibitors for the WT-PHD2 and the PHD2 variants. The D-/L-Phe analogues **17** and **18** were shown to substantially inhibit NODD hydroxylation catalysed by the PHD2 variants and WT-PHD2, however, to a lesser degree in the latter. Notably, D-Ala-BIQ **15** was shown to selectively inhibit NODD hydroxylation catalysed by the L343A-PHD2 over WT-PHD2. Comparison with its effect on CODD hydroxylation suggests that D-Ala-BIQ **15** is the most potent L343A-variant-sensitive inhibitor in this 'bump-pocket' approach.

Interestingly, when the NODD hydroxylation assays were carried out in the presence of the same concentration of CODD peptide (*i.e.* both substrates were present in a competitive experiment), all the WT-PHD2 and PHD2 variants were shown to be totally selective for CODD hydroxylation under the standard conditions, as there was no hydroxylated-NODD peak detectable in the MS spectra (data not shown). Similar observation (*i.e.* CODD over NODD substrate selectivity of PHD2) has previously been reported.[35] Therefore, to simplify the analysis, subsequent studies focused primarily on CODD hydroxylation.

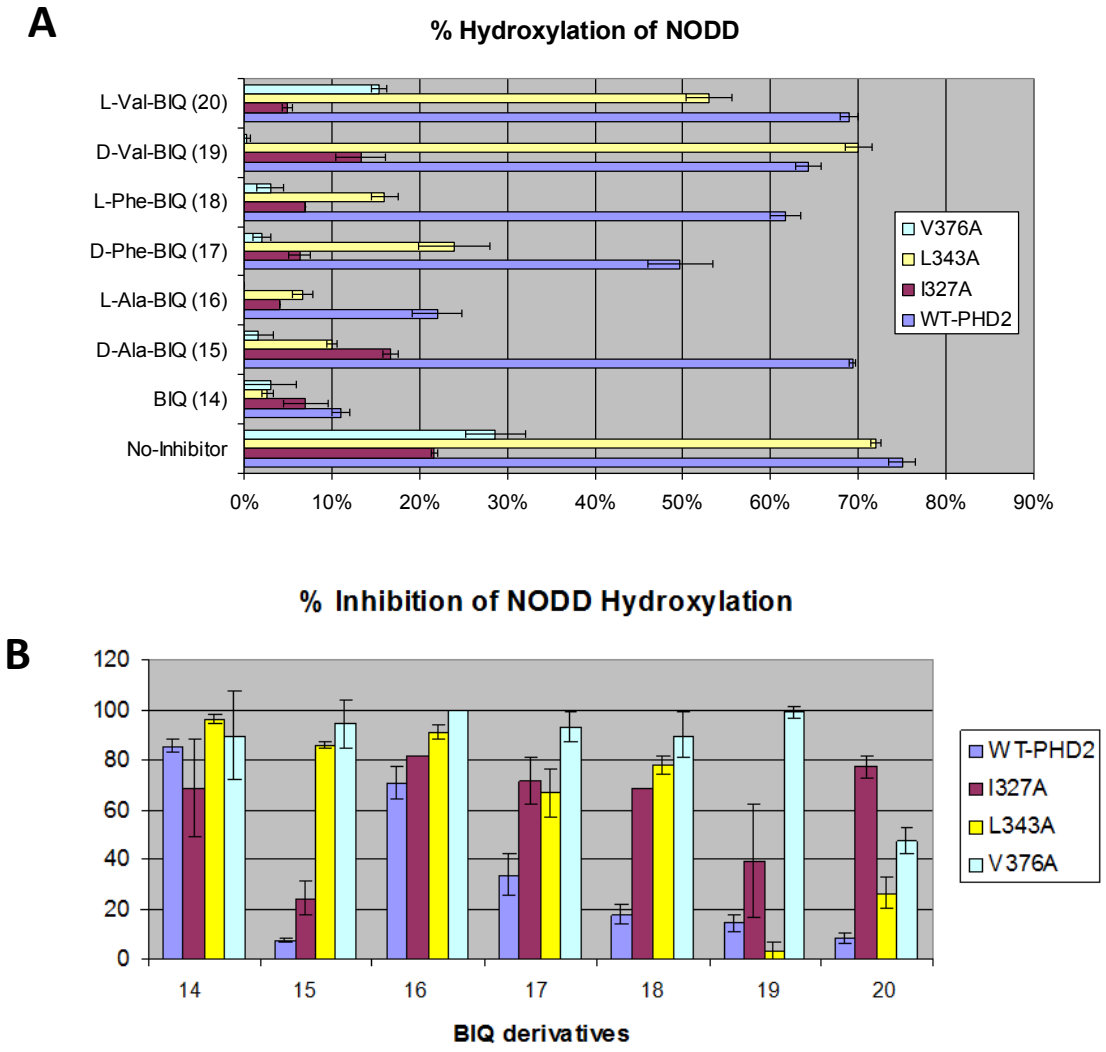


Figure 5.14: (**A**) Percentage of NODD hydroxylation in the presence of BIQ analogue inhibitors (structures refer to **Fig. 5.13 A**). (**B**) Data from (**A**) were plotted as percentage of inhibition on the enzyme activity; values were normalized to no inhibitor control which was set to 0 %. The MALDI MS PHD2 hydroxylation assays were carried out for 10 min at 37°C at 4 μM enzyme, in the presence of NODD (100 μM), 2OG (300 μM), inhibitor (300 μM) ascorbate (4 mM), and Fe(II) (50 μM). (**B**) Values have been normalized to negative controls (no enzyme). Error bars represent standard deviations (n > 3). NODD peptide peak appears on MS spectra at ~ 1916 *m/z*, NODD hydroxylation peak at ~ 1933 *m/z* (+ 16 Da).

5.2.7 Potential combination: L343A-PHD2 variant and D-Ala-BIQ (15)

Although the MALDI MS hydroxylation assay is often used for inhibitor screening, its requirement for relatively high concentrations of enzyme (1-4 μM) places a lower limit on the IC_{50} values that can be determined, making it a less desirable assay for the determination of IC_{50} values. The IC_{50} values of the BIQ analogues in the presence of WT-PHD2 or L343A-PHD2 variant were therefore obtained using the AlphaScreen PHD2 hydroxylation assay described in **Chapter 2**.

Time course experiments were first carried out to determine the reaction time in which L343A-PHD2 shows similar CODD hydroxylation activity to WT-PHD2 under the standard assay conditions. The results show for a standard reaction time of 10 min using 1 nM WT-PHD2, an equimolar amount of L343A-PHD2 requires 18 min to achieve similar hydroxylation activity (**Fig. 5.15**). Subsequent experiments were therefore carried out at these reaction times. The IC_{50} values for the BIQ analogues for WT-PHD2 and L343A-PHD2 obtained from the AlphaScreen hydroxylation assays are summarised in **Table 5.3**.

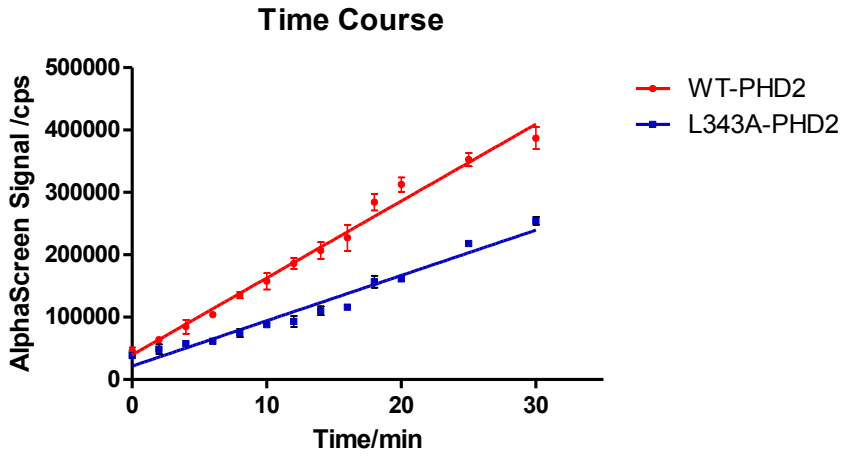


Figure 5.15: Time course experiments for WT-PHD2 and L343A-PHD2 carried out under the standard AlphaScreen hydroxylation assay conditions. Reaction mixtures consisted of 1 nM PHD2, 20 μM Fe(II), 200 μM ascorbate, 60 nM biotinylated CODD peptide, and 2 μM 2OG.

	BIQ (**14**)	D-Ala-BIQ (**15**)	L-Ala-BIQ (**16**)	D-Phe-BIQ (**17**)	L-Phe-BIQ (**18**)	D-Val-BIQ (**19**)	L-Val-BIQ (**20**)
WT-PHD2	1.4 μM	> 300 μM	1.1 μM	> 300 μM	> 300 μM	> 300 μM	> 300 μM
L343A-PHD2	4.3 μM	47.9 μM	3.9 μM	241.6 μM	> 300 μM	> 300 μM	> 300 μM

Table 5.3: IC_{50} values for the BIQ analogues (**14-20**, **Fig. 5.14 A**) for WT-PHD2 and L343A-PHD2 obtained from AlphaScreen PHD2 hydroxylation assays.

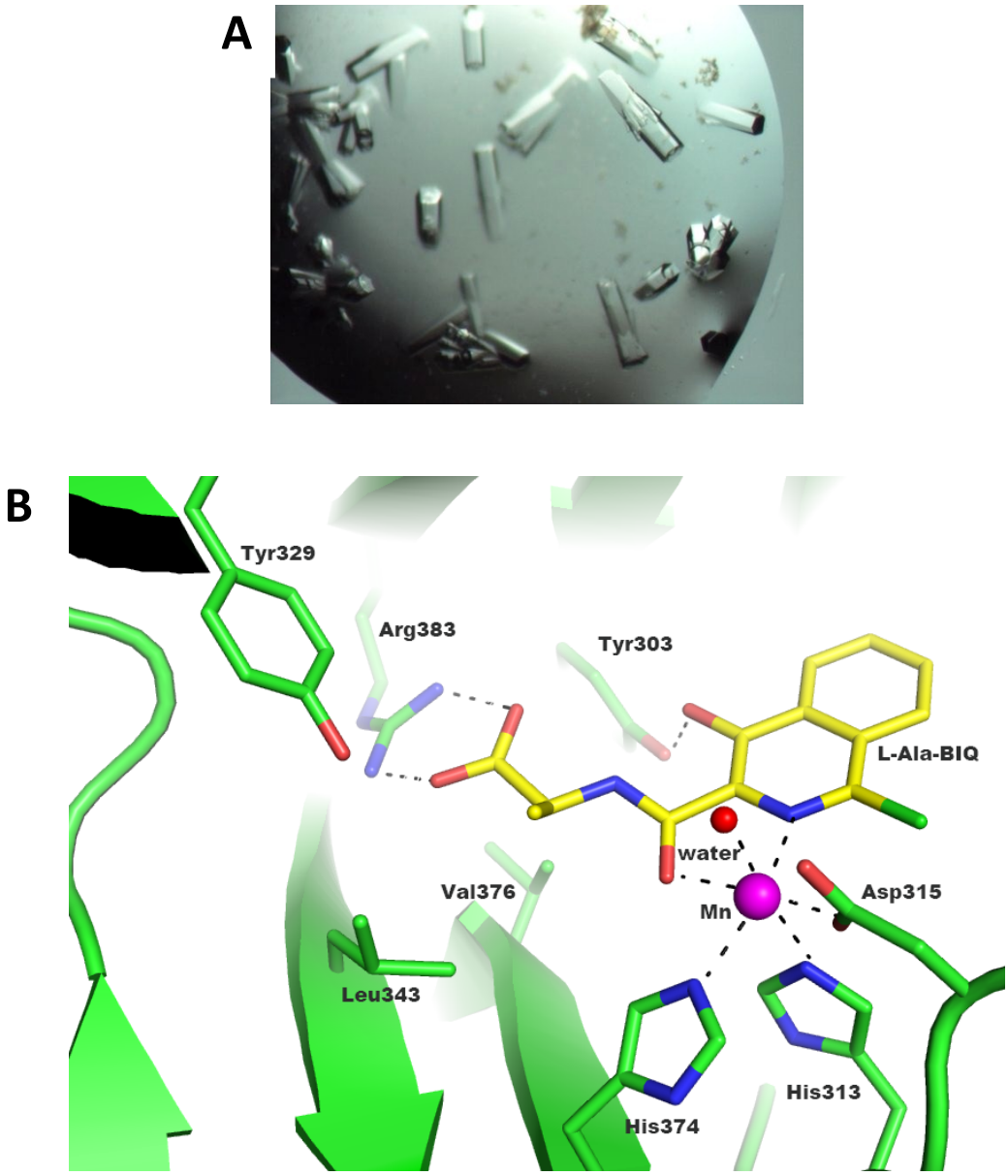
The AlphaScreen inhibition data for the WT-PHD2 and L343A-PHD2 (**Table 5.2**) are in broad concordance with the results obtained from the above MALDI MS hydroxylation assays (**Fig. 5.13 B**). Whilst both BIQ **14** and L-Ala-BIQ **16** exhibit similar IC_{50} values for WT-PHD2 and L343A-PHD2, D-Ala-BIQ **15** selectively inhibited L343A-PHD2 with an IC_{50} value of 47.9 μM (IC_{50} for **15** for WT-PHD2 > 300 μM). Considering the results obtained from the above kinetic and inhibition studies, L343A-PHD2 and D-Ala-BIQ **15** was considered the best combination of variant and inhibitor of those tested in this study, and therefore evaluated further in cell-based experiments.

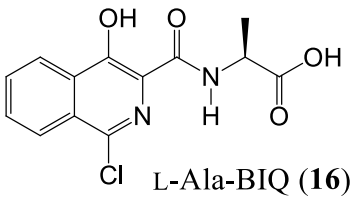
(Note: The differential selectivities of the D-Ala-BIQ **15** (IC_{50} > 300 μM) and L-Ala-BIQ **16** (IC_{50} 1.1 μM) against WT-PHD2 have been employed in two separate studies involving the development of (i) a proteolysis/mass spectrometry method[165] which allows screening of inhibitors based on their stabilising/destabilising effects with respect to nature and rate of proteolysis and (ii) an NMR solvent water relaxation method[254] which enables quantitative determination of ligand binding and mechanistic investigations of enzymes. These works have been published in *Journal of Medicinal Chemistry* (2009)[165] and (2010).[254])

5.2.8 Crystallographic and docking studies

Extensive efforts have been carried out to obtain structural information on the WT-PHD2 and the PHD2 variants in complex with the BIQ analogues. The proteins were co-crystallised with 10 equivalents of the inhibitors using vapor diffusion methods.[31] Under these conditions, none of the PHD2 variants formed crystals, however, hexagonal rod crystals (**Fig. 5.16 A**) were obtained for WT-PHD2 co-crystallised with L-Ala-BIQ **16**. A high resolution (1.2 Å) crystal structure of the catalytic domain of WT-PHD2$_{181\text{-}426}$ in complex with **16** was later solved by Dr M. McDonough and refined by Dr R. Chowdhury. To date, this is the first PHD2 crystal structure solved in complex with an inhibitor with an L-alanine side-chain. The isoquinoline nitrogen atom and the amide carbonyl oxygen of L-Ala-BIQ **16** bind in a bidentate fashion to metal in the PHD2 catalytic site, in a manner similar to its parent compound, BIQ **14** and the 8-iodo bicyclic isoquinoline inhibitior (see also **Section 2.2.4**).[31, 162] The carboxylic acid side chain of **16** occupies the 2OG binding pocket and is positioned to form a salt bridge with the Arg383 residue, wheares the 3-hydroxy group in the bicyclic moiety hydrogen bonds with the nearby Try303 residue in WT-PHD2 active site. The crystal structure also indicates that the methyl group in the L-Ala analogue **16** points in the opposite direction to the Leu343 and Val376 residues in the active site (**Fig. 5.16 B**).

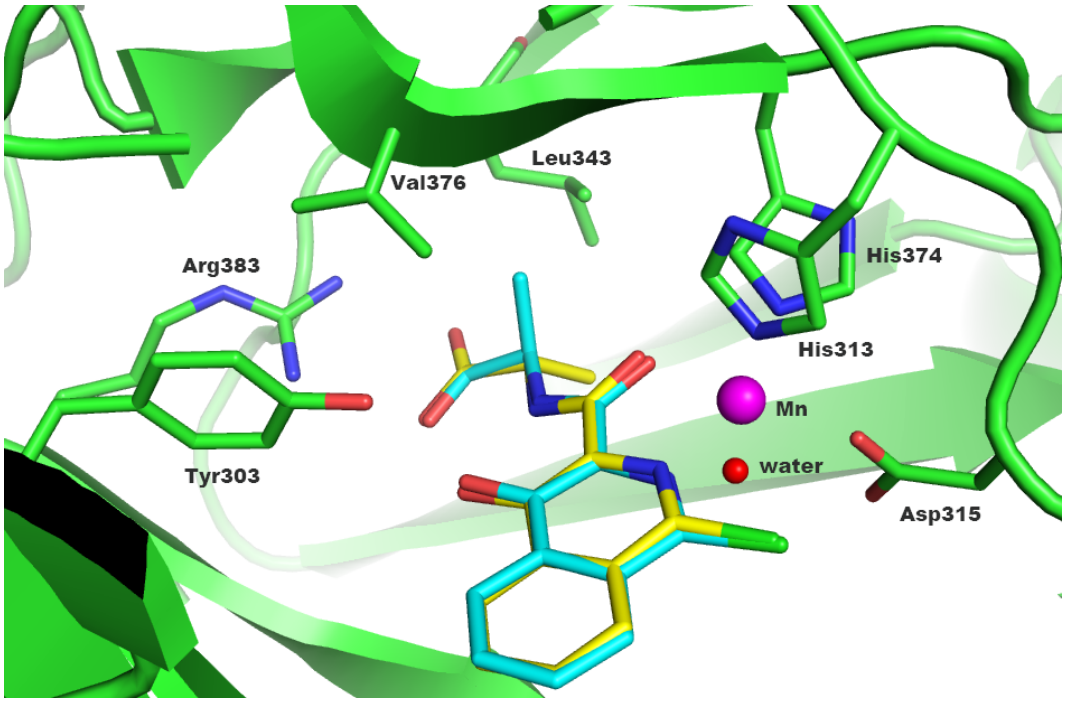
Docking studies overlaying D-Ala-BIQ **15** and L-Ala-BIQ **16** in the PHD2 crystal structure (**Fig. 5.17**) clearly show that the D-alanine substituent may clash with the Leu343 or Val376 residues in the WT-PHD2 active site, explaining why D-Ala-BIQ **15** is a poor inhibitor for WT-PHD2 and the I327A variant. D-Ala-BIQ **15** was shown to be a potent inhibitor of the L343A variant and a modest inhibitor for the V376A variant in the MALDI MS hydroxylation assays.

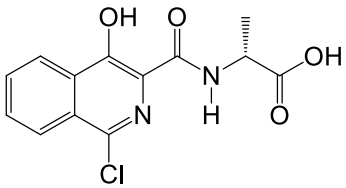




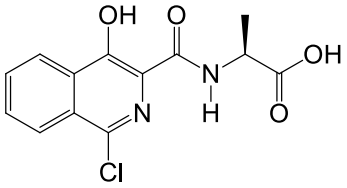
L-Ala-BIQ (**16**)

Figure 5.16: (**A**) WT-PHD2 co-cyrstallises with L-Ala-BIQ **16** to form hexagonal rod crystals. (**B**) View of the crystal structure of the WT-PHD2 catalytic domain in complex with **16** shows the compound binds in a bidentate manner to the active site metal (Mn), in a manner similar to the previously reported PHD2 crystal structure in complex with BIQ **14** (PDB ID 2HBT).





D-Ala-BIQ (**15**) (cyan)



L-Ala-BIQ (**16**) (yellow)

Figure 5.17: Modeling studies of D-Ala-BIQ **15** (cyan) overlaying with L-Ala-BIQ **16** (yellow) show the D-alanine substituent of **15** may clash with Leu343 and Val376 active site residues.

5.2.9 Cell-based studies

From the *in vitro* findings, L343A-PHD2 was identified as a potential variant for functional assignment work. D-Ala-BIQ **15** and several NOG analogues **5-9** were shown to selectively inhibit the L343A variant but not the WT-PHD2 *in vitro*. In **Chapter 2** (**Section 2.2.4**), compounds **15**, **8**, and **9** (and their di-ester forms of the NOG analogues) were shown to be ineffective inhibitors of WT-PHDs in cells. Therefore, the work next aimed to investigate whether L343A variant is active (*i.e.* able to catalyse the CODD and NODD hydroxylation in cells) and can be inhibited by these variant-sensitive analogue inhibitors in mammalian cells. WT-PHD2 was used as a control in the cell-based experiments.

The chemical-genetic strategy has been widely used as a versatile and effective tool for dissecting kinase function in yeast,[243, 255, 256] however its application to mammalian cells and animal models has been limited. Due to the simple physiology of yeast, the target enzyme of interest can relatively easy to replace with a variant using basic genetic-microbial techniques.[243] In contrast, labour intensive specially tailored transgenic cells or 'knock in' mice are usually required for the successful application of this approach in higher organisms.[234, 235] However, there is a study demonstrating the successful application of the chemical-genetic strategy in natural mammalian cell-system employing overexpression of the kinases.[242]

5.2.9.1 L343A-PHD2 variant is functionally active in the cells

With the lack of a suitable transgenic cell-system, it was attempted to test the 'bump-pocket' approach using a natural cell-line, human fibrosarcoma HT1080. In HT1080 cells, all three PHDs and HIF are present at endogenous levels. HIF-α is continously hydroxylated by the PHDs under normoxia and targeted for proteasomal degradation. However, in the presence of a proteasome inhibitor or under hypoxia, HIF-α is stabilised and the activities of the PHDs can be directly probed using hydroxy-residue specific

antibodies (**Chapter 2**). The latter condition was excluded because the PHDs were expected to be inactive (or less active) at low oxygen availability; therefore a proteasome inhibitor was used to maintain high HIF levels.

Exogenous source of HIF-1α was required to increase substrate concentrations because endogenous HIF-1α was expected to be substantially hydroxylated (i.e hydroxylation close to a saturated level) by the activities of the PHDs in the presence of proteasome inhibitor. High concentrations of HIF-1α were to ensure an excess of substrates was present for the catalytic activities of the endogenous and exogenous expressed PHDs. Increased levels of HIF prolyl hydroxylation were therefore expected to be detected for cells with overexpressed WT- or L343A-PHD2. Introduction of variant-sensitive inhibitor analogues were anticipated to suppress the activities of the L343A variant but not the wild-type enzyme.

In the cell-based experiments, L343A-PHD2 was first engineered into a human (full length) PHD2-pcDNA3 plasmid (previously prepared by Dr J. M. Gleadle)[17] using site-directed mutagenesis PCR (Stratagene). The PHD2 plasmids bearing the L343A mutation and WT-PHD2 were then transiently transfected into HT1080 cells using Fugene HD Transfection reagent[14]. The full-length WT-PHD2 or L343A-PHD2 were overexpressed in the presence of high (plasmid) concentrations of a truncated form of HIF-1α (HIF-1α/PK) (HIF-1α residue 344-826, with a nine amino-acid *C*-terminal PK-epitope tag (prepared by Dr Y-M Tian)) as an exogenous source of HIF-1α in HT1080 cells. 24 h after transfection, cells were treated for 5 h with the proteasome inhibitor MG132 and in the presence or absence of the PHD inhibitors (*i.e.* BIQ or NOG analogues). Cells were then lysed and analysed by immunoblotting. The proteins were probed by HIF-1α and hydroxy-residue specific antibodies; allowing simultaneous detection of endogenous HIF-1α (~105 kDa) and exogenous HIF-1α/PK (~76 kDa) and their hydroxylation states (**Fig. 5.18**).

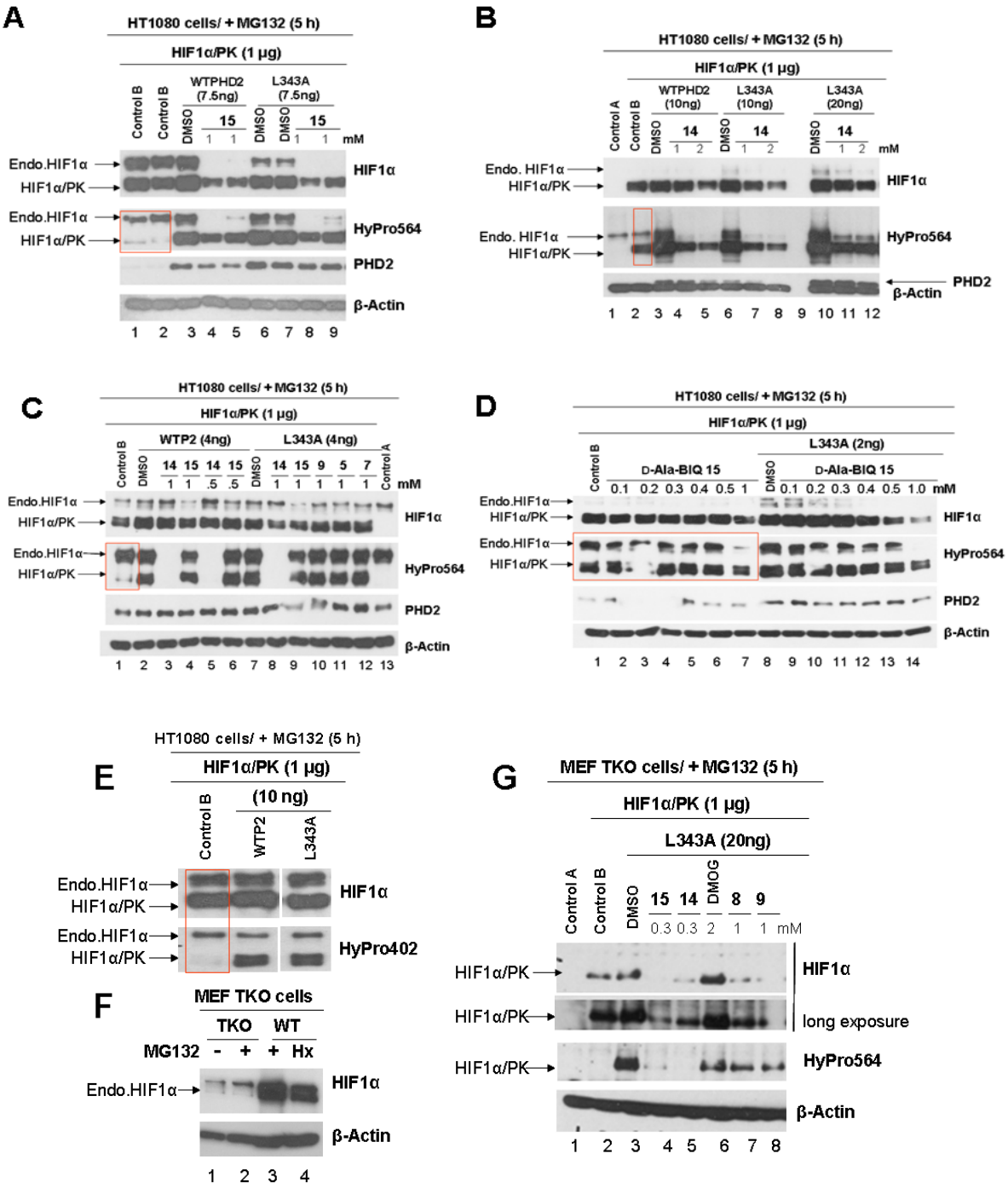


Figure 5.18: Summary of initial cell-based experiments carried out in human fibrosarcoma HT1080 and PHD null mouse embryonic fibroblast (TKO MEF). WT- or L343A-PHD2 were overexpressed in the presence of a truncated form of HIF-1α (HIF-1α/PK) using transient transfection. The transfected cells were then treated with PHD or variant-sensitive inhibitors in the presence of proteasome inhibitor MG132 for 5 h. (NOG analogues **12-16** were tested in their corresponding di-ester forms) Immunoblots probed with indicated antibodies (**A-E** HT1080 cells. **F-G** TKO MEF). Brackets ( ) showing amount of HIF-1α/PK and WT- or L343A-PHD2 plasmid DNA used per well (1 mL) in the transfection experiments. Control A represents untreated sample. Control B represents sample trasnfected with HIF-1α/PK but in the absence of PHD2-overexpression.

In agreement with the *in vitro* findings, the L343A-PHD2 variant was shown to catalyse the hydroxylation of NODD (Pro402) and CODD (Pro564) in HIF-1α in HT1080 cells at a level comparable to WT-PHD2. As observed from the hydroxy-residue specific immunoblots (Hyp564 and Hyp402) (**Fig. 5.18 A,** compare lanes 1, 3, 6, and **Fig 5.18 E**), WT-PHD2 and L343A-PHD2 transfected cells have significantly higher levels of CODD and NODD hydroxylation on HIF-1α/PK compared to the negative controls (without PHD2 overexpression) despite the samples having similar levels of HIF-1α/PK (HIF-1α immunoblots, lower band). Furthermore, the levels of prolyl hydroxylation were also shown to increase when higher L343A-PHD2 plasmid concentration was used in the transfection (**Fig. 5.18 B**, compare lanes 6 and 10), thus further confirming that the hydroxylation was a result of the L343A-PHD2 variant activity.

Although experiments were carried out at similar conditions, variable HIF-1α/PK hydroxylation levels were observed in the negative controls (without PHD2 transfections) (**Fig 5.18 A-D**, shown in red box) in more than ten independent experiments (some data not shown). In some experiments (e.g. **Fig 5.18 C**), the hydroxylation status of exogenous substrates (*i.e.* HIF-1α/PK) were much lower than the endogenous HIF-1α; the endogenous PHDs appeared to preferentially hydroxylate the natural substrates despite the presence of excess HIF-1α/PK. However, in other cases, high levels of HIF-1α/PK hydroxylation were observed in the negative controls (**Fig. 5.18 B** and **D**). One of the major disadvantages of transient transfections is the variable transfection efficiencies between experiments which lead to different degrees of protein expression. It cannot be ruled out that this is the reason for the differences observed in the hydroxylation status of HIF-1α/PK controls between experiments.

In the first instance, both BIQ **14** (a potent PHD inhibitor) and D-Ala-BIQ **15** (L343A-variant-sensitive analogue) (1 and 2 mM) appeared to have little or no effect on the hydroxylase activities of the WT-PHD2 or L343A-PHD2 transfectants (plasmid concentrations ~7.5 - 20 ng/100 µL media) *i.e.* similar levels of HIF-1α and Hyp564 signals were observed in the immunoblots (**Fig. 5.18 A and B**). It was therefore proposed high concentrations of inhibitors might be required to observe inhibition, given that

overexpression of the exogenous PHD2 enzymes in these cells markedly increased the hydroxylase activities. Lower levels of PHD2 overexpression would therefore be expected to result in inhibition of hydroxylation.

To achieve this, HT1080 cells were then transfected at lower plasmid concentrations (*i.e.* 4 ng/100 μL media) of WT-PHD2 and L343A-PHD2. However, under these conditions, the PHD2 protein levels of both the endogenous and exogenous were observed to be similar (**Fig 5.18 C**), meaning dissection of the endogenous and exogenous enzyme activities is almost impossible. High background levels of endogenous PHD activity might lead to a wrong interpretation of the results. This could be the reason why **BIQ 14** was observed to substantially inhibit the activities of the WT-PHD2 and L343A-PHD2 transfected cells (**Fig. 5.18 C**, Hypro564 immunoblot, lanes 3, 5, 8), whereas the L343A-variant-sensitive analogue inhibitors **15**, **5**, **7**, and **9** appeared to have no apparent effect on the activity of L343A-PHD2 transfectants (**Fig. 5.18 C**, lanes 9-12). This may be because **BIQ 14** not only inhibits the exogenous trasnfected PHD2s, but also the endogenous PHDs (as demonstrated in **Chapter 2 Section 2.2.4** in RCC4 cells), resulting in the observation of significant inhibition in these samples. Conversely, the variant-sensitive inhibitors did not inhibit the wild-type PHDs. The hydroxylation signals observed might be contributed to by the activities of endogenous PHDs. In addition, the inhibitor-treated transfectants were found to be highly susceptible to compound toxicity (observed from reduced HIF-1α levels and cell-morphological changes, for instance, D-Ala-BIQ **15** > 0.5 mM was found to gradually reduce the HIF-1α level (**Fig. 5.18 D**)), adding extra complexity to this system.

5.2.9.2 PHD null cell-system

Given that interference from the activity of endogenous PHDs was the major concern in HT1080 cells, it was judged that a PHD null cell-line (*i.e.* PHD1-2-3 triple-knockout (TKO) mouse embryonic fibroblast (MEF)) might be a better option for this study (the TKO MEF cell-line was obtained from Dr J. Adam.[257]) These cells stabilise HIF-1α due

to the absence of endogenous PHDs. Re-expressing PHD was expected to destabilise HIF-1α, while treatment of the PHD transfected cells with inhibitor was expected to increase HIF-1α activity.

Surprisingly, these PHD null cells have relatively low levels of HIF-1α compared to the wild-type cells (**Fig. 5.18 F**), making protein measurements difficult. Therefore, WT-PHD2 or L343A-PHD2 was overexpressed concurrently with the truncated version HIF-1α/PK. The PHD2 and HIF-1α/PK transfected PHD null cells were exposed to PHD inhibitors in the presence of proteasome inhibitor MG132 for 5 h. Under these assay conditions, BIQ analogues **14** and **15** and NOG analogues **8** and **9** (tested in their di-ester forms) were all shown to cause HIF-1α reduction, while DMOG (dimethyl ester of NOG) showed no apparent effect on the HIF-1α protein level (**Fig. 5.18 G**). The reasons for these differences are not clear. It may be compounds **14**, **15**, **8**, and **9** exerted greater toxicity effects or other possible mechanisms that promoted HIF-1α degradation under the tested conditions. Although extensive work has been carried out to optimise the cell-based experiment conditions. However, the PHD triple-knockout cells were found to have low transfection efficiencies and the transfected cells were highly susceptible to compound toxicity.

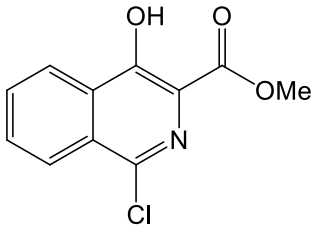
In conclusion, the presence of multiple endogenous PHDs makes dissection of the endogenous and exogenous PHD activity difficult in HT1080 cell-line, meaning that at least this natural mammalian cell-line (and possibily other natural mammaliam cell-lines) is probably not suitable to be used to determine PHD variant-analogue selectivity. PHD null cells were found to be resistant to further genetic alterations and highly susceptible to drug-induced toxicity. Therefore, without a suitable cell-system, this work is not yet able to demonstrate PHD variant-analogue selective inhibition in mammalian cells.

5.3 Conclusions and future directions

The work in this chapter demonstrates the feasibility of selective inhibition of PHD2 employing analogue-sensitive variants *in vitro*. Of the tested PHD2 variants, L343A-PHD2 was identified as the most active variant, retaining similar activity to WT-PHD2. D-Ala-BIQ (**15**) (IC_{50} 47.9 μM) was identified as a potent inhibitor which selectively inhibits the L343A-PHD2, but not the WT-PHD2. Attempts to test this 'bump-hole' (chemical-genetic) approach in mammalian cells have not been successful, possibly due to the lack of a suitable cell-system. Therefore, future research may focus on the further development of variant-sensitive analogue inhibitors and the generation of stable cell-lines expressing WT-PHD2 and L343A-PHD2 in PHD null cells.

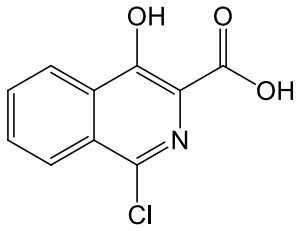
5.4 Synthesis and characterisation of the BIQ analogues

Methyl 1-chloro-4-hydroxyisoquinoline-3-carboxylate (21)[77]



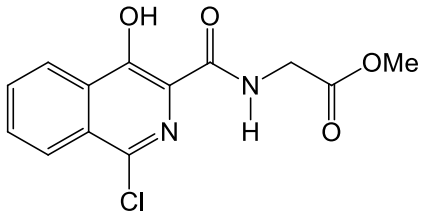
Methyl 1,4-dihydroxyisoquinoline (1.30 g, 5.9 mmol) was added to phosphorus oxychloride (10 mL, excess). The resulting mixture was stirred under reflux at 80^{o}C. TLC analysis indicated that the reaction was complete after 2 h. The excess phosphorus oxychloride was then removed under reduced pressure and the crude residue dissolved in EtOAc (30 mL). The organic layer was then washed with sodium hydrogen carbonate (3 x 30 mL) and brine (30 mL), dried ($MgSO_4$), filtered, and concentrated *in vacuo* to give methyl 1-chloro-4-hydroxyisoquinoline-3-carboxylate **21** (1.39 g, 98%) as a white solid; mp 137-140^{o}C; R_f (hexane: EtOAc, 4:1) 0.5; ν_{max} (KBr) 3454 (OH), 1619 (C=O), 1566, 1467, 1407, 1335 cm^{-1}; ^{1}H NMR (500 MHz, $CDCl_3$) δ 4.08 (3H, s, CH_3O), 7.82-7.86 (2H, m, 2 x Ar-H), 8.27-8.30 (1H, m, Ar-H), 8.39-8.42 (1H, m, Ar-H), 11.76 (1H, s, ArOH); ^{13}C NMR (125 MHz, $CDCl_3$) δ 53.1 (CH_3O), 119.3 (ArC), 123.7 (ArCH), 126.5 (ArCH), 129.6 (ArC), 129.7 (ArC), 131.0 (ArCH), 131.5 (ArCH), 140.9 (ArC), 156.5 (ArC), 170.2 (C=O) ; MS (ES$^-$) *m/z* 236.1 (60) [M-H]$^-$; HMRS (ESI) calcd. for $C_{11}H_7ClNO_3$ [M-H]$^-$ 236.0120; found 236.0113.

1-Chloro-4-hydroxyisoquinoline-3-carboxylic acid (22)[77]



A mixture of compound **21** (1.30 g, 5.5 mmol) and 1 N NaOH: EtOH (1:1) (50 ml, excess) was stirred under reflux at 85°C. TLC analysis (hexane: EtOAc, 4:1) indicated complete consumption of starting material (R_f 0.5) after 2 h. The reaction mixture was then washed with EtOAc (3 x 50 mL). The aqueous layer was acidified with 1 N HCl to pH 1 and then extracted with EtOAc (3 x 50 mL), dried ($MgSO_4$), filtered and concentrated *in vacuo* to give 1-chloro-4-hydroxyisoquinoline-3-carboxylic acid **22** (1.10 g, 90%) as a white solid; mp 318-320°C; ν_{max} (KBr) 3403 (OH), 1660 (C=O), 1570, 1475, 1315, 1235, 1173, 774 cm^{-1}; ^1H NMR (500 MHz, DMSO-d_6) δ 7.96-8.01 (2H, m, 2 x Ar-H), 8.21-8.25 (1H, m, Ar-H), 8.31-8.36 (1H, m, Ar-H); ^{13}C NMR (125 MHz, DMSO-d_6) δ 119.5 (ArC), 123.2 (ArCH), 125.9 (ArCH), 128.8 (ArC), 129.1 (ArC), 131.8 (ArCH), 132.1 (ArCH), 138.8 (ArC), 156.0 (ArC), 171.5 (C=O) ; MS (ES^-) *m/z* 222.0 (100) $[M-H]^-$; HMRS (ESI) calcd. for $C_{10}H_5ClNO_3$ $[M-H]^-$ 221.9963; found 221.9955.

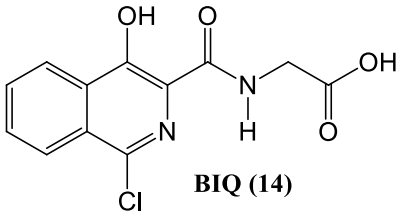
Methyl 2-(1-chloro-4-hydroxyisoquinoline-3-carboxamido)acetate (23)[77]



To a solution of glycine methyl ester hydrochloride (336 mg, 2.7 mmol, 1.2 equiv) and triethylamine (0.8 mL, 5.6 mmol, 2.5 equiv.) in CH_2Cl_2 (50 mL) were added compound **22** (500 mg, 2.2 mmol, 1 equiv.) followed by benzotriazol-1-yl-oxytripyrrolidinophosphonium hexafluorophosphate (1.28 g, 2.45 mmol, 1.1 equiv.). The resulting mixture was then stirred at room temperature. TLC analysis indicated that the reaction was complete after 20 h. The organic solvents were removed and the residue was

purified by flash chromatography (hexane: EtOAc, 4:1) to afford methyl 2-(1-chloro-4-hydroxyisoquinoline-3-carboxamido)acetate **23** (490 mg, 75%) as a white solid, mp 101-103^{o}C; R_f (hexane: EtOAc, 4:1) 0.3; ν_{max} (KBr) 3401 (NH), 2955 (C-H), 1743 (C=O), 1636 (C=O), 1569, 1538, 1401, 1344, 981, 770 cm^{-1}; ^{1}H NMR (500 MHz, $CDCl_3$) δ 3.82 (3H, s, CH_3O), 4.29 (2H, d, J 5.5, CH_2), 7.76-7.81 (2H, m, 2 x Ar-H), 8.20-8.25 (2H, m, Ar-H, NH), 8.33-8.46 (1H, m, Ar-H), 12.83 (1H, s, ArOH); ^{13}C NMR (125 MHz, $CDCl_3$) δ 40.7 (CH), 52.5 (CH_3O), 120.3 (ArC), 123.4 (ArCH), 126.4 (ArCH), 129.4 (ArC), 130.1 (ArC), 130.8 (2 x ArCH), 139.4 (ArC), 154.5 (ArC), 169.1 (C=O), 169.6 (C=O) ; MS (ES$^-$) *m/z* 293.1 (90) [M-H]$^-$.

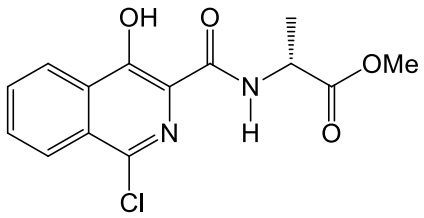
2-(1-Chloro-4-hydroxyisoquinoline-3-carboxamido)acetic acid (14)[77]



BIQ (14)

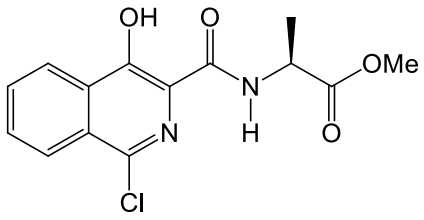
A mixture of compound **23** (470 mg, 1.6 mmol) and 1 N NaOH: MeOH (1:1) (20 ml, excess) was stirred at room temperature. TLC analysis (hexane: EtOAc, 4:1) indicated complete consumption of starting material (R_f 0.3) after 2 h. The reaction mixture was then washed with EtOAc (3 x 10 mL). The aqueous layer was acidified with 1 N HCl to pH 1 and then extracted with EtOAc (3 x 10 mL), dried ($MgSO_4$), filtered, and concentrated *in vacuo* to give 2-(1-chloro-4-hydroxyisoquinoline-3-carboxamido)acetic acid **14** (420 mg, 94%) as a white solid; mp 222-225^{o}C; ν_{max} (KBr) 3400 (NH), 2913 (C-H), 1712 (C=O), 1640 (C=O), 1586, 1568, 1530, 1355, 1255, 954, 794 cm^{-1}; ^{1}H NMR (500 MHz, MeOD) δ 4.20 (2H, s, CH_2), 7.91-7.94 (2H, m, 2 x Ar-H), 8.33-8.35 (1H, m, Ar-H), 8.41-8.43 (1H, m, Ar-H); ^{13}C NMR (125 MHz, MeOD) δ 41.5 (CH_2), 122.0 (ArC), 124.3 (ArCH), 127.4 (ArCH), 130.6 (ArC), 131.4 (ArC), 132.3 (2 x ArCH), 140.6 (ArC), 155.8 (ArC), 170.8 (C=O), 172.8 (C=O) ; MS (ES$^-$) *m/z* 279.0 (100) [M-H]$^-$. Anal. ($C_{12}H_9ClN_2O_4$) requires: C, 51.35; H, 3.23; N, 9.98%; found C, 51.26; H, 3.19; N, 9.89%.

***(R)*-Methyl 2-(1-chloro-4-hydroxyisoquinoline-3-carboxamido)propanoate (24)**



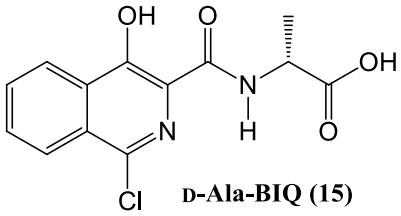
To a solution of D-alanine methyl ester hydrochloride (98 mg, 0.7 mmol, 1.2 equiv.) and triethylamine (0.2 mL, 1.5 mmol, 2.5 equiv.) in CH_2Cl_2 (10 mL) were added compound **22** (130 mg, 0.6 mmol, 1 equiv.) followed by benzotriazol-1-yl-oxytripyrrolidinophosphonium hexafluorophosphate (332 mg, 0.6 mmol, 1.1 equiv.). The resulting mixture was then stirred at room temperature. TLC analysis indicated that the reaction was complete after 20 h. The organic solvents were removed and the residue was purified by flash chromatography (hexane: EtOAc, 4:1) to afford (*R*)-methyl 2-(1-chloro-4-hydroxyisoquinoline-3-carboxamido)propanoate **24** (110 mg, 67%) as a white solid, mp 116-118^{o}C; R_f (hexane: EtOAc, 4:1) 0.5; $[\alpha]_D^{22}$ - 20.2 (*c*, 1.0 in CH_2Cl_2); ν_{max} (KBr) 3394 (NH), 2941 (C-H), 1740 (C=O), 1638 (C=O), 1568, 1531, 1329, 955, 772 cm^{-1}; ^{1}H NMR (500 MHz, $CDCl_3$) δ 1.61 (3H, d, J 6.9, CH_3), 3.82 (3H, s, CH_3O), 4.78-4.84 (1H, m, CH), 7.80-7.85 (2H, m, 2 x Ar-H), 8.20 (1H, d, J 7.5, NH), 8.27-8.31 (1H, m, Ar-H), 8.39-8.42 (1H, m, Ar-H), 12.96 (1H, s, ArOH); ^{13}C NMR (125 MHz, $CDCl_3$) δ 18.2 (CH_3), 47.9 (CH), 52.6 (CH_3O), 120.4 (ArC), 123.4 (ArCH), 126.5 (ArCH), 129.5 (ArC), 130.2 (ArC), 130.8 (2 x ArCH), 139.5 (ArC), 154.9 (ArC), 168.5 (C=O), 172.7 (C=O) ; MS (ES$^-$) *m/z* 307.1 (100) [M-H]$^-$; HMRS (ESI) calcd. for $C_{14}H_{12}ClN_2O_4$ [M-H]$^-$ 307.0491; found 307.0493.

***(R)*-Methyl 2-(1-chloro-4-hydroxyisoquinoline-3-carboxamido)propanoate (25)**



To a solution of L-alanine methyl ester hydrochloride (98 mg, 0.7 mmol, 1.2 equiv.) and triethylamine (0.2 mL, 1.5 mmol, 2.5 equiv.) in CH_2Cl_2 (10 mL) were added compound **22** (130 mg, 0.6 mmol, 1 equiv.) followed by benzotriazol-1-yl-oxytripyrrolidinophosphonium hexafluorophosphate (332 mg, 0.6 mmol, 1.1 equiv). The resulting mixture was then stirred at room temperature. TLC analysis indicated that the reaction was complete after 20 h. The organic solvents were removed and the residue was purified by flash chromatography (hexane: EtOAc, 4:1) to afford (*R*)-methyl 2-(1-chloro-4-hydroxyisoquinoline-3-carboxamido)propanoate **25** (105 mg, 59%) as a white solid, mp 178-180^{o}C; R_f (hexane: EtOAc, 4:1) 0.5; $[\alpha]_D^{22}$ + 21.6 (*c*, 1.0 in CH_2Cl_2); ν_{max} (KBr) 3394 (NH), 2941 (C-H), 1740 (C=O), 1638 (C=O), 1568, 1530, 1328, 955, 771 cm^{-1}; ^{1}H NMR (500 MHz, $CDCl_3$) δ 1.61 (3H, d, J 7.5, CH_3), 3.82 (3H, s, CH_3O), 4.78-4.84 (1H, m, CH), 7.79-7.85 (2H, m, 2 x Ar-H), 8.20 (1H, d, J 7.5, NH), 8.27-8.30 (1H, m, Ar-H), 8.38-8.41 (1H, m, Ar-H), 12.97 (1H, s, ArOH); ^{13}C NMR (125 MHz, $CDCl_3$) δ 18.2 (CH_3), 47.9 (CH), 52.6 (CH_3O), 120.4 (ArC), 123.4 (ArCH), 126.4 (ArCH), 129.5 (ArC), 130.2 (ArC), 130.8 (2 x ArCH), 139.5 (ArC), 154.9 (ArC), 168.5 (C=O), 172.7 (C=O) ; MS (ES$^-$) *m/z* 307.1 (100) [M-H]$^-$; HMRS (ES$^-$) calcd. for $C_{14}H_{12}ClN_2O_4$ [M-H]$^-$ 307.0491; found 307.0495.

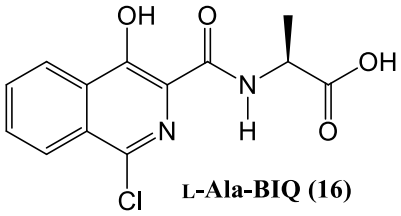
***(R)*-2(1-Chloro-4-hydroxyisoquinoline-3-carboxamido)propanoic acid (15)**



D-Ala-BIQ (15)

A mixture of compound **24** (90 mg, 0.3 mmol) and 1 N NaOH: MeOH (1:1) (10 ml, excess) was stirred at room temperature. TLC analysis (hexane: EtOAc, 4:1) indicated complete consumption of starting material (R_f 0.5) after 2 h. The reaction mixture was then washed with EtOAc (3 x 10 mL). The aqueous layer was acidified with 1 N HCl to pH 1 and then extracted with EtOAc (3 x 10 mL), dried ($MgSO_4$), filtered, and concentrated *in vacuo* to give (*R*)-2(1-chloro-4-hydroxyisoquinoline-3-carboxamido)propanoic acid **15** (84 mg, 98%) as a white solid; mp 116-118^oC; $[\alpha]_D^{22}$ -26.8 (*c*, 1.0 in MeOH); ν_{max} (KBr) 3441 (OH), 3372 (NH), 2942 (C-H), 1737 (C=O), 1619 (C=O), 1586, 1573, 1547, 1359, 1286, 771 cm^{-1}; ^1H NMR (500 MHz, DMSO-d_6) δ 1.50 (3H, d, J 7.3, CH_3), 4.54-4.60 (1H, m, CH), 7.98-8.03 (2H, m, 2 x Ar-H), 8.29-8.32 (1H, m, Ar-H), 8.34-8.37 (1H, m, Ar-H), 9.08 (1H, d, J 8.0, NH), 13.67 (1H, s, OH); ^{13}C NMR (125 MHz, DMSO-d_6) δ 16.9 (CH_3), 47.6 (CH), 120.4 (ArC), 123.0 (ArCH), 126.1 (ArCH), 128.6 (ArC), 129.5 (ArC), 131.7 (ArCH), 131.8 (ArCH), 138.5 (ArC), 154.4 (ArC), 168.2 (C=O), 173.2 (C=O) ; MS (ES^-) *m/z* 293.0 (100) $[M-H]^-$; HMRS (ES^-) calcd. for $C_{13}H_{10}ClN_2O_4$ $[M-H]^-$ 293.0335; found 293.0342. Anal. ($C_{13}H_{11}ClN_2O_4$) requires: C, 52.98; H, 3.76; N, 9.51%; found C, 52.93; H, 3.83; N, 9.40%.

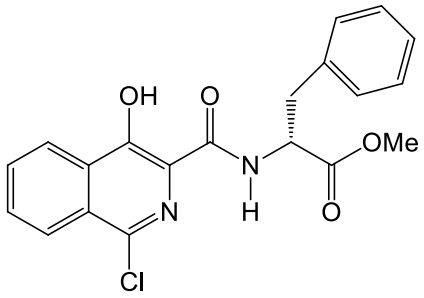
***(S)*-2(1-Chloro-4-hydroxyisoquinoline-3-carboxamido)propanoic acid (16)**



L-Ala-BIQ (16)

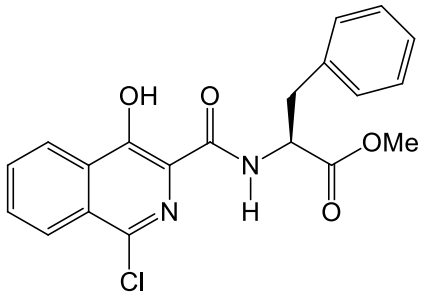
A mixture of compound **25** (85 mg, 0.3 mmol) and 1 N NaOH: MeOH (1:1) (10 ml, excess) was stirred at room temperature. TLC analysis (hexane: EtOAc, 4:1) indicated complete consumption of starting material (R_f 0.5) after 2 h. The reaction mixture was then washed with EtOAc (3 x 10 mL). The aqueous layer was acidified with 1 N HCl to pH 1 and then extracted with EtOAc (3 x 10 mL), dried ($MgSO_4$), filtered, and concentrated *in vacuo* to give (*S*)-2(1-chloro-4-hydroxyisoquinoline-3-carboxamido)propanoic acid **16** (77 mg, 93%) as a white solid; m.p. 178-180^oC; $[\alpha]_D^{25}$ + 25.0 (*c*, 1.0 in MeOH); ν_{max} (KBr) 3441 (OH), 3372 (NH), 2942 (C-H), 1737 (C=O), 1618 (C=O), 1586, 1574, 1547, 1360, 1286, 771 cm^{-1}; ^1H NMR (500 MHz, DMSO-d_6) δ 1.50 (3H, d, J 7.3, CH_3), 4.54-4.60 (1H, m, CH), 7.98-8.02 (2H, m, 2 x Ar-H), 8.28-8.31 (1H, m, Ar-H), 8.33-8.36 (1H, m, Ar-H), 9.07 (1H, d, J 7.5, NH), 13.66 (1H, s, OH); ^{13}C NMR (125 MHz, DMSO-d_6) δ 16.9 (CH_3), 47.6 (CH), 120.4 (ArC), 123.0 (ArCH), 126.1 (ArCH), 128.6 (ArC), 129.5 (ArC), 131.7 (ArCH), 131.8 (ArCH), 138.5 (ArC), 154.4 (ArC), 168.2 (C=O), 173.2 (C=O) ; MS (ES^-) *m/z* 293.0 (100) $[M-H]^-$; HMRS (ES^-) calcd. for $C_{13}H_{10}ClN_2O_4$ $[M-H]^-$ 293.0335; found 293.0335. Anal. ($C_{13}H_{11}ClN_2O_4$) requires: C, 52.98; H, 3.76; N, 9.51%; found C, 52.95; H, 3.65; N, 9.43%.

***(R)*-2-(1-Chloro-4-hydroxyisoquinoline-3-carboxamido)-3-phenylpropanoate (26)**



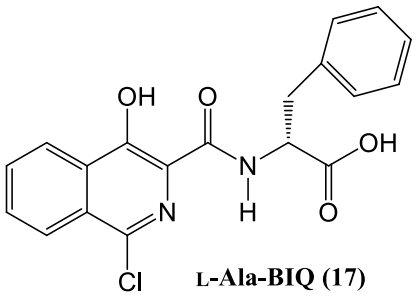
To a solution of D-phenylalanine methyl ester hydrochloride (151 mg, 0.7 mmol, 1.2 equiv.) and triethylamine (0.2 mL, 1.5 mmol, 2.5 equiv.) in CH_2Cl_2 (10 mL) were added compound **22** (130 mg, 0.6 mmol, 1 equiv.) followed by benzotriazol-1-yl-oxytripyrrolidinophosphonium hexafluorophosphate (332 mg, 0.6 mmol, 1.1 equiv.).The resulting mixture was then stirred at room temperature. TLC analysis indicated that the reaction was complete after 20 h. The organic solvents were removed and the residue was purified by flash chromatography (hexane: EtOAc, 4:1) to afford *(R)*-2-(1-chloro-4-hydroxyisoquinoline-3-carboxamido)-3-phenylpropanoate **26** (147 mg, 66%) as yellow oil; R_f (hexane: EtOAc, 4:1) 0.4; $[\alpha]_D^{22}$ - 16.8 (*c*, 1.0 in CH_2Cl_2); ν_{max} (KBr disc) 3384 (N-H), 2925 (C-H), 1745 (C=O), 1638 (C=O), 1568, 1531, 1323, 943, 718 cm^{-1}; ^1H NMR (500 MHz, $CDCl_3$) δ 3.25 (1H, dd, J 14.0, 6.9, $PhCH_2$), 3.31 (1H, dd, J 14.0, 6.0, $PhCH_2$), 3.77 (3H, s, CH_3O), 5.02-5.06 (1H, m, CH), 7.23-7.34 (5H, m, 5 x Ph-H), 7.77-7.81 (2H, m, 2 x Ar-H), 8.21 (1H, d, J 8.0, NH), 8.23-8.26 (1H, m, Ar-H), 8.34-8.37 (1H, m, Ar-H), 12.85 (1H, s, ArOH); ^{13}C NMR (125 MHz, $CDCl_3$) δ 37.9 ($PhCH_2$), 52.2 (CH_3O), 52.9 (CH), 120.4 (ArC), 123.1 (ArCH), 126.1 (ArCH), 127.0 (PhCH), 128.5 (2 x ArCH), 128.9 (2 x PhCH), 129.1 (ArC), 130.0 (ArC), 130.5 (2 x PhCH), 135.9 (PhC), 139.3 (ArC), 154.5 (ArC), 168.2 (C=O), 171.0 (C=O) ; MS (ES^-) *m/z* 383.1 (100) $[M-H]^-$; HMRS (ESI) calcd. for $C_{20}H_{16}ClN_2O_4$ $[M-H]^-$ 383.0804; found 383.0805.

_(S)_-2-(1-Chloro-4-hydroxyisoquinoline-3-carboxamido)-3-phenylpropanoic acid (27)



To a solution of L-phenylalanine methyl ester hydrochloride (151 mg, 0.7 mmol, 1.2 equiv) and triethylamine (0.2 mL, 1.5 mmol, 2.5 equiv.) in CH_2Cl_2 (10 mL) were added compound **22** (130 mg, 0.6 mmol, 1 equiv.) followed by benzotriazol-1-yl-oxytripyrrolidinophosphonium hexafluorophosphate (332 mg, 0.6 mmol, 1.1 equiv.). The resulting mixture was then stirred at room temperature. TLC analysis indicated that the reaction was complete after 20 h. The organic solvents were removed and the residue was purified by flash chromatography (hexane: EtOAc, 4:1) to afford *(S)*-2-(1-chloro-4-hydroxyisoquinoline-3-carboxamido)-3-phenylpropanoate **27** (130 mg, 59%) as yellow oil; R_f (hexane: EtOAc, 4:1) 0.4; $[\alpha]_D^{22}$ - 17.5 (*c*, 1.0 in CH_2Cl_2); ν_{max} (KBr disc) 3384 (N-H), 2925 (C-H), 1745 (C=O), 1639 (C=O), 1568, 1531, 1323, 943, 719 cm^{-1}; ^1H NMR (500 MHz, $CDCl_3$) δ 3.25 (1H, dd, J 13.9, 6.9 Hz, $PhCH_2$), 3.31 (1H, dd, J 13.9, 6.0 Hz, $PhCH_2$), 3.77 (3H, s, CH_3O), 5.02-5.06 (1H, m, CH), 7.23-7.34 (5H, m, 5 x Ph-H), 7.77-7.81 (2H, m, 2 x Ar-H), 8.21 (1H, d, J 8.0, NH), 8.25-8.26 (1H, m, Ar-H), 8.35-8.37 (1H, m, Ar-H), 12.86 (1H, s, ArOH); ^{13}C NMR (125 MHz, $CDCl_3$) δ 38.0 ($PhCH_2$), 52.2 (CH_3O), 52.9 (CH), 120.1 (ArC), 123.1 (ArCH), 126.2 (ArCH), 127.0 (PhCH), 128.5 (2 x ArCH), 128.9 (2 x PhCH), 129.2 (ArC), 130.0 (ArC), 130.5 (2 x PhCH), 135.4 (PhC), 139.3 (ArC), 154.5 (ArC), 168.2 (C=O), 171.1 (C=O) ; MS (ES^-) *m/z* 383.1 (100) $[M-H]^-$; HMRS (ESI) calcd. for $C_{20}H_{16}ClN_2O_4$ $[M-H]^-$ 383.0804; found 383.0804.

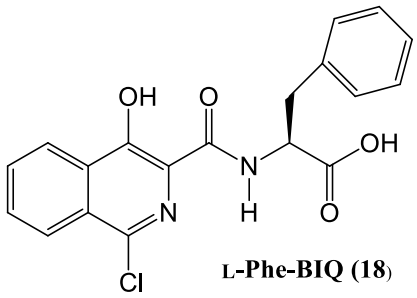
***(R)*-2-(1-Chloro-4-hydroxyisoquinoline-3-carboxamido)-3-phenylpropanoic acid (17)**



L-Ala-BIQ (17)

A mixture of compound **26** (110 mg, 0.3 mmol) and 1 N NaOH: MeOH (1:1) (10 ml, excess) was stirred at room temperature. TLC analysis (hexane: EtOAc, 4:1) indicated complete consumption of starting material (R_f 0.4) after 2 h. The reaction mixture was then washed with EtOAc (3 x 10 mL). The aqueous layer was acidified with 1 N HCl to pH 1 and then extracted with EtOAc (3 x 10 mL), dried ($MgSO_4$), filtered, and concentrated *in vacuo* to give *(R)*-2-(1-Chloro-4-hydroxyisoquinoline-3-carboxamido)-3-phenylpropanoic acid **17** (100 mg, 95%) as a pale yellow solid; mp 184-186^{o}C; $[\alpha]_D^{22}$ – 13.0 (*c*, 1.0 in MeOH); ν_{max} (KBr) 3448 (OH), 3362 (NH), 2930 (C-H), 1736 (C=O), 1637 (C=O), 1570, 1540, 1323, 1258, 941, 771 cm^{-1}; ^{1}H NMR (500 MHz, DMSO-d_6) δ 3.28-3.33 (2H, m, $PhCH_2$), 4.79-4.84 (1H, m, CH), 7.16-7.20 (1H, m, Ph-H), 7.26-7.27 (4H, m, 4 x Ph-H), 7.93-7.96 (2H, m, 2 x Ar-H), 8.22-8.24 (1H, m, Ar-H), 8.29-8.27 (1H, m, Ar-H), 8.93 (1H, d, J 8.0, NH), 13.49 (1H, s, ArOH); ^{13}C NMR (125 MHz, DMSO-d_6) δ 35.9 ($PhCH_2$), 53.2 (CH), 120.3 (ArC), 123.0 (ArCH), 126.1 (ArCH), 126.6 (PhCH), 128.3 (2 x PhCH), 128.6 (ArC), 129.1 (2 x ArCH), 129.4 (ArC), 131.7 (PhCH), 131.8 (PhCH), 137.5 (PhC), 138.5 (ArC), 154.3 (ArC), 168.4 (C=O), 172.1 (C=O); MS (ES$^-$) *m/z* 369.1 (100) [M-H]$^-$; HMRS (ES$^-$) calcd. for $C_{19}H_{14}ClN_2O_4$ [M-H]$^-$ 369.0648; found 369.0651. Anal. ($C_{19}H_{15}ClN_2O_4$) requires: C, 61.55; H, 4.08; N, 7.56%; found C, 61.45; H, 4.00; N, 7.63%.

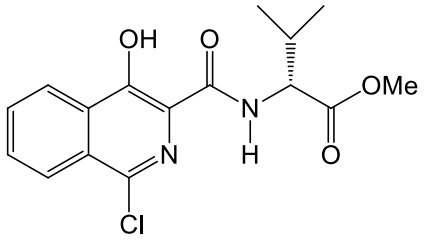
***(S)*-2-(1-Chloro-4-hydroxyisoquinoline-3-carboxamido)-3-phenylpropanoic acid (18)**



L-Phe-BIQ (18)

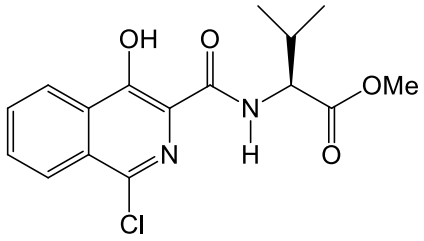
A mixture of compound **27** (100 mg, 0.3 mmol) and 1 N NaOH: MeOH (1:1) (10 ml, excess) was stirred at room temperature. TLC analysis (hexane: EtOAc, 4:1) indicated complete consumption of starting material (R_f 0.4) after 2 h. The reaction mixture was then washed with EtOAc (3 x 10 mL). The aqueous layer was acidified with 1 N HCl to pH 1 and then extracted with EtOAc (3 x 10 mL), dried ($MgSO_4$), filtered, and concentrated *in vacuo* to give *(S)*-2-(1-Chloro-4-hydroxyisoquinoline-3-carboxamido)-3-phenylpropanoic acid **18** (90 mg, 92%) as a pale yellow solid; mp 185-188 ^oC; $[\alpha]_D^{22}$ + 12.9 (*c*, 1.0 in MeOH); ν_{max} (KBr) 3448 (OH), 3362 (NH), 2929 (C-H), 1736 (C=O), 1637 (C=O), 1570, 1540, 1322, 1259, 941, 773 cm^{-1}; ^1H NMR (500 MHz, DMSO-d_6) δ 3.27-3.32 (2H, m, $PhCH_2$), 4.79-4.83 (1H, m, CH), 7.17-7.21 (1H, m, Ph-H), 7.26-7.27 (4H, m, 4 x Ph-H), 7.97-7.99 (2H, m, 2 x Ar-H), 8.26-8.28 (1H, m, Ar-H), 8.30-8.32 (1H, m, Ar-H), 8.94 (1H, d, J 8.0, NH), 13.50 (1H, s, ArOH); ^{13}C NMR (125 MHz, DMSO-d_6) δ 35.9 ($PhCH_2$), 53.2 (CH), 120.3 (ArC), 123.0 (ArCH), 126.1 (ArCH), 126.6 (PhCH), 128.3 (2 x PhCH), 128.6 (ArC), 129.1 (2 x ArCH), 129.5 (ArC), 131.7 (PhCH), 131.8 (PhCH), 137.4 (PhC), 138.5 (ArC), 154.3 (ArC), 168.4 (C=O), 172.1 (C=O); MS (ES^-) *m/z* 369.1 (100) $[M-H]^-$; HMRS (ES^-) calcd. for $C_{19}H_{14}ClN_2O_4$ $[M-H]^-$ 369.0648; found 369.0651. Anal. ($C_{19}H_{15}ClN_2O_4$) requires: C, 61.55; H, 4.08; N, 7.56%; found C, 61.61; H, 4.01; N, 7.62%.

***(R)*-Methyl 2-(1-chloro-4-hydroxyisoquinoline-3-carboxamido)-3-methylbutanone (28)**



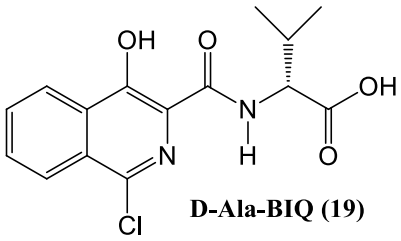
To a solution of D-valine methyl ester hydrochloride (118 mg, 0.7 mmol, 1.2 equiv.) and triethylamine (0.2 mL, 1.5 mmol, 2.5 equiv.) in CH_2Cl_2 (10 mL) were added compound **22** (130 mg, 0.6 mmol, 1 equiv.) followed by benzotriazol-1-yl-oxytripyrrolidinophosphonium hexafluorophosphate (332 mg, 0.6 mmol, 1.1 equiv.). The resulting mixture was then stirred at room temperature. TLC analysis indicated that the reaction was complete after 20 h. The organic solvents were removed and the residue was purified by flash chromatography (hexane: EtOAc, 9:1) to afford *(R)*-methyl 2-(1-chloro-4-hydroxyisoquinoline-3-carboxamido)-3-methylbutanone **28** (97 mg, 50%) as yellow oil; R_f (hexane: EtOAc, 9:1) 0.4; $[\alpha]_D^{22}$ - 19.5 (*c*, 1.0 in CH_2Cl_2); ν_{max} (KBr disc) 3390 (NH), 2965 (C-H), 1745 (C=O), 1640 (C=O), 1568, 1531, 1321, 965, 718 cm^{-1}; ^1H NMR (500 MHz, $CDCl_3$) δ 1.07 (6H, d, J 6.9, 2 x CH_3), 2.32-2.38 (1H, m, C<u>H</u>$(CH_3)_2$), 3.81 (3H, s, CH_3O), 4.71 (1H, dd, J 5.5, J 9.0, α-CH), 7.79-7.84 (2H, m, 2 x Ar-H), 8.21 (1H, d, J 9.0, NH), 8.26-8.30 (1H, m, Ar-H), 8.37-8.41 (1H, m, Ar-H), 13.00 (1H, s, ArOH); ^{13}C NMR (125 MHz, $CDCl_3$) δ 18.1 (CH_3), 19.1 (CH_3), 31.4 (<u>C</u>H$(CH_3)_2$), 52.3 (CH_3O), 57.1 (α-CH), 120.5 (ArC), 123.4 (ArCH), 126.5 (ArCH), 129.5 (ArC), 130.2 (ArC), 130.8 (2 x ArCH), 139.5 (ArC), 154.9 (ArC), 168.8 (C=O), 171.7 (C=O) ; MS (ES^-) *m/z* 335.1 (100) $[M-H]^-$; HMRS (ESI) calcd. for $C_{16}H_{16}ClN_2O_4$ $[M-H]^-$ 335.0804; found 335.0802.

***(S)*-Methyl 2-(1-chloro-4-hydroxyisoquinoline-3-carboxamido)-3-methylbutanone (29)**



To a solution of L-valine methyl ester hydrochloride (118 mg, 0.7 mmol, 1.2 equiv.) and triethylamine (0.2 mL, 1.5 mmol, 2.5 equiv.) in CH_2Cl_2 (10 mL) were added compound **22** (130 mg, 0.6 mmol, 1 equiv.) followed by benzotriazol-1-yl-oxytripyrrolidinophosphonium hexafluorophosphate (332 mg, 0.6 mmol, 1.1 equiv).The resulting mixture was then stirred at room temperature. TLC analysis indicated that the reaction was complete after 20 h. The organic solvents were removed and the residue was purified by flash chromatography (hexane: EtOAc, 9:1) to afford *(S)*-methyl 2-(1-chloro-4-hydroxyisoquinoline-3-carboxamido)-3-methylbutanone **29** (108 mg, 55%) as yellow oil; R_f (hexane: EtOAc, 9:1) 0.4; $[\alpha]_D^{22}$ +17.4 (*c*, 1.0 in CH_2Cl_2); ν_{max} (KBr disc) 3389 (NH), 2964 (C-H), 1744 (C=O), 1641 (C=O), 1568, 1531, 1321, 965, 719 cm^{-1}; ^1H NMR (500 MHz, $CDCl_3$) δ 1.07 (6H, d, J 7.0 Hz, 2 x CH_3), 2.30-2.40 (1H, m, C<u>H</u>$(CH_3)_2$), 3.81 (3H, s, CH_3O), 4.71 (1H, dd, J 5.5, 9.0, α-CH), 7.78-7.83 (2H, m, 2 x Ar-H), 8.21 (1H, d, J 9.0, NH), 8.26-8.29 (1H, m, Ar-H), 8.37-8.40 (1H, m, Ar-H), 13.00 (1H, s, ArOH); ^{13}C NMR (125 MHz, $CDCl_3$) δ 18.1 (CH_3), 19.1 (CH_3), 31.4 (<u>C</u>H$(CH_3)_2$), 52.3 (CH_3O), 57.1 (α-CH), 120.5 (ArC), 123.4 (ArCH), 126.5 (ArCH), 129.5 (ArC), 130.2 (ArC), 130.8 (2 x ArCH), 139.5 (ArC), 154.9 (ArC), 168.8 (C=O), 171.7 (C=O) ; MS (ES^-) *m/z* 335.1 (100) $[M-H]^-$; HMRS (ESI) calcd. for $C_{16}H_{16}ClN_2O_4$ $[M-H]^-$ 335.0804; found 335.0810.

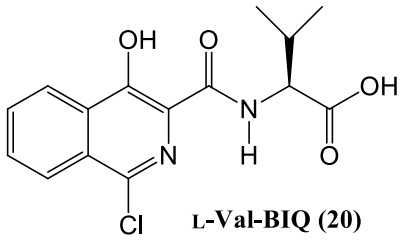
***(R)*-Methyl 2-(1-chloro-4-hydroxyisoquinoline-3-carboxamido)-3-methylbutanoic acid (19)**



D-Ala-BIQ (19)

A mixture of compound **28** (80 mg, 0.2 mmol) and 1 N NaOH: MeOH (1:1) (10 ml, excess) was stirred at room temperature. TLC analysis (hexane: EtOAc, 9:1) indicated complete consumption of starting material (R_f 0.4) after 2 h. The reaction mixture was then washed with EtOAc (3 x 10 mL). The aqueous layer was acidified with 1 N HCl to pH 1 and then extracted with EtOAc (3 x 10 mL), dried ($MgSO_4$), filtered, and concentrated *in vacuo* to give *(R)*-methyl 2-(1-chloro-4-hydroxyisoquinoline-3-carboxamido)-3-methylbutanoic acid **19** (69 mg, 88%) as a white solid; mp 178-180^{o}C; $[\alpha]_D^{22}$ – 31.1 (*c*, 1.0 in MeOH); ν_{max} (KBr) 3449 (OH), 3373 (NH), 2965 (C-H), 1758 (C=O), 1619 (C=O), 1572, 1544, 1325, 1259, 970, 778 cm^{-1}; ^{1}H NMR (500 MHz, DMSO-d_6) δ 1.00 (6H, dd, J 7.0, 5.5, 2 x CH_3), 2.28-2.36 (1H, m, C<u>H</u>$(CH_3)_2$), 4.44 (1H, dd, J 5.7, 8.5, α-CH), 7.98-8.02 (2H, m, 2 x Ar-H), 8.28-8.31 (1H, m, Ar-H), 8.33-8.37 (1H, m, Ar-H), 8.50 (1H, d, J 8.5, NH), 13.40 (1H, s, ArOH); ^{13}C NMR (125 MHz, DMSO-d_6) δ 18.1 (CH_3), 19.1 (CH_3), 30.1 (<u>C</u>H$(CH_3)_2$), 57.1 (α-CH), 120.1 (ArC), 123.0 (ArCH), 126.2 (ArCH), 128.6 (ArC), 129.5 (ArC), 131.8 (ArCH), 131.9 (ArCH), 138.7 (ArC), 154.3 (ArC), 168.2 (C=O), 172.1 (C=O); MS (ES$^-$) *m/z* 321.1 (100) [M-H]$^-$; HMRS (ES$^-$) calcd. for $C_{15}H_{14}ClN_2O_4$ [M-H]$^-$ 321.0648; found 321.0635. Anal. ($C_{15}H_{15}ClN_2O_4$) requires: C, 55.82; H, 4.68; N, 8.68%; found C, 55.93; H, 4.73; N, 8.74%.

***(S)*-Methyl 2-(1-chloro-4-hydroxyisoquinoline-3-carboxamido)-3-methylbutanoic acid (20)**



L-Val-BIQ (20)

A mixture of compound **29** (78 mg, 0.2 mmol) and 1 N NaOH: MeOH (1:1) (10 ml, excess) was stirred at room temperature. TLC analysis (hexane: EtOAc, 9:1) indicated complete consumption of starting material (R_f 0.4) after 2 h. The reaction mixture was then washed with EtOAc (3 x 10 mL). The aqueous layer was acidified with 1 N HCl to pH 1 and then extracted with EtOAc (3 x 10 mL), dried ($MgSO_4$), filtered, and concentrated *in vacuo* to give *(S)*-methyl 2-(1-chloro-4-hydroxyisoquinoline-3-carboxamido)-3-methylbutanoic acid **20** (70 mg, 94%) as a white solid; mp 178-180^oC; $[\alpha]_D^{22}$ + 29.5 (*c*, 1.0 in MeOH); ν_{max} (KBr) 3449 (OH), 3373 (NH), 2965 (C-H), 1758 (C=O), 1619 (C=O), 1572, 1544, 1325, 1259, 970, 778 cm^{-1}; ^1H NMR (500 MHz, DMSO-d_6) δ 1.00 (6H, dd, J 5.5., 7.0, 2 x CH_3), 2.28-2.36 (1H, m, C<u>H</u>$(CH_3)_2$), 4.44 (1H, dd, J 5.5, 8.5, α-CH), 7.98-8.02 (2H, m, 2 x Ar-H), 8.28-8.31 (1H, m, Ar-H), 8.33-8.36 (1H, m, Ar-H), 8.50 (1H, d, J 8.5, NH), 13.40 (1H, s, ArOH); ^{13}C NMR (125 MHz, DMSO-d_6) δ 18.1 (CH_3), 19.1 (CH_3), 30.2 (<u>C</u>H$(CH_3)_2$), 57.1 (α-CH), 120.2 (ArC), 123.0 (ArCH), 126.2 (ArCH), 128.7 (ArC), 129.5 (ArC), 131.9 (2 x ArCH), 138.7 (ArC), 154.3 (ArC), 168.2 (C=O), 172.1 (C=O); MS (ES^-) *m/z* 321.1 (100) $[M-H]^-$; HMRS (ES^-) calcd. for $C_{15}H_{14}ClN_2O_4$ $[M-H]^-$ 321.0648; found 321.0648. Anal. ($C_{15}H_{15}ClN_2O_4$) requires: C, 55.82; H, 4.68; N, 8.68%; found C, 55.74; H, 4.78; N, 8.58%.

Chapter 6: Dual-Action HIF Prolyl Hydroxylase Inhibitors That Induce Binding of a Second Iron Ion

6.1 Background and Objectives

Most, if not all, of the reported PHD inhibitors likely bind to the single active site iron in a bidentate manner and compete with 2OG co-substrate for binding to the active sites of PHDs.[32, 74, 222, 258] Representative examples of 2OG-competitive inhibitors include the generic 2OG oxygenase inhibitor *N*-oxalylglycine (NOG), its cell-penetrating prodrug, dimethyloxalylglycine (DMOG) and the bicyclic isoquinoline inhibitors BIQ (**Fig. 6.1 A**) and L-Ala-BIQ described in **Chapter 2**. Iron chelators and transition metal ions also inhibit PHD activity, both *in vitro* and in cells, likely due to chelation in solution and competition with iron for binding to the enzyme active sites (see also **Chapter 2**).[2, 66]

PHD inhibition can therefore be achieved by limiting iron availability (e.g. as in the case of iron chelators) or by specific binding of the inhibitors to the active sites of the PHDs (*i.e*. PHDs 1-3). Given that the natural hypoxic response may potentially involve contributions from oxygenases other than the HIF hydroxylases, from a therapeutic perspective, it may be that relatively non-specific inhibitors may better mimic the natural hypoxic response.

The aim of the work described in this chapter was to identify compounds that both bind to the PHD active site and simultaneously deplete cellular iron levels, *i.e*. have specific and non-specific components to their mode of action. In this chapter, the design, synthesis, structure-activity analysis and cell-based evaluation of such dual-function inhibitors is reported. Non-denaturing electrospray ionization mass spectrometry (ESI-MS), which has previously been shown to be a useful tool for assaying ligand binding to PHD2,[222, 259] was employed as a lead analytical tool to identify inhibitors leading to the desired metal binding stoichiometry. The work in this chapter was carried out in

collaboration with Dr J. Mecinovic (who pioneered the development of this new class of PHD inhibitors) and A. Thalhmmer. Synthesis of some of the diacylhydrazine compounds, some ESI-MS binding studies, and part of the cell-based results (see text) were reported in Dr J. Mecinovic's D. Phil thesis (Oxford University, 2009).[260]

6.2 Results and Discussion

6.2.1 Inhibitor design and synthesis

The objective of this work was to design inhibitors that bind specifically to the PHDs, and additionally deplete cellular iron levels by promoting the binding of a second iron in the active site. Reports on the crystal structures of diacylhydrazine-iron complexes demonstrate that diacylhydrazine compounds can form octahedral complexes with iron, characterised by a tridentate chelation mode (**Fig. 6.1 B** and **C**).[261, 262] Notably, the studies also revealed that when appropriately functionalized with metal-chelating groups (e.g. phenolic hydroxyl groups or heteroaromatic sp^2 nitrogens), the diacylhydrazines are capable of simultaneously chelating a second transition metal ion (**Fig. 6.1 D** and **E**).[263] It was therefore anticipated that the diacylhyrazine moiety might be a potential template for PHD inhibitor design.

Initial docking studies suggested that the diacylhydrazine succinate derivative **1 (Fig. 6.2)** might bind to the PHD2 active site. Diacylhydrazine **1** and a set of analogues of **1** were therefore prepared and tested for their binding affinities and inhibitory potencies against PHD2. The compounds were obtained from the monoacylhydrazines either *via* a single-step ring-opening reaction of the corresponding carboxylic acid anhydrides (**Method A**),[260] *via* coupling with the monomethyl adipate in the presence of 1-hydroxybenzotriazole (HOBt) and 1-ethyl-3-(3-dimethylaminopropyl) carbodiimide hydrochloride (EDCI) followed by basic hydrolysis (**Method B**) (**Fig. 6.3**),[260] or by nucleophilic substitution with ethyl pentafluorophenyl fumarate followed by basic hydrolysis (**Method C**) (**Fig 6.4**).

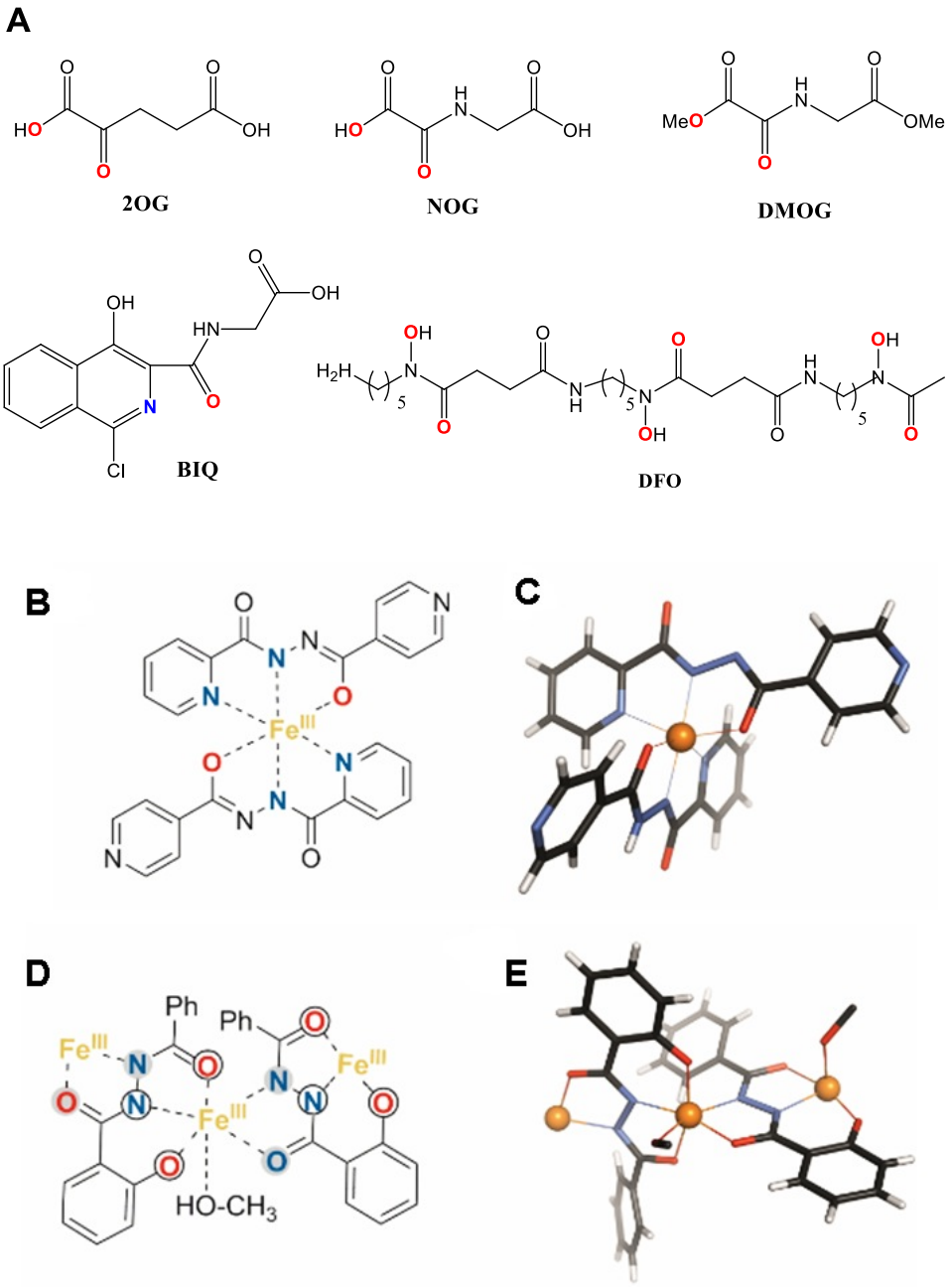


Figure 6.1: Structural considerations for the design of diacylhydrazines as potential 'dual-action' PHD inhibitors (**A**) Structures of reported PHD inhibitors. *N*-oxalylglycine (NOG) and bicyclic isoquinoline compound (BIQ) compete with 2OG co-substrate for binding to the PHD active sites.[32, 258] Dimethyloxalylglycine (DMOG) is a cell-penetrating form of NOG. Desferrioxamine (DFO) acts *via* generic iron chelation.[66] Ligand atoms involved in Fe(II) chelation are shown in red (or blue). (**B**, **C**) Views derived from a crystal structure of a diacylhydrazine-iron complex with tridentate iron chelation (CSD ID OKUGIK).[264] (**D**, **E**) Views derived from a crystal structure of a diacylhydrazine-iron complex with concomitant bidentate and tridentate iron chelation (CSD ID QEVBEY).[263] (**Fig. B-E** were prepared by A. Thalhmmer)

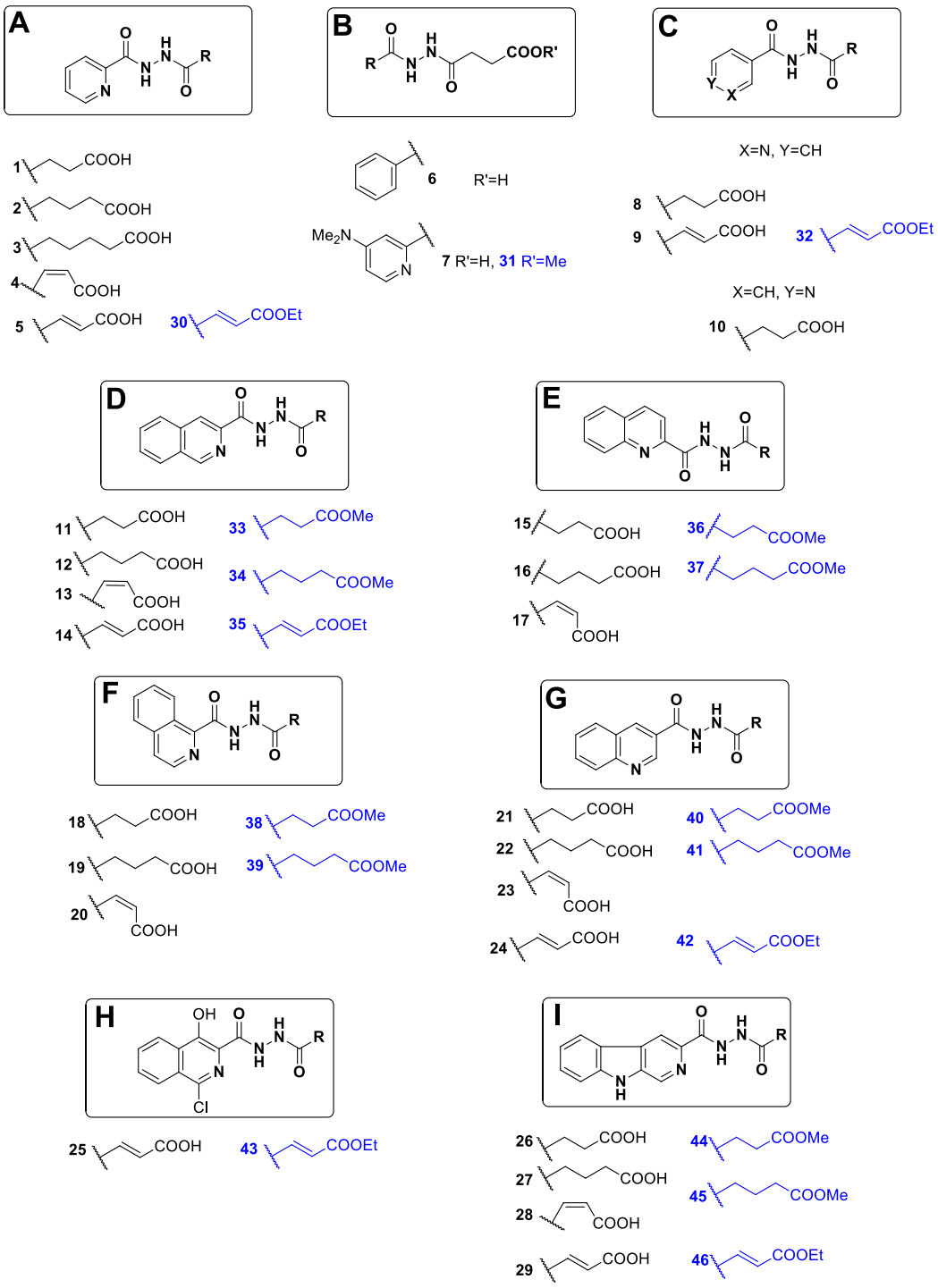


Figure 6.2: Diacylhydrazine derivatives tested as potential PHD2 inhibitors. Cell-based activity assays were carried out for selected diacylhydrazines (in their methyl or ethyl ester forms, compounds highlighted in blue). *In vitro* potency and cell-based activity data are summarized in **Table 3.1**. Some compounds were not tested, including those with limited solubility or due to interference with biochemical assays. Compounds (with the exception of fumarate derivatives 5,9,14,20,24,25,29,30,32,35,42,43,46) were synthesised by Dr J. Mecinovic and reported in his D.Phil thesis (University of Oxford, 2009).[260]

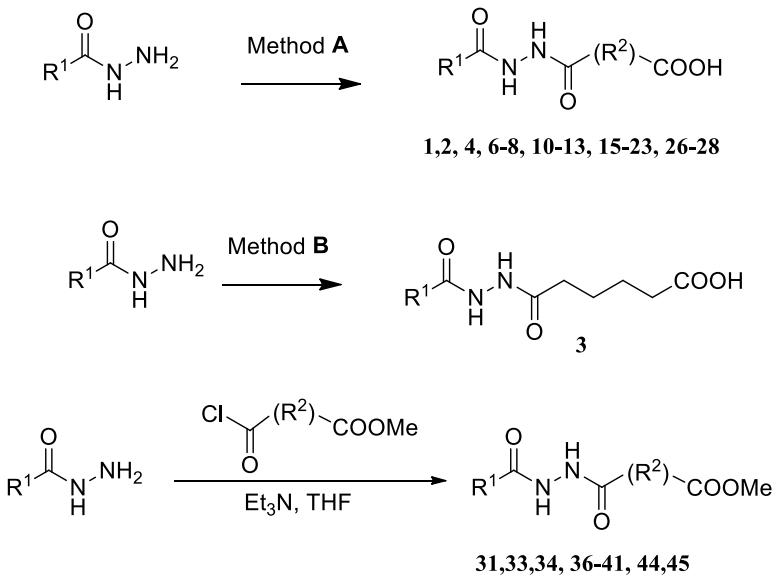


Figure 6.3: Synthetic procedures for the preparation of some of the diacylhydrazine derivatives. **Method A**: carboxylic acid anhydride, EtOAc. **Method B**: monomethyl adipate, 1-hydroxybenzotriazole (HOBt), 1-ethyl-3-(3-dimethylaminopropyl) carbodiimide (EDCI), Et_3N, THF; then NaOH, THF. See **Fig. 6.2** for compound structures. Compounds were synthesized by Dr J. Mecinovic and reported in his D.Phil thesis (University of Oxford, 2009).

6.2.1.1 Synthesis of diacylhydrazine fumarate derivatives

With the exception of the diacylhydrazine fumarate derivatives, other diacylhydrazine compounds were synthesized by Dr J. Mecinovic and reported in his D.Phil thesis (University of Oxford, 2009).[260] The diacylhydrazine fumarate derivatives were prepared in three steps (**Method C**). The precursor ethyl pentafluorophenyl fumarate (**47**) was first prepared via a nucleophilic substitution of ethyl fumaryl chloride with pentafluorophenol[265] The diacylhydrazine fumarate compounds (**5**, **9**, **14**, **24**, **29**) were then obtained from the corresponding monoacylhydrazines (**48**-**52**) via an acylation reaction with the reactive intermediate ethyl pentafluorophenyl fumarate, followed by basic hydrolysis (**Fig. 6.4**). Characterisation of the fumarate derivatives is described in **Section 6.4**.

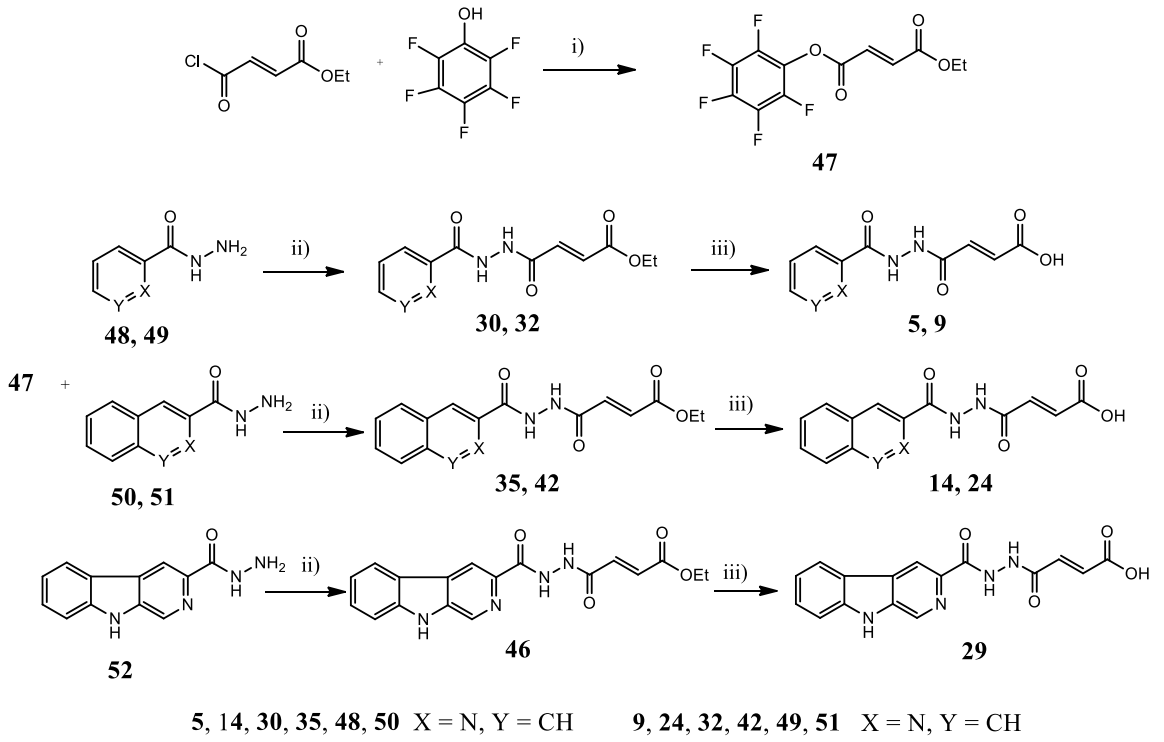


Figure 6.4: Schematic presentation of the reaction steps used in the synthesis of the diacylhydrazide fumarate derivatives (**Method C**). *Reagents and conditions:* i) Et_3N, THF, RT, overnight; **47**, 70%; ii) DMF: EtOAc, 1:1, RT, overnight; **30**, 43%; **32**, 63%; **35**, 62%; **42**, 51%; **46**, 95%; iii) $LiOH.H_2O$, THF, RT, overnight; **5**, 98%; **9**, 65%; **14**, 88%; **24**, 63%, **29**, 76%.

6.2.2 Binding affinities and inhibitory potencies of the diacylhydrazines

6.2.2.1 Monocyclic diacylhydrazines

Non-denaturing ESI-MS[222]was used as an analytical method to investigate the binding affinities and potential abilities of the diacylhydrazines to induce a second iron binding to PHD2. In the ESI-MS assays, the diacylhydrazine compounds were incubated with the catalytic domain of PHD2/pET-24a(+) (residues 181-426) (expressing with pET-24a(+) vector in *E. coli* and purified by cation exchange method by Dr E. Flashman)[25] in the presence of two equivalents of Fe(II) ions. The inhibitory potencies of the diacylhydrazines towards PHD2 catalysis were studied using a time resolved fluorescence resonance energy transfer (FRET) turnover assay[46, 266] (The FRET

experiments were conducted by Dr L. A. McNeill and Dr J. Mecinovic).[260] The structure-activity data (*i.e*. ESI-MS and FRET-based results) are summarised in **Table 6.1**.

Interestingly, the ESI-MS results implied that diacylhydrazide **1** formed a PHD2·Fe_2·**1** complex as the only observed new species under the standard assay conditions (**Fig. 6.5 A**). The PHD2·Fe_2·**1** complex peak (27990 Da, peak D, **Fig. 6.5 A**) has a molecular mass of 290 Da larger than that of the no inhibitor control (PHD2.Fe, 27700 Da, peak B, **Fig. 6.5 A**). The molecular mass of 290 Da thus corresponds to the intact masses of diacylhydrazide **1** (237 Da) and a second iron (56 Da). Note that there is a small peak (27755 Da, peak C, **Fig. 6.5 A**) corresponding to a PHD2.Fe_2 complex in the no inhibitor control which may result from non-specific binding of Fe(II) ions to the PHD2 protein under the standard assay conditions. (In a separate ESI-MS experiment carried out by Dr J. Mecinovic[260] using catalytic domain of PHD2/pET-28(a) (residues 181-426, expressing with pET-28a(+) vector in *E. coli* and purified using His-tag affinity column by Dr R. Chowdhury)[259] under similar conditions, this PHD2.Fe_2 peak is almost undetectable in the control). However, **1** was shown to significantly increase the ability of PHD2 to bind to a second iron. Diacylhyrazide **1** was later found to inhibit PHD2 activity with a half-maximal inhibitory concentration (IC_{50}) of 93 μM.

The binding affinities of diacylhydrazines were shown to gradually decrease with increased size of the side chains (**Fig. 6.5 A**). Glutarate derivative **2** (IC_{50} 108 μM) formed a two-iron complex with PHD2 (PHD2.Fe_2.**2,** peak E, **Fig. 6.5 A**); however, no detectable complex was observed with adipate derivative **3**, possibly due to the extended aliphatic side chain of **3** which might hinder efficient binding of the compound into the PHD2 2OG binding pocket. Interestingly, the maleate derivative (**4,** IC_{50} 84 μM) was able to induce binding of a second iron to PHD2 (PHD2·Fe_2·**4**, peak G, **Fig. 6.5 A**), whereas the isomeric fumarate derivative (**5,** IC_{50} 20 μM) only bound to one iron (PHD2·Fe·**5**, peak H, **Fig. 6.5 B**), revealing the stereochemistry of the olefinic side chain affects the binding of the second iron ion.

Of the tested 2-pyridyl diacylhydrazines, variations to the aliphatic side-chain also suggested a trend of decreasing potencies in the order of fumarate (**5**, IC_{50} 20 μM) > maleate (**4**, IC_{50} 84 μM) > succinate (**1**, IC_{50} 93 μM), glutarate (**2**, IC_{50} 108 μM) >> adipate (**3**, IC_{50} 227 μM) (**Table 6.1**). Therefore, the results suggest the ability of a compound to induce the binding of a second iron to PHD2 active site (e.g. **1**, **2**, **4**) does not generally make it a more potent inhibitor. Modest inhibition exhibited by **3** (IC_{50} 227 μM) may be due to iron chelation in solution.

When the 2-pyridyl group of the parent compound **1** (IC_{50} 93μM) was replaced by a phenyl (**6,** IC_{50} **>** 1000 μM), 3-pyridyl (**8,** IC_{50} 195 μM), or 4-pyridyl (**10,** IC_{50} 202 μM) group, the analogues lost their ability to chelate a second iron (**Fig. 6.5 B**), suggesting a specific regiochemical requirement of the pyridyl-*N* to bind a second iron. These replacements were also found to generally result in reduced inhibitory potencies of the compounds (**Table 6.1**). The above observations generally consistent with the results obtained from a separate set of ESI-MS experiments by Dr J. Mecinovic.[260]

Introduction of an electron-donating dimethylamino group to the *para*-position of aromatic ring of **1** (compound **7**) was speculated to increase its binding affinity for a second iron. However, this substitution actually led to a decreased formation of the two iron binding complex (PHD2.Fe_2.**7**, peak K, **Fig. 6.5 B**) and an increased formation of a single iron complex (PHD2.Fe.**7**, peak J, **Fig. 6.5 B**) (however, this single iron peak was only weakly detectable in a seperate experiment carried out by Dr J. Mecinovic).[260] **7** (IC_{50} 133 μM) was also found to be slightly less potent than **1** (IC_{50} 93 μM). Due to its larger molecular size, it is possible that **7** binds in a different orientation and binds less tightly to the PHD2 active site compared to **1**.

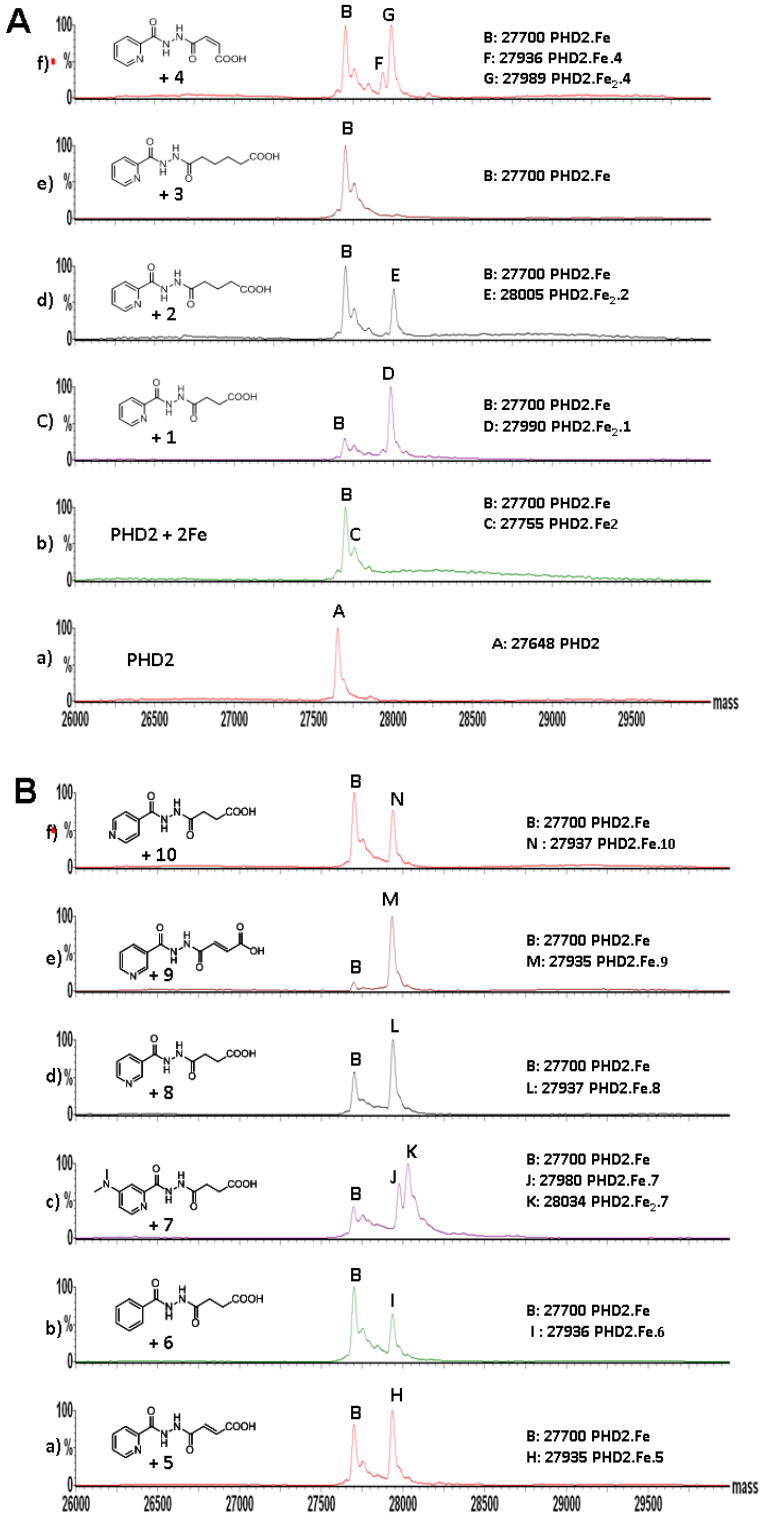


Figure 6.5: (**A**, **B**) Non-denaturing ESI-MS studies of PHD2 in the presence of 2 equiv. of Fe(II) ions and 1 equiv. of monocyclic diacylhydrazine derivatives **1**-**10**. There is a small peak (peak C) in the control (without inhibitors) corresponding to a PHD2.Fe_2 complex which may result from non-specific binding of Fe(II) ions to the PHD2 under the standard assay conditions.

6.2.2.2 Bicyclic and tricylic diacylhydrazines

Appropriately functionalised bicyclic PHD inhibitors generally appear to be more potent compared to their monocyclic analogues, partly because the second ring of the inhibitors can form hydrophobic interactions with the amino acid residues located at the entrance of the PHD2 active site.[31, 34, 74] A series of bicyclic (**11-24, Fig. 6.2**) and tricyclic (**26-29, Fig. 6.2**) diacylhydrazide derivatives were therefore prepared and tested as above (**Table 6.1**).

Consistent with the ESI-MS results of the monocyclic derivatives, most of the bicyclic and tricyclic (**11**-**29**) compounds were able to induce a second iron binding to the PHD2 (**Fig. 6.6** and **6.7**). In contrast, fumarate derivatives (**24**, **29**) and 3-quinolinyl derivatives (**21**-**23)** (scaffold **G, Fig. 6.2**) were observed to bind to PHD2 with a single iron under standard conditions (see also **Table 6.1**). Substantial single iron complex peaks (e.g. PHD2.Fe.**15**, peak G, **Fig. 6.6 A**; PHD2.Fe.**26**, peak D, **Fig. 6.7**; PHD2.Fe.**29**, peak G, **Fig. 6.7**) were detected in some of the two iron binding compounds (*i.e*. succinates **15, 26** and maleate **29**) (however, the formation of PHD2.Fe.**15** and PHD2.Fe.**26** peaks were again not substantially present in Dr J. Mecinovic's experiments),[260] showing that their abilities to induce a second iron binding are not only affected by their side chains, but are also strongly affected by the orientation and size of the aromatic rings.

The results show that binding affinities and inhibitory potencies of the bicyclic compounds also substantially depend on the position of the second aromatic ring (*i.e*. in the isomeric scaffolds **D**, **E** and **F, Fig. 6.2**). Compounds with scaffolds **E** (**15**, **16**) and **F** (**18**, **19**) tend to give weaker complexes compared to compounds with scaffold **D** (**11**, **12**) (**Fig. 6.6 A** and **B**). As exemplified in the series of relatively potent maleate derivatives, the isoquinoline-3- (**13,** scaffold **D**), quinoline-2- (**17,** scaffold **E**) and isoquinoline-1-derivatives (**20,** scaffold **F**) exhibited IC_{50} values of 9 μM, 84 μM and 149 μM, respectively. The tricyclic compounds **26**-**29** were shown to display similar inhibition potencies to their bicyclic analogues **11**-**14** with IC_{50} values ranging from 10-40 μM **(Table 6.1)**.

Beside the descrepencies observed in the detection of the PHD2.Fe_2 complex peak in the no inhibitor control, and the formation of single iron complex peaks in some of the two-iron binding compounds (e.g. **7**, **15**, **26**) (as discussed above), the ESI-MS results obtained in this study are in great concordance with the results obtained by Dr J. Mecinovic (reported in his D. Phil thesis).[260] It is possible that the differences observed are due to the different PHD2 proteins (*i.e*. PHD2/pET24(a) and PHD2/pET28(a)) used in the tests.

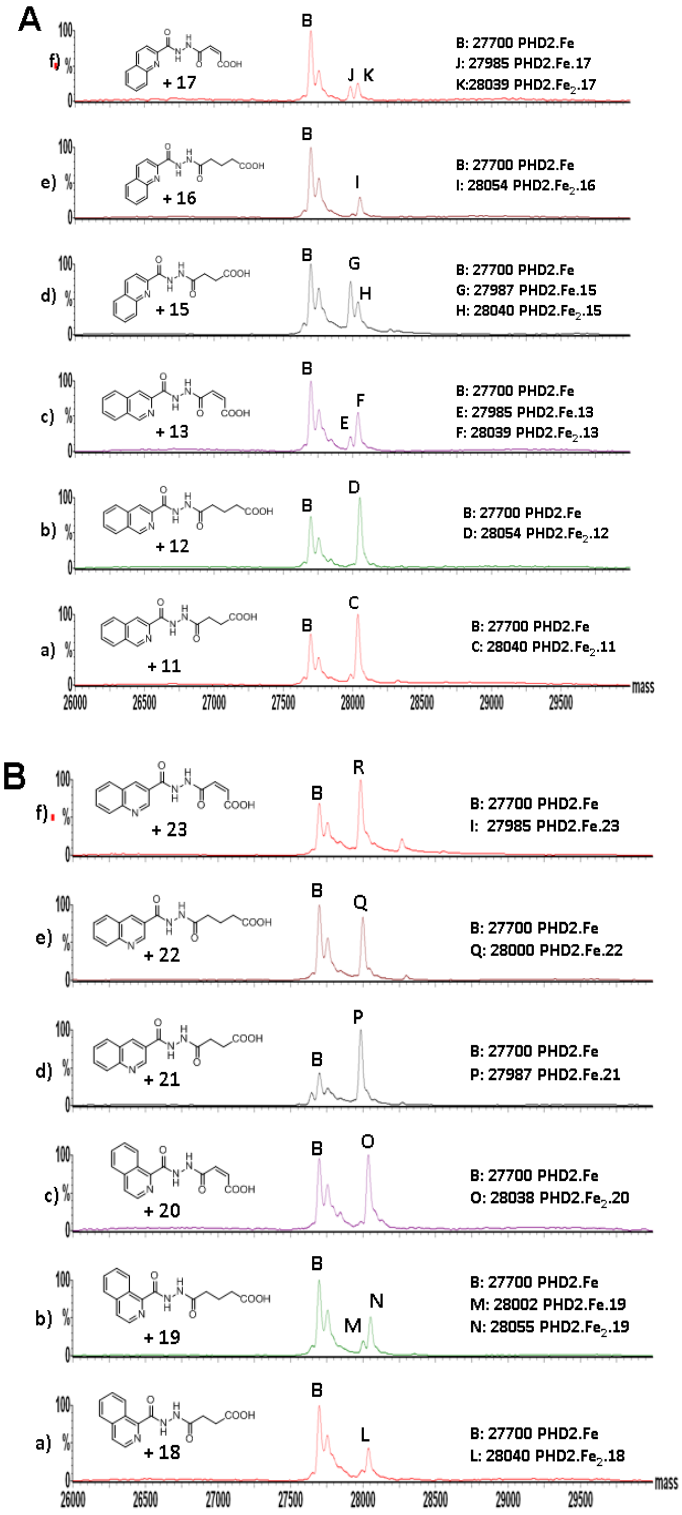


Figure 6.6: (**A**, **B**) Non-denaturing ESI-MS studies of PHD2 in the presence 2 equiv. of Fe(II) ions and 1 equiv. of bicyclic diacylhydrazine derivatives **11**-**23**. Compound **14** was not tested because it was not very soluble.

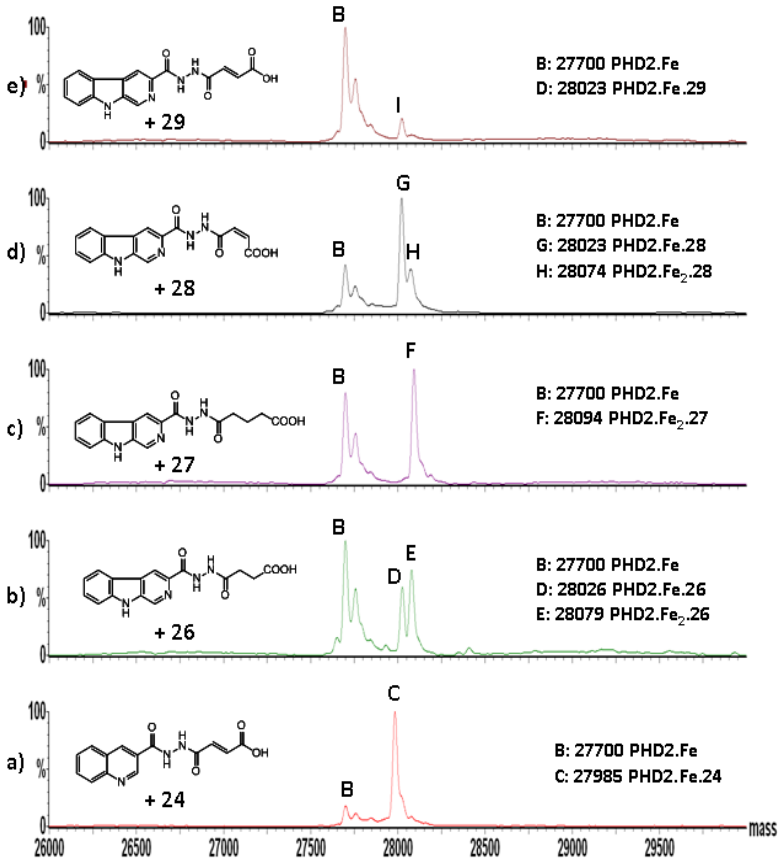


Figure 6.7: Non-denaturing ESI-MS studies of PHD2 in the presence 2 equiv. of Fe(II) ions and 1 equiv. of bicyclic diacylhydrazine **24** and tricylic diacylhydrazines **26**-**29**. Compound **25** was not tested because it was not very soluble.

6.2.3 *N*-Oxalylglycine (NOG) competition studies

Further studies were carried out to compare the binding affinities towards PHD2 of selected diacylhydrazide derivatives to the unreactive 2OG analogue *N*-oxalylglycine (NOG, IC_{50} 18.5 μM).[165] ESI-MS assays were carried out in the presence of equimolar quantities of the diacylhydrazides and NOG, and two equivalents of Fe(II). Interestingly, the competition experiments revealed that in the presence of equimolar NOG, the relatively potent 2-pyridyl derivatives **1**-**5** (IC_{50} 20-90 μM) did not give rise to any detectable complexes with PHD2 (**Fig. 6.8 A**). The results show that NOG substantially

competes these compounds for binding to the PHD2 active site (*i.e.* the NOG and the diacylhydrazides bind to the same site).

In contrast, despite their generally weak potencies in PHD2 inhibition and the lack of abilities to induce the binding of a second iron, diacylhydrazides with 3-pyridyl (**8**, **9**) and 3-quinolinyl moieties (**21**, **24**) (IC_{50} 200-300 μM) effectively compete with NOG (IC_{50} 18.5 μM)[165] to bind to the PHD2 (**Fig. 6.8 B**). Compound **9** was also shown to substantially compete with the potent PHD inhibitor, bicyclic isoquinoline compound (BIQ, IC_{50} 0.073 μM)[165] to bind to the PHD2 active site (**Fig. 6.8 B**); however, its ethyl ester **32** (cell-penetrating prodrug of **9**) was later found to be an inefficient PHD inhibitor in the cell-based experiments (**Section 6.2.7**).

Overall, the binding studies indicate that the affinities of the diacylhydrazines to bind to the PHD2 and their abilities to induce the binding of a second iron to the enzyme active sites may at least to a certain extent reflect their inhibitory potencies (*i.e.* a stronger ligand is generally expected to be a more potent inhibitor); however, it is not always the case (as demonstrated by compounds **8**, **9**, **21**, **24**). The differences observed in the binding affinities and inhibitory potencies of the inhibitors may be due to the different assay conditions used in the ESI-MS (*i.e.* gas phase) and FRET-based (*i.e.* aqueous phase) experiments.

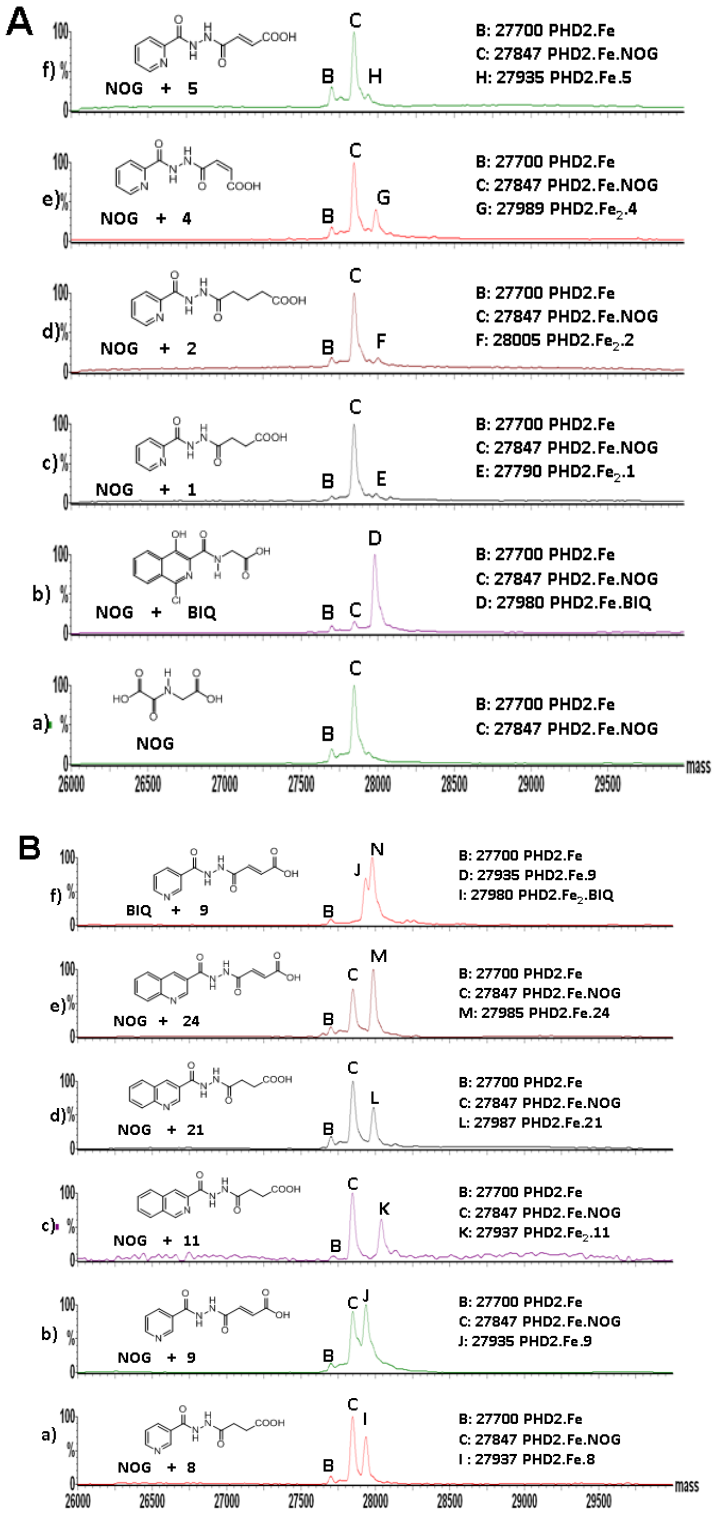


Figure 6.8: (**A**, **B**) Non-denaturing ESI-MS competitive experiments in the presence of equimolar amounts of PHD2, *N*-oxalylglycine (NOG), and diacylhydrazine compounds, and 2 equiv. of Fe(II) ions. (B, f) Equimolar amounts of PHD2, bicyclic isoquinoline inhibitor (BIQ), and diacylhydrazine **9** and 2 equiv. of Fe(II) ions.

6.2.4 Docking studies

Docking studies were performed (by A. Thalhmmer) to investigate the potential binding modes of the diacylhydrazines to PHD2 using GOLD program.[267, 268] **Fig. 6.9 A** shows the proposed binding mode of dual-action diacylhydrazine inhibitor that induces a second iron binding to the active site. In the docking studies, succinate (**1**), maleate (**3**) and fumarate (**4**) diacylhydrazine derivatives display at least one predicted binding mode, with bidentate coordination to the active site iron of PHD2 and salt bridge formation with Arg383 **(Fig. 6.9 B-D**), similar to NOG and BIQ binding seen in crystal structures of PHD2 (see **Chapter 2**, **Fig. 2.4 A** and **Fig. 2.10,** respectively).

The docking models for the compounds that are capable of chelating a second iron suggest that at least three ligand atoms of the diacylhydrazine (typically an sp^2-hybridized nitrogen atom, a diacylhydrazine nitrogen atom and a diacylhydrazine oxygen atom) are required to enable tridentate coordination with a second iron, as exemplified by succinate (**2**) and maleate (**3**) derivatives (**Fig. 6.9 B** and **C**). It is possible that the binding of the first active site iron by the diacylhydrazine motif might facilitate structural pre-organization that supports the chelation of a second iron.

Interestingly, the *trans*-geometry side chain in the fumarate derivative **4** gave rise to docking models with the amide carbonyl group of the fumarate side chain directed towards the entrance of the PHD2 active site (**Fig. 6.9 D**), so preventing the arrangement proposed to be required for second iron binding. This proposal is consistent with the ESI-MS results, demonstrating that none of the fumarate derivatives (**5**, **9**, **14**, **29)** are able to induce second iron binding (**Table 6.1**).

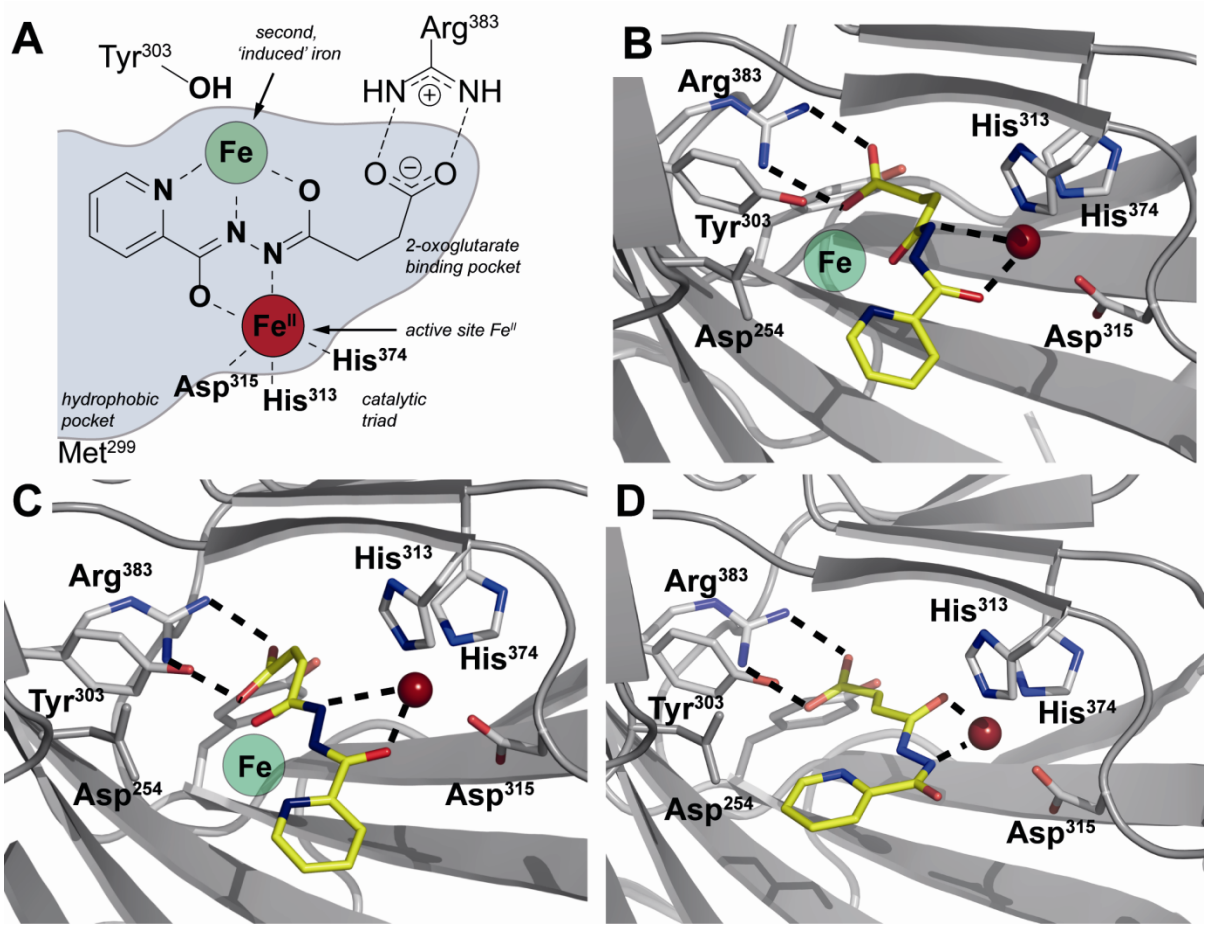


Figure 6.9: Possible binding modes of the diacylhydrazine inhibitors that induce binding of a second iron in the PHD2 active site. The models were derived from structure-activity data (**Table 3.1**) followed by docking analyses using the GOLD software.[267, 268] Note that experimental results revealed that the succinate-(**6**) and maleate-(**9**) derivatives induce the binding of a second iron, but the fumarate-(**10**) derivative binds with only one iron. (**A**) Graphical presentation of the proposed binding mode. (**B**, **C** and **D**): Representative binding modes for diacylhydrazines **6, 9** and **10**. Selected residues and the active site catalytic iron atom of PHD2 (red) are highlighted. For docking studies, protein coordinates were derived from the crystal structure of PHD2 in complex with the bicyclic isoquinoline (BIQ) inhibitor (PDB ID 2HBT). Proposed locations for binding of the second iron (green) are indicated. (Figures obtained from A. Thalhmmer)

6.2.5 Cell-based studies

The potencies of selected diacylhydrazide compounds were then investigated in cells by examining their abilities to induce HIF-1α as an indicator of cellular PHD2 inhibition (**Figure 6.10**). Initially, it was considered possible that at least some of the compounds might be cell-permeable in their free acid forms due to their structural similarities to the known cell-permeable PHD inhibitor **BIQ** (see **Section 2.2.4.1**). However, diacylhydrazine derivatives bearing a free carboxylate group that showed inhibition of PHD2 activity *in vitro* (**4**, **13**, **28, Table 6.1**) failed to upregulate HIF-1α levels in human hepatoma Hep3B cells (data not shown), possibly because the diacylhydrazine or carboxylic acid moieties negatively affect cell-penetrating ability. Ester derivatives which in general are more cell-penetrating than the respective free acids were therefore synthesised and used in the cell-based experiments. The requisite methyl or ethyl esters (**30-46, Fig. 6.2**) were obtained from the corresponding monoacylhydrazines by acylation (**Fig. 6.3**, final step and **Method C**).

Human hepatoma Hep3B cells were treated with the esters **30**-**46** at two concentrations (0.1 mM and 1 mM) for 6 h and the resulting cell extracts were probed using a HIF-1α antibody (these experiments were carried out by Dr I. Stolze and reported in Dr J. Mecinovic's D. Phil thesis).[260] The cell-based HIF hydroxylase inhibitor DMOG was used as a positive control for HIF-1α induction and DMSO as a negative control. In agreement with *in vitro* inhibition data of their corresponding acids (*i.e*. **7**, **11**, **12**, **15**, **16**, **18**, and **19**) (**Table 6.1**), compounds **31, 33**, **34,** and **36**-**39** clearly caused HIF-1α induction in a concentration-dependent manner (**Fig. 6.10 A** and **B**); (compounds **44** and **45** were not tested in cell-based assays due to their low solubilities in DMSO). The esters **40-41** failed to cause HIF-1α accumulation (Dr J. Mecinovic's D. Phil thesis),[260] consistent with the weak *in vitro* potencies of the corresponding acids (**21**-**22**) (**Table 6.1**).

For selected compounds, the contribution of iron chelating ability to their cellular 2OG oxygenase inhibitory potencies were then investigated. For this purpose, Hep3B cells were incubated with iron chelator DFO (which inhibits PHD by limiting iron availability) or DMOG (which inhibits PHD by competitive inhibiton) as controls and compound **31**, in the presence (or absence) of equimolar amounts of Fe(II), which were added either at the beginning or during the final 2 h of the 6 h incubation period (these experiments were carried out by Dr I. Stolze and reported in Dr J. Mecinovic's D. Phil thesis).[260]

As anticipated, DFO, DMOG and **31** substantially induced HIF-1α accumulation (**Fig. 6.10 B**). However, in the presence of an equimolar amount of Fe(II), HIF-1α accumulation was not observed with **DFO** or **31** (**Fig. 6.10 B**). Titrations using different Fe(II) concentrations demonstrate that induction of HIF-1α by **31** was reduced as the Fe(II) concentration was increased (**Fig. 6.10 C**). These observations suggest that, at least in part, the cellular activity of **31** is due to iron chelation. Interestingly, however, the addition of an equimolar amount of Fe(II) with DMOG also resulted in a reduction in HIF-1α stabilization, compared to DMOG alone. NOG and DMOG are relatively poor iron chelators, hence these results suggest a more complex relationship between iron availability and the HIF system than currently understood. The possibility that the addition of iron may shift the equilibrium between uncomplexed compound and (charged) compound-Fe(II) complexes, thus altering the amount of compound that is available for cellular uptake cannot be ruled out.[261, 264]

Diacylhydrazine derivatives containing the fumarate sidechains (**30, 32, 35, 42,** and **46**) were then tested in Hep3B cells. In contrast to non-olefinic derivatives which stabilised HIF-1α in a concentration-dependent manner (**Fig. 6.10 A**), the fumarate derivatives, **30** and **35,** displayed better HIF-1α stabilization at a lower concentration (*i.e.* HIF-1α stabilization at 0.1 mM compound >> HIF-1α stabilization at 1 mM compound) (**Fig. 6.10 D**), possibly due to cytotoxic effects or the interaction of these compounds with factors working to destabilize HIF-1α at higher concentrations. Notably, **35** gave rise to detectable HIF-1α induction at concentrations as low as 25 μM, and HIF-1α levels obtained at 50 μM of **35** were in fact greater than those obtained with the established cell-

active HIF hydroxylase inhibitor DMOG at 100 μM. On the other hand, **30** showed a similar level of HIF-1α stabilization with DMOG at 100 μM (**Fig. 6.10 E**). Compounds **32** and **42** were inactive in the tested cells; compound **46** was not very soluble and precipitated in the cell media.

Notably, in RCC4/VHL cells (renal carcinoma RCC4 cells re-expressing functional VHL), some compounds including **31** displayed better HIF-1α induction at a higher concentration (1mM), while the fumarate derivatives **30** and **35** again gave rise to higher HIF-1α levels at a lower concentration (200 μM) (consistent with the observation in Hep3B cells). In the RCC4/VHL cell line, **30** displayed better HIF-1α induction than **35**; in contrast in Hep3B cells where these compounds displayed similar potencies (**Fig. 6.10 B**), suggesting the cell-type dependent effect of these compounds. The free acid of **30** (**5**) at 1mM, also stabilised HIF-1α, but to a lesser extent than its ester, possibly due to reduced cell permeability. Similarly, the free acid of **35** (**14**) was ineffective in causing HIF-1α induction (**Fig 6.10 F**). On the other hand, the ethyl ester form of diacylhydrazine derivative of BIQ (**43**) substantially stabilised HIF-1α in RCC4/VHL cells (**Fig. 6.10 G**). However, morphological evidence of toxicity (*i.e.* detachment of cells) was observed when **43** was used at higher concentrations (>200 μM).

To test the specificities of the diacylhydrazine derivatives againts HIF prolyl and asparaginyl hydroxylases, selected compounds were then tested in the HIF hydroxy-residue specific antibody assay described in **Chapter 2**. Experiments were performed in VHL-defective renal carcinoma cells (RCC4) using compounds **30, 31**, and **43**, along with DMOG and BIQ serving as positive controls (**Fig. 6.10 H and I**). In contrast to DMOG, which clearly showed selectivity for inhibition of FIH over the PHDs, and BIQ, which specifically inhibited HIF prolyl hydroxylation, **30** and **43** substantially inhibited both HIF prolyl hydroxylation (Hyp564) and asparaginyl hydroxylation (HyAsn803). **31** showed partial selectivity against HIF prolyl hydroxylation over asparaginyl hydroxylation (**Fig. 6.10 H**).

Interestingly, despite the similar level of HIF-1α induction by DMOG (1mM), **30** (0.2 mM) and **31** (1 mM) (**Fig. 6.10 F**) in RCC4/VHL cells, these compounds showed different levels of inhibition on HIF prolyl hydroxylation (Hyp564) in RCC4 cells (**Fig. 6.10 H**). HIF prolyl hydroxylation was only partially inhibited by **31** at high concentrations (1 mM and 2 mM), compared to **30**, which inhibited HIF prolyl hydroxylation almost completely at lower concentrations (0.2 and 0.5 mM). Therefore, it was speculated that the upregulation of HIF-1α **31** may not solely be due to the inhibition of HIF prolyl hydroxylation.

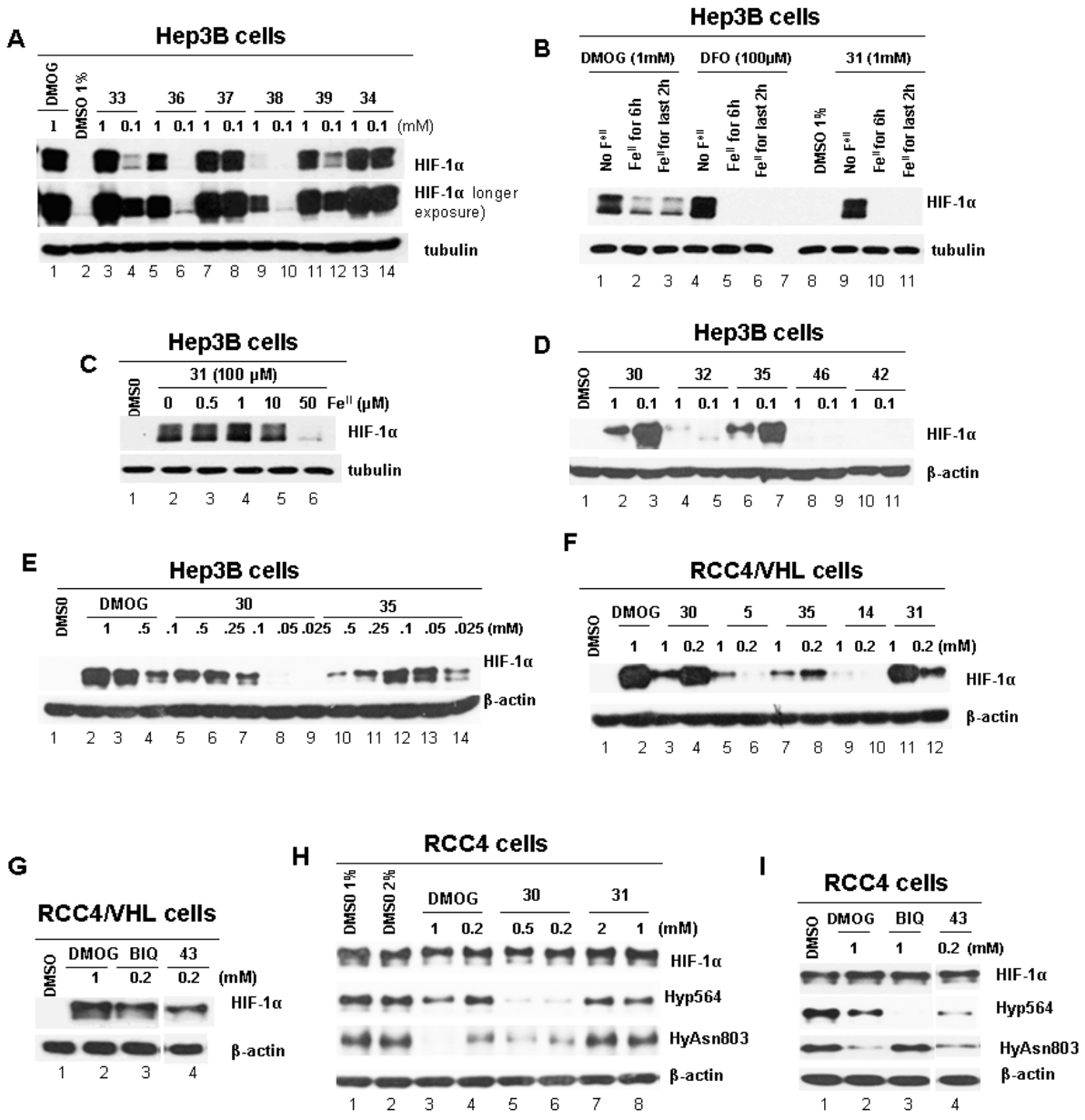
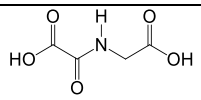
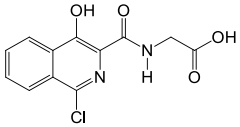
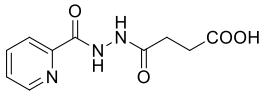
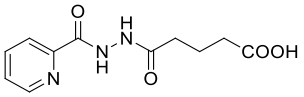
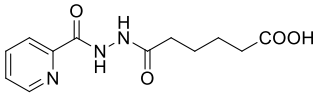
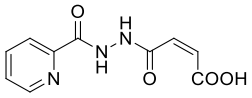
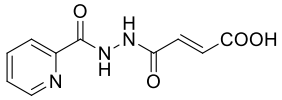
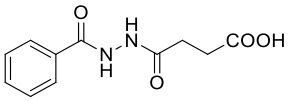
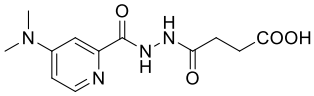
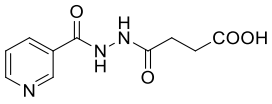
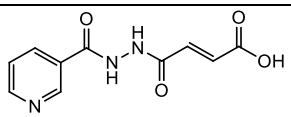
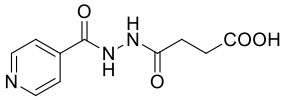
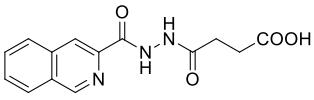
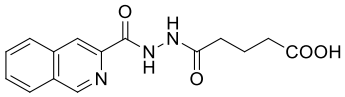
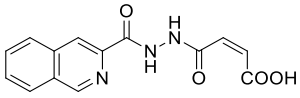
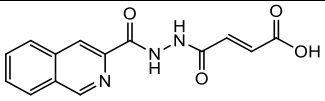
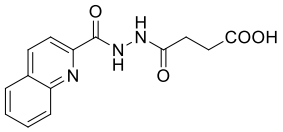
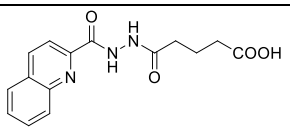
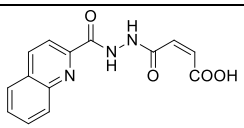
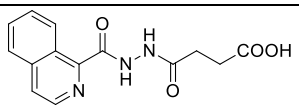
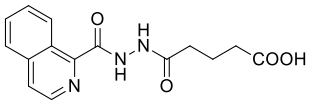
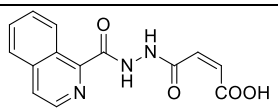
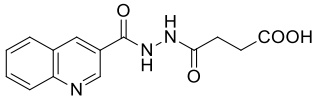
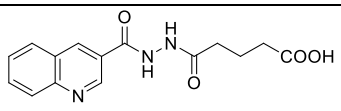
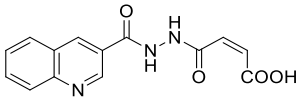


Figure 6.10: Effects of diacylhydrazine-based compounds on cellular HIF-1α levels. (**A**, **D**) Immunoblots demonstrating HIF-1α stabilisation in the presence of diacylhydrazine derivatives (1 mM and 0.1 mM) in Hep3B cells after 6 h incubation. (**B**, **C**) Effects of the addition of Fe(II) ions on the HIF-1α induction caused by **31** after 6 h incubation. (**E**) Dose-dependent HIF-1α induction caused by **30** and **35** after 6 h incubation. (**F**) Concentration-dependent stabilisation of HIF-1α in RCC4/VHL cells by diacylhydrazine derivatives **5**, **14**, **43, 30** and **35**. (**G**) Stabilization of HIF-1α caused by **43** in RCC4/VHL cells. (**H**, **I**) Effects of **30**, **35**, and **43** on HIF prolyl and asparaginyl hydroxylation in VHL-defective RCC4 cells after 5 h incubation (HIF-1α band intensities were used to normalize hydroxylation signals, tubulin/β-actin protein levels were used as loading controls). DMSO (1%) was used as a negative control and dimethyloxalylglycine (DMOG) and bicyclic isoquinoline inhibitor (BIQ) were used as positive controls in the cell-based experiments. (Figures **A-C** were obtained from Dr I. Stolze and reported in Dr Mecinovic's D. Phil thesis).[260]

Compd.	Structure	PHD2 FRET IC_{50} (μM)[a]	Cell-based activity[b] HIF-1α induction	PHD2·Fe_n·Cmpd. Complexes in ESI-MS[c]	
				n=1	n=2
NOG (DMOG)		18.5[165]	Active	+	
BIQ		0.073[165]	Active	+	
1		93	-		+
2		108	-		+
3		227	-	no binding	
4		84	-		+
5 (30)		20	Active	+	
6		>1000	-	+	
7 (31)		133	Active		+
8		195	-	+	
9 (32)		ND	Inactive	+	
10		202	-	+	
11 (33)		24	Active		+

Compd.	Structure	PHD2 FRET IC_{50} (μM)[a]	Cell-based activity[b] HIF-1α induction	PHD2·Fe_n·Cmpd. Complexes in ESI-MS[c]	
				n=1	n=2
12 **(34)**		34	Active		+
13		9	-		+
14 **(35)**		ND	Active	ND	
15 **(36)**		106	Active		**+**
16 **(37)**		141	Active		+
17		84	-		+
18 **(38)**		166	Active		+
19 **(39)**		205	Active		+
20		149	-		+
21 **(40)**		350	Inactive	+	
22 **(41)**		>1000	Inactive	+	
23		340	-	+	

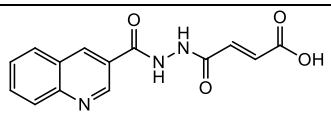
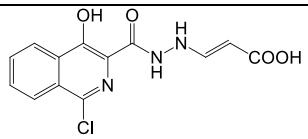
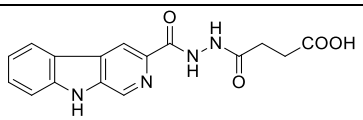
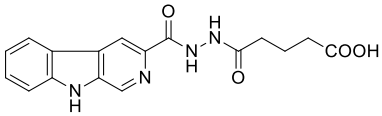
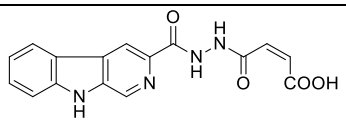
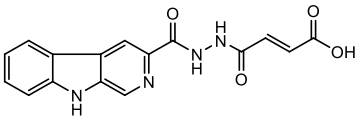
24 **(42)**		ND	Inactive	+	
25 **(43)**		ND	Active	ND	
26 **(44)**		27	ND		+
27 **(45)**		27	ND		+
28		10	-	+	
29 **(46)**		ND	ND	+	

Table 6.1: Summary of the *in vitro* and cell-based potencies of the diacylhydrazines as PHD inhibitors. [a]Determined by FRET-based turnover endpoint assay in the presence of 20 nM recombinant PHD2 enzyme and 750 nM of 2OG co-substrate[46, 266]. Data for DMOG and BIQ have been reported.[165] [b]The corresponding methyl or ethyl esters (compound numbers in parentheses) of the diacylhydrazines were tested in the cell-based assays. ND, not determined (including compounds that were not well soluble, or interfered with the assay). [c]Number of iron ions bound in the most abundant PHD2·Fe_n·compound complex in non-denaturing protein ESI-MS experiments (n=1, 2).

6.3 Conclusions and future directions

Following structure-activity studies and application of non-denaturing protein mass spectrometry to assess PHD2 : iron : inhibitor stoichiometry, a set of diacylhydrazine-based compounds were identified as a new class of dual-action HIF prolyl hydroxylase inhibitors in which they can bind specifically to the enzyme active site and simultaneously induce the binding of a second iron ion. The results show that the inhibitory potencies and the ability of these inhibitors to promote second iron binding strongly depend on the substitution pattern on the aromatic rings and the side chain structures of the aryl-diacylhydrazines.

The mode of action of these diacylhydrazine inhibitors is related to that of a family of serine protease inhibitors (e.g. 5-amidino-2-benzimidazolyl)methane, BABIM) that inhibits activity by inducing the binding of a zinc ion that is not normally present at the active site of the target enzyme (**Fig. 6.11**).[269] The inhibitory potency of BABIM against trypsin was reported to increase by a factor of over 1000 in the presence of Zn(II) ions.[269] In the case of the HIF hydroxylases, depletion of cellular iron levels has functional consequences causing HIF-1α accumulation and thereby activation of the HIF-mediated response, as demonstrated by iron chelators and metal ions.[2, 3, 66, 270] Therefore, the diacylhydrazine-based PHD inhibitors have the potential to act as dual-action inhibitors in cells, by both directly inhibiting the HIF hydroxylases and generally depleting the cellular iron levels by chelating an additional iron at the enzyme active sites. However, there is no clear evidence that shows the two-iron binding inhibitors are more potent than the single-iron binding inhibitors *in vitro* or in cells.

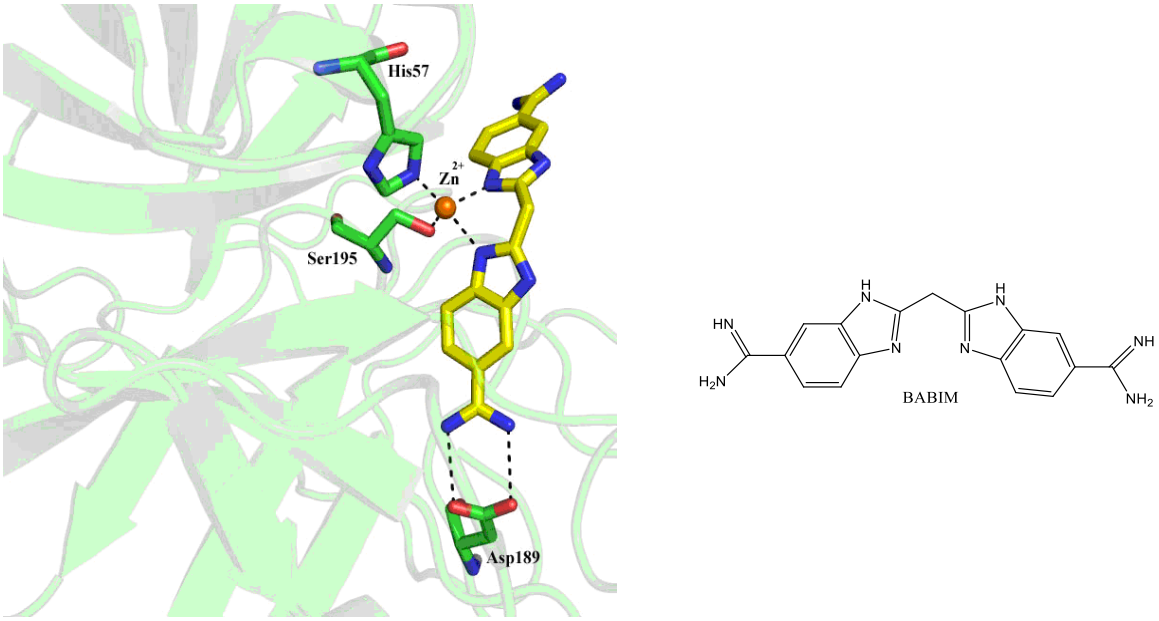


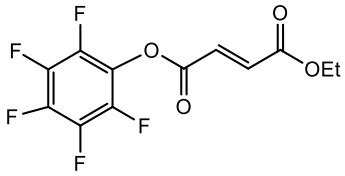
Fig. 6.11: A view derived from a crystal structure of trypsin in complex with BABIM (yellow). BABIM induced the binding of a Zn(II) ion (orange) in the enzyme active site (PDB: 1XUG). Active site residues that coordinate the Zn(II) ion (His57, Ser195) and hydrogen bond (Asp189) with BABIM are highlighted.

The cell-based results indicate that these diacylhydrazine-based PHD inhibitors also inhibit the activity of FIH. It is most likely that they may also inhibit other 2OG oxygeneses, given that these enzymes also require Fe(II) for their catalysis and have a conserved (but not identical) Fe(II) and 2OG binding domain.[32] However, as discussed previously, the natural hypoxic response may involve other 2OG oxygenases, the action of these dual-action HIF hydroxylase inhibitors may be physiologically more relevant. The potential application of these inhibitors for therapeutic manipulation of HIF-mediated response could be further investigated. Further structure-activity studies should enable the development of dual-action diacylhydrazine-based inhibitors that target other 2OG oxygenases.

Finally, non-heme iron-dependent oxygenases can be classified into mono- or di-iron oxygenases (*i.e.* those employ one or two active site irons),[271] the identification of diacylhydrazines as compounds that induce the binding of a second iron to a mono-iron oxygenase (*i.e.* PHD2) presents a link between the two subfamilies, and may provide insights to future studies that are aimed at the development of di-iron oxygenase inhibitors.

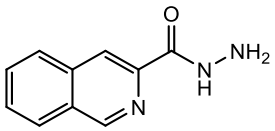
6.4 Synthesis and characterisation of the diacylhydrazine fumarate derivatives

Ethyl perfluorophenyl fumarate (47)[265]



47 was prepared according to the reported method[265]. To a stirred suspension of pentaflurophenol (3.87 g, 21.0 mmol) and ethyl fumaryl chloride (3.45 g, 21.0 mmol) in THF was added triethylamine (3.2 mL, 23.1 mmol) over 10 min. The resulting mixture was then stirred at room temperature overnight. The reaction mixture was filtered, concentrated in *vacuo*, and the residue was purified by flash chromatography (hexane: EtOAc, 4:1) to afford ethyl perfluorophenyl fumarate (**47**) as colourless oil (4.5 g, 70%); R_f (hexane: EtOAc, 4:1) 0.5; FT-IR (film) 2990, 2360, 1775, 1731, 1520, 1286, 1005, 762 cm^{-1}; ^1H NMR (500 MHz, $CDCl_3$) δ 1.36 (3H, t, J 7.0, CH_3), 4.33 (2H, q, J 7.0, OCH_2), 7.07 (1H, d, J 16.0, =C-H), 7.13 (1H, d, J 16.0, =C-H); ^{13}C NMR (125 MHz, $CDCl_3$) δ 14.0 (CH_3), 62.0 (OCH_2), 130.0 (=C), 137.0 (Ar-C), 138.8 (=C), 140.0 (Ar-C), 140.8 (ArCH), 142.0 (ArC), 160.7 (C=O), 164.2 (C=O); ^{19}F NMR (376 MHz, $CDCl_3$) δ -152.3 - - 152.4 (2F, m, Ar-F), -157.1- -157.2 (1F, m, Ar-F), -161.9 - -162.0 (2F, m, Ar-F).

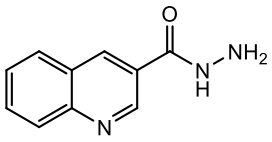
Isoquinoline-3-carbohydrazide (50)[272]



50 was prepared according to the reported method[272]. A stirred solution of methyl isoquinoline-3-carboxylate (1 g, 5 mmol) and hydrazine monohydrate (1.06 g, 20 mmol) in MeOH (40 mL) was heated under reflux for 6 h and then cooled to room temperature. The organic solvent was removed under vacuo and the resulting residue was recrystallised withμ EtOH to afford isoquinoline-3-carbohydrazide (**50**) as a yellowish

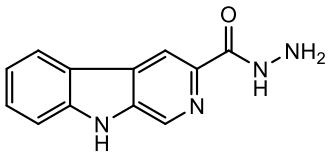
white solid (710 mg, 71%), mp 114-117°C [260]; R_f (CH_2Cl_2:MeOH, 9:1) 0.5; FT-IR (KBr) 3292, 1673, 1607, 1503 cm^{-1}; ^1H NMR (500 MHz, DMSO-d_6) δ 4.61 (2H, bs, NH_2),7.78-7.81 (1H, m, ArCH), 7.86-7.79 (1H, m, ArCH), 8.18 (1H, d, J 8.0, ArCH), 8.23 (1H, J 8.0, ArCH), 8.51 (1H, s, ArCH), 9.35 (1H, s, ArCH), 10.0 (1H, bs, NH); ^{13}C NMR (125 MHz, DMSO-d_6) δ 119.4 (ArCH), 127.8 (ArCH), 127.9 (ArCH), 129.0 (ArCH), 129.1 (ArC), 131.3 (ArCH), 135.4 (ArC), 143.5 (ArC), 151.6 (ArCH), 162.8 (ArCO); MS (ES^-) m/z 186.1 (100) $[M-H]^-$.

Quinoline-3-carbohydrazide (51)[272]



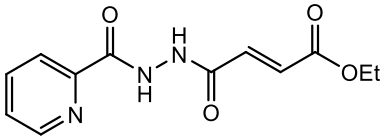
51 was prepared according to the reported method[272]. A stirred solution of methyl quinoline-3-carboxylate (1 g, 5 mmol) and hydrazine monohydrate (1.06 g, 20 mmol) in MeOH (40 mL) was heated under reflux for 6 h and then cooled to room temperature. The organic solvent was removed under vacuo and the resulting residue was recrystallised with absolute EtOH to afford quinoline-3-carbohydrazide (**51**) as a yellowish white solid (988 mg, 100%), mp 176-178°C[260, 272]; R_f (CH_2Cl_2:MeOH, 9:1) 0.5; FT-IR (KBr) 3308, 1655, 1618, 1314 cm^{-1}; ^1H NMR (500 MHz, DMSO-d_6) δ 4.65 (2H, bs, NH_2), 7.79 (1H, dd, J 1.0, 7.0, ArCH), 7.86 (1H, dd, J 7.0, 7.0, ArCH), 7.87 (1H, dd, J 7.0, 7.0, ArCH), 8.07-8.11 (2H, m, 2 x ArCH), 8.80 (1H, d, J 2.0, ArCH), 9.26 (1H, d, J 2.0, ArCH), 9.26 (1H, d, J 2.0, ArCH), 10.12 (1H, bs, NH); ^{13}C NMR (125 MHz, DMSO-d_6) δ 126.1 (ArC), 126.6 (ArC), 127.4 (ArCH), 128.7 (ArCH), 129.1 (ArCH), 131.1 (ArCH), 135.3 (ArCH), 148.4 (ArC), 148.5 (ArCH), 164.5 (C=O); MS (ES^-) *m/z* 186.1 (100) $[M-H]^-$.

***9H*-pyrido[3,4-*b*]indole-3-carbohydrazide (52)**[273]



52 was prepared according to the reported method[273]. A stirred solution of ethyl β-carboline-3carboxylate (1 g, 4.2 mmol) and hydrazine monohydrate (1.06 g, 20 mmol) in MeOH (40 mL) was heated under reflux for 6 h and then cooled to room temperature. The organic solvent was removed under vacuo and the resulting residue was recrystallised with absolute EtOH to afford *9H*-Pyrido[3,4-*b*]indole-3-carbohydrazide (**52**) as a brown solid (900 mg, 96%), mp 272-276^{o}C[260, 273]; R_f (CH_2Cl_2:MeOH, 9:1) 0.4; FT-IR (KBr) 3245, 1648, 1618, 1496, 1457, 1340, 721 cm^{-1}; ^{1}H NMR (500 MHz, DMSO-d_6) δ) 4.55 (2H, bs, NH_2), 7.29-7.32 (1H, m, ArCH), 7.58-7.61 (1H, m, ArCH), 7.66 (1H, d, J 8.0, ArCH), 8.41 (1H, d, J 8.0, ArCH), 8.82 (1H, s, ArCH), 8.88 (1H, s, ArCH), 9.65 (1H, bs, NH), 11.93(1H, bs, indole NH);^{13}C NMR (125 MHz, DMSO-d_6) δ 112.2 (ArCH), 113.8 (ArCH), 120.0 (ArCH), 120.9 (ArC), 122.3 (ArCH), 128.0 (ArC), 128.6 (ArCH), 132.5 (ArCH),137.0 (ArC), 139.4 (ArC), 141.0 (ArC), 164.0 (C=O); MS (ES$^-$) *m/z* 225.1 (100) [M-H]$^-$

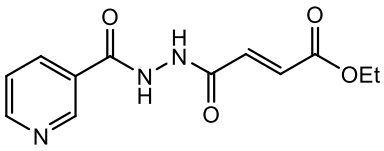
(*E*)-Ethyl 4-oxo-4-(2-picolinoylhydrazinyl)but-2-enoate (30)



Compound **47** (1.24 g, 4.0 mmol) was added to a stirred suspension of 2-picolinyl hydrazide (500 mg, 3.6 mmol) in THF: EtOAc (1:1) (50 ml) and the reaction mixture was stirred at room temperature overnight. The organic solvents were removed in *vacuo*, the resulting solid residue washed with EtOAc (50 mL), filtered, and co-evaporated with diethyl ether to give (*E*)-ethyl 4-oxo-4-(2-picolinoylhydrazinyl)but-2-enoate (**30**) as a white solid (411 mg, 43%); mp 188-192^{o}C; R_f (EtOAc:MeOH, 4:1) 0.6; FT-IR (KBr) 3357, 3188, 3115, 1717, 1665, 1570, 1368, 749 cm^{-1}; ^{1}H NMR (500 MHz, DMSO-d_6) δ

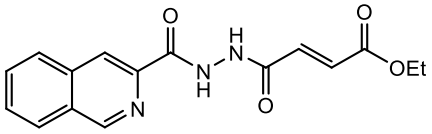
1.27 (3H, t, J 7.0, CH_3), 4.22 (2H, q, J 7.0, OCH_2), 6.71 (1H, d, J 16.0, =C-H), 7.12 (1H, d, J 16.0, =C-H), 7.66-7.68 (1H, m, ArCH), 8.04-8.05 (2H, m, 2 x ArCH), 8.69-8.70 (1H, m, ArCH), 10.75 (1H, bs, NH), 10.79 (1H, bs, NH); ^{13}C NMR (125 MHz, DMSO-d_6) δ 14.1 (CH_3), 60.8 (OCH_2), 122.4 (ArCH), 127.1 (ArCH), 129.8 (=CH), 134.8 (=CH), 137.9 (ArCH), 148.8 (ArCH), 149.0 (ArC), 161.5 (C=O), 162.3 (C=O), 164.7 (C=O); MS (ES^-) *m/z* 262.1 (100) $[M-H]^-$; HMRS (ESI) calcd. for $C_{12}H_{13}N_3O_4Na$ $[M+Na]^+$ 286.0798; found 286.0802. Anal. ($C_{12}H_{13}N_3O_4$) requires: C, 54.75; H, 4.98; N, 15.96%; found C, 54.69, H, 4.98, N, 15.87%.

(*E*)-Ethyl 4-(2-nicolinoylhydrazinyl)-4-oxobut-2-enoate (32)



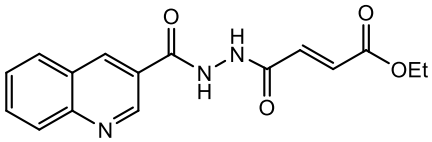
Compound **47** (1.24 g, 4.0 mmol) was added to a stirred suspension of nicotinic hydrazide (500 mg, 3.6 mmol) in THF: EtOAc (1:1) (50 ml) and the reaction mixture was stirred at room temperature overnight. The organic solvents were removed in *vacuo*, the resulting solid residue washed with EtOAc (50 mL), filtered, and co-evaporated with diethyl ether to give (*E*)-ethyl 4-(2-nicolinoylhydrazinyl)-4-oxobut-2-enoate (**32**) as a white solid (600 mg, 63%); mp 177-180^{o}C; R_f (EtOAc:MeOH, 4:1) 0.6; FT-IR (KBr) 3256, 2992, 1724, 1636, 1506, 1367, 700 cm^{-1}; ^{1}H NMR (500 MHz, DMSO-d_6) δ 1.27 (3H, t, J 7.1, CH_3), 4.23 (2H, q, J 7.1, OCH_2), 6.73 (1H, d, J 15.5, =C-H), 7.12 (1H, d, J 15.5, =C-H), 7.56-7.58 (1H, m, ArCH), 8.23 (1H, dt, J 2.0, 8.0, ArCH), 8.78 (1H, dd, J 2.0, 5.0, ArCH), 9.04 (1H, d, J 2.0, ArCH), 10.74 (1H, bs, NH), 10.90 (1H, bs, NH); ^{13}C NMR (125 MHz, DMSO-d_6) δ 14.1 (CH_3), 61.0 (OCH_2), 123.8 (ArCH), 128.0 (ArC), 130.0 (=CH), 134.6 (=CH), 135.3 (ArCH), 148.5 (ArCH), 152.6 (ArCH), 162.0 (C=O), 163.9 (C=O), 164.7 (C=O); MS (ES^-) *m/z* 262.1 (100) $[M-H]^-$; HMRS (ESI) calcd. for $C_{12}H_{12}N_3O_4$ $[M-H]^-$ 262.0833; found 262.0827. Anal. ($C_{12}H_{13}N_3O_4$) requires: C, 54.75; H, 4.98; N, 15.96%; found C, 54.79, H, 4.97, N, 15.95%.

(*E*)-Ethyl 4-(2-(isoquinoline-3-carbonyl)hydrazinyl)-4-oxobut-2-enoate (35)



Compound **47** (726 mg, 2.3 mmol) was added to a stirred suspension of compound **50** (400 mg, 2.1 mmol) in THF: EtOAc (1:1) (50 ml) and the reaction mixture was stirred at room temperature overnight. The organic solvents were removed in *vacuo*, the resulting solid residue washed with EtOAc (50 mL), filtered, and co-evaporated with diethyl ether to give (*E*)-ethyl 4-(2-(isoquinoline-3-carbonyl)hydrazinyl)-4-oxobut-2-enoate (**9**) as a off-white solid (410 mg, 62%); mp 230-233^{o}C; R_f (EtOAc:MeOH, 4:1) 0.5; FT-IR (KBr) 3359, 3215, 1712, 1663, 1503, 1304 cm^{-1}; ^{1}H NMR (500 MHz, DMSO-d$_6$) δ 1.27 (3H, t, J 7.0, CH_3), 4.23 (2H, q, J 7.0, OCH_2), 6.73 (1H, d, J 15.5, =C-H), 7.15 (1H, d, J 15.5, =C-H), 7.84-7.87 (1H, m, ArCH), 7.90-7.93 (1H, m, ArCH) 8.24 (1H, d, J 8.0, ArCH), 8.29 (1H, d, J 8.0, ArCH), 8.61 (1H, s, ArCH), 9.43 (1H, s, ArCH), 10.87 (1H, bs, NH), 10.93 (1H, bs, NH); ^{13}C NMR (125 MHz, DMSO-d$_6$) δ 14.1 (CH_3), 61.0 (OCH_2), 120.5 (ArCH), 127.9 (ArCH), 128.1 (ArCH), 129.4 (ArC), 129.5 (ArCH), 130.0 (=CH), 131.5 (ArCH), 135.0 (=CH), 135.2 (ArC), 142.5 (ArC), 151.9 (ArCH) 161.3 (C=O), 162.4 (C=O), 164.8 (C=O); MS (ES$^-$) *m/z* 312.1 (100) [M-H]$^-$; HMRS (ESI) calcd. for $C_{16}H_{15}N_3O_4Na$ [M+Na]$^+$ 336.0955; found 336.0960. Anal. ($C_{16}H_{15}N_3O_4$) requires: C, 58.95; H, 3.89; N, 14.73%; found C, 59.03, H, 3.88, N, 14.70%.

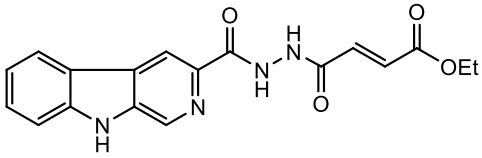
(*E*)-Ethyl 4-oxo-4-(2-(quinoline-3-carbonyl)hydrazinyl)but-2-enoate (42)



Compound **47** (520 mg, 1.6 mmol) was added to a stirred suspension of compound **51** (280 mg, 1.5 mmol) in THF: EtOAc (1:1) (50 ml) and the reaction mixture was stirred at room temperature overnight. The organic solvents were removed in *vacuo*, the resulting solid residue washed with EtOAc (50 mL), filtered, and co-evaporated with diethyl ether

to give **(***E*)-Ethyl 4-oxo-4-(2-(quinoline-3-carbonyl)hydrazinyl)but-2-enoate (**42**) as a off-white solid (240 mg, 51%); mp 223-226^{o}C; R_f (EtOAc:MeOH, 4:1) 0.5; FT-IR (KBr) 3209, 1714, 1605, 1486, 1300, 1186 cm^{-1}; ^{1}H NMR (500 MHz, DMSO-d_6) δ 1.27 (3H, t, J 7.0, CH_3), 4.23 (2H, q, J 7.0, OCH_2), 6.75 (1H, d, J 16.0, =C-H), 7.16 (1H, d, J 16.0, =C-H), 7.74 (1H, dd, J 7.5, 7.6, ArCH), 7.92 (1H, dd, J 7.5, 7.6, ArCH), 8.10-8.16 (2H, m, 2 x ArCH) 8.91 (1H, d, J 2.0, ArCH), 9.30 (1H, d, J 2.0, ArCH), 10.93 (2H, bs, 2 x NH); ^{13}C NMR (125 MHz, DMSO-d_6) δ 14.1 (CH_3), 61.0 (OCH_2), 125.0 (ArC), 126.4 (ArC), 127.6 (ArCH), 128.8 (ArCH), 129.3 (ArCH), 130.1 (=CH), 131.7 (ArCH), 134.7 (=CH), 136.3 (ArCH), 148.6 (ArCH), 148.7 (ArC) 161.9 (C=O), 163.9 (C=O), 164.7 (C=O); MS (ES$^-$) *m/z* 312.1 (100) [M-H]$^-$; HMRS (ESI) calcd. for $C_{16}H_{15}N_3O_4Na$ [M+Na]$^+$ 336.0955; found 336.0949. Anal. ($C_{16}H_{15}N_3O_4$) requires: C, 61.34; H, 4.83; N, 13.41%; found C, 61.35, H, 4.81, N, 13.43%.

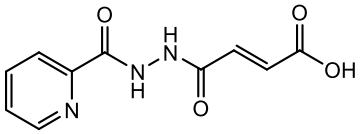
***(E)*-Ethyl 4-(2-(9H-pyrido[3,4-*b*]indole-3carbonyl)hydrazinyl)-4-oxobut-2-enoate (46)**



Compound **47** (454 mg, 1.5 mmol) was added to a stirred suspension of compound **52** (400 mg, 1.3 mmol) in THF: EtOAc (1:1) (50 ml) and the reaction mixture was stirred at room temperature overnight. The organic solvents were removed in *vacuo*, the resulting solid residue washed with EtOAc (50 mL), filtered, and co-evaporated with diethyl ether to give *(E)*-ethyl 4-(2-(9H-pyrido[3,4-b]indole-3carbonyl)hydrazinyl)-4-oxobut-2-enoate (**46**) as a white solid (447 mg, 95%); mp > 330^{o}C; R_f (EtOAc:MeOH, 4:1) 0.5; FT-IR (KBr) 3350, 3262, 1719, 1611, 1490, 1459, 741 cm^{-1}; ^{1}H NMR (500 MHz, DMSO-d_6) δ 1.28 (3H, t, J 7.0, CH_3), 4.23 (2H, q, J 7.0, OCH_2), 6.73 (1H, d, J 15.5, =C-H), 7.17 (1H, d, J 15.5, =C-H), 7.33 (1H, dd, J 7.5, 8.0, ArCH), 7.62 (1H, dd, J 7.5, 8.0, ArCH), 7.69 (1H, d, J 8.0, ArCH), 8.44 (1H, d, J 8.0, ArCH), 8.89 (1H, s, ArCH), 8.95 (1H, s, ArCH), 10.64 (1H, bs, NH), 10.94 (1H, bs, NH), 12.05 (1H, bs, indole NH); ^{13}C NMR (125 MHz, DMSO-d_6) δ 14.0 (CH_3), 61.0 (OCH_2), 112.3 (ArCH), 114.8 (ArCH), 120.2 (ArCH),

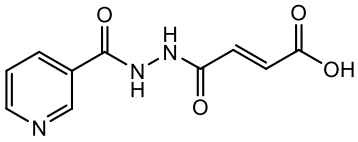
120.9 (ArC), 122.4 (ArCH), 128.0 (ArC), 128.8 (ArCH), 129.7 (=CH), 132.6 (ArCH), 135.0 (=CH), 137.4 (ArC), 138.1 (ArC), 141.0 (ArC) 161.2 (C=O), 163.0 (C=O), 164.8 (C=O); MS (ES^-) *m/z* 351.1 (100) $[M-H]^-$; HMRS (ESI) calcd. for $C_{18}H_{16}N_4O_4Na$ $[M+Na]^+$ 375.1064; found 375.1071.

(*E*)- 4-Oxo-4-(2-picolinoylhydrazinyl)but-2-enoic acid (5)



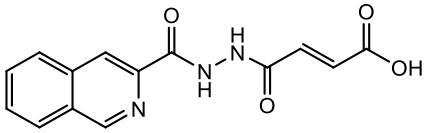
Compound **30** (150 mg, 0.6 mmol) was added to a solution of $LiOH.H_2O$ (75 mg, 1.8 mmol) in H_2O:THF (1:2) (15 ml) and the mixture was stirred at room temperature. TLC analysis (EtOAc: MeOH, 4:1) indicated complete consumption of starting material (R_f 0.6) after 3 h. The reaction mixture was then washed with EtOAc (3 x 10 mL). The aqueous layer was acidified with 1 N HCl to pH 3, and the white precipitate formed was filtered, washed with H_2O, and dried under *vacuo* to give (*E*)- 4-oxo-4-(2-picolinoylhydrazinyl)but-2-enoic acid (**5**) as a white solid (130 mg, 98%); mp 272-275^oC; FT-IR (KBr) 3400-3100 (br), 3317, 3213, 1724, 1630, 1153 cm^{-1}; ^1H NMR (500 MHz, DMSO-d_6) δ 6.66 (1H, d, J 15.5, =C-H), 7.04 (1H, d, J 15.5, =C-H), 7.65-7.68 (1H, m, ArCH), 8.02-8.06 (2H, m, 2 x ArCH), 8.69-8.70 (1H, m, ArCH), 10.73 (1H, bs, NH), 10.75 (1H, bs, NH); ^{13}C NMR (125 MHz, DMSO-d_6) δ 122.4 (ArCH), 127.1 (ArCH), 131.2 (=CH), 134.2 (=CH), 138.0 (ArCH), 148.7 (ArCH), 148.8 (ArC), 161.8 (C=O), 162.4 (C=O), 166.1 (COOH); MS (ES^-) *m/z* 234.1 (100) $[M-H]^-$; HMRS (ESI) calcd. for $C_{10}H_8N_3O_4$ $[M-H]^-$ 234.0520; found 234.0512.

(*E*)- 4-(2-Nicolinoylhydrazinyl)-4-oxobut-2-enoic acid (9)



Compound **32** (150 mg, 0.6 mmol) was added to a stirring solution of $LiOH.H_2O$ (75 mg, 1.8 mmol) in H_2O:THF (1:2) (15 ml) at room temperature. TLC analysis (EtOAc: MeOH, 4:1) indicated complete consumption of starting material (R_f 0.6) after 3 h. The reaction mixture was then washed with EtOAc (3 x 10 mL). The aqueous layer was acidified with 1 N HCl to pH 3, and the white precipitate formed was filtered, washed with H_2O, and dried under *vacuo* to give (*E*)- 4-oxo-4-(2-picolinoylhydrazinyl)but-2-enoic acid (**9**) as a white solid (87 mg, 65%); mp 274-276^oC; FT-IR (KBr) 3400-3100 (br), 3206, 3076, 1702, 1619, 1596, 1153 cm^{-1}; ^1H NMR (500 MHz, DMSO-d_6) δ 6.68 (1H, d, J 15.5, =C-H), 7.05 (1H, d, J 15.5, =C-H), 7.68-7.71 (1H, m, ArCH), 8.36-8.40 (1H, m, ArCH), 8.83-8.85 (1H, m, ArCH), 9.10 (1H, d, J 2.0, ArCH), 10.76 (1H, bs, NH), 10.99 (1H, bs, NH); ^{13}C NMR (125 MHz, DMSO-d_6) δ 124.3 (ArCH), 128.5 (ArC), 131.4 (=CH), 134.1 (=CH), 137.0 (ArCH), 147.2 (ArCH), 151.1 (ArCH), 162.3 (C=O), 163.3 (C=O), 166.1 (COOH); MS (ES^-) *m/z* 234.1 (100) $[M-H]^-$; HMRS (ESI) calcd. for $C_{10}H_8N_3O_4$ $[M-H]^-$ 234.0520; found 234.0514.

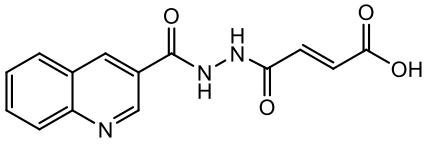
(*E*)- 4-(2-(Isoquinoline-3-carbonyl)hydrazinyl)-4-oxobut-2-enoic acid (14)



Compound **35** (150 mg, 0.5 mmol) was added to a stirring solution of $LiOH.H_2O$ (63 mg, 1.5 mmol) in H_2O:THF (1:2) (15 ml) at room temperature. TLC analysis (EtOAc: MeOH, 4:1) indicated complete consumption of starting material (R_f 0.5) after 3 h. The reaction mixture was then washed with EtOAc (3 x 10 mL). The aqueous layer was acidified with 1 N HCl to pH 3, and the white precipitate formed was filtered, washed with H_2O, and dried under *vacuo* to give(E)- 4-(2-(isoquinoline-3-carbonyl)hydrazinyl)-4-oxobut-2-enoic acid (**14**) as a yellow solid (120 mg, 88%) ; mp > 330^oC; FT-IR (KBr) 3209, 1714,

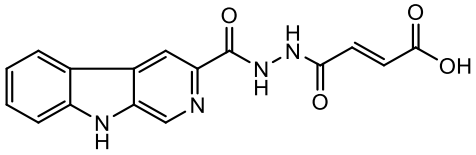
1605, 1486, 1300, 1186 cm^{-1}; ^{1}H NMR (500 MHz, DMSO-d_6) δ 6.67 (1H, d, J 15.5, =C-H), 7.05 (1H, d, J 15.5, =C-H), 7.84-7.87 (1H, m, ArCH), 7.90-7.93 (1H, m, ArCH) 8.24 (1H, d, J 8.0, ArCH), 8.29 (1H, d, J 8.0, ArCH), 8.61 (1H, s, ArCH), 9.43 (1H, s, ArCH), 10.85 (1H, bs, NH), 10.89 (1H, bs, NH); ^{13}C NMR (125 MHz, DMSO-d_6) δ 120.5 (ArCH), 127.9 (ArCH), 128.1 (ArCH), 129.4 (ArC), 129.5 (ArCH), 131.1 (=CH), 131.6 (ArCH), 134.3 (=CH), 135.2 (ArC), 142.8 (ArC), 151.9 (ArCH) 161.7 (C=O), 162.5 (C=O), 164.8 (COOH); MS (ES^-) *m/z* 284.1 (100) $[M-H]^-$; HMRS (ESI) calcd. for $C_{14}H_{10}N_3O_4$ $[M-H]^-$ 284.0677; found 284.0670.

(*E*)- 4-Oxo-4-(2-(quinoline-3-carbonyl)hydrazinyl)but-2-enoic acid (24)



Compound **42** (90 mg, 0.3 mmol) was added to a stirring solution of $LiOH.H_2O$ (38 mg, 0.9 mmol) in H_2O:THF (1:2) (15 ml) at room temperature. TLC analysis (EtOAc: MeOH, 4:1) indicated complete consumption of starting material (R_f 0.5) after 3 h. The reaction mixture was then washed with EtOAc (3 x 10 mL). The aqueous layer was acidified with 1 N HCl to pH 3, and the white precipitate formed was filtered, washed with H_2O, and dried under *vacuo* to give (*E*)- 4-oxo-4-(2-(quinoline-3-carbonyl)hydrazinyl)but-2-enoic acid (**15**) as a yellow solid (50 mg, 63%) ; mp > 330^oC; FT-IR (KBr) 3450 (br), 3186, 1698, 1607, 1487 cm^{-1}; ^{1}H NMR (500 MHz, DMSO-d_6) δ 6.70 (1H, d, J= 15.5 Hz, =C-H), 7.08 (1H, d, J 15.5 Hz, =C-H), 7.75 (1H, dd, J 7.5, 7.6 Hz, ArCH), 7.93 (1H, dd, J 7.5, 7.6, ArCH), 8.12-8.17 (2H, m, 2 x ArCH) 8.93 (1H, d, J 2.0, ArCH), 9.31 (1H, d, J 2.0, ArCH), 10.79 (H, bs, NH), 11.06 (H, bs, NH); ^{13}C NMR (125 MHz, DMSO-d_6) δ 125.0 (ArC), 126.4 (ArC), 127.7 (ArCH), 128.6 (ArCH), 129.3 (ArCH), 131.3 (=CH), 131.7 (ArCH), 134.1 (=CH), 136.5 (ArCH), 148.5 (ArCH), 148.6 (ArC) 162.4 (C=O), 163.9 (C=O), 166.1 (COOH); MS (ES^-) *m/z* 284.1 (100) $[M-H]^-$; HMRS (ESI) calcd. for $C_{14}H_{12}N_3O_4$ $[M-H]^-$ 286.0822; found 286.0822.

(*E*)-4-(2-(9H-Pyrido[3,4-b]indole-3-carbonyl)hydrazinyl)-4-oxobut-2-enoic acid (29)



Compound **42** (340 mg, 1.0 mmol) was added to a stirring solution of $LiOH.H_2O$ (125 mg, 3.0 mmol) in H_2O:THF (1:2) (30 ml) at room temperature. TLC analysis (EtOAc: MeOH, 4:1) indicated complete consumption of starting material (R_f 0.5) after 3 h. The reaction mixture was then washed with EtOAc (3 x 10 mL). The aqueous layer was acidified with 1 N HCl to pH 3, and the white precipitate formed was filtered, washed with H_2O, and dried under *vacuo* to give (*E*)-4-(2-(9H-pyrido[3,4-b]indole-3-carbonyl)hydrazinyl)-4-oxobut-2-enoic acid (**29**) as a yellow solid (240 mg, 76%); mp > 330^oC; R_f (EtOAc:MeOH, 4:1) 0.5; FT-IR (KBr) 3425 (br), 1688, 1611, 1493, 1458 cm^{-1}; ^1H NMR (500 MHz, DMSO-d_6) δ 6.67 (1H, d, J 15.5, =C-H), 7.10 (1H, d, J 15.5, =C-H), 7.33 (1H, dd, J 7.5, 8.0, ArCH), 7.62 (1H, dd, J 7.5, 8.0, ArCH), 7.69 (1H, d, J 8.0, ArCH), 8.44 (1H, d, J 8.0, ArCH), 8.89 (1H, s, ArCH), 8.95 (1H, s, ArCH), 10.62 (1H, d, J 2.0, NH), 10.91 (1H, d, J 2.0, NH), 12.09 (1H, bs, indole NH); ^{13}C NMR (125 MHz, DMSO-d_6) δ 112.3 (ArCH), 114.8 (ArCH), 120.2 (ArCH), 120.9 (ArC), 122.4 (ArCH), 128.0 (ArC), 128.8 (ArCH), 130.9 (=CH), 132.7 (ArCH), 134.5 (=CH), 137.4 (ArC), 138.1 (ArC), 141.0 (ArC) 161.5 (C=O), 163.0 (C=O), 166.1 (COOH); MS (ES^-) *m/z* 323.1 (100) $[M-H]^-$; HMRS (ESI) calcd. for $C_{18}H_{16}N_4O_4Na$ $[M-H]^-$ 323.0786; found 323.0794.

Chapter 7: Aspirin Metabolites Suppress HIF-α Levels in von Hippel-Lindau (VHL)-Defective Renal Cell Carcinomas

7.1 Introduction

7.1.1 Aspirin and salicylic acid

Acetylsalicylic acid, more commonly known as aspirin (ASA, **Fig. 7.1**), remains the most widely used medicine of all time. It was first synthesised by the German chemist Felix Hoffmann in 1897.[274] At one or two grams a day, aspirin is used to relieve fever and minor aches and pains whereas at high prescription dosages between four and eight grams daily, it is used to reduce swelling and to treat gout, rheumatoid arthritis, and inflammatory ailments.[275, 276] Many people also take low dosages (below 100 mg) of aspirin daily to prevent recurrent stroke or cardiovascular events such as heart attack.[277-280]

It is worth noting that synthetic aspirin is not the only source of salicylic acid (SA, direct metabolites of aspirin, **Fig. 7.1**) and salicylate derivatives. Natural salicylates are commonly found in our daily diet; food products such as berries, fresh orange, vegetables, tea, honey, curry powder and many others all contain salicylates. The average daily intake of salicylates from food alone is estimated to be in a range of 10-200 mg/day in the Western diet.[281, 282]

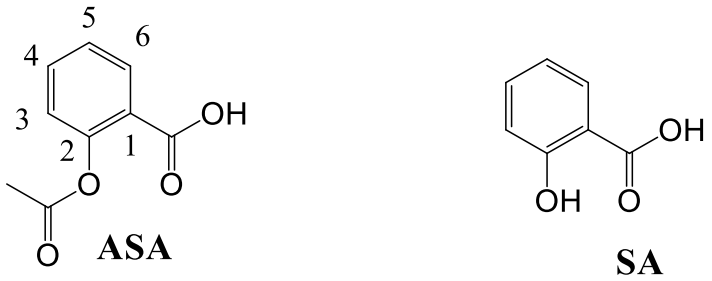


Figure 7.1: Aspirin (ASA) and its immediate metabolite salicylic acid (SA).

7.1.2 Aspirin and cancers

Aspirin has also been associated with cancer prophylaxis (*i.e.* prevention of cancers). Evidence shows that moderate or high doses of aspirin can decrease the risks of colorectal and lung cancer, and possibly breast cancer and other cancers.[283-288] However, long term use of aspirin (> 10 years) may be necessary to see the protective effects.[289-291] The dosages used for cancer prevention vary substantially across the studies. Two reports have suggested that 80 mg of daily aspirin is the optimum dose,[292, 293] whereas some investigators demonstrated increased benefits with larger daily doses (300-1200 mg).[283, 285, 294]

A recent large scale long term follow-up study on patients from eight randomised trials (25 570 patients, 674 deaths) has shown that daily aspirin intake (taken at daily doses of at least 75 mg for several years) can reduce deaths caused by several common cancers including colorectal, stomach, pancreatic, lung and prostate cancer. Its benefits are also found to increase with duration of treatment.[295] The biological processes by which healthy cells are transformed into cancer cells are highly complex and despite substantial research, the mechanisms in which aspirin (or salicylates) might directly affect tumorigenesis remain undetermined.[296]

7.1.3 Inhibition of cyclooxygenases

Non-steroidal anti-inflammatory drugs (NSAIDs), including aspirin, Ibuprofen, Naproxen, and many others, are cyclooxygenase (COX) inhibitors. Aspirin inhibits COX-1 and COX-2 in prostaglandin (PG) synthesis via inhibition of the enzymatic oxidation of arachidonic acid.[297, 298] Many kinds of prostaglandins are produced by the body to serve different physiological functions, some of which are beneficial, others deleterious.[275, 296, 299]

COX-1 is constitutively produced in the endoplasmic reticulum and is responsible for normal homeostatic functions including platelet aggregation, vascular homoeostasis, and renal blood flow, whereas COX-2 is rapidly induced in response to mediators such as inflammation, growth factors and endotoxins, and is associated with cell proliferation and tumour growth.[299-301] Inhibition of COX-2 is proposed to be responsible for the therapeutic effects of aspirin in reducing pain, inflammation and fever and prevention of cancers whereas inhibition of COX-1 is associated with the drug's undesirable side effects including severe stomach irritation, gastrointestinal bleeding, and promotion of peptic ulcers.[275, 302, 303]

The therapeutic effect of aspirin in preventing myocardial infarction (heart attack) is attributed to COX-1 inhibition in platelets. Aspirin at low dosages irreversibly inhibits COX-1 activity by acetylating serine-530 in the enzyme active site. This modification hinders substrate (arachidonic acid) binding and inhibits thromboxane generation, thus inhibiting platelet aggregation.[304] It has been proposed that inhibition of COX-2 by aspirin might not be caused by acetylation of its catalytic site.[304]

Despite the structural similarities between the COX-1 and COX-2 isoforms, aspirin is reported to be 160 times more specific at inhibiting COX-1 whereas its major metabolite SA is reported to be 100 times more potent at inhibiting COX-2 *in vitro*.[305, 306] SA at therapeutic concentrations has been reported to inhibit COX-2 expression by suppressing COX-2 messenger RNA (mRNA) and protein synthesis in human endothelial cells. Similar effects were observed in mice fed with salicylate-rich diets.[307, 308] Because COX-2 has been associated with carcinogenesis, pharmaceutical salicylates and salicylate-rich diets are therefore suggested to be beneficial for cancer prevention.[296, 309]

The therapeutic effects of aspirin vary with the doses used, of which three dose ranges are commonly examined.[310] Low dosages ($\leq$ 80 mg/day) of aspirin irreversibly inhibit COX-1 and are anti-thrombotic. Medium dosages (2-4 g/day) inhibit both COX-1 and COX-2, and are analgesic and anti-pyretic. At millimolar range of serum concentrations (6-8 g/day), aspirin is effective in the treatments of rheumatic disorders; however, the mechanisms underlying these different effects remain uncertain.[310]

7.1.4. Other possible mechanisms

Evidence has shown that the acquired ability of cells to resist apoptosis is a hallmark of most cancers, whilst the pro-apoptotic effects of aspirin are commonly attributed to inhibition of COX-2.[311, 312] However, the chemopreventive effects of aspirin and other NSAIDs cannot be solely associated with inhibition of prostaglandin synthesis, as several NSAIDs also demonstrate anti-proliferative effects in cells lacking of COX-activity.[296] High concentrations of aspirin and SA have been shown to stimulate apoptosis via COX-independent pathways by upregulation of several pro-apoptotic genes such as 15-LOX-1 (15-lipoxygenase-1)[313] and Par-4 (prostate apoptosis response-4)[314] and the activation of the p38 MAPK (mitogen-activated protein kinase) pathway.[315] In addition, the pro-apoptotic effects of aspirin have also been associated with the upregulation of several tumour suppressor genes and the downregulation of anti-apoptotic genes.[316]

NF_KB (nuclear factor kappaB) transcriptional activities include the inflammatory responses which are associated with solid tumours and the induction of survival genes (which protect the cells from apoptosis). High doses of aspirin or SA (4 -10 g/day) have been shown to inhibit the activation of the NF_KB transcriptional pathway by preventing phosphorylation (possibly through inhibition of the kinase IKKβ) and subsequent degradation of its inhibitory factor $I_KB\alpha$.[317, 318] However, the effects of aspirin on NF_KB response have been shown to be cell-type specific.[319, 320]

7.1.5 Metabolism of aspirin

Most drugs are metabolised in the liver in where enzymes catalyse various biochemical reactions (most commonly oxidations, catalysed by oxidase enzymes mainly from the cytochrome P450 family) to produce water soluble and less lipid-soluble molecules. Metabolites which are insufficiently water soluble for excretion by the kidney will undergo conjugation reactions with endogenous amino acids present in the liver in which the formation of glycine adducts is common. The resulting compounds are then excreted

by the kidney. Less water soluble metabolites can be excreted in the bile, which contains sufficient cholesterol to dissolve the lipid soluble molecules for further breakdown. Drug metabolism may also take place in the intestine, plasma, lungs and skin. Similarly to many other drugs, aspirin undergoes intensive biotransformation after oral administration; different metabolites have been detected in patients under treatment.[276, 321, 322]

The formation of aspirin metabolites such as salicyluric acid (SUA), SA, 2,3-dihydroxybenzoic acid (2,3-DHBA), 2,5-dihydroxybenzoic acid (2,5-DHBA or gentisic acid), 2,5-dihydroxybenzoylglycine (or gentisuric acid, GUA) and the acyl and phenolic glucuronide conjugates have been extensively characterised.[321-324] A recent study has also reported the detection of 2,3-dihydroxybenzoylglycine (DHBG) (**Fig. 7.2**) as an aspirin metabolite.[82, 276]

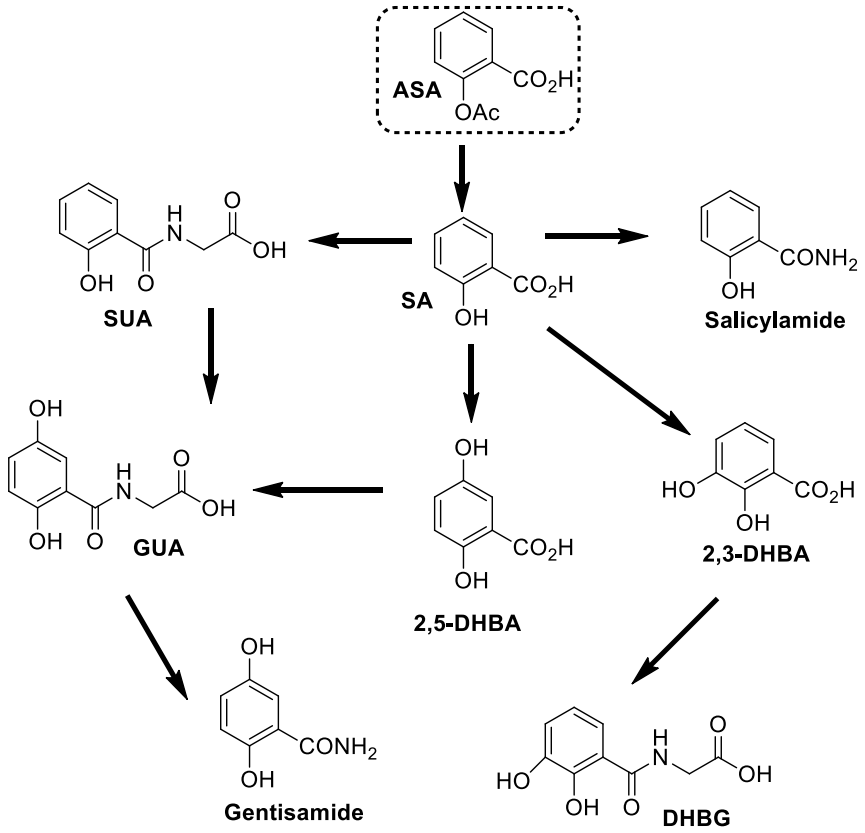


Figure 7.2: Aspirin and its reported metabolites.

Aspirin is first converted into SA by the activity of esterases in the intestine, or by trans-acylation of targeted proteins, which then undergoes glycine coupling via mitochondrial glycine-*N*-acyltransferase in the liver and kidney to form SUA (**Fig. 7.3**).[325, 326] Aspirin or SA are also metabolised into 2,3- and 2,5-DHBA by the reactions of hydroxyl radicals generated by activated neutrophils (the most abundant white blood cells and commonly found at inflammatory sites) or by enzymatic oxidation catalysed by cytochrome P450 in the liver.[276, 324, 327]

DHBG and GUA are expected to be formed either by glycine coupling to the corresponding acids or by hydroxylation of SUA.[82, 328] Glucuronate and sulphate conjugates of the 2,3- and 2,5-DHBA, trihydroxybenzoates and quinones have also been proposed as potential metabolites.[327] In addition, SUA and GUA have been shown to be converted to salicyamide, gentisamide, and glyoxylate by the bi-functional peptidylglycine α-amidating monooxygenase (PAM) (**Fig. 7.3**), however their proportions are very low (< 5%) compared to the unconverted SUA and GUA.[276, 329]

Discrepancies have been reported in the identification and abundance of metabolites in patients who undergo aspirin treatment. However, SA and its glycine conjugate, SUA (ranging between 10-65% and 22-75% of total recovered salicylates, respectively) have consistently been reported as the major metabolites in the urinary samples of volunteers who took therapeutic doses (< 1 g/day) or high doses (4-8 g/day) of aspirin for different durations.[276, 322, 330]

Proportions as high as 75% and as low as 2% of GUA of total recovered salicylates have been detected in the urine samples of patients under intensive treatment.[328, 331] A later report suggested GUA may also remain for a long time in a living body.[332] A single oral therapeutic dose (600 mg) has been reported to result in plasma SUA concentrations of 10-25 μM for up to 10 h.[333, 334] For patients on long-term treatment (4 x 600 mg/day for 3 months), plasma concentrations of 2,5-DHBA and 2,3-DHBA were detected at about 2 μM, while SA was estimated to be at least a hundred times higher and SUA at least fifteen times more than the concentrations of 2,5-DHBA and 2,3-DHBA.[324]

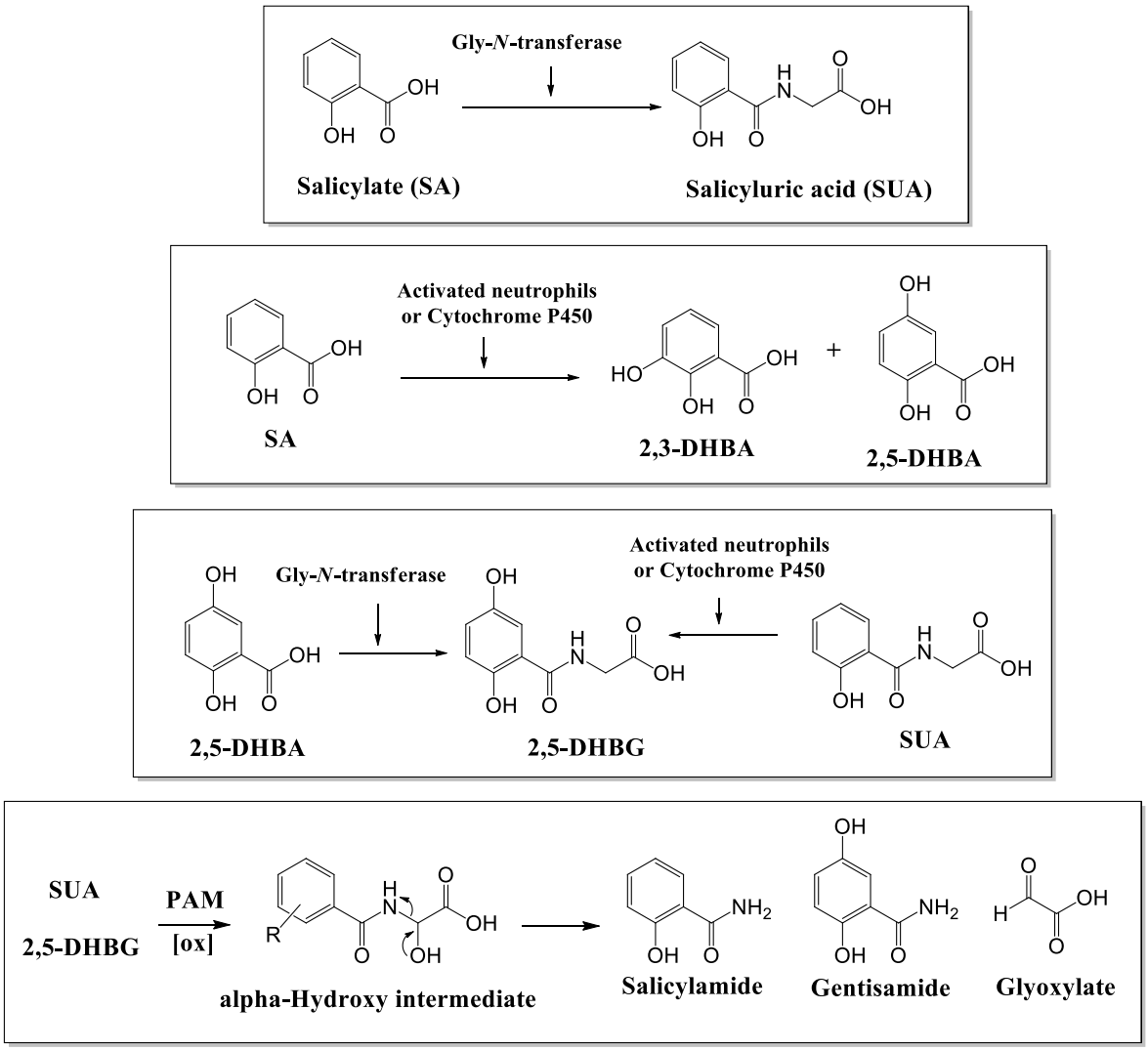


Figure 7.3: Possible metabolic pathways leading to the formation of different aspirin metabolites. PAM, peptidylglycine α-amidating monooxygenase.[276]

7.2 Background and Objectives

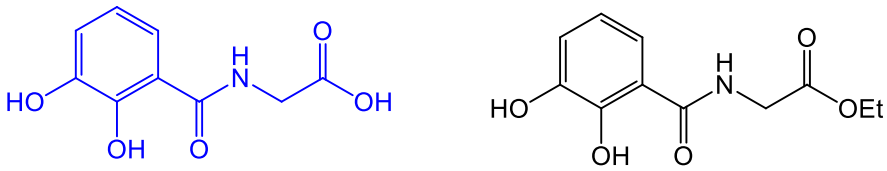
Renal cell carcinoma (RCC) accounts for approximately 2% of adult malignancies worldwide[335] and is resistant to radiation and chemotherapy.[336] A common feature found in renal cancer patients is somatic mutation of the von Hippel-Lindau (VHL) tumour suppression gene.[337] pVHL (VHL protein) recruits an E3 ubiquitin ligase complex and targets HIF-α for proteasomal degradation under normoxic conditions (see also **Chapter 1**).[338] pVHL mutants, however, are defective in this regard, leading to excessive accumulation of HIF-α and thus elevated levels of VEGF (vascular endothelial growth factor), which promote tumour progression and result in poor outcomes of RCC patients despite current treatments.[339, 340] Elevated HIF-α levels are commonly found in cancers, in contrast to the undetectably low levels observed in most normal human tissues[341]. Suppression of HIF mediated gene expression has therefore been proposed as a potential therapeutic strategy for the treatments of RCC and other cancers.[1, 342-344]

The aspirin metabolite 2,3-dihydroxybenzoylglycine (DHBG) has previously been identified as a HIF prolyl hydroxylase (PHD) inhibitor that causes HIF-1α accumulation in cells.[82] Surprisingly, when DHBG was tested in the HIF hydroxy-residue specific antibody assays developed in **Chapter 2**, the compound was found to substantially destabilise HIF-1α in the RCC4 cells. This interesting observation prompted me to further evaluate aspirin, its metabolites and other structurally related compounds as potential HIF-1α inhibitors in this chapter. (HIF-1α inhibitors are defined as agents which suppress HIF-1α activity via one of the following or other mechanisms:[345] (i) inhibiting HIF-1α mRNA expression, (ii) inhibiting HIF-1α protein translation, (iii) promoting HIF-1α protein degradation, (iv) inhibiting HIF-1α DNA binding to hypoxia responsive element (HRE), (v) inhibiting HIF-1α transcriptional activity.) The work in this chapter was carried out in collaboration with Dr Y-M Tian at the Centre for Cellular and Molecular Physiology, University of Oxford.

7.3 Results and Discussion

7.3.1 Aspirin metabolites DHBG and GUA are HIF-1α Inhibitors

Whilst the anti-inflammatory and analgesic effects of aspirin are apparently attributed to the mechanisms of the inhibition of cyclooxgenases COX-1 and COX-2 (**Section 7.1.3**), its preventive effects on heart disease and various cancers are still under intensive investigation. It is possible that salicylate metabolites (**Fig. 7.2**) may also contribute substantially to the observed therapeutic effects of aspirin. Lienard *et al.* have previously evaluated these metabolites as PHD inhibitors; DHBG (**1**) (**Fig. 7.4**) was identified as a PHD inhibitor with an IC_{50} value of 27.4 μM[82] using a fluorescence-based assay.



1 **(DHBG)** **2**

Figure 7.4: 2,3-Dihydroxybenzoylglycine (DHBG) **1** and its ethyl ester derivative **2** have been previously identified as PHD inhibitors *in vitro* and in cells respectively.[82] Structure in blue indicates the compound is an aspirin metabolite. (Compounds **1** and **2** were synthesized by Dr A. Conejo-Garcia).

The work in this chapter first investigated the effect of DHBG on HIF prolyl and asparaginyl hydroxylation in RCC4 cells. (Unless otherwise stated, all compounds were tested in their methyl or ethyl ester forms in the cell-based experiments). Consistent with the previous results which demonstrated the HIF-1α accumulation effect of DHBG,[82] the compound at 0.2 mM substantially inhibited HIF-1α Pro564 hydroxylation (and moderately inhibited Asn803 hydroxylation) in RCC4 cells (**Fig. 7.5 A**). Unexpectedly, at a higher concentration (0.5 mM), DHBG reduced HIF-1α levels in RCC4 cells, therefore suggesting DHBG may inhibit HIF-1α expression or induce HIF-1α degradation via a VHL-independent pathway.

When DHBG was used to treat RCC4 VHL-competent cells (*i.e.* RCC4 re-expressing functional VHL, RCC4/VHL), the compound was shown to induce HIF-1α accumulation as anticipated (**Fig. 7.5 B**). Interestingly, at 0.5 mM (**Fig. 7.5 B**, but not 0.1 or 0.2 mM), a slower-mobility HIF-1α species (higher molecular weight protein) was clearly detected, indicating DHBG at high concentrations may promote HIF-1α modification and eventually lead to its degradation. (A slower-mobility HIF-1α species was also detected in RCC4 cells treated with DHBG, however at relatively low abundance (**Fig. 7.6 A**, lane 3)). It is also possible that the DHBG mediated reduction of HIF-1α levels observed in the cells could be due to the potential inhibitory effects of DHBG on the HIF-1α mRNA transcription or protein translation. In this regard, 'HIF-1α suppression' will be used in the following to refer to reduced HIF-1α activity caused by HIF-1α degradation or inhibition of HIF-1α expression.

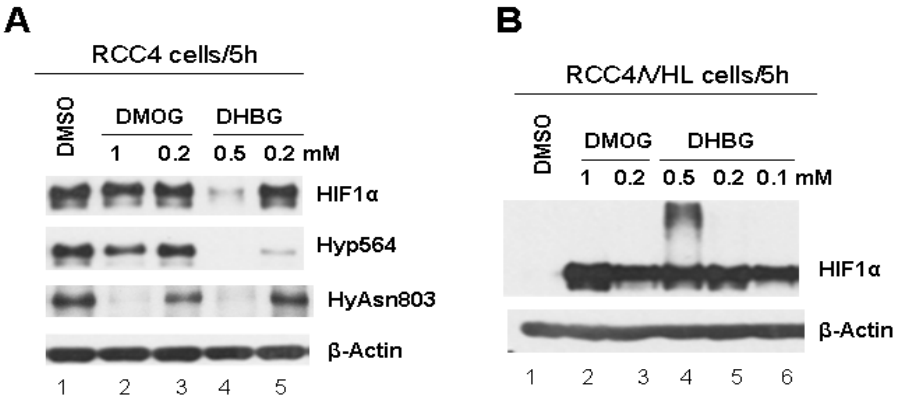


Figure 7.5: (**A**) DHBG **2** substantially inhibits Pro564 hydroxylation at 0.2 mM, and induces HIF-1α suppresion at 0.5mM in RCC4 cells. (**B**) DHBG **2** promotes HIF-1α accumulation in RCC4/VHL cells. The formation of a slower-mobility species (lane 4) indicates DHBG promotes HIF-1α modification at high concentrations. Dimethyloxaylgylcine (DMOG) was used as a positive control.

These cell-based results demonstrate that DHBG displays concentration-dependent dichotomous effect on HIF-1α stabilisation and HIF-1α suppression in RCC4/VHL cells. Furthermore, DHBG was also shown to suppress HIF-1α protein levels in RCC4 cells at high concentrations. The work next sought to investigate whether other DHBG derivatives would also exhibit similar effects. A number of DHBG derivatives with

hydroxyl groups at different positions (*i.e.* 2,4-, 2,5-, and 2,6-) in the aromatic ring (**Fig. 7.6,** compounds **4**, **6**, **8**,) and different amino acid side chains (D/L-alanine, and D/L-valine, **Fig. 7.6,** compounds **10**, **12**, **14**, **16**) were tested in RCC4 and RCC4/VHL cells (**Fig. 7.7 A-D**).

While the 2,4- and 2,6-dihydroxybenzoylglycine derivatives **4** and **8** did not have apparent effects on HIF-1α levels in the RCC4 cells, the 2,5-dihydroxybenzoylgylcine **6** (GUA, a known aspirin metabolite) significantly reduced HIF-1α levels in this VHL-defective cell-line (**Fig. 7.7 A**). This observation suggests that the position of the hydroxyl group in the aromatic ring is an important determinant of suppression in HIF-α activity. Unlike DHBG which exerted its suppressive effects at high concentrations (**Fig. 7.7 A**, lane 3), GUA reduced HIF-1α levels at both concentrations (0.2 and 1 mM) (**Fig. 7.7 A** lanes 7 and 8).

GUA was also shown to weakly induce HIF-1α accumulation in RCC4/VHL cells at 0.2 mM (**Fig. 7.7 B**, lane 8, HIF-1α long exposure film), however, the induction was relatively weak compared to DHBG (**Fig. 7.7 B**, lanes 4 and 8). This observation is consistent with previous data indicating that GUA is an inffective PHD inhibitor[82]. In RCC4 cells, the HIF-1α suppression effect of GUA (at 0.2 mM) is expected to be greater than its stabilising effect. Suprisingly, when the 5-hydroxyl group in the GUA aromatic ring is replaced with a chloro- (**17**) or methyl-group (**18**), the compound instantly lost its ability to suppress HIF-1α in RCC4 cells (**Fig. 7.7 E**), indicating the important role of the hydroxyl group at the C-5 position.

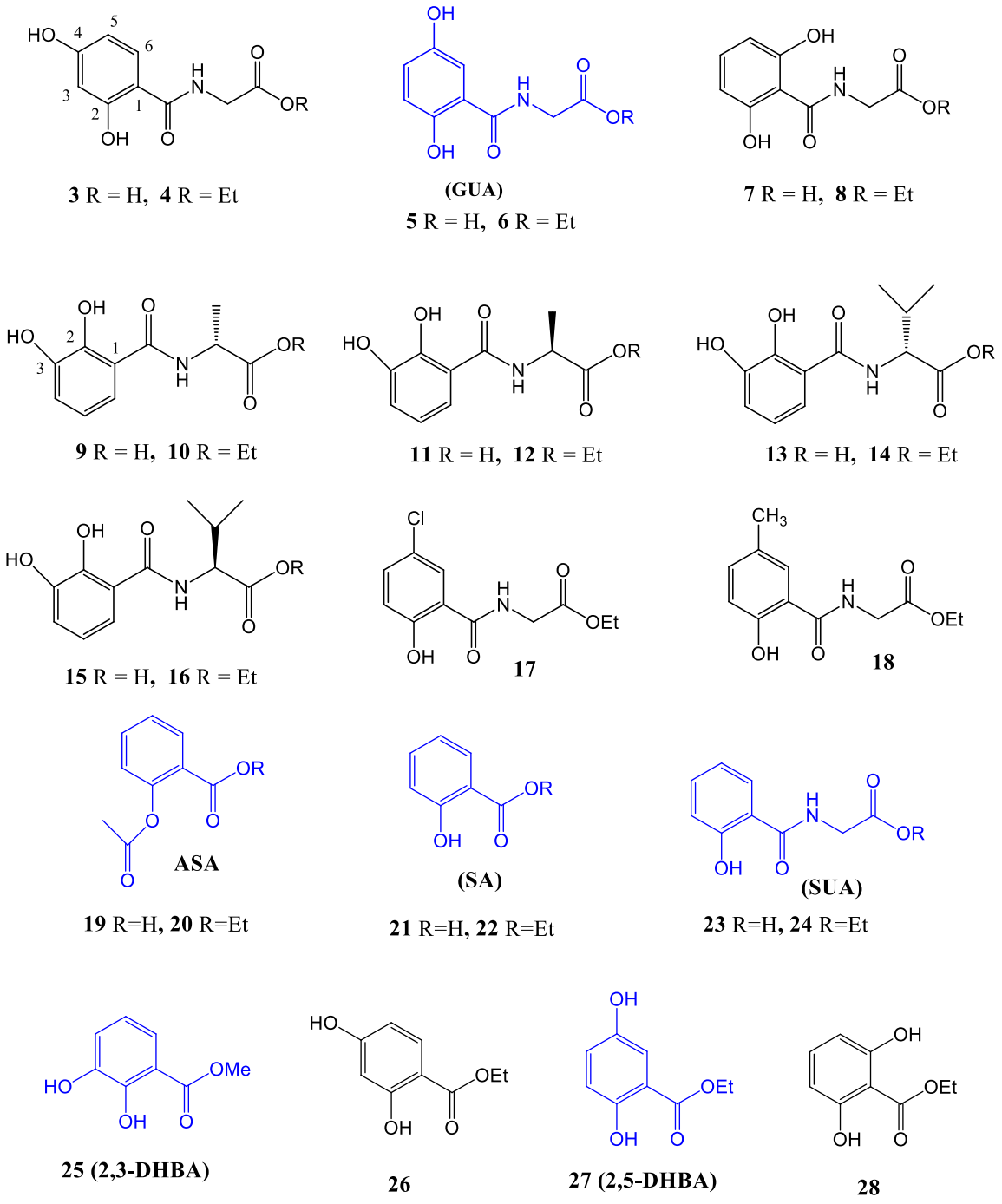


Figure 7.6: The structures of DHBG and salicylate derivatives tested in the *in vitro* and cell-based assays. Structures in blue indicate the corresponding acids are aspirin metabolites (see introduction). (Compounds **3-8**, **17-18**, **23-24** were synthesized by Dr A. Conejo-Garcia; compounds **9-16** were synthesised by Dr Esther C.Y. Woon; other compounds were from Sigma)

Interestingly, a glycine side-chain was not required for the observed HIF-α suppression effects. Compounds with a D/L-alanine (**10**, **12**) or D/L-valine (**14**, **16**) side-chain were all found to display concentration-dependent dichotomous effects similar to DHBG. At 0.2 mM, the D/L- alanine and D/L-valine derivatives substantially inhibited prolyl hydroxylation in RCC4 cells (**Fig. 7.7 C**), and induced HIF-1α accumulation in RCC4/VHL cells (**Fig. 7.7 D**); while at 1.0 mM, they promoted HIF-1α suppression in both cells. On the other hand, the compounds were also shown to moderately inhibit the Asn803 hydroxylation in RCC4 cells. The IC_{50} values of the corresponding free acids (**9**, **11**, **13**, **15**) for PHD2 were later determined using the AlphaScreen PHD2 hydroxylation assay (**Table 7.1**) described in **Chapter 2.** The PHD2 hydroxylation assays were carried out by Andrew M. C. Chan.

In keeping with the cell-based data, the D/L- alanine and valine derivatives (**9**, **11**, **13**, **15**) inhibited the purified PHD2 with IC_{50} values ranging from 20 – 90 μM (**Table 7.1**). The inhibition by the D-alanine and D/L-valine derivatives (**9**, **13**, **15**) was rather unexpected because the corresponding *N*-oxalylglycine (NOG) and bicyclic isoquinoline compound (BIQ) analogues were shown to be ineffective in inhibiting PHDs activity (see **Chapter 2 Section 2.2.3.1**). The results suggest that these DHBG derivatives may inhibit PHD via a different inhibition mode.

Given that the glycine side-chain was not required for the observed HIF-1α suppression effects, it was considered that aspirin (ASA, **19**, **Fig. 7.6**) and other salicylate derivatives (**20-28**, **Fig. 7.6**) (especially the 2,3- and 2,5-dihydroxybenzoate derivatives (**25**, **27**)) may exhibit similar effects. Therefore, these compounds were then tested in the cell-based assays. Compared to DHBG and GUA which substantially suppressed the HIF-1α levels in RCC4 cells, the salicylates **19-28** exhibited little or almost no effects, at least at the tested concentrations (0.2 and 1 mM) (**Fig. 7.7 F** and **G**). Interestingly, the major aspirin metabolite salicylurate (SUA, **24**) moderately reduced the HIF-1α level at high concentration (2 mM) (**Fig. 7.7 F**, lane 14). It is possible that SUA (**24**) was metabolised to DHBG or GUA by the enzymatic reactions of oxidases in the cells (**Section 7.1.4** and **Fig. 7.3**).

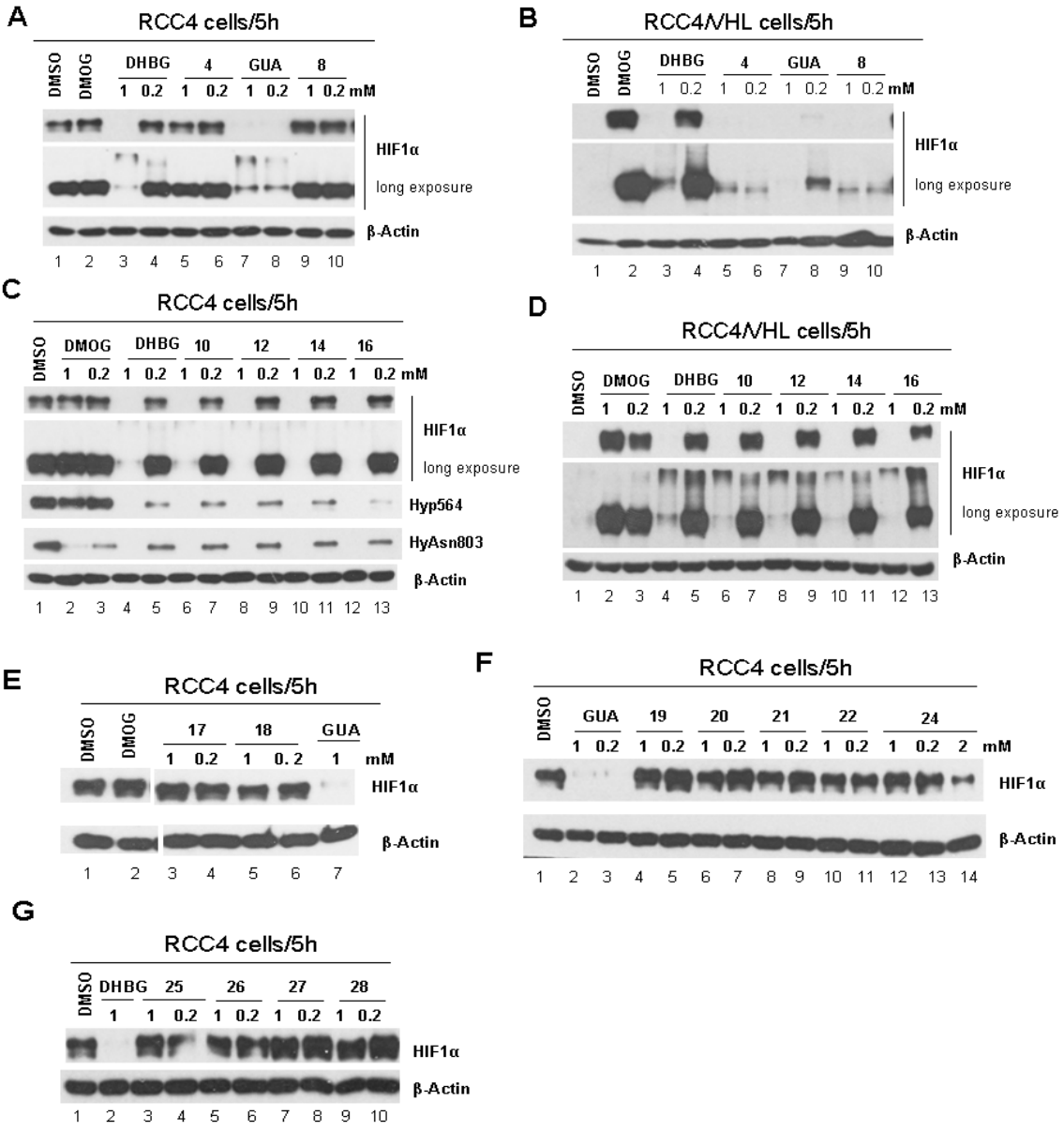


Figure 7.7: (**A**, **C**, **E-G**) The effects of DHBG and salicylate derivatives on HIF-1α levels in RCC4 cells. (**B**, **D**) The dichotomous effects of DHBG derivatives on HIF-1α levels in RCC4/VHL cells. Dimethyloxalygylcine (DMOG) (1 mM or at indicated concentration) was used as controls.

Compound no.	PHD2 IC_{50} (μM)	Compound no.	PHD2 IC_{50} (μM)
NOG	4.6	**BIQ**	1.4
DHBG (1)	18.4	**9**	19.1
3	> 1000	**11**	64.6
GUA (5)	598	**13**	90.1
7	> 1000	**15**	48.2

Table 7.1: The IC_{50} values of the DHBG derivatives (acids) obtained using the AlphaScreen PHD2 hydroxylation assays. IC_{50} values of *N*-oxalylglycine (NOG) and bicylic isoquinoline compound (BIQ) obtained from the same assay were shown for comparison. (Data obtained from Andrew M. C. Chan).

7.3.2 Concentration-dependent effects of DHBG and GUA

The aspirin metabolites DHBG and GUA were identified as potent HIF-1α inhibitors in the above cell-based assays. The work then further investigated their concentration-dependent effects on HIF-1α suppression. For this purpose, DHBG (**2**) and GUA (**6**) were incubated in RCC4 cells at various concentrations and times (**Fig. 7.8**). Immunoblots in **Fig. 7.8 A** and **B** clearly show that DHBG gradually suppressed HIF-1α levels at increased concentrations; high concentrations (> 0.5 mM) are required to achieve complete suppression in 5 h in both RCC4 and RCC4/VHL cells.

Gradual decrease of HIF-1α levels was demonstrated by RCC4 cells treated with 1 mM DHBG over time. Complete (or close to complete) suppression was achieved at approximately 2 h (**Fig. 7.8 C**, lane 10). Previous reports showed that HIF-1α protein in RCC4 cells was still clearly detected after 3 h of cycloheximide (100 μg/ml) (a biosynthesis inhibitor) treatment and HIF-1α half-life in RCC4 cells has been estimated at the region of 1 h.[142, 346] On the other hand, concentrations lower than 100 μM of DHBG were shown to be ineffective in suppressing HIF-1α levels even over 24 h of incubation time (**Fig. 7.8 D**).

It is interesting to note that the extent of formation of the slow-mobility HIF-1α species in DHBG treated in RCC4/VHL cells is much more abundant than in RCC4 cells (**Fig. 7.8 A** and **B**), which may suggest the HIF-1α suppression effects in these cells involves different *in vivo* mechanisms. This observation strongly suggests the mechanism involved in the VHL-competent cells may utilise the VHL-ubiquitination proteasomal degradation pathway.

GUA was shown to be a more potent HIF-1α suppressor than DHBG at low concentrations. Substantial suppression was achieved at GUA concentrations of ~ 0.2 mM in 5 h. Lower concentrations of GUA were shown to be less effective on suppressing HIF-1α at this time point (**Fig. 7.8 C**). In cells exposed to GUA for 24 h, 100 μM (but not lower than 50 μM) of the compound was found to substantially suppress the HIF-1α levels (**Fig. 7.8 D**). Concentrations higher than 100 μM of DHBG and GUA were observed to cause severe morphological changes in cells in 24 h, which indicate toxic effects.

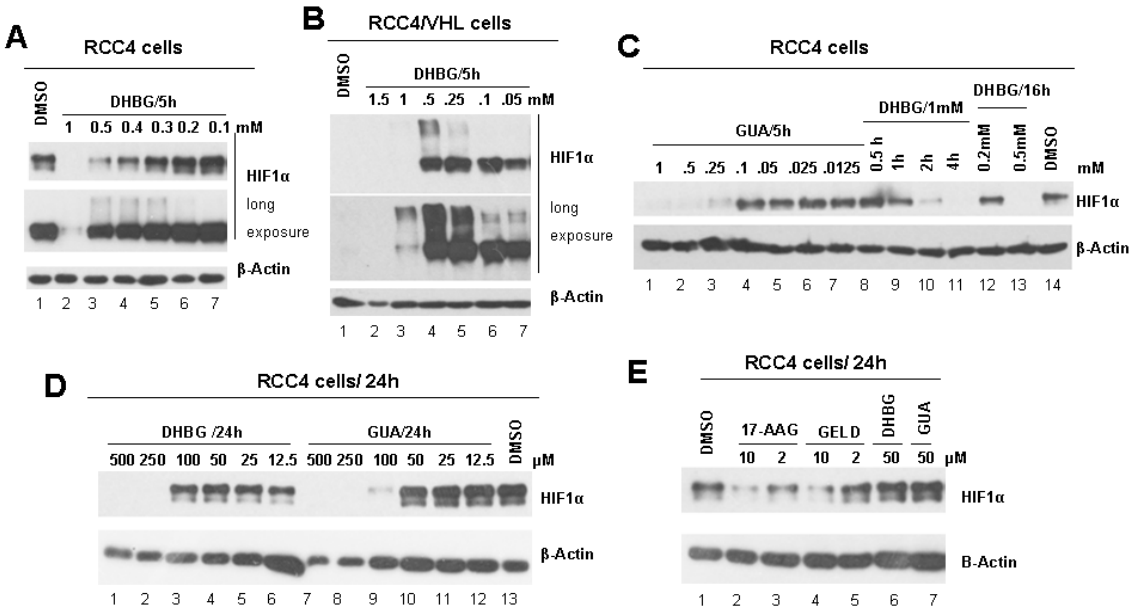


Figure 7.8: Concentration and time-dependent effects of DHBG and GUA. (**A-D**) DHBG and GUA were treated at indicated concentrations and times in RCC4 or RCC4/VHL cells. (**E**) The potencies of DHBG and GUA were compared to the Hsp90 inhibitors 17-allylaminogeldamycin (17-AAG) and geldamycin (GELD).

7.3.3 DHBG and GUA are ineffective Hsp90 inhibitors *in vitro*

The molecular chaperone heat shock protein 90 (Hsp90) is one of the most abundant proteins expressed in cells. Hsp90 is important in maintaining the conformation, stability and function of a large numbers of client proteins, many of which are key oncogenic proteins including HIF-1α.[347] Inhibition of Hsp90 has been reported to lead to O_2/VHL-independent HIF-1α degradation in RCC4 cells by promoting the binding of the receptor of activated protein kinase C (RACK1) to HIF-1α.[348] RACK1 recruits Elongin-C and other components of E3 ligase complex, in a manner mechanistically similar to pVHL, which eventually leads to ubiquitination and proteasomal degradation of HIF-1α[348](**Fig. 7.9**). On the other hand, the Copper Metabolism MURR1 Domain 1 protein (COMMD1) has also been associated with promotion of O_2/VHL/ubiquitin-independent proteolysis of HIF-1α by competition with Hsp90.[349]

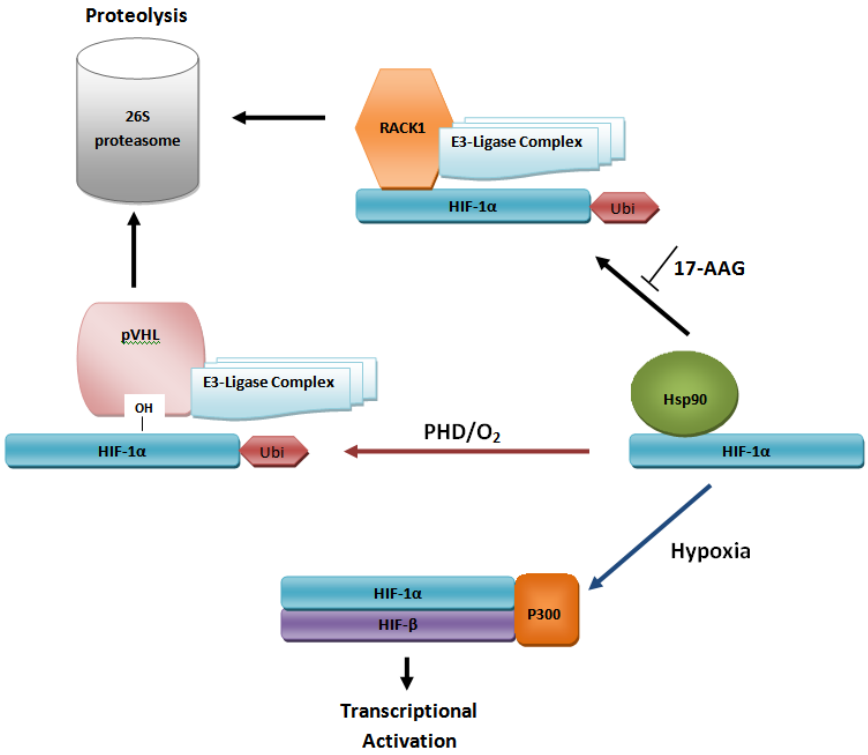


Figure 7.9: Receptor of activated protein kinase C (RACK1) is a crucial component of the O_2/VHL-independent HIF-1α proteasomal degradation pathway. RACK1 regulates HIF-1α stability through competition with Hsp90, and recruitment of E3-ligase-ubiquitin complex. Inhibition of Hsp90 promotes RACK1 binding to HIF-1α, therefore promotes HIF-1α degradation.[348]

17-Allylaminogeldamycin (17-AAG) and geldamycin (**Fig. 7.10**) are commonly used as Hsp90 inhibitors and have been reported to induce HIF-1α degradation in RCC4 cells.[348-350] The potencies of DHBG and GUA on HIF-1α suppression were then compared to 17-AAG and geldamycin in RCC4 cells (**Fig 7.8 E**). The results demonstrate substantial HIF-1α suppression for the 17-AAG and geldamycin treated cells at 10 μM for 24 h, indicating that DHBG and GUA were at least 10 times less potent in this regard (compare **Fig. 7.8 D** and **E**). (17-AAG and geldamycin at high doses (> 100 μM) and short incubation times were found to be ineffective in HIF-1α suppression and toxic to the cells (data not shown).)

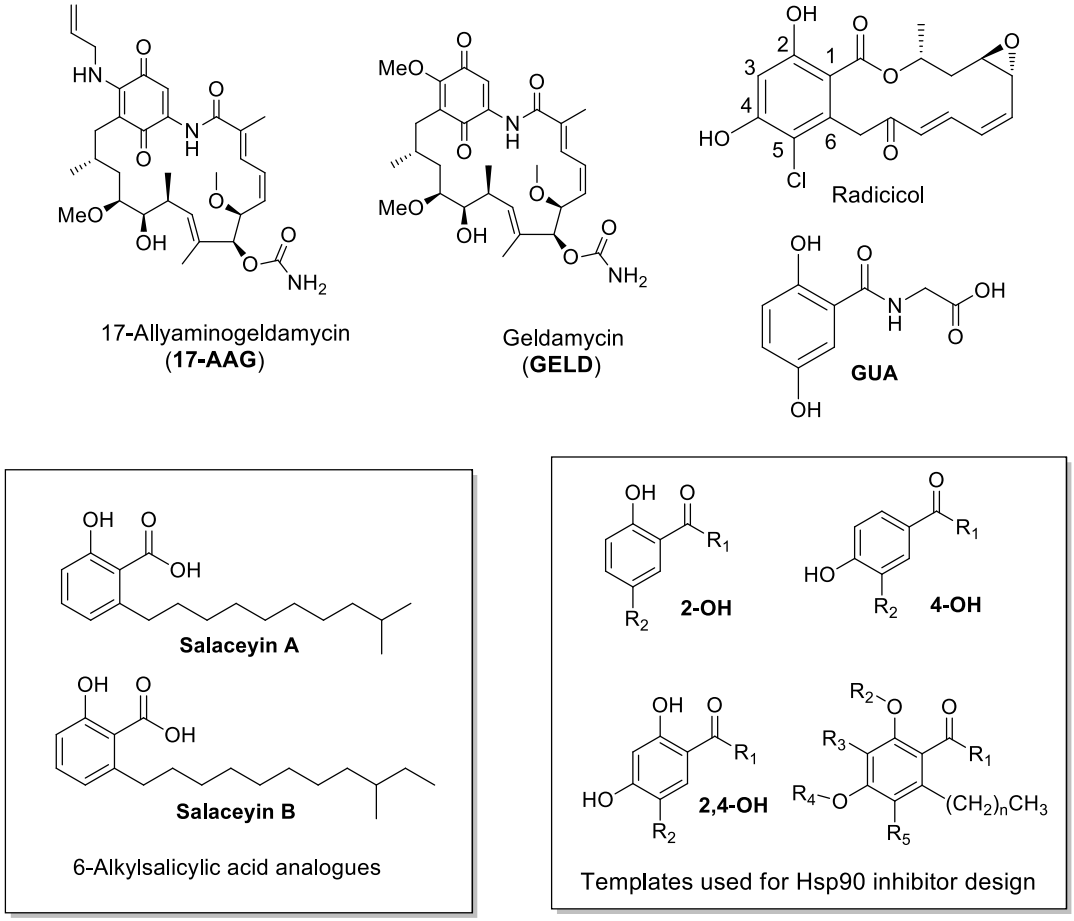


Figure 7.10: Structures of Hsp90 inhibitors and benzoic acid scaffolds used for inhibitor design. Structure of GUA is shown for comparison.

The Hsp90 chaperone cycle consists of turnover of ATP to ADP through an intrinsic ATPase activity associated with the *N*-terminal domain of Hsp90.[351] Inhibition of Hsp90 has been shown to lead to destabilisation of its client proteins (e.g. HIF-1α).[352] Crystallographic studies revealed that most of the inhibitors including 17-AAG, geldamycin, and radicicol (**Fig. 7.10**) inhibit Hsp90 by binding to its ATP binding site.[280, 351, 353]

Recently, two 6-alkylsalicylic acid analogues, salaceyin A and salaceyin B (**Fig. 7.10**) (natural products extracted from *Streptomyces*), have been identified as Hsp90 inhibitors with IC_{50} values of 68.3 and 65.2 μM, respectively.[354] Furthermore, benzoic acid and salicylic acid scaffolds have also been widely used for Hsp90 inhibitor design (**Fig. 7.10**).[355-357] Given the structural similarities of DHBG and GUA to the Hsp90 inhibitors, and their similar effects on promoting VHL-independent HIF-1α suppression, it was considered that the DHBG and GUA mechanisms of action may involve Hsp90 inhibition.

To investigate the above proposal, the work next sought to investigate the binding potencies of DHBG and GUA (and other salicylates) to Hsp90 using thermal shift protein assay (Hsp90 preparation and thermal shift experiments were carried out by Dr E. P. Williams).[355] In this assay, Hsp90 protein solution (*i.e.* full-length Hsp90 (2 μM) in 10 mM HEPES buffer at pH 7.5) was heated at a constant rate in the presence or absence of a ligand (compound was added to the protein solution at 10 μM final concentration), and the denaturing process was then monitored by fluorescence. Ligand binding normally leads to stabilisation (sometimes destabilistation) of the protein which results in higher denaturation temperature T_m in the termal shift assay (as shown in **Fig. 7.11**).[358]

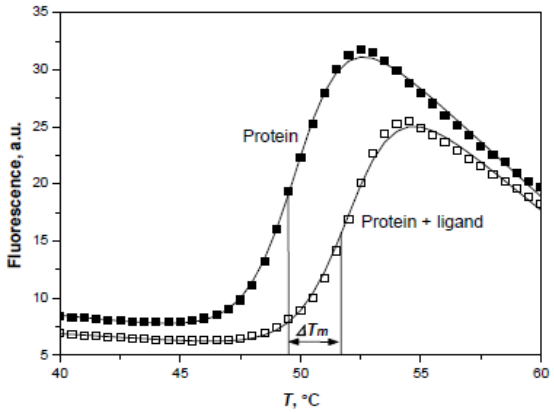


Figure 7.11: Thermal shift assay (Hsp90) protein melting curves. The midpoint of denaturation (T_m) is shifted to higher temperature upon ligand binding. Figure adapted from Petrikaite *et. al*.[358]

The results of the Hsp90 thermal shift assay are shown in **Fig. 7.12**. The rise of fluorescence close to 50°C (**Fig. 7.12**) indicated the protein unfolding and the binding of the fluorescent compound (*i.e.* 8-anilinonaphthalene-1-sulfonate) to the hydrophobic patches of the Hsp90 interior.[358] Addition of 17-AAG (positive control) was shown to shift the midpoint of denaturation (T_m) by about 6°C, however, neither DHBG (**1**) nor its ethyl ester (**2**) or GUA (**5**) or other salicylate derivatives (**2**, **3**, **18**, **19**, **21**, **23**, **24**) were demonstrated to have any effect on the unfolding processes of Hsp90 (**Fig. 7.12**) (*i.e.* causing no significant shift in T_m). The thermal shift results therefore indicate that the salicylate derivatives may not be effective Hsp90 ligands/inhibitors. However, negative thermal shift assay results do not always indicate a lack of ligand binding.

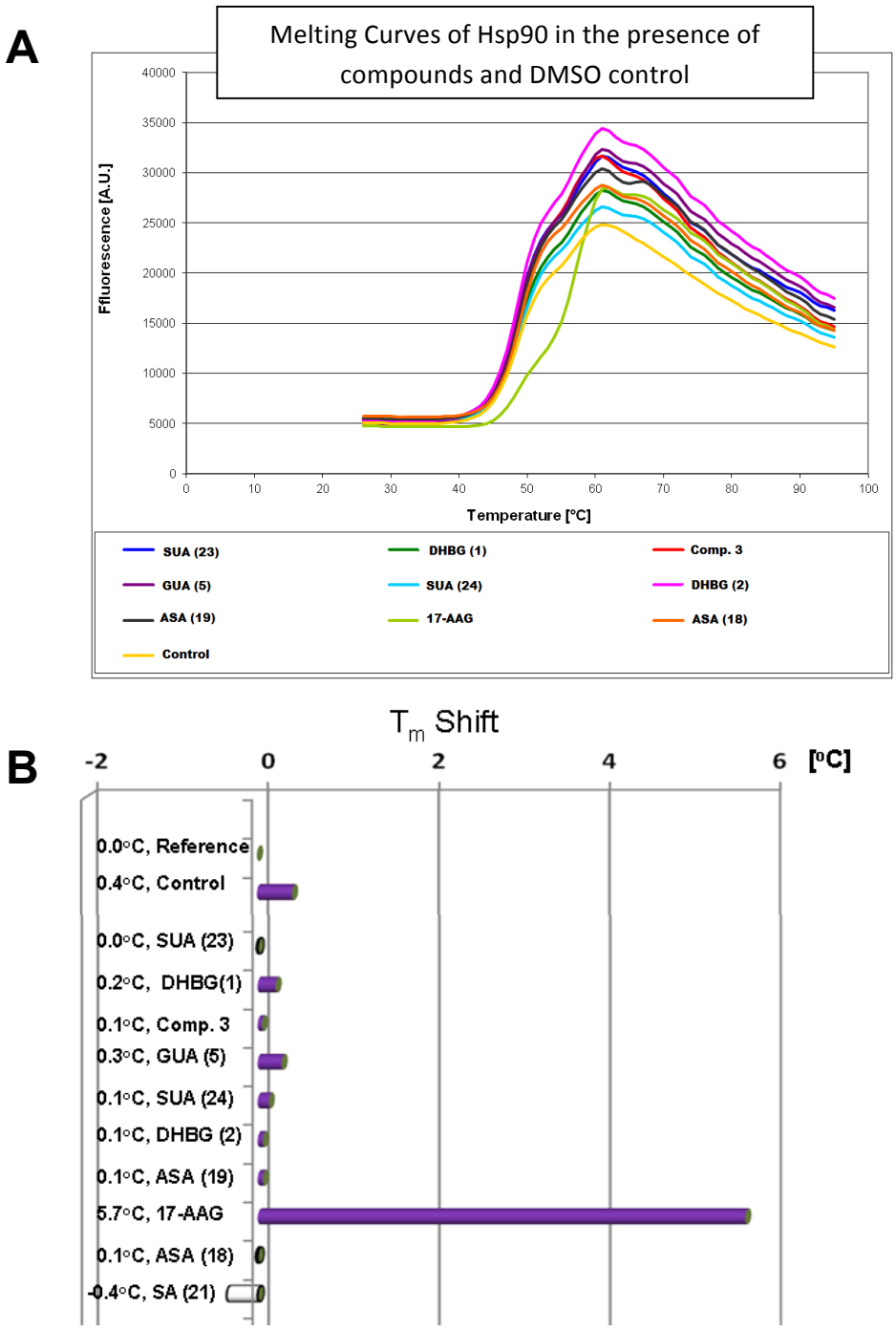


Figure 7.12: The results from the thermal shift assay suggest that the salicylate derivatives may be ineffective ligands of Hsp90 (at least judging by this assay). (**A**) Hsp90 melting curves in the presence of compounds or DMSO control. (**B**) Graphic representation of T_m shift data in experiments (**A**). (Data obtained from Dr E. P. Williams) .

To further investigate this, the compounds were characterised according to competition for the Hsp90 ATPase site using nuclear magnetic resonance (NMR) water-LOGSY (water-Ligand Observed via Gradient SpectroscopY) method based on the reported protocols[356] (experiments were carried out by Ivanhoe K. H. Leung). The competition experiments were carried out in the presence of ADP (**Fig. 7.13**), which binds weakly to the ATPase site of Hsp90 under the screening conditions (*i.e.* 10 μM Hsp90; 200 μM ADP; 1 mM compound; 50 mM Tris-D11; 150 mM NaCl; pH 8.0; 95% H_2O + 5% D_2O (<1% DMSO) at 280 K). A compound that binds to the nucleotide binding site (therefore causing displacement of ADP) would be reflected in the reduction of the ADP water-LOGSY signal. In the water-LOGSY experiments, the large bulk water magnetisation is partially transferred via the protein-ligand complex to the free ligand in a selective manner. The resonance of the non-binding compound appears with opposite sign and tends to be weaker than those of the binding compound in the NMR spectrum (**Fig. 7.14**).[275, 359] The results of the ADP competition experiments in the presence of 5-fold excess of the salicylates are summarised in **Table 7.2**.

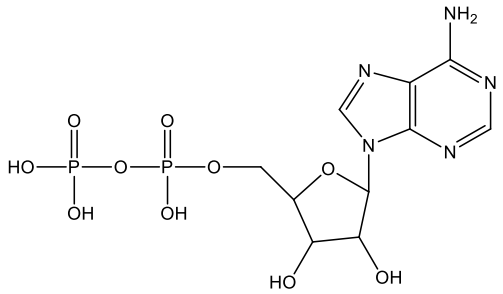


Figure 7.13: The structure of adenosine diphosphate (ADP).

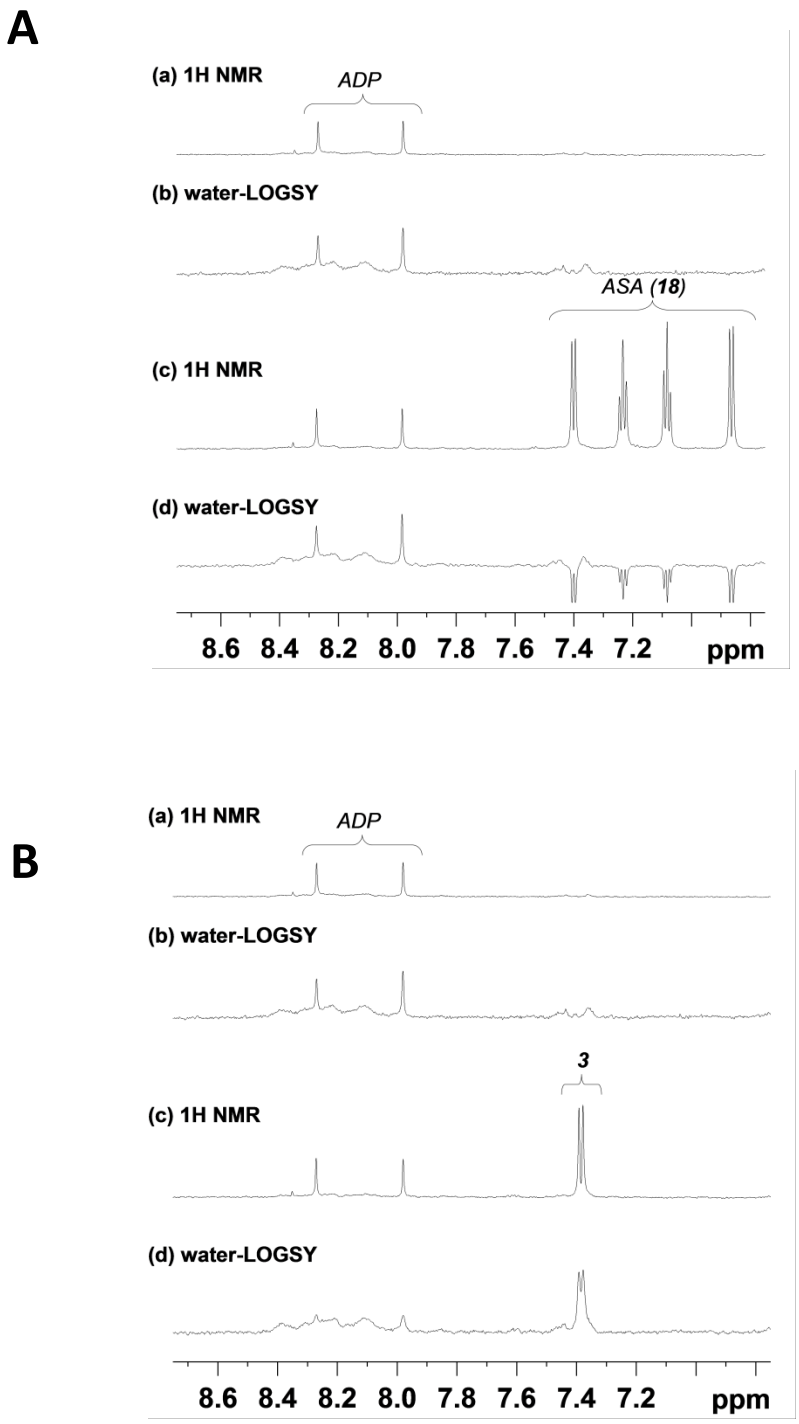


Figure 7.14: (**A**) and (**B**) show examples of the NMR spectra of the Hsp90 water-LOGSY ADP competition experiments in the presence of salicylates. Assay conditions: 10 µM Hsp90; 200 µM ADP; 1 mM compound; 50 mM Tris-D11; 150 mM NaCl; pH 8.0; 95% H_2O + 5% D_2O (<1% DMSO) at 280 K. In the water-LOGSY NMR experiments, resonance of a non-binding compound (ASA (**18**), **A**) appears with opposite sign in comparison to binding compound (2,4-dihydroxybenzoylglycine (**3**), (**B**)). Compound **3** substantially competed with ADP to bind to the ATPase binding domain of Hsp90 (reflected by the reduction of the ADP water-LOGSY signal). The NMR peaks are corresponding to the aromatic hydrogens of the ADP and the salicylates (only NMR peaks at the region of 7.0- 8.7 ppm are shown).

Consistent with the thermal shift data, most of the tested salicylates show weak binding to the Hsp90 ATPase domain, with the exception of 2,4-dihydroxybenzoylglycine (**3**) which substantially displaced the ADP (42 ± 2.8% reduction of ADP waterLOGSY signal, n = 3 and with a dissociation constant K_D ~ 1.2 mM). DHBG (**1**) was only found to weakly substitute the active site ADP (11.3 ± 7.6% reduction of ADP waterLOGSY signal remaining, n =3). All other salicylates including GUA (**5**) and the D/L- alanyl and -valinyl derivatives (**9**, **11**, **14**, **15**) which substantially suppress HIF-1α levels in the cells show little change (< 5%, n = 1) in the ADP waterLOGSY signal.

Compound	Binding to Hsp90 ATPase domain	Compound	Binding to Hsp90 ATPase domain
17-AAG	Strong (K_D = 0.3 μM)[a]	**13**	Weak/No
DHBG (**1**)	Weak	**15**	Weak/No
DHBG (**2**)	Weak/No	ASA (**18**)	Weak/No
3	Moderate (K_D ~ 1.2 mM)	ASA (**19**)	Weak/No
GUA (**5**)	Weak/No	SA (**21**)	Weak/No
9	Weak/No	SUA (**23**)	Weak/No
11	Weak/No	SUA (**24**)	Weak/No

Table 7.2: Summary of the Hsp90 water-LOGSY ADP competition assay results. Assay conditions: 10 μM HSP90; 200 μM ADP; 1 mM compound; 50 mM Tris-D11; 150 mM NaCl; pH 8.0; 95% H_2O + 5% D_2O (<1% DMSO) at 280 K. [a] K_D of 17-AAG was obtained from reported value in Zurawska *et al.*[360]

The weak binding of 2,4-dihydroxybenzoylglycine (**3**) to the Hsp90 ATPase binding site is not entirely unexpected as the natural product radicicol and a number of synthetic Hsp90 inhibitors[355, 356] contain the 2,4-OH benzoic acid scaffold (**Fig. 7.10**), whereas 2,3- and 2,5-OH benzoic acid analogues have not been reported (to date) as Hsp90 inhibitors. Interestingly, in this study, compound **3** (**4**) was not shown to suppress HIF-1α in the cells, whereas DHBG and GUA (with the 2,3- and 2,5-OH benzoic acid scaffolds, respectively) were shown to be potent HIF-1α inhibitors (**Fig. 7.7**).

In conclusion, the thermal shift and water-LOGSY results indicate that DHBG and GUA are probably ineffective inhibitors for Hsp90, suggesting that DHBG and GUA-mediated HIF-1α suppression effects may not involve the Hsp90 pathway.

7.3.4 HIF-1α degradation or modification?

The nonsteroidal anti-inflammatory drugs (NSAIDs) including indomethacin[361] and sodium salicylate (a metabolite of aspirin)[362] have been shown to inhibit angiogenesis by increasing VHL expression (through an unknown mechanism) and thus downregulating HIF-1α and VEGF in hypoxia-induced VHL-competent cancer cell-lines. Both the O_2/VHL-dependent (*i.e.* dependent on prolyl hydroxylation state of HIF-1α) and O_2/VHL-independent (e.g. RACK-1 mediated) HIF-1α degradation pathways involve the actions of 26S proteasome (**Fig. 7.9**).[12, 348, 349] It was considered that if the aspirin metabolites DHBG and GUA suppress HIF-1α by promoting its degradation, inhibiting the proteasome activity could substantially reduce the drug effects.

To study the above hypothesis, cells were treated with DHBG/GUA in the presence or absence of a proteasome inhibitor (*i.e.* MG132 (25 μM) (a potent and specific inhibitor to 26S proteasome, K_i 4 nM)[363, 364] or ALLnL (25 μM) (a general proteasome inhibitor; K_i value of 670 nM for 26S proteasome)[363, 365] (**Fig. 7.15 A-C**). Surprisingly, the results shown blocking the proteasomal degradation pathways did not significantly affect the HIF-1α suppression effects of DHBG and GUA. The compounds were shown to substantially reduce the HIF-1α levels in the presence of proteasome inhibitor in both RCC4 and RCC4/VHL cell-lines (**Fig. 7.15 A-C**).

DHBG also demonstrated similar suppression effects on HIF-2α accumulation in RCC4 cells (**Fig. 7.15 D**). Furthermore, the DHBG and GUA were shown to substantially suppress the HIF-1α levels in a PHD null mouse embryonic fibroblast (MEF) cell-line (HIF-1α was constitutively activated in this cell-line due to the lack of PHD activity) (**Fig.**

7.15 E), which further suggests the compounds' suppression effects are PHD-independent (and therefore independent of prolyl hydroxylation state of HIF-1α).

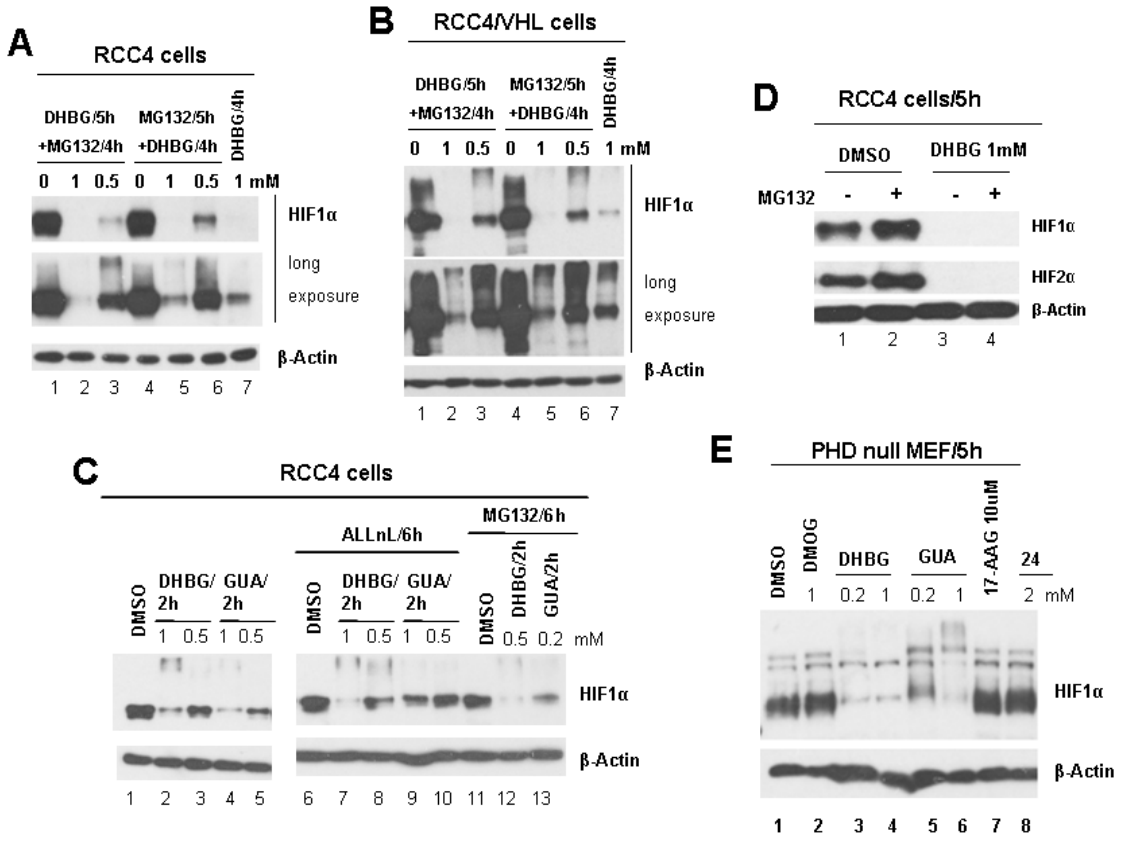


Figure 7.15: (**A**-**D**) DHBG and GUA suppressed HIF-α levels in the presence of proteasome inhibitor. RCC4 or RCC4/VHL cells were either pretreated with the proteasome inhibitor or DHBG/GUA at indicated times. (**E**) DHBG (1 mM) and GUA (1 mM) substantially suppressed HIF-1α levels in the PHD null mouse embryonic fibroblast cells (PHD null MEF). ALLnL, *N*-acetyl leucyl-leucyl norlucinal.

It has been reported that the RACK-1 mediated HIF-1α degradation pathway (through Hsp90 inhibition, see **Fig. 7.9**) involves binding of RACK-1 to the PAS-A domain of HIF-1α. The loss of function of RACK-1 abolished HIF-1α degradation.[348] It was considered that if the suppression effects of DHBG and GUA on HIF-1α involved the action of RACK-1 (and therefore Hsp90), the suppression effects would at least be reduced in cell-lines expressing a truncated version of HIF-1α without the PAS domain. For this purpose, DHBG and GUA suppression effects were investigated using the Clone3 human osteosarcoma (C3 U2OS) stable cell-line.[183] In this cell-line, truncated

HIF-1α protein (residues 344-826, without the PAS domain) was heterologously expressed under the control of a doxycyline-inducible promoter. The effects of this was then compared to the results obtained using WT4 U2OS stable cell-line[142] with doxycyline-inducible wild-type (full length) HIF-1α.

The C3 and WT4 U2OS cell-lines were first induced with doxycyline at indicated doses 24 h prior to compound treatments (5 h). The doxycyline-induced controls clearly demonstrated higher levels of HIF-1α compared to the untreated controls (**Fig 7. 16 A,** lanes 2 and 8). Interestingly, in the absence of the HIF-1α PAS domain (C3 U2OS cell-line) which is crucial for the interaction of HIF-1α and RACK-1, DHBG at 1 mM still strongly suppressed the accumulation of the inducible truncated HIF-1α, in a manner similar to the inducible full-length HIF-1α (WT4 U2OS cell-line) (**Fig. 7.16 A,** compare lanes 3 and 9). This result further suggests that DHBG suppression effects may not directly involve Hsp90-RACK-1 pathway, in keeping with the *in vitro* results which demonstrated that DHBG and GUA are ineffective Hsp90 inhibitors.

Consistent with the RCC4/VHL results which demonstrated DHBG dichotomous effect, DHBG (at 0.2 mM) was shown to elevate the HIF-1α levels in both C3 and WT4 U2OS cell-lines (**Fig. 7.16 A**, lanes 4 and 10). GUA at both tested concentrations (0.2 and 1 mM) was also found to moderately suppress the inducible HIF-1α levels in both the U2OS cell-lines.

The effects of DHBG and GUA were further studied in the PHD inhibitor treated (*i.e.* DMOG (general) and BIQ (specific), **Chapter 2**) and hypoxia treated wild-type U2OS cells. Wild-type U2OS cells were pre-incubated in the presence of PHD inhibitor (1 mM) or hypoxia (1% oxygen), DHBG (1 mM) and GUA (1 mM) were later added at the indicated times (**Fig. 7.16 B**). (MG132 treated samples (**Fig. 7.16 B**, lanes 8-10) were shown for comparison). Both DHBG and GUA were found to substantially suppress the PHD inhibitor-induced HIF-1α accumulation in U2OS cells, however, to a lesser extent for the latter (**Fig. 7.16 B**). These results further support the observations in the PHD null

cells (**Fig. 7.15 E**) which shown the DHBG and GUA suppression effects are largely independent of the prolyl hydroxylation state of HIF-1α in VHL-competent cells.

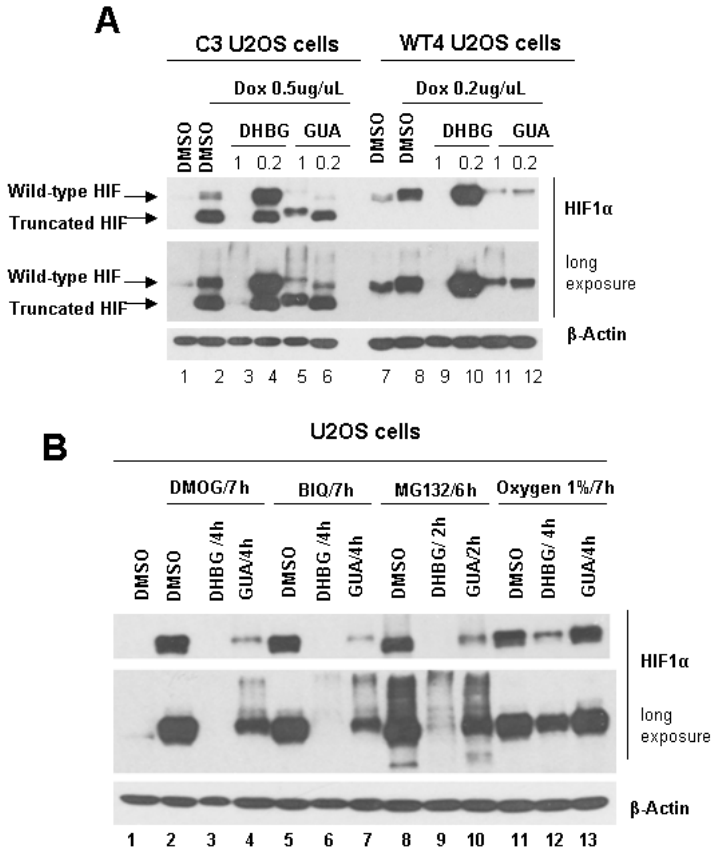


Figure 7.16: (**A**) DHBG (1 mM) significantly suppressed the doxycyline-inducible truncated (residues344-826, without the PAS-domain) and full-length HIF-1α in these modified U2OS cells. (**B**) DHBG (1 mM) and GUA (1 mM) substantially suppressed the PHD inhibitor-induced HIF-1α levels, whereas their effects are partially abolished at low oxygen availability. DMOG, dimethyloxalylglycine; BIQ, bicyclic isoquinoline compound.

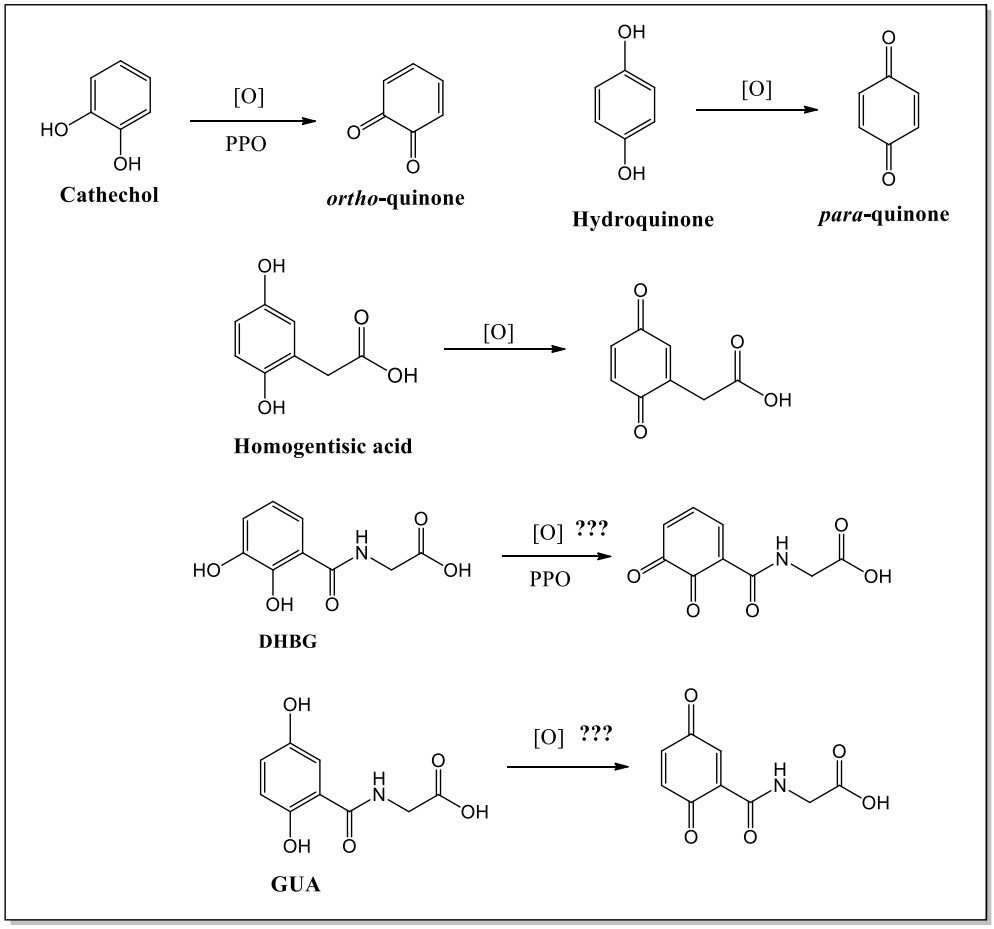
Interestingly, hypoxia (1% oxygen) treatment was observed to partially abolish the HIF-1α suppression effect of DHBG, whereas in the case of GUA, its suppression effect was almost completely ablated (**Fig. 7.16 B**, compare lanes 11, 12 and 13, long exposure film). As it was shown above (in PHD null cells (**Fig. 7.15 E**) and in PHD inhibitor treated cells (**Fig. 7.16 B**)), the hydroxylation state did not significantly affect the HIF-1α suppression; the partial loss of the compound's functions at low oxygen levels is therefore expected to be attributed to the intrinsic chemical nature of the compounds.

DHBG is a catechol (2-hydroxyphenol) derivative which has been shown to undergo auto-oxidation to form its corresponding *ortho*-quinone under atmospheric oxygen levels ($t_{½}$ = 9 hr)[366] (**Fig. 7.17**). In cells, catechol oxidation is reported to be accelerated in the presence of polyphenol oxidase (PPO) (*i.e.* tyrosinase or catechol oxidase), a copper-containing enzyme found in plants and animals and known to catalyse the conversion of phenols and catechols to quinones using molecular oxygen (dioxygen) (**Fig. 7.17**).[366-369]

GUA which contains a hydroquinone (4-hydroxyphenol) scaffold is also expected to be highly susceptible to oxidation (**Fig. 7.17**).[370] The proposal is supported by the observation of the naturally occurring hydroquinone metabolite, homogentisic acid (a key component in the development of inflammatory arthritis disorder). Homogentisic acid has been reported to undergo rapid auto-oxidation to produce its corresponding *para*-quinone under physiological conditions, in an oxygen dependent manner (**Fig. 7.17**).[371] In addition, the oxidation reaction generates oxygen radicals, superoxide, and hydrogen peroxide (**Fig. 7.17**, lower panel); these reactive oxygen species (ROS) have also been shown to have a regulatory role in the HIF pathway.[30, 372]

Quinones are both biological active and highly susceptible to modifications in physiological systems. A large number of nucleophilic amino acid residues including cysteines, lysines, and histidines can react with quinones leading to protein covalent modifications (**Fig. 7.18**).[366, 373, 374] Both the enzymatic or auto-oxidation of DHBG and GUA require molecular oxygen, and their suppression effects are largely reduced at low oxygen availability. It was proposed that the mechanisms of action of these aspirin metabolites may involve their conversion to quinones. This subsequently leads to protein modifications and results in HIF-1α suppression. This hypothesis is further supported by the observations that only the 2,3- and 2,5-OH DHBG derivatives (*i.e.* **2**, **6**, **10**, **12**, **14**, **16**) which bear a reactive catechol or hydroquinone scaffold (and are therefore susceptible to be converted to *ortho*- and *para*-quionones), but not the 2,4- or 2,6-OH DHBG derivatives (*i.e.* **4**, **8**) which bear a stable resorcinol (3-hydroxyphenol) scaffold, are active in the cells (**Fig. 7.7**).

It is also worth noting that some protein modifications may lead to protein aggregation which results in insoluble complexes that cannot be separated by SDS PAGE electrophoresis, or cannot be detected by the HIF-1α antibody and therefore leads to false interpretations of immunoblot results.



$$QH_2 + O_2 \rightleftharpoons QH\cdot + O_2^- + H^+ \quad (1)$$

$$QH\cdot + O_2 \rightleftharpoons Q + O_2^- + H^+ \quad (2)$$

$$QH\cdot + QH\cdot \rightleftharpoons QH_2 + Q \quad (3)$$

$$O_2^- + O_2^- + 2H^+ \rightleftharpoons H_2O_2 + O_2 \quad (4)$$

Figure 7.17: Upper panel: the enzymatic reaction or auto-oxidation of catechol and hydroquinone derivatives under physiological conditions, PPO, polyphenol oxidase. Lower panel: reaction schemes of auto-oxidation of hydroquinone. QH_2, $QH\cdot$, and Q represent the three oxidation states of hydroquinone (see discussion in text).

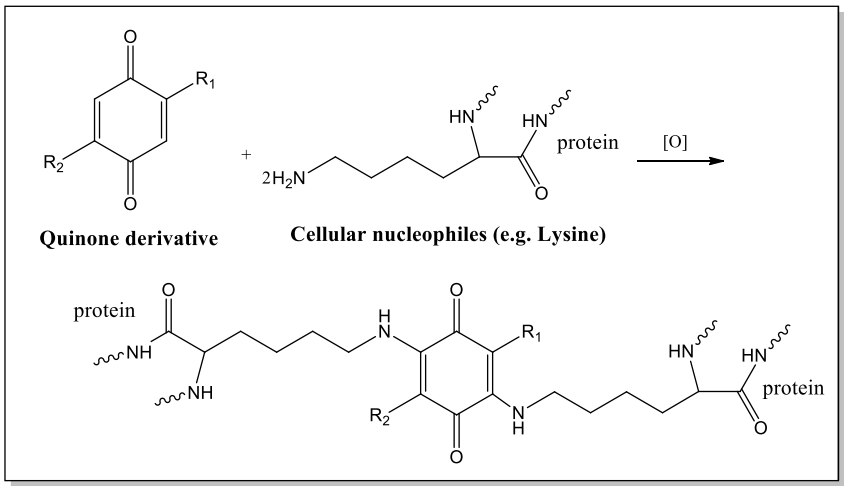


Figure 7.18: Possible protein modification by quinone derivative in the physiological system.

7.3.5 Precursors of DHBG and GUA exhibit HIF-1α suppression effects

In the human body, it seems likely that the oxidation and glycine coupling reactions that lead to the formation of DHBG and GUA take place largely in the liver (the major organ for drug metabolism) (see **Section 7.1.4**).[325, 326] It was thus considered that the oxidation and glycine coupling reactions may occur in hepatic cell-lines. Therefore, it may be possible to observe similar suppression effects by incubating the potential precursors of DHBG and GUA (**Fig. 7.3**) (*i.e.* aspirin (**19**) and its ethyl ester (**20**); and ester derivatives of SUA (**24**), 2,3-DHBA (**25**), and 2,5-DHBA (**27**), **Fig. 7.6**) in human hepatoma (Hep3B) cell-line at higher doses. A human epithelial (Hela) cell-line was used for comparison. The cells were first pretreated with the generic 2OG oxygenase inhibitor DMOG (0.5 mM) to induce HIF-α accumulation, the salicylates were then added at the indicated concentrations and times (**Fig. 7.19 A** and **B**).

Interestingly, aspirin (**20**), SUA (**24**), 2,3-DHBA (**25**), 2,5-DHBA (**27**) substantially suppressed the HIF-1α accumulation induced by DMOG in Hep3B and Hela cell-lines. However, the effects are slightly more prominent in Hep3B which may indicate a better turnover rate of drug metabolism in the Hep3B cell-line. The HIF-1α suppression effects of these precursors might be due to the subsequent formation of DHBG or GUA in the

cells; however, this proposal does not exclude the potential involvements of other mechanisms.

The HIF-1α suppression potencies of the salicylate derivatives (precursors of DHBG and GUA) at 2 mM in both Hep3B and Hela cell-lines were ranked as **27** > **20** > **24** > **25** > **19**. Given that DHBG requires higher concentrations (> 0.5 mM, **Fig. 7.8**) to exhibit its HIF-1α suppression effect, it could be the reason why 2,3-DHBA (**25)** (non-gylcinated precursor of DHBG) was less potent on HIF-1α suppression compared to the precusors of GUA **(20**, **24**, and **27**) which possibly metabolised to GUA in cells (GUA exhibits HIF-1α suppression effect at lower concentrations, **Fig. 7.8**). The ethyl ester analogue of aspirin (**20**) was clearly more potent than its acid (**19**) for HIF-1α suppression, suggesting better cell-permeability of the ester derivative.

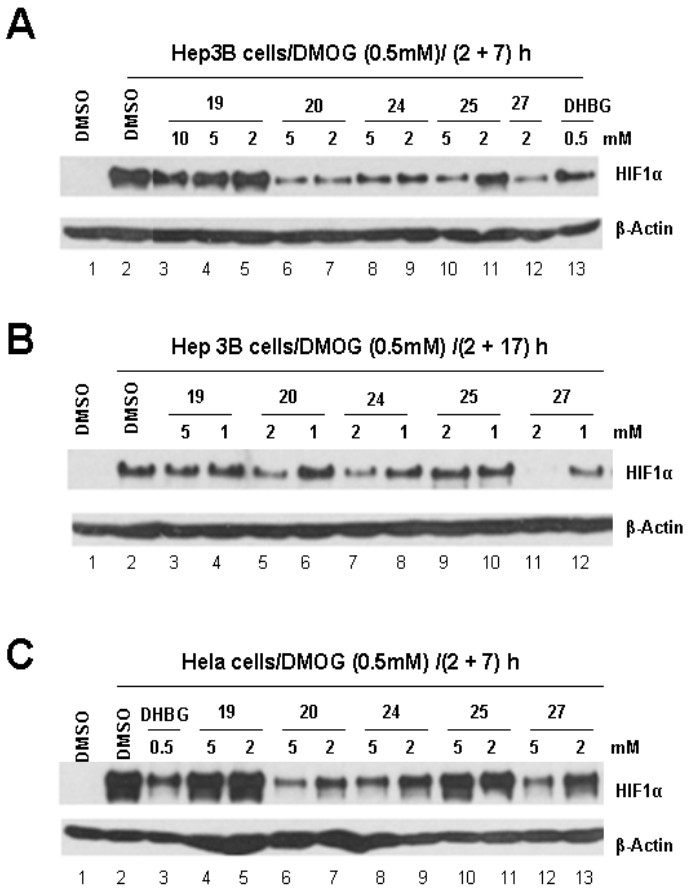


Figure 7.19: The effects of the precursors of DHBG and GUA (**19**, **20**, **24**, **25**, and **27**, see **Fig. 7.6** for structures) in the DMOG-induced HIF-1α accumulation in human hepatoma (Hep3B) and epithelial (Hela) cell-lines.

7.3.6 Effects of DHBG and GUA on HIF-α mRNA expression

Induction of tumour hypoxia and chemotherapy have been commonly used in the treatment of various cancers (e.g hepatocellular carcinoma).[375] Oxygen deprivation arrests cancer progression which leads to cell necrosis and apoptosis;[376] whilst chemo-cytotoxicity of drugs "kills" the cancer cells.[377] Overexpression of HIF-1α (which leads to upregulation of VEGF and multidrug resistance gene (MDR1)) resulting from hypoxia and chemotherapy treatments has been associated with poor tumour response rate to these treatment protocols.[362, 375, 378] Interestingly, high doses of sodium salicylate (5 mM) have been demonstrated to suppress HIF-1α (and VEGF) mRNA and protein expression levels in the hypoxia (by hepatic artery ligation) and chemotherapy drug (*i.e.* cisplatin) treated rat orthotopic hepatoma models.[362] HIF-1α transcriptional blockage achieved by administration of high dosage of sodium salicylate (mechanism unknown) has also been associated with decreased tumour progression and improved therapeutic efficacy of hypoxia and chemotherapy treatments in the rat hepatoma models.[362]

It was considered possible that the HIF-1α transcriptional blockage by sodium salicylate (sodium salt of salicylic acid) may be a direct action of DHBG and/or GUA, given that salicylic acid itself is a potential precursor of DHBG and GUA (**Fig. 7.3**). Therefore, the effects of DHBG and GUA on the mRNA levels of HIF-1α, HIF-2α and several HIF target genes including pyruvate dehydrogenase kinase-1 (PDK1), glucose transporter-1 (GLUT1), carbonic anhydrase-9 (CA9), vascular endothelial growth factor-A (VEGFA), cyclin D1 (CCND1) and transforming growth factor-α (TGFα) were therefore investigated in RCC4 cells.[4, 379-381]

DHBG, GUA and a DMSO control were first incubated in RCC4 cells for 6 h. RNA was extracted from confluent cells using a total RNA isolation reagent (*i.e.* TRI Reagent (Sigma)). The mRNA levels of the targets of interest were then determined by quantitative reverse transcription-polymerase chain reactions (qRT-PCR). The method of log (-ΔCT) was used for quantification calculations and the results are summarised in

Fig. 7.20. (The qRT-PCR experiments were carried out by Dr P. J. Pollard, Centre for Cellular and Molecular Physiology, University of Oxford). Interestingly, DHBG and GUA were shown to demonstrate some differential regulatory effects on the mRNA expression of HIF-1α, HIF-2α and their downstream genes.

Overexpression of HIF-2α has been reported to be relatively more common in RCC4 cells. The pro-tumourigenic genes encoding VEGFA, CCND1, and TGFα, and the glycolitic gene GLUT-1 were shown to be preferentially regulated by HIF-2α RCC4 cells, whereas PDK1 and CA9 were shown to be preferentially regulated by HIF-1α in this cell-line.[346, 382, 383] In contrast, some investigators have reported that HIF-1α does play a predominant role in VEGF secretion in renal cell carcinomas (RCC) expressing both HIF-1α and HIF-2α.[343]

DHBG, which is a PHD inhibitor,[82] was shown to suppress HIF-1α and HIF-2α accumulation in RCC4 cells (**Fig. 7.15 D)**, and demonstrated a concentration-dependent dichotomous effect on HIF-1α regulation in VHL-competent cells (**Fig. 7.5 B**). Surprisingly, the qRT-PCR results show that DHBG moderately elevated the HIF-1α mRNA expression in RCC4 cells despite its HIF-1α suppression effect observed at 0.5 mM (**Fig. 7.8 A**). In contrast, DHBG moderately suppressed the HIF-2α mRNA expression (**Fig. 7.20 A** and **B**). The decrease of HIF-2α mRNA level may be a direct result of increased HIF-1α mRNA and *vice versa*, as these HIF-α isoforms have been demonstrated to display reciprocal suppressive interactions in RCC4 cells.[346, 383]

The above observation may suggest that the HIF-1α stabilisation by DHBG in VHL-competent cells is not solely a result of PHD inhibition, because DHBG can also regulate HIF-1α transcription (*i.e.* mRNA expression). It is possible that DHBG first increased the HIF-1α expression (as observed in the RCC4/VHL cells) and the HIF-1α was subsequently targeted for modification which eventually resulted in HIF-1α suppression.

The suppression effects on HIF-2α by DHBG were also reflected in the downregulation of GLUT1 and TGFα mRNA expression, as HIF-2α has been shown to specifically

regulate these genes in RCC4 cells.[346] Furthermore, DHBG was shown to upregulate the PDK1, CA9, and VEGFA mRNA levels, which are HIF-1α downstream targets. However, the compound did not have any apparent effect on the LDHA and CCND1 mRNA expression (**Fig. 7.20**).

Unlike DHBG, GUA (which is an ineffective HIF-upregulator in VHL-competent cells), displayed no apparent effect on the mRNA expression of HIF-1α and HIF-1α target genes (*i.e.* PDK1, CA9, VEGFA) in RCC4 cells. However, GUA was demonstrated to moderately inhibit the HIF-2α mRNA expression. GUA was also shown to suppress the mRNA expression of its target genes GLUT1 and TGFα to a certain extent and had no apparent effect on LDHA and CCND1 mRNA expression (**Fig. 7.20**). It is also worth noting that the degree of mRNA regulation of a particular gene does not always correlate to its protein synthesis; therefore this point has to be taken into consideration in interpreting the results. For instance, despite having no apparent effect on HIF-1α mRNA levels, the DNA damaging inducing agents campthothecin and mitomycin C have been reported to suppress HIF-1α accumulation by specifically inhibiting HIF-1α protein translation[384]. Therefore, further investigation should be carried out to examine the potential regulatory effects of DHBG and GUA on HIF-1α protein synthesis.

Overall, the results indicate that DHBG and GUA moderately inhibited the HIF-2α, but not HIF-1α, mRNA expression in RCC4 cells. Therefore, the HIF-1α protein suppression effects observed in the cell-based experiments may not be a direct result of inhibition of HIF-1α transcription. The dual functionality of DHBG appears contradictory in that it suppresses HIF-1α at high concentrations, and yet promotes the transcription of some of its key target genes. In this regard, DHBG may provide a measure of selectivity by enhancing the activation of only a subset of HIF-1α downstream targets while suppressing HIF-1α. On the other hand, given that HIF-2α has been regarded as an important therapeutic target for RCC therapy (particularly in HIF-1α defective renal cancer cells),[343, 346] DHBG and GUA suppression effects on HIF-2α may make these aspirin metabolites potential drug candidates for RCC treatment.

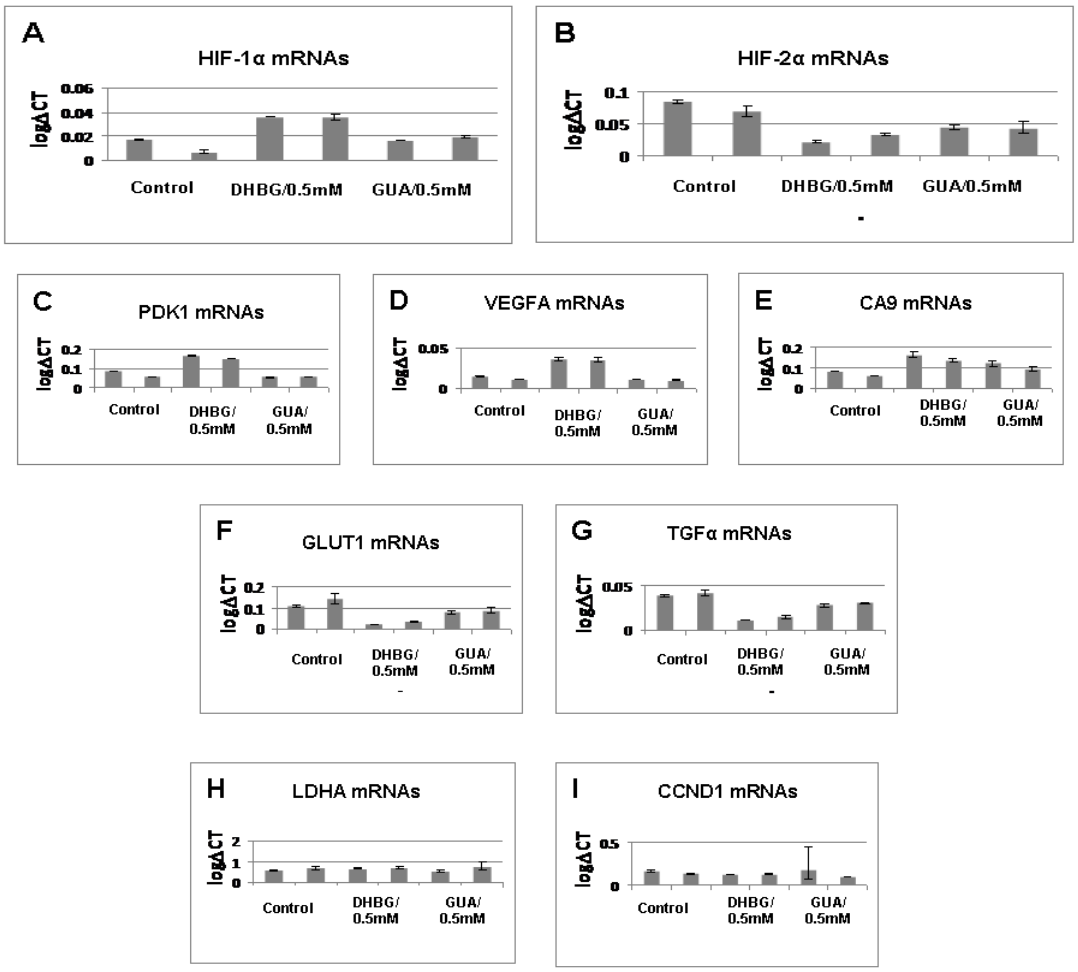


Figure 7.20: The effects of DHBG and GUA on the mRNA levels of (**A**) HIF-1α, (**B**) HIF-2α, (**C**) PDK1, (**D**) VEGFA, (**E**) CA9, (**F**) GLUT1, (**G**) TGFα, (**H**) LDHA, and (**I**) CCND1 in RCC4 cells. HIF-1α direct target genes in RCC4: PDK1, and CA9; HIF-2α direct target genes in RCC4 cells: VEGFA, GLUT1, TGFα and CCND1.[346, 382, 383] PDK1, pyruvate dehydrogenase kinase-1; VEGFA, vascular endothelial growth factor-A; CA9, carbonic anhydrase-9; GLUT1, glucose transporter-1; TGFα, transforming growth factor-α, LDHA, lactate dehydrogenase-A; and CCND1, cyclin D1. (Results obtained from Dr P. J. Pollard)

7.3.7 DHBG can regulate multiple potential cancer targets

The specificity of DHBG on HIF-α suppression was then investigated by probing the protein levels of several non-HIF downstream targets including *MINA53* (Myc-Induced-Nuclear Antigen 53 kDa), FIH (Factor Inhibiting HIF), nucleophosmin/B23, Hsp90, PKCλ (atypical isoform of protein kinase C), Akt/PKB (protein kinase B), and NF_KB-p105 (nuclear factor kappaB 105kDa) using their corresponding antibodies. **Fig. 7.21** shows the immunoblot results, DMOG treated samples are shown for comparison.

Interestingly, DHBG (1 mM) displayed no apparent effect on the protein levels of MINA53, FIH, and nucleophosmine/B23. In contrast, the drug substantially suppressed PKCλ, Akt and NF_KB-p105 levels (**Fig. 7.21**). Similar to most reported HIF-α inhibitors,[345] the results indicate DHBG suppression effect is not limited to HIF-α, however, DHBG does confer a certain degree of specificity.

The detection of the observed slower-mobility species (upper band) on the Hsp90 and NF_KB-p105 immunoblots (**Fig. 7.21**, lane 4) was particularly interesting (which might indicate the formation of higher molecular weight protein complexes via protein modifications as speculated). However, these slower-mobility species were unable to be detected when the experiments were repeated.

As discussed previously (**Section 7.3.3**), inhibition of Hsp90 activity has been reported to promote HIF-1α degradation.[348, 349] Although the *in vitro* results (**Section 7.3.3**) indicate DHBG (and other aspirin metabolites) are probably not direct competitive Hsp90 inhibitors, the results did not exclude the possibility of *in vivo* Hsp90 inhibition via another cellular mechanism (e.g. protein modification or by an unidentified metabolite of DHBG).

Beside HIF-1α, Akt is a major client protein of Hsp90. Inhibition of Hsp90 has been shown to lead to direct downregulation of Akt activity.[385, 386] In addition, Hsp90 has also been associated with the regulation of the PKC and $NF\text{-}_KB$ signaling pathways.[387-389]

Therefore, it is unclear whether the observed suppressions of PKCλ, Akt and NF_KB-p105 levels are the direct effects of DHBG or via the inhibition of other associated proteins including Hsp90.

Interestingly, Akt suppression by siRNA (a small interfering RNA) has been shown to suppress hypoxia or DMOG-induced HIF-1α accumulation by inhibiting HIF-1α protein translation.[118] Furthermore, inhibition of the Akt-dependent PI3K/Akt/mTOR pathway (see **Introduction** in **Section 1.3.4**) has been associated with decreased HIF-1α activity and shown to have therapeutic effects in RCC therapy.[390-393] Genetic inhibition of Akt has also been reported to inhibit NF_KB transcriptional activity, whereas inhibition of NF_KB has been demonstrated to block HIF-1α protein expression.[394, 395] Therefore, it is not impossible that DHBG may inhibit HIF-α expression via acting on PI3K/Akt/mTOR or NF_KB pathways, given the observations that DHBG also reduced Akt and NF_KB-p105 protein levels (**Fig. 7.21**).

High doses of aspirin and salicylate (from 5 mM up to 20 mM) have been reported to inhibit the activity of NF_KB, Akt, mTOR, and PKC in cells.[396, 397] It is conceivable that the mechanism of action maybe in part involve the aspirin metabolite DHBG (and GUA), therefore the work in this chapter may help to identify the actual 'active compound' in aspirin treatment. Furthermore, HIF-α, NF_KB, PI3K/Akt/mTOR, and PKC signal transduction pathways have been proposed as potential therapeutic targets for RCC (and other cancers) treatment,[344, 398-401] antitumour selectivity may derive from the simultaneous combinatorial effects of DHBG (and GUA) on multiple cancer targets and pathways.

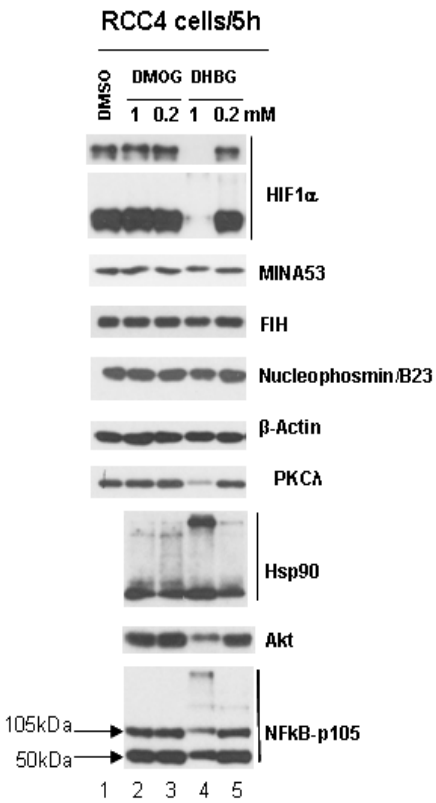


Figure 7.21: Suppression effect of DFBG is not specific to HIF-α. DHBG is shown to directly regulate the potential therapeutic targets for RCC including NF_KB-p105, and PKCλ. Howevr, DHBG has no apparent effect on the levels of MINA53, FIH, and nucleophosmine/B23. The slow-mobility species in the (top bands) Hsp90 and NF_KB-p105 immunoblots were unable to be detected when the experiments were repeated. (NF_KB-p105 undergoes proteasomal processing to produce the mature NF_KB-p50 subunit[402] detected in the lower band in the western blot)

7.4 Conclusions and future directions

This chapter has described investigations on the potential of two aspirin metabolites, DHBG and GUA, as HIF-α inhibitors in RCC4 VHL-defective and other VHL-competent cell-lines. DHBG was found to demonstrate concentration-dependent dichotomous effect on HIF-α regulation (*i.e.* DHBG stablises HIF-α at low concentrations (e.g. 0.2 mM) but suppresses HIF-α accumulation at high concentrations (> 0.5 mM), whilst GUA exhibited HIF-α suppression effect at concentrations higher than 0.1 mM.

Potential salicylate precursors of DHBG and GUA including aspirin, SUA, 2,3-DHBA, and 2,5-DHBA were also demonstrated to exhibit similar suppression effects on HIF-1α at high concentrations (> 2 mM). The findings suggest that the therapeutic effects of aspirin may in part be attributed to the formation and the abundance of its different metabolites including DHBG and GUA in a concentration-dependent manner.

The results so far indicate that DHBG and GUA may exert their HIF-α suppression effects through multiple cellular pathways including regulation of HIF-α mRNA levels and gene expression or by interacting with other proteins that are involved in HIF-α regulation (e.g. PHDs, Hsp90, RACK-1). The possibilities of the formation of biologically active quinones and subsequent covalent modifications to proteins or nucleic acids need further investigations.

At the concentration that substantially suppressed protein levels of HIF-1α, HIF-2α PKCλ, Akt and NF_KB-p105 levels, DHBG (1 mM) was shown to have no apparent effect on MINA53, FIH, nucleophosmine/B23 and Hsp90 levels. The work in this chapter thus demonstrates that DHBG (and possibly GUA) can regulate multiple cancer targets (*i.e.* HIF-1α, HIF-2α, Akt and NF_KB-p105). The antitumour selectivity of these aspirin metabolites (*i.e.* DHBG and GUA) warrants further studies. Future experiments may include:

i) UV-visible spectrometry which allows investigation of potential conversion of DHBG/GUA to quinones (via auto-oxidation or enzymatic reaction) by monitoring the changes in the wavelengths of the parent compounds.
ii) Mass spectrometry-based proteomic analyses which allow the studies of potential protein modifications.
iii) The studies of potential effects of DHBG and GUA on the NF_KB and P13K/Akt/mTOR pathways.

Chapter 8: Summary

The work presented in this thesis first describes the development of cell-based antibody assays that employ immunoblotting and the HIF hydroxy-residue specific antibodies. These antibody assays enable the simultaneous measurement of the effects of chemical inhibition on the three known hydroxylation sites (i.e. Pro402, Pro564, and Asn803) of human HIF-1α. Unexpectedly, the results reveal substantial differences on the effects of the supposedly nonspecific hypoxia mimetic chemical reagents including iron chelators, transition metal ions, and the cell-permeable 2OG analogue DMOG on the inhibition of HIF prolyl and asparaginyl hydroxylation in cells. In contrast to the *in vitro* predictions, HIF prolyl hydroxylation was more susceptible to iron chelator and transition metal ion inhibition while asparaginyl hydroxylation was more sensitive to DMOG inhibition. The newly developed antibody assays were further used to provide biological selectivity data on both previously reported and novel HIF hydroxylase inhibitors. The work led to the identification of several specific cell-permeable PHD inhibitors and one specific FIH inhibitor (see **Chapter 2**).

By employing the newly developed antibody assays and the cell-permeable 2HG ester derivatives, the current work also demonstrates that the oncometabolite *R*-2HG is an ineffective PHD inhibitor in cells. The results therefore argue against the hypothesis of HIF upregulation being the direct action of *R*-2HG inhibition on the PHDs in IDH-associated cancers. However, *R*-2HG elevation was found to inhibit FIH activity, suggesting a possible pathway in which *R*-2HG could potentially regulate HIF transcriptional activity. Notably, 2HG elevation was demonstrated to inhibit the activities of 2OG-dependent histone lysine demethylases including JMJD2A and JMJD2C, therefore suggesting that IDH-mediated oncogenic pathways might involve epigenetic chromatin alterations.

Contrary to expectations, elevated cellular 2OG levels were demonstrated to result in HIF-1α upregulation in all of the tested VHL-competent cell-lines (*i.e.* RCC4/VHL, U2OS, and 293T cells). Initial cell-based results suggest that the 2OG-mediated HIF-1α upregulation may be the direct result of 2OG (co-substrate) inhibition of the PHDs in cells. This proposal is supported by the *in vitro* findings which show that recombinant PHD2 activity can be inhibited by high concentrations of 2OG. The 2OG-mediated PHD inhibition/HIF-1α upregulation can also be reversed by the addition of ascorbate (a PHD stimulant) which results in an increased PHD activity *in vitro* and in cells. However, the results by no means exclude other possible cellular mechanisms, including the possible involvement of 2OG direct metabolites such as succinate and fumarate, which have been shown to inhibit PHD activity in cells.

A series of PHD2 variants and potential variant-sensitive analogue inhibitors were then prepared and investigated in the first attempts to apply the 'bump-hole' (chemical-genetic) approach for the functional studies of 2OG oxygenases. The kinetic parameters of the PHD2 variants were determined and the inhibitory potencies of the analogue inhibitors were evaluated using MALDI MS and AlphaScreen PHD hydroxylation assays. L343A-PHD2 was identified as an active variant, which exhibits similar activity to wild-type PHD2. D-Ala-BIQ (IC_{50} 47.9 μM) was demonstrated to selectively inhibit the L343A-PHD2, but not the wild-type PHD2. The *in vitro* results clearly demonstrate the feasibility of selective inhibition of the PHD variants using the 'bump-hole' approach. These *in vitro* findings should assist in guiding future attempts at functional studies of the PHD isoforms in cellular systems.

A series of aromatic diacylhydrazine-based PHD inhibitors were also developed. ESI-MS studies reveal that some these diacylhydrazine-based inhibitors are capable of specifically binding to the PHD active site and simultaneously chelating a second iron. The induction of second iron binding substantially depends on the position of nitrogen in the aromatic rings and the structures of the side chains of the diacylhydrazine-based inhibitors. The biochemical assay results indicate that some these diacylhydrazine-based compounds are potent PHD inhibitors (IC_{50} ~ 10 μM). These compounds were shown to upregulate HIF-

1α in VHL-competent cells and inhibited HIF prolyl hydroxylation in VHL-defective RCC4 cells. However, they were also found to inhibit HIF asparaginyl hydroxylation.

Lastly, the work in this thesis describes the evaluation of a series of aspirin metabolites including 2,3-dihydroxybenzoylglycine (DHBG) and gentisuric acid (GUA) as potential HIF inhibitors. DHBG, GUA and several DHBG derivatives were shown to substantially suppress the HIF-1α and HIF-1α levels in VHL deficient RCC4 cells. Thermal shift and NMR data suggest that the modes of action of DHBG and GUA on HIF-1α suppression may not involve the Hsp90-mediated HIF degradation pathway. Possible mechanisms of action of DHBG and GUA may involve the conversion of the compounds to bioactive quinones which then promote covalent modifications to proteins in cells. This hypothesis warrants further investigations. The findings of HIF-α suppression effect mediated by aspirin metabolites DHBG and GUA suggest that the therapeutic effects of aspirin in cancers may involve potential regulation of HIF-α activity, implying a novel mechanism of action for aspirin in cancer therapy.

Chapter 9: Materials and Methods

9.1 Chemicals

Desferrioxamine (DFO), 2,2′-dipyridine (DIP), and ethyl-3,4-dihydroxybenzoate (EDHB), dimethyl 2-oxoglutarate (DM-2OG) were from Sigma-Aldrich. 4-oxo-1,4-dihydro-1,10-phenanthroline-3-carboxylic acid (DPCA) was synthesised by Dr A. Conejo-Garcia.[147] (Z)-2-(3-hydroxy-2-((naphthalene-2-ylmethyl)sulfonyl)acetyl)imino)-2,3-dihydrothiazol-4-yl) acetic acid (BNS) was a kind gift from Amgen.[178] Dimethyloxalylglycine (DMOG) was from Frontier Scientific. All other chemicals were from Sigma-Aldrich unless otherwise stated.

9.2 General methods used in chemical synthesis

Chemicals and solvents were purchased from Sigma. Melting points were recorded on a Kőfler hot block. Proton and carbon nuclear magnetic resonance (δ_H, δ_C) spectra were recorded Bruker AVC 500 (500 MHz) or Bruker AMX 500 (500 MHz) spectrometers. Chemical shifts are quoted on the δ-scale in ppm using residual solvent as an internal standard. Coupling constant (J) is reported to the nearest 0.5 Hz. Low resolution mass spectra were recorded on a Micromass Platform 1 spectrometer using electrospray ionisation in either positive or negative ion modes (ES^+ or ES^-) or using a VG Micromass spectrometer. High resolution mass spectra were recorded using a Walters 2790-Micromass LCT electrospray ionisation mass spectrometer. *M/z* values are reported in Daltons and are followed by their percentage abundance in parentheses. Optical rotations were measured using a Perkin-Elmer 241 polarimeter with a path length of 1 dm. Concentrations are given in g/100 mL. Microanalyses were performed by the Science Centre Elemental Analysis Service, London Metropolitan University, London. Thin Layer Chromatography (TLC) was carried out using Merck Kieselgel $60F_{254}$ pre-coated glass-backed plates. Visualisation of the plates was achieved using a U.V. lamp (l_{max} = 254 or 365 nm), and/or ammonium molybdate (5% in 2 M sulphuric acid), or

sulphuric acid (5% in ethanol). Flash column chromatography was carried out using Sorbsil C60 40/60 silica. Figures of the crystal structures were drawn using PyMOL software.

9.3 Cell-lines

Cells were cultured in DMEM each supplemented with 10% fetal calf serum, 2 mM l-glutamine, 50 U/mL of penicillin, and 50 μg/mL of streptomycin. Stable RCC4 transfectants expressing empty vector alone (referred to here as RCC4) or *C*-haemagglutinin-tagged functional (wild-type) VHL (RCC4/VHL) were previously prepared at Ratcliffe laboratory as reported.[12] Human hepatoma Hep3B, breast cancer MCF7, human embryonic kidney 293T, and human bone osteosarcoma U2OS cells were obtained from European Collection of Cell Cultures (ECACC). C3 U2OS cell-line expressing doxycyline-inducible truncated HIF-1α (residues 344-826) was jointly prepared by Dr Y-M Tian and Dr N. Masson.[183] WT4 U2OS cell-line expressing doxycyline-inducible wild-type HIF-1α was prepared by Dr Y-M Tian.[142] PHD 1-2-3 triple-knockout mouse embryonic fibroblast was prepared by Dr J. Adam.[257] Cells were seeded at 40-60 % confluency 12-16 h prior to inhibitor treatments at 70-100% cell confluency in 12-well plate. DMSO or inhibitors were exposed to the cells for 4-6 h, at 0-2% DMSO. All assays were performed at least in duplicate.

9.4 Protein immunoblotting analyses

Cells were lysed in urea/SDS buffer supplemented with 1 mM dithiothreitol and Complete Protease Inhibitor Mixture (Roche Applied Science). Extracts were resolved by SDS-PAGE, electroblotted onto PVDF membranes (Millipore), and probed with primary antibodies followed by HRP-conjugated secondary antibodies. SuperSignal Chemiluminescent Substrates (Pierce) were used to visualize immunoreactive species.

9.5 Antibodies

Rabbit polyclonal anti-HIF-1α Hyp402 (Hyp402) was developed in collaboration with Millipore Biosciences (catalog number 07-1585). Mouse monoclonal anti-HIF-1α hydroxy-Asn803 (HyAsn803) was a gift from Dr S. H. Lee.[143] Other antibodies were as follows: anti-HIF-1α Hyp564 (Hyp564) (clone-D43B5, New England Biolabs); pan-anti-HIF-1α (clone-54, BD Transduction Laboratories), HRP(horseradish peroxidase)-conjugated anti-β-Actin (clone-AC15, Abcam), anti-HIF-2α (clone-190b, Ratcliffe laboratory)[403], anti-Hsp90 (clone-68, BD Transduction Laboratories), anti-Akt (clone-9272, New England BioLabs), anti-nucleophosmin/B23 (clone-42, Santa Cruz Biotechnology), anti-MINA53(clone-M532, Invitrogen), anti-P105[170], anti- FIH[183], anti-PKCλ[404].

9.6 Plasmids and transient transfections

Expression vectors for full length human PHD2 (*i.e.* PHD2-pcDNA3)[17]and the truncated HIF-1α (residues 344-826) (*i.e.* HIF-1α/PK) were prepared by Dr J. M. Gleadle and Dr Y-M. Tian, respectively. Transient transfections were performed following the reported method.[14] In brief, for each well to be transfected 3 μl Fugene 6 (Roche, Mannheim, Germany) per μg plasmid DNA were suspended in 100 μl DMEM/well. After 5 min incubation at room temperature plasmid DNA was added. The mixture was incubated for another 30 min at room temperature and then added to the cell culture medium. Cells were incubated for 24 h and then subjected to the experimental conditions.

9.7 Heat shock protein 90

Full-length heat shock protein (Hsp90) was produced in *E. Coli* and purified by Dr E. P. Williams (The Structural Genomic Consortium, University of Oxford).

9.8 Preparation of the PHD2 variants

Four active site residues of human PHD2 were identified for single point mutations *i.e.* I327A, L343A, F366L and V376A. The variants were cloned, expressed and purified to obtain I327A-, L343A-, F366L- and V376A-PHD2. Below are the materials and methods used in the preparation of the PHD2 variants in this study.

9.8.1 Materials

Water was from a Millipore Elix® 10 system, and purified further through a 0.22 μm filter by a Millipore Milli-Q system. All equipment and media used were sterilised prior to use by autoclaving at 121°C for 20 mins. *E. Coli* XL10-Gold and *E.coli* BL21 (DE3) competent cells were purchased from Strategene. Kanamycin and isopropyl β-D-1-thiogalactopyranoside (IPTG) was obtained from Melford Laboratories Ltd. DNase used is from bovine pancreas; grade II, purchased from Roche. Agarose was purchased from Bioline. Tryptone, yeast extract and agar (bacteriological) for use in culture media were obtained from Oxoid. SYBR Safe™ DNA gel stain and 2-log DNA Ladder 0.1-10 kb were purchased from Invitrogen. Standard sterile practices were followed throughout, with procedures carried out in a Biological Safety Hood (Heraeus KJ12) where appropriate.

Bacterial growth media: *LB media* (per Litre): Tryptone (10 g), NaCl (10 g), Yeast extract (5 g). To obtain a solid medium, agar (20 g) was added to media before autoclaving. *2TY media* (per Litre): Tryptone (16 g), NaCl (5 g), Yeast extract (10 g). The medium was adjusted to pH 7.0 before autoclaving. *SOC media* (per Litre): 2TY (980 mL), 1 M $MgCl_2$ (10 mL), 2 M glucose (10 mL). The final concentration of kanamycin in all media is 30 μg mL^{-1} and was added post-autoclaving.

Agarose Gel electrophoresis gel buffers: *50 x TAE (running buffer solution)* – 2 M Tris, 1 M acetic acid, 0.5 M EDTA, pH 8.0. *5 x sample loading buffer* – glycerol (30%), xylene cyanol FF (0.25%), bromophenol blue (0.25%), TAE buffer (2%).

SDS-PAGE buffers: *Separating gel*, *15% acrylamide* (per gel): 30% acrylamide (1.25 mL), 2 x separating gel buffer (750 mM Tris-HCl, 0.2% SDS, pH 8.8) (1.25 mL), tetramethylethylenediamine (TEMED) (5 µL), ammonium persulfate (APS) (15 µL). *Stacking gel, 4.5% acrylamide* (per gel): Milli-Q H_2O(700 µL), 30% acrylamide (300 µL), 2 x stacking gel buffer (350 mM Tris-HCl, 0.2% SDS, pH6.8) (1 mL), TEMED (5 µL), APS (15 µL). (TEMED and APS were added to the mixture immediately prior to pouring of both gels). *10 x running buffer*: 250 mM Tris, 1.92 M glycine, 10% SDS, pH 8.8. *2 x sample loading buffer*: 10% 0.5 M Tris-HCl; pH 6.8, 0.5% bromophenol blue, 2% SDS, 12% Glycerol, 0.5% β-mercaptoethanol, 53%-MilliQ H_2O. *Stain*: 0.5% Coomassie Brilliant Blue, 50% methanol, 10% glacial acetic acid. *Destain*: 10% methanol, 10% glacial acetic acid. *Molecular weight marker*: SeeBlue® Plus 2 (Invitrogen).

FPLC buffers: *S Buffer A*: 0.1 M MES, pH 5.8. *S Buffer B*: 0.1 M MES, 1 M NaCl, pH 5.8.*Gel filtration buffer*: 100 mM NaCl, 100 mM Tris, pH 7.5. All buffers were freshly prepared with Milli-Q water and filtered with a 0.20 µm filter.

9.7.2 Generation of PHD2 variant plasmids

The methods used for the generation and purification of the PHD2 variant plasmids are described as follows:

(i) Polymerase chain reaction (PCR): Predesigned oligonucleide primers (**Fig. 9.1 A**) were synthesised to order by Sigma-Genosys and obtained as lyophilised samples. The primers were resuspended in sterile water to 100 µM. The forward (F) and reverse (R) primers were then mixed and used directly as F-R primer mixtures (10 µM) in the PCR reaction. DNA coding for the N terminally truncated $PHD2_{181-426}$ construct had

previously been cloned by Dr K. S. Hewitson into the pET-28a(+)vector (Novagen) and was used as the plasmid template in the reactions. The PCR reactions were carried out in a Techne TC-312 PCR thermocycler. The thermal cycling used was shown in **Fig. 8.1 B**. All reactions were carried out according to the Stratagene QuikChange® site-directed mutagenesis protocol. Each reaction mixture contained:

Reagent	Volume/µL
pET-28a PHD-2 Plasmid template (10 ng/µL)	2
F-R primers mixture (10 µM)	2.2
10 x reaction buffer	5
dNTP mix (10 mM)	5
$MgCl_2$ (2 mM)	5
Sterile water	29.8
Pfu Turbo polymerase	1
Total	50

(ii) Agarose gel electrophoresis: Agarose gel electrophoresis was then used for DNA plasmid separation and visualisation. 1.0% agarose gel was prepared by dissolving agarose (0.4 g) in TAE buffer (40 mL) by boiling. SYBR Safe™ DNA gel stain (2 µL) was added when the solution had cooled to 60 ^{o}C before pouring into a Bio-Rad agorose gel cast. 12µL PCR product was loaded onto the gel, and run on a Bio-Rad system at a constant potential of 80 V for approximately 30 minutes; bands were visualised with a UV transilluminator (Gel logic 200). Samples were run against a 2-log DNA Ladder 0.1-10 kb, allowing molecular weight determination.

(iii) Template plasmid digestion*: Dpn*I (1 µL) was added to each PCR amplified plasmid mixture and incubated at 37 ^{o}C for 2 hours followed by transformation step.

(iv) Transformation: *E. coli* XL10-Gold ultracompetent cells were thawed on ice and β-mecaptoethanol (4 µL) was then added and gently mixed with the cells (100 µL) . The mixture was allowed to chill on ice for 10 minutes. 25 µL cells were then added to the mutated DNA plasmid (2 µL) in a sterile eppendorf tube. This was incubated on ice for 30 mins before the cells underwent heat shock at 42°C for another 30 min, followed by returning them to ice for 2 min. SOC medium (200 µL) was added to cells which were then incubated at 37°C for 1 h. The transformation mixture (100 µL) was then spread

onto a kanamycin LB agar plate and incubated overnight at 37°C in a Gallenkamp Duostat incubator.

(v) Preparation of cell culture: A single colony was picked from the agar plate and inoculated into kanamycin 2TY medium (10 mL) in a 50 mL falcon tube. The tubes were incubated overnight at 37°C with vigorous shaking (250 rpm) in a New Brunswick Scientific G25 environmental shaker to allow cell growth.

(vi) Preparation of glycerol stocks: A cell pellet was obtained from an overnight starter culture (1 mL). The pellet was resuspended in 2TY media (400 μL), glycerol stock solution (400 μL) added, and the mixture stored at -80°C. (*Glycerol stock solution*: 65% glycerol, 0.1 M $MgSO_4$, 25 mM Tris, pH 7.5)

(vii) DNA Purification: A Qiagen Miniprep DNA purification kit was used for DNA extraction and purification from 8-10 mL cell culture of according to the manufacturer's protocols.

(viii) DNA quantification: Plasmid concentration was determined through measurement of light absorbance at 260 nm using a NanoDrop ND-1000 UV/Vis Spectrophotometer. Abs_{260} of 1.00 ≈ [dsDNA] = 50 mg mL^{-1}.

(ix) DNA sequencing: Determination of DNA sequences to ensure correct incorporation of each mutation, was carried by Geneservice Ltd., Department of Biochemistry, University of Oxford using T7 promoter and terminator sequence primers on a 48-capillary AppliedBiosystems 3730 DNA Analyser.

A

(i) I327A-PHD2 Primers
Forward 5' GA TGT GTG ACA TGT GCA TAT TAT CTT AAT AAA G 3' Reverse 5' T ATT AAG ATA ATA TGC ACA TGT CAC ACA TCT TC 3'
(ii) L343A-PHD2 Primers
Forward 5' GTA AGT GGA GGT ATA GCT CGA ATT TTT CCA GAA G 3' Reverse 5' C TGG AAA AAT TCG AGC TAT ACC TCC ACT TAC CTT G 3'
(iii) F366L-PHD2 Primers
Forward 5' T AGA CTG CTG TTT CTC TGG TCT GAC CGT CGC 3' Reverse 5' G ACG GTC AGA CCA GAG AAA CAG CAG TCT ATC3'
(i) V376A-PHD2 Primers
Forward 5' GC AAC CCT CAT GAA GCA CAA CCA GCA TAT GCT AC 3' Reverse 5' GC ATA TGC TGG TTG TGC TTC ATG AGG GTT GCG AC3'

B

Segment	Cycles	Step	Temperature	Time
1	1	Denaturation	95 °C	1 minute
2	8	i) Denaturation	95 °C	50 seconds
		ii) Annealing	50 °C	50 seconds
		iii) Extension	68 °C	8 minutes
3	10	i) Denaturation	95 °C	50 seconds
		ii) Annealing	60 °C	50 seconds
		iii) Extension	68 °C	8 minutes
4	1	Final extension	68 °C	10 minutes
5	1	Final hold	4 °C	-

C

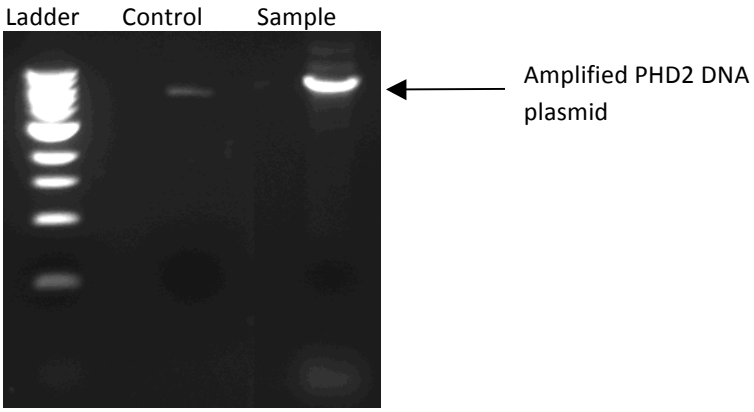


Figure 9.1: **(A)** Designed primers for the intended site directed mutagenesis. The DNA sequence of the corresponding amino acid residue selected for substitution is highlighted in red. (The primers were synthesised to order by Sigma-Genosys). **(B)** Thermal cycling used in the Polymerase Chain Reactions. (**C**) A representative agarose gel showing amplification of L343A-PHD2 DNA plasmid in the PCR product. Gel sample mixture: Ladder: 2-log DNA Ladder 0.1-10 kb (2 µL), loading buffer (2 µL), sterile water (8 µL); Control: pET-28a(+) *phd2* plasmid template (2 µL), loading buffer (2 µL), sterile water (8 µL); Sample: PCR product mixture (10 µL), loading buffer (2 µL).

9.7.3 Protein expression and fast protein liquid chromatography purification

The methods used for the expression and purification of the PHD2 variants are described as follows:

(i) Transformations: *E. coli* BL21 (DE3) competent cells were used for protein production of the PHD2 variant protiens. The cells were thawed on ice before added (25 μL) to the corresponding mutated DNA plasmid (2.0 μL) in a sterile eppendorf tube. This was incubated on ice for 30 min before heat shock at 42°C for 30 s and returning to ice for 2 mins. SOC medium (200 μL) was added to cells which were then incubated in a 37°C water bath for 1 h. The transformation mixture (100 μL) was then spread onto a kanamycin LB agar plate and incubated overnight at 37 ^{o}C in a Gallenkamp Duostat incubator.

(ii) Preparation of starter culture: A single colony was then picked from the LB plate and inoculated into kanamycin 2TY medium (10 mL) in a 50 mL falcon tube. The tubes were incubated overnight at 37^{o}C with vigorous shaking (250 rpm) in a New Brunswick Scientific G25 environmental shaker.

(iii) Expression trials: Starter culture (1 mL) of each PHD2 variant was then used to inoculate 4 x 500 mL flasks containing kanamycin 2TY media (100 mL). These flasks were then incubated at 37°C with vigorous shaking at 220 rpm in a New Brunswick Scientific G25 environmental shaker. Once an Optical Density (OD) 0.6-0.8 at 600 nm was reached (measured using a sample of bacterial culture (1 mL) compared to initial growth medium (1 mL) as a reference solution in a Novaspec II spectrophotometer, Pharmacia), 0.5 M IPTG (100 μL) was added to induce protein expression (except for the control). Flasks were then incubated at either 15°C, 28°C or 37°C, shaking at 220 rpm for 3 hours and 20 hours. 50 mL of each culture was harvested at each stage in an S-4180 rotor in a Beckman Allegra™ 21R bench top centrifuge at 4000 rpm and 4°C for 20 mins. Resulting cell pellets were stored at -20°C. Cell pellets were resuspended in 50 mM Tris pH 7.5 (5 mL), and lysed on ice using an MSE Soniprep 150 sonicator with two 30 s

pulses separated by a 30 s pause at an amplitude of 10 µm. 1 mL of the cell suspension was transferred to a sterile Eppendorf and spun at 13 000 rpm for 1 min in a Jouan A-14 microcentrifuge. The supernatant (soluble protein) was removed and the remaining precipitate (insoluble protein) resuspended in 50 mM Tris pH 7.5 (1 mL). The samples were then used for SDS PAGE.

(iv) SDS PAGE: Polyacrylamide gels were run for 60 mins at 200 V at room temperature on a Bio-Rad Mini-PROTEAN II system. Protein (5 µL), loading buffer (20 µL) and 50 mM Tris (35 µM) were mixed in an eppendort tube. The protein samples were then denatured by heating at 100°C for 5 mins prior to loading (20 µL). The gels were stained for 10 mins, and destained overnight. SDS PAGE was carried out to determine conditions under which greatest soluble expression of PHD2 variants occurred. Negative (variant PHD2 without induction) control was run on the same gel for comparison.

(v) Large scale growths: Starter culture (7 mL) of each PHD2 variant was used to inoculate 12 x 2L flasks containing kanamycin 2TY media (600 mL). Flasks were then incubated at 37°C with vigorous shaking at 220 rpm in a New Brunswick Scientific G25 environmental shaker. Once an OD of 0.6-0.8 at 600 nm was reached, 0.5 M IPTG (600 µL) was added to induce protein expression. Cultures were further incubated at 15^{o}C for 20 hours, then cells harvested by centrifugation in a JA-10 rotor in a Beckman Avanti J25 centrifuge at 9000 rpm and 4°C for 10 mins. The resulting cell pellet was weighed and stored at -80°C.

(vi) Preparation of cell lysate: Cell pellets obtained from large scale growths were resuspended in Sepharose Buffer A (250 mL). 1 M $MgCl_2$ (100 µL) and DNase (1 mg) were added and the mixture was stirred at 4°C until homogeneous. Cells were sonicated for 4 x 45 s separated by 45 s breaks with a Sonics VibraCell VCX-500 (13 mm probe at 60% intensity). Insoluble cell debris was then removed by centrifugation in a JLA-16.250 rotor in a Beckman Avanti J25 centrifuge at 15 000 rpm for 20 mins, then a JA-25.50 rotor at 23 000 rpm for 10 mins, each at 4°C. The supernatant was filtered through a 0.20 µm filter prior to purification.

(vii) Protein purification: Protein purification was carried out using AKTA FPLC systems at 4^{o}C. Cation exchange column (SP sepharose fast flow 50) was equilibrated with Milli-Q water (2CV), 1 M NaCl (2CV) and S buffer A (2CV) prior to loading of the filtered supernatant (via a 50 mL superloop at 4 mL min^{-1}). The column was washed with S buffer A until the UV trace returned to its initial level. A gradient of 0-100% S buffer B was then run over a period of 35 mins to elute the protein, and 5 mL fractions were collected. Following use the column was washed with 2CV each of Milli-Q water, 1 M NaOH, water, 1 M NaCl, 1 M AcOH and water. UV trace analysis and SDS PAGE were used to determine fractions containing the required protein, which were then combined and concentrated to 2 mL using a 10 kDa MWCO concentrator in an S-4180 rotor in a Beckman Allegra™ 21R bench top centrifuge at 4000 rpm and 4°C.

Prior to use the 320 mL gel filtration Superdex 75 column (Pharmacia) containing S75 gel filtration resin (Amersham Biosciences) was equilibrated by washing with Milli-Q water (1CV), and gel filtration buffer (1CV). The concentrated protein was then loaded onto the column via a 2 mL injection loop at 0.5 ml min^{-1}, and subsequently run at 1.5 mL min^{-1}. The loop was washed with one volume each of Milli-Q water and gel filtration buffer before use. Protein was eluted with gel filtration buffer (1CV), with 5 mL fractions collected when the UV absorption exceeded 40 mAU. Following use, the column was washed with Milli-Q water (2CV). SDS PAGE was used to identify protein fractions with highest purity, they were then combined and concentrated. The resulting protein was desalted into 50 mM Tris pH 7.5 by further concentration. The concentration of the desalted protein was determined and stored at -80°C in appropriate aliquots for future use.

(viii) Determination of protein concentration: Concentrated, desalted proteins were spun in a microcentrifuge at 13 000 rpm for 1 min to remove precipitate or dust prior to measurement. Concentration was determined using a NanoDrop ND-1000 UV/Vis Spectrophotometer by measurement of the absorbance at 280 nm. 50 mM Tris buffer was used as a blank, 3 µL of sample was used in each measurement.

9.8 AlphaScreen PHD2 hydroxylation assay[163]

Inhibition assay was carried out in 384-well white ProxiPlates (PerkinElmer) in 10ul of reaction volume. Standard reaction mixture consisted of the compound (in 2% DMSO final concentration), enzyme mix (1 nM of PHD2, 20 μM of Fe(II), 200 μM of ascorbate) and peptide mix (60 nM of biotinylated CODD peptide (HIF-1α residues 556-574) , 2 μM of 2OG) in 50 mM HEPES pH7.5, 0.01% Tween-20 and 0.1% BSA buffer. Compound was pre-incubated with the enzyme mix for 15 min before being incubated with peptide mix for 10 min at 22°C. Each reaction was quenched with 5 ul of 30 mM EDTA. Bead mix containing AlphaScreen beads (AlphaScreen streptavidin-conjugated donor and ProteinA-conjugated acceptor beads; PerkinElmer) was pre-incubated with rabbit monoclonal HIF-1α hydroxy-Pro564 antibody (Cell Signaling) and were added to the wells for a further 1 h at 22°C. The plates were then analysed with an Envision (PerkinElmer) plate reader.

9.9 MALDI MS PHD2 hydroxylation assay[35]

Standard assay mixtures contained: 100 μM substrate (CODD (HIF-1α residues 556-574) or NODD HIF-1α residues 395-413)), 300 μM 2OG, 300 μM inhibitor, 4 mM ascorboate, 50 μM $FeSO_4.7H_2O$ (dissolved first to 250 mM with 20 mM HCl, then 2.5 mM with Milli-Q water) and enzyme (concentration was varied as necessary). Assay mixtures were made up to 100 μL with 50 mM Tris pH 7.5. Reagents were pipetted into the base of a 5 ml tube as three separate spots: enzyme, substrate, and all other reagents prepared as a master mix. Assays were incubated at 37°C for 10 min in a shaking incubator then quenched by 1:1 addition of 0.1% formic acid and stored at -20°C. Samples were analysed by MALDI MS. For comparison, positive controls were without inhibitor, and negative controls without enzyme. Assays were carried at one time out as triplicate. Matrix-assisted laser desorption/ionization mass spectrometry (MALDI MS) was performed on a Waters Micromass™ MALDI micro MX™ mass spectrometer in negative ion reflectron mode with the following parameters: Laser energy 170, Pulse

2000, Detector 2700 and Suppression 700. Calibration was carried out using 1 µl PepMix4 (Trypsinogen Enolase BSA) in 9 µl CHCA (recrystallized α-cyano-4-hydroxy-cinnamic acid) matrix, (both Laser BioLabs). Samples were prepared by spotting 2 µL sample mixture of 1:1 quenched assay solution: CHCA matrix on a MALDI 96 well sample plate and allowing to air dry before measurements.

References

1. Semenza, G. L., Targeting HIF-1 for cancer therapy. *Nat Rev Cancer* 2003, 3, (10), 721-732.
2. Schofield, C. J.; Ratcliffe, P. J., Oxygen sensing by HIF hydroxylases. *Nat Rev Mol Cell Biol* 2004, 5, (5), 343-54.
3. Kaelin, W. G., Jr.; Ratcliffe, P. J., Oxygen sensing by metazoans: the central role of the HIF hydroxylase pathway. *Mol Cell* 2008, 30, (4), 393-402.
4. Chowdhury, R.; Hardy, A.; Schofield, C. J., The human oxygen sensing machinery and its manipulation. *Chem Soc Rev* 2008, 37, (7), 1308-19.
5. Ortiz-Barahona, A.; Villar, D.; Pescador, N.; Amigo, J.; del Peso, L., Genome-wide identification of hypoxia-inducible factor binding sites and target genes by a probabilistic model integrating transcription-profiling data and in silico binding site prediction. *Nucleic Acids Res* 2010, 38, (7), 2332-45.
6. Schodel, J.; Oikonomopoulos, S.; Ragoussis, J.; Pugh, C. W.; Ratcliffe, P. J.; Mole, D. R., High-resolution genome-wide mapping of HIF-binding sites by ChIP-seq. *Blood* 2011, 117, (23), e207-17.
7. Rankin, E. B.; Biju, M. P.; Liu, Q.; Unger, T. L.; Rha, J.; Johnson, R. S.; Simon, M. C.; Keith, B.; Haase, V. H., Hypoxia-inducible factor-2 (HIF-2) regulates hepatic erythropoietin in vivo. *J Clin Invest* 2007, 117, (4), 1068-77.
8. Percy, M. J.; Furlow, P. W.; Lucas, G. S.; Li, X.; Lappin, T. R.; McMullin, M. F.; Lee, F. S., A gain-of-function mutation in the HIF2A gene in familial erythrocytosis. *N Engl J Med* 2008, 358, (2), 162-8.
9. Furlow, P. W.; Percy, M. J.; Sutherland, S.; Bierl, C.; McMullin, M. F.; Master, S. R.; Lappin, T. R.; Lee, F. S., Erythrocytosis-associated HIF-2alpha mutations demonstrate a critical role for residues C-terminal to the hydroxylacceptor proline. *J Biol Chem* 2009, 284, (14), 9050-8.
10. Fong, G. H., Regulation of angiogenesis by oxygen sensing mechanisms. *J Mol Med (Berl)* 2009, 87, (6), 549-60.
11. Li, Q. F.; Wang, X. R.; Yang, Y. W.; Lin, H., Hypoxia upregulates hypoxia inducible factor (HIF)-3alpha expression in lung epithelial cells: characterization and comparison with HIF-1alpha. *Cell Res* 2006, 16, (6), 548-58.
12. Maxwell, P. H.; Wiesener, M. S.; Chang, G. W.; Clifford, S. C.; Vaux, E. C.; Cockman, M. E.; Wykoff, C. C.; Pugh, C. W.; Maher, E. R.; Ratcliffe, P. J., The tumour suppressor protein VHL targets hypoxia-inducible factors for oxygen-dependent proteolysis. *Nature* 1999, 399, (6733), 271-5.
13. Jaakkola, P.; Mole, D. R.; Tian, Y. M.; Wilson, M. I.; Gielbert, J.; Gaskell, S. J.; Kriegsheim, A.; Hebestreit, H. F.; Mukherji, M.; Schofield, C. J.; Maxwell, P. H.; Pugh, C. W.; Ratcliffe, P. J., Targeting of HIF-alpha to the von Hippel-Lindau ubiquitylation complex by O2-regulated prolyl hydroxylation. *Science* 2001, 292, (5516), 468-72.

14. Masson, N.; Willam, C.; Maxwell, P. H.; Pugh, C. W.; Ratcliffe, P. J., Independent function of two destruction domains in hypoxia-inducible factor-alpha chains activated by prolyl hydroxylation. *EMBO J* 2001, 20, (18), 5197-206.
15. Masson, N.; Ratcliffe, P. J., HIF prolyl and asparaginyl hydroxylases in the biological response to intracellular O(2) levels. *J Cell Sci* 2003, 116, (Pt 15), 3041-9.
16. Lando, D.; Peet, D. J.; Whelan, D. A.; Gorman, J. J.; Whitelaw, M. L., Asparagine hydroxylation of the HIF transactivation domain a hypoxic switch. *Science* 2002, 295, (5556), 858-61.
17. Epstein, A. C.; Gleadle, J. M.; McNeill, L. A.; Hewitson, K. S.; O'Rourke, J.; Mole, D. R.; Mukherji, M.; Metzen, E.; Wilson, M. I.; Dhanda, A.; Tian, Y. M.; Masson, N.; Hamilton, D. L.; Jaakkola, P.; Barstead, R.; Hodgkin, J.; Maxwell, P. H.; Pugh, C. W.; Schofield, C. J.; Ratcliffe, P. J., C. elegans EGL-9 and mammalian homologs define a family of dioxygenases that regulate HIF by prolyl hydroxylation. *Cell* 2001, 107, (1), 43-54.
18. Ivan, M.; Haberberger, T.; Gervasi, D. C.; Michelson, K. S.; Gunzler, V.; Kondo, K.; Yang, H.; Sorokina, I.; Conaway, R. C.; Conaway, J. W.; Kaelin, W. G., Jr., Biochemical purification and pharmacological inhibition of a mammalian prolyl hydroxylase acting on hypoxia-inducible factor. *Proc Natl Acad Sci U S A* 2002, 99, (21), 13459-64.
19. Bruick, R. K.; McKnight, S. L., A conserved family of prolyl-4-hydroxylases that modify HIF. *Science* 2001, 294, (5545), 1337-40.
20. Rose, N. R.; McDonough, M. A.; King, O. N.; Kawamura, A.; Schofield, C. J., Inhibition of 2-oxoglutarate dependent oxygenases. *Chem Soc Rev* 2011.
21. McNeill, L. A.; Hewitson, K. S.; Gleadle, J. M.; Horsfall, L. E.; Oldham, N. J.; Maxwell, P. H.; Pugh, C. W.; Ratcliffe, P. J.; Schofield, C. J., The use of dioxygen by HIF prolyl hydroxylase (PHD1). *Bioorg Med Chem Lett* 2002, 12, (12), 1547-50.
22. Berra, E.; Benizri, E.; Ginouves, A.; Volmat, V.; Roux, D.; Pouyssegur, J., HIF prolyl-hydroxylase 2 is the key oxygen sensor setting low steady-state levels of HIF-1alpha in normoxia. *EMBO J* 2003, 22, (16), 4082-90.
23. Willam, C.; Nicholls, L. G.; Ratcliffe, P. J.; Pugh, C. W.; Maxwell, P. H., The prolyl hydroxylase enzymes that act as oxygen sensors regulating destruction of hypoxia-inducible factor alpha. *Adv Enzyme Regul* 2004, 44, 75-92.
24. Koivunen, P.; Hirsila, M.; Gunzler, V.; Kivirikko, K. I.; Myllyharju, J., Catalytic properties of the asparaginyl hydroxylase (FIH) in the oxygen sensing pathway are distinct from those of its prolyl 4-hydroxylases. *J Biol Chem* 2004, 279, (11), 9899-904.
25. Ehrismann, D.; Flashman, E.; Genn, D. N.; Mathioudakis, N.; Hewitson, K. S.; Ratcliffe, P. J.; Schofield, C. J., Studies on the activity of the hypoxia-inducible-factor hydroxylases using an oxygen consumption assay. *Biochem J* 2007, 401, (1), 227-34.
26. Hirsila, M.; Koivunen, P.; Gunzler, V.; Kivirikko, K. I.; Myllyharju, J., Characterization of the human prolyl 4-hydroxylases that modify the hypoxia-inducible factor. *J Biol Chem* 2003, 278, (33), 30772-80.

27. Loenarz, C.; Schofield, C. J., Physiological and biochemical aspects of hydroxylations and demethylations catalyzed by human 2-oxoglutarate oxygenases. *Trends Biochem Sci* 2011, 36, (1), 7-18.
28. Lavista-Llanos, S.; Centanin, L.; Irisarri, M.; Russo, D. M.; Gleadle, J. M.; Bocca, S. N.; Muzzopappa, M.; Ratcliffe, P. J.; Wappner, P., Control of the hypoxic response in Drosophila melanogaster by the basic helix-loop-helix PAS protein similar. *Mol Cell Biol* 2002, 22, (19), 6842-53.
29. Fong, G. H.; Takeda, K., Role and regulation of prolyl hydroxylase domain proteins. *Cell Death Differ* 2008, 15, (4), 635-641.
30. Schofield, C. J.; Ratcliffe, P. J., Signalling hypoxia by HIF hydroxylases. *Biochem Biophys Res Commun* 2005, 338, (1), 617-26.
31. McDonough, M. A.; Li, V.; Flashman, E.; Chowdhury, R.; Mohr, C.; Lienard, B. M.; Zondlo, J.; Oldham, N. J.; Clifton, I. J.; Lewis, J.; McNeill, L. A.; Kurzeja, R. J.; Hewitson, K. S.; Yang, E.; Jordan, S.; Syed, R. S.; Schofield, C. J., Cellular oxygen sensing: Crystal structure of hypoxia-inducible factor prolyl hydroxylase (PHD2). *Proc Natl Acad Sci U S A* 2006, 103, (26), 9814-9.
32. Clifton, I. J.; McDonough, M. A.; Ehrismann, D.; Kershaw, N. J.; Granatino, N.; Schofield, C. J., Structural studies on 2-oxoglutarate oxygenases and related double-stranded beta-helix fold proteins. *J Inorg Biochem* 2006, 100, (4), 644-69.
33. Ozer, A.; Bruick, R. K., Non-heme dioxygenases: cellular sensors and regulators jelly rolled into one? *Nat Chem Biol* 2007, 3, (3), 144-53.
34. Chowdhury, R.; McDonough, M. A.; Mecinovic, J.; Loenarz, C.; Flashman, E.; Hewitson, K. S.; Domene, C.; Schofield, C. J., Structural basis for binding of hypoxia-inducible factor to the oxygen-sensing prolyl hydroxylases. *Structure* 2009, 17, (7), 981-9.
35. Flashman, E.; Bagg, E. A.; Chowdhury, R.; Mecinovic, J.; Loenarz, C.; McDonough, M. A.; Hewitson, K. S.; Schofield, C. J., Kinetic rationale for selectivity toward N- and C-terminal oxygen-dependent degradation domain substrates mediated by a loop region of hypoxia-inducible factor prolyl hydroxylases. *J Biol Chem* 2008, 283, (7), 3808-15.
36. Ivan, M.; Kondo, K.; Yang, H.; Kim, W.; Valiando, J.; Ohh, M.; Salic, A.; Asara, J. M.; Lane, W. S.; Kaelin, W. G., Jr., HIFalpha targeted for VHL-mediated destruction by proline hydroxylation: implications for O2 sensing. *Science* 2001, 292, (5516), 464-8.
37. Appelhoff, R. J.; Tian, Y. M.; Raval, R. R.; Turley, H.; Harris, A. L.; Pugh, C. W.; Ratcliffe, P. J.; Gleadle, J. M., Differential function of the prolyl hydroxylases PHD1, PHD2, and PHD3 in the regulation of hypoxia-inducible factor. *J Biol Chem* 2004, 279, (37), 38458-65.
38. Takeda, K.; Aguila, H. L.; Parikh, N. S.; Li, X.; Lamothe, K.; Duan, L. J.; Takeda, H.; Lee, F. S.; Fong, G. H., Regulation of adult erythropoiesis by prolyl hydroxylase domain proteins. *Blood* 2008, 111, (6), 3229-35.
39. Cummins, E. P.; Berra, E.; Comerford, K. M.; Ginouves, A.; Fitzgerald, K. T.; Seeballuck, F.; Godson, C.; Nielsen, J. E.; Moynagh, P.; Pouyssegur, J.; Taylor, C. T., Prolyl hydroxylase-1 negatively regulates IkappaB kinase-beta, giving insight into hypoxia-induced NFkappaB activity. *Proc Natl Acad Sci U S A* 2006, 103, (48), 18154-9.

40. Schmid, J. A.; Birbach, A., IkappaB kinase beta (IKKbeta/IKK2/IKBKB)--a key molecule in signaling to the transcription factor NF-kappaB. *Cytokine Growth Factor Rev* 2008, 19, (2), 157-65.
41. Tanaka, H.; Fujita, N.; Tsuruo, T., 3-Phosphoinositide-dependent protein kinase-1-mediated IkappaB kinase beta (IkkB) phosphorylation activates NF-kappaB signaling. *J Biol Chem* 2005, 280, (49), 40965-73.
42. Kuznetsova, A. V.; Meller, J.; Schnell, P. O.; Nash, J. A.; Ignacak, M. L.; Sanchez, Y.; Conaway, J. W.; Conaway, R. C.; Czyzyk-Krzeska, M. F., von Hippel-Lindau protein binds hyperphosphorylated large subunit of RNA polymerase II through a proline hydroxylation motif and targets it for ubiquitination. *Proc Natl Acad Sci U S A* 2003, 100, (5), 2706-11.
43. Xie, L.; Xiao, K.; Whalen, E. J.; Forrester, M. T.; Freeman, R. S.; Fong, G.; Gygi, S. P.; Lefkowitz, R. J.; Stamler, J. S., Oxygen-regulated beta(2)-adrenergic receptor hydroxylation by EGLN3 and ubiquitylation by pVHL. *Sci Signal* 2009, 2, (78), ra33.
44. Luo, W.; Hu, H.; Chang, R.; Zhong, J.; Knabel, M.; O'Meally, R.; Cole, R. N.; Pandey, A.; Semenza, G. L., Pyruvate kinase M2 is a PHD3-stimulated coactivator for hypoxia-inducible factor 1. *Cell* 2011, 145, (5), 732-44.
45. Luo, W.; Semenza, G. L., Pyruvate kinase M2 regulates glucose metabolism by functioning as a coactivator for hypoxia-inducible factor 1 in cancer cells. *Oncotarget* 2011, 2, (7), 551-6.
46. Dao, J. H.; Kurzeja, R. J.; Morachis, J. M.; Veith, H.; Lewis, J.; Yu, V.; Tegley, C. M.; Tagari, P., Kinetic characterization and identification of a novel inhibitor of hypoxia-inducible factor prolyl hydroxylase 2 using a time-resolved fluorescence resonance energy transfer-based assay technology. *Anal Biochem* 2009, 384, (2), 213-23.
47. Flashman, E.; Hoffart, L. M.; Hamed, R. B.; Bollinger, J. M., Jr.; Krebs, C.; Schofield, C. J., Evidence for the slow reaction of hypoxia-inducible factor prolyl hydroxylase 2 with oxygen. *FEBS J* 2010, 277, (19), 4089-99.
48. Taylor, M. S., Characterization and comparative analysis of the EGLN gene family. *Gene* 2001, 275, (1), 125-32.
49. Huang, J.; Zhao, Q.; Mooney, S. M.; Lee, F. S., Sequence determinants in hypoxia-inducible factor-1alpha for hydroxylation by the prolyl hydroxylases PHD1, PHD2, and PHD3. *J Biol Chem* 2002, 277, (42), 39792-800.
50. Dupuy, D.; Aubert, I.; Duperat, V. G.; Petit, J.; Taine, L.; Stef, M.; Bloch, B.; Arveiler, B., Mapping, characterization, and expression analysis of the SM-20 human homologue, c1orf12, and identification of a novel related gene, SCAND2. *Genomics* 2000, 69, (3), 348-54.
51. Oehme, F.; Ellinghaus, P.; Kolkhof, P.; Smith, T. J.; Ramakrishnan, S.; Hutter, J.; Schramm, M.; Flamme, I., Overexpression of PH-4, a novel putative proline 4-hydroxylase, modulates activity of hypoxia-inducible transcription factors. *Biochem Biophys Res Commun* 2002, 296, (2), 343-9.
52. Lieb, M. E.; Menzies, K.; Moschella, M. C.; Ni, R.; Taubman, M. B., Mammalian EGLN genes have distinct patterns of mRNA expression and regulation. *Biochem Cell Biol* 2002, 80, (4), 421-6.

53. Cioffi, C. L.; Liu, X. Q.; Kosinski, P. A.; Garay, M.; Bowen, B. R., Differential regulation of HIF-1 alpha prolyl-4-hydroxylase genes by hypoxia in human cardiovascular cells. *Biochem Biophys Res Commun* 2003, 303, (3), 947-53.
54. Metzen, E.; Berchner-Pfannschmidt, U.; Stengel, P.; Marxsen, J. H.; Stolze, I.; Klinger, M.; Huang, W. Q.; Wotzlaw, C.; Hellwig-Burgel, T.; Jelkmann, W.; Acker, H.; Fandrey, J., Intracellular localisation of human HIF-1 alpha hydroxylases: implications for oxygen sensing. *J Cell Sci* 2003, 116, (Pt 7), 1319-26.
55. Soilleux, E. J.; Turley, H.; Tian, Y. M.; Pugh, C. W.; Gatter, K. C.; Harris, A. L., Use of novel monoclonal antibodies to determine the expression and distribution of the hypoxia regulatory factors PHD-1, PHD-2, PHD-3 and FIH in normal and neoplastic human tissues. *Histopathology* 2005, 47, (6), 602-10.
56. Koivunen, P.; Tiainen, P.; Hyvarinen, J.; Williams, K. E.; Sormunen, R.; Klaus, S. J.; Kivirikko, K. I.; Myllyharju, J., An endoplasmic reticulum transmembrane prolyl 4-hydroxylase is induced by hypoxia and acts on hypoxia-inducible factor alpha. *J Biol Chem* 2007, 282, (42), 30544-52.
57. Takeda, K.; Ho, V. C.; Takeda, H.; Duan, L. J.; Nagy, A.; Fong, G. H., Placental but not heart defects are associated with elevated hypoxia-inducible factor alpha levels in mice lacking prolyl hydroxylase domain protein 2. *Mol Cell Biol* 2006, 26, (22), 8336-46.
58. Holscher, M.; Silter, M.; Krull, S.; von Ahlen, M.; Hesse, A.; Schwartz, P.; Wielockx, B.; Breier, G.; Katschinski, D. M.; Zieseniss, A., Cardiomyocyte-specific prolyl-4-hydroxylase domain 2 knock out protects from acute myocardial ischemic injury. *J Biol Chem* 2011, 286, (13), 11185-94.
59. Ameln, A. K.; Muschter, A.; Mamlouk, S.; Kalucka, J.; Prade, I.; Franke, K.; Rezaei, M.; Poitz, D. M.; Breier, G.; Wielockx, B., Inhibition of HIF prolyl hydroxylase-2 blocks tumor growth in mice through the antiproliferative activity of TGFbeta. *Cancer Res* 2011, 71, (9), 3306-16.
60. Tian, M.; Schiemann, W. P., The TGF-beta paradox in human cancer: an update. *Future Oncol* 2009, 5, (2), 259-71.
61. Siddiq, A.; Aminova, L. R.; Troy, C. M.; Suh, K.; Messer, Z.; Semenza, G. L.; Ratan, R. R., Selective inhibition of hypoxia-inducible factor (HIF) prolyl-hydroxylase 1 mediates neuroprotection against normoxic oxidative death via HIF- and CREB-independent pathways. *J Neurosci* 2009, 29, (27), 8828-38.
62. Eggert, U. S.; Field, C. M.; Mitchison, T. J., Small molecules in an RNAi world. *Mol Biosyst* 2006, 2, (2), 93-6.
63. Shrivastava, N.; Srivastava, A., RNA interference: an emerging generation of biologicals. *Biotechnol J* 2008, 3, (3), 339-53.
64. Lehar, J.; Stockwell, B. R.; Giaever, G.; Nislow, C., Combination chemical genetics. *Nat Chem Biol* 2008, 4, (11), 674-81.
65. Sharom, J. R.; Bellows, D. S.; Tyers, M., From large networks to small molecules. *Curr Opin Chem Biol* 2004, 8, (1), 81-90.
66. Hirsila, M.; Koivunen, P.; Xu, L.; Seeley, T.; Kivirikko, K. I.; Myllyharju, J., Effect of desferrioxamine and metals on the hydroxylases in the oxygen sensing pathway. *FASEB J* 2005, 19, (10), 1308-10.

67. Semenza, G. L., Defining the role of hypoxia-inducible factor 1 in cancer biology and therapeutics. *Oncogene* 2010, 29, (5), 625-34.
68. Sekirnik, R.; Rose, N. R.; Mecinovic, J.; Schofield, C. J., 2-Oxoglutarate oxygenases are inhibited by a range of transition metals. *Metallomics* 2010, 2, (6), 397-9.
69. Chen, H.; Costa, M., Iron- and 2-oxoglutarate-dependent dioxygenases: an emerging group of molecular targets for nickel toxicity and carcinogenicity. *Biometals* 2009, 22, (1), 191-6.
70. Muchnik, E.; Kaplan, J., HIF prolyl hydroxylase inhibitors for anemia. *Expert Opin Investig Drugs* 2011, 20, (5), 645-56.
71. Hirota, S. A.; Beck, P. L.; MacDonald, J. A., Targeting hypoxia-inducible factor-1 (HIF-1) signaling in therapeutics: implications for the treatment of inflammatory bowel disease. *Recent Pat Inflamm Allergy Drug Discov* 2009, 3, (1), 1-16.
72. Miyata, T.; Takizawa, S.; van Ypersele de Strihou, C., Hypoxia. 1. Intracellular sensors for oxygen and oxidative stress: novel therapeutic targets. *Am J Physiol Cell Physiol* 2011, 300, (2), C226-31.
73. Gunaratnam, L.; Bonventre, J. V., HIF in kidney disease and development. *J Am Soc Nephrol* 2009, 20, (9), 1877-87.
74. Yan, L.; Colandrea, V. J.; Hale, J. J., Prolyl hydroxylase domain-containing protein inhibitors as stabilizers of hypoxia-inducible factor: small molecule-based therapeutics for anemia. *Expert Opin Ther Pat* 2010, 20, (9), 1219-45.
75. Fisher, J. W., Erythropoietin: pharmacology, biogenesis and control of production. *Pharmacol Rev* 1972, 24, (3), 459-508.
76. Hsieh, M. M.; Linde, N. S.; Wynter, A.; Metzger, M.; Wong, C.; Langsetmo, I.; Lin, A.; Smith, R.; Rodgers, G. P.; Donahue, R. E.; Klaus, S. J.; Tisdale, J. F., HIF prolyl hydroxylase inhibition results in endogenous erythropoietin induction, erythrocytosis, and modest fetal hemoglobin expression in rhesus macaques. *Blood* 2007, 110, (6), 2140-7.
77. Thevis, M.; Kohler, M.; Schlorer, N.; Schanzer, W., Gas phase reaction of substituted isoquinolines to carboxylic acids in ion trap and triple quadrupole mass spectrometers after electrospray ionization and collision-induced dissociation. *J Am Soc Mass Spectrom* 2008, 19, (1), 151-8.
78. R Provenzano, G. F., M Bernardo, C James, G Kochendoerfer, T Lee, S Nakayama, T Neff, BA Piper *FG2216, A NOVEL ORAL HIF-PHI, STIMULATES ERYTHROPOIESIS AND INCREASES HEMOGLOBIN CONCENTRATION IN PATIENTS WITH NON-DIALYSIS CKD* 2008; p 120.
79. Bernhardt, W. M.; Wiesener, M. S.; Scigalla, P.; Chou, J.; Schmieder, R. E.; Gunzler, V.; Eckardt, K. U., Inhibition of prolyl hydroxylases increases erythropoietin production in ESRD. *J Am Soc Nephrol* 2010, 21, (12), 2151-6.
80. Pan, Y.; Mansfield, K. D.; Bertozzi, C. C.; Rudenko, V.; Chan, D. A.; Giaccia, A. J.; Simon, M. C., Multiple factors affecting cellular redox status and energy metabolism modulate hypoxia-inducible factor prolyl hydroxylase activity in vivo and in vitro. *Mol Cell Biol* 2007, 27, (3), 912-25.

81. Hewitson, K. S.; Lienard, B. M.; McDonough, M. A.; Clifton, I. J.; Butler, D.; Soares, A. S.; Oldham, N. J.; McNeill, L. A.; Schofield, C. J., Structural and mechanistic studies on the inhibition of the hypoxia-inducible transcription factor hydroxylases by tricarboxylic acid cycle intermediates. *J Biol Chem* 2007, 282, (5), 3293-301.
82. Lienard, B. M.; Conejo-Garcia, A.; Stolze, I.; Loenarz, C.; Oldham, N. J.; Ratcliffe, P. J.; Schofield, C. J., Evaluation of aspirin metabolites as inhibitors of hypoxia-inducible factor hydroxylases. *Chem Commun (Camb)* 2008, (47), 6393-5.
83. Mace, K. A.; Yu, D. H.; Paydar, K. Z.; Boudreau, N.; Young, D. M., Sustained expression of Hif-1alpha in the diabetic environment promotes angiogenesis and cutaneous wound repair. *Wound Repair Regen* 2007, 15, (5), 636-45.
84. Botusan, I. R.; Sunkari, V. G.; Savu, O.; Catrina, A. I.; Grunler, J.; Lindberg, S.; Pereira, T.; Yla-Herttuala, S.; Poellinger, L.; Brismar, K.; Catrina, S. B., Stabilization of HIF-1alpha is critical to improve wound healing in diabetic mice. *Proc Natl Acad Sci U S A* 2008, 105, (49), 19426-31.
85. Pajusola, K.; Kunnapuu, J.; Vuorikoski, S.; Soronen, J.; Andre, H.; Pereira, T.; Korpisalo, P.; Yla-Herttuala, S.; Poellinger, L.; Alitalo, K., Stabilized HIF-1alpha is superior to VEGF for angiogenesis in skeletal muscle via adeno-associated virus gene transfer. *FASEB J* 2005, 19, (10), 1365-7.
86. Rey, S.; Semenza, G. L., Hypoxia-inducible factor-1-dependent mechanisms of vascularization and vascular remodelling. *Cardiovasc Res* 2010, 86, (2), 236-42.
87. Pichiule, P.; Agani, F.; Chavez, J. C.; Xu, K.; LaManna, J. C., HIF-1 alpha and VEGF expression after transient global cerebral ischemia. *Adv Exp Med Biol* 2003, 530, 611-7.
88. Fraisl, P.; Aragones, J.; Carmeliet, P., Inhibition of oxygen sensors as a therapeutic strategy for ischaemic and inflammatory disease. *Nat Rev Drug Discov* 2009, 8, (2), 139-52.
89. Semenza, G. L., HIF-1 and tumor progression: pathophysiology and therapeutics. *Trends Mol Med* 2002, 8, (4 Suppl), S62-7.
90. Boulahbel, H.; Duran, R. V.; Gottlieb, E., Prolyl hydroxylases as regulators of cell metabolism. *Biochem Soc Trans* 2009, 37, (Pt 1), 291-4.
91. DeBerardinis, R. J.; Lum, J. J.; Hatzivassiliou, G.; Thompson, C. B., The biology of cancer: metabolic reprogramming fuels cell growth and proliferation. *Cell Metab* 2008, 7, (1), 11-20.
92. Vander Heiden, M. G.; Cantley, L. C.; Thompson, C. B., Understanding the Warburg effect: the metabolic requirements of cell proliferation. *Science* 2009, 324, (5930), 1029-33.
93. Board, M.; Humm, S.; Newsholme, E. A., Maximum activities of key enzymes of glycolysis, glutaminolysis, pentose phosphate pathway and tricarboxylic acid cycle in normal, neoplastic and suppressed cells. *Biochem J* 1990, 265, (2), 503-9.
94. Piva, T. J.; McEvoy-Bowe, E., Oxidation of glutamine in HeLa cells: role and control of truncated TCA cycles in tumour mitochondria. *J Cell Biochem* 1998, 68, (2), 213-25.

95. Kannan, R.; Lyon, I.; Baker, N., Dietary control of lipogenesis in vivo in host tissues and tumors of mice bearing Ehrlich ascites carcinoma. *Cancer Res* 1980, 40, (12), 4606-11.
96. Ookhtens, M.; Kannan, R.; Lyon, I.; Baker, N., Liver and adipose tissue contributions to newly formed fatty acids in an ascites tumor. *Am J Physiol* 1984, 247, (1 Pt 2), R146-53.
97. Warburg, O., On the origin of cancer cells. *Science* 1956, 123, (3191), 309-14.
98. Lum, J. J.; Bauer, D. E.; Kong, M.; Harris, M. H.; Li, C.; Lindsten, T.; Thompson, C. B., Growth factor regulation of autophagy and cell survival in the absence of apoptosis. *Cell* 2005, 120, (2), 237-48.
99. Isaacs, J. S.; Jung, Y. J.; Mole, D. R.; Lee, S.; Torres-Cabala, C.; Chung, Y. L.; Merino, M.; Trepel, J.; Zbar, B.; Toro, J.; Ratcliffe, P. J.; Linehan, W. M.; Neckers, L., HIF overexpression correlates with biallelic loss of fumarate hydratase in renal cancer: novel role of fumarate in regulation of HIF stability. *Cancer Cell* 2005, 8, (2), 143-53.
100. Koivunen, P.; Hirsila, M.; Remes, A. M.; Hassinen, I. E.; Kivirikko, K. I.; Myllyharju, J., Inhibition of hypoxia-inducible factor (HIF) hydroxylases by citric acid cycle intermediates: possible links between cell metabolism and stabilization of HIF. *J Biol Chem* 2007, 282, (7), 4524-32.
101. Kaelin, W. G., Jr., SDH5 mutations and familial paraganglioma: somewhere Warburg is smiling. *Cancer Cell* 2009, 16, (3), 180-2.
102. O'Flaherty, L.; Adam, J.; Heather, L. C.; Zhdanov, A. V.; Chung, Y. L.; Miranda, M. X.; Croft, J.; Olpin, S.; Clarke, K.; Pugh, C. W.; Griffiths, J.; Papkovsky, D.; Ashrafian, H.; Ratcliffe, P. J.; Pollard, P. J., Dysregulation of hypoxia pathways in fumarate hydratase-deficient cells is independent of defective mitochondrial metabolism. *Hum Mol Genet* 2010, 19, (19), 3844-51.
103. Zhao, S.; Lin, Y.; Xu, W.; Jiang, W.; Zha, Z.; Wang, P.; Yu, W.; Li, Z.; Gong, L.; Peng, Y.; Ding, J.; Lei, Q.; Guan, K. L.; Xiong, Y., Glioma-derived mutations in IDH1 dominantly inhibit IDH1 catalytic activity and induce HIF-1alpha. *Science* 2009, 324, (5924), 261-5.
104. MacKenzie, E. D.; Selak, M. A.; Tennant, D. A.; Payne, L. J.; Crosby, S.; Frederiksen, C. M.; Watson, D. G.; Gottlieb, E., Cell-permeating alpha-ketoglutarate derivatives alleviate pseudohypoxia in succinate dehydrogenase-deficient cells. *Mol Cell Biol* 2007, 27, (9), 3282-9.
105. Parsons, D. W.; Jones, S.; Zhang, X.; Lin, J. C.; Leary, R. J.; Angenendt, P.; Mankoo, P.; Carter, H.; Siu, I. M.; Gallia, G. L.; Olivi, A.; McLendon, R.; Rasheed, B. A.; Keir, S.; Nikolskaya, T.; Nikolsky, Y.; Busam, D. A.; Tekleab, H.; Diaz, L. A., Jr.; Hartigan, J.; Smith, D. R.; Strausberg, R. L.; Marie, S. K.; Shinjo, S. M.; Yan, H.; Riggins, G. J.; Bigner, D. D.; Karchin, R.; Papadopoulos, N.; Parmigiani, G.; Vogelstein, B.; Velculescu, V. E.; Kinzler, K. W., An integrated genomic analysis of human glioblastoma multiforme. *Science* 2008, 321, (5897), 1807-12.

106. Yan, H.; Parsons, D. W.; Jin, G.; McLendon, R.; Rasheed, B. A.; Yuan, W.; Kos, I.; Batinic-Haberle, I.; Jones, S.; Riggins, G. J.; Friedman, H.; Friedman, A.; Reardon, D.; Herndon, J.; Kinzler, K. W.; Velculescu, V. E.; Vogelstein, B.; Bigner, D. D., IDH1 and IDH2 mutations in gliomas. *N Engl J Med* 2009, 360, (8), 765-73.
107. Mardis, E. R.; Ding, L.; Dooling, D. J.; Larson, D. E.; McLellan, M. D.; Chen, K.; Koboldt, D. C.; Fulton, R. S.; Delehaunty, K. D.; McGrath, S. D.; Fulton, L. A.; Locke, D. P.; Magrini, V. J.; Abbott, R. M.; Vickery, T. L.; Reed, J. S.; Robinson, J. S.; Wylie, T.; Smith, S. M.; Carmichael, L.; Eldred, J. M.; Harris, C. C.; Walker, J.; Peck, J. B.; Du, F.; Dukes, A. F.; Sanderson, G. E.; Brummett, A. M.; Clark, E.; McMichael, J. F.; Meyer, R. J.; Schindler, J. K.; Pohl, C. S.; Wallis, J. W.; Shi, X.; Lin, L.; Schmidt, H.; Tang, Y.; Haipek, C.; Wiechert, M. E.; Ivy, J. V.; Kalicki, J.; Elliott, G.; Ries, R. E.; Payton, J. E.; Westervelt, P.; Tomasson, M. H.; Watson, M. A.; Baty, J.; Heath, S.; Shannon, W. D.; Nagarajan, R.; Link, D. C.; Walter, M. J.; Graubert, T. A.; DiPersio, J. F.; Wilson, R. K.; Ley, T. J., Recurring mutations found by sequencing an acute myeloid leukemia genome. *N Engl J Med* 2009, 361, (11), 1058-66.
108. Dang, L.; Jin, S.; Su, S. M., IDH mutations in glioma and acute myeloid leukemia. *Trends Mol Med* 2010, 16, (9), 387-97.
109. Dang, L.; White, D. W.; Gross, S.; Bennett, B. D.; Bittinger, M. A.; Driggers, E. M.; Fantin, V. R.; Jang, H. G.; Jin, S.; Keenan, M. C.; Marks, K. M.; Prins, R. M.; Ward, P. S.; Yen, K. E.; Liau, L. M.; Rabinowitz, J. D.; Cantley, L. C.; Thompson, C. B.; Vander Heiden, M. G.; Su, S. M., Cancer-associated IDH1 mutations produce 2-hydroxyglutarate. *Nature* 2009, 462, (7274), 739-44.
110. Gross, S.; Cairns, R. A.; Minden, M. D.; Driggers, E. M.; Bittinger, M. A.; Jang, H. G.; Sasaki, M.; Jin, S.; Schenkein, D. P.; Su, S. M.; Dang, L.; Fantin, V. R.; Mak, T. W., Cancer-associated metabolite 2-hydroxyglutarate accumulates in acute myelogenous leukemia with isocitrate dehydrogenase 1 and 2 mutations. *J Exp Med* 2010, 207, (2), 339-44.
111. Ward, P. S.; Patel, J.; Wise, D. R.; Abdel-Wahab, O.; Bennett, B. D.; Coller, H. A.; Cross, J. R.; Fantin, V. R.; Hedvat, C. V.; Perl, A. E.; Rabinowitz, J. D.; Carroll, M.; Su, S. M.; Sharp, K. A.; Levine, R. L.; Thompson, C. B., The common feature of leukemia-associated IDH1 and IDH2 mutations is a neomorphic enzyme activity converting alpha-ketoglutarate to 2-hydroxyglutarate. *Cancer Cell* 2010, 17, (3), 225-34.
112. Bauer, D. E.; Harris, M. H.; Plas, D. R.; Lum, J. J.; Hammerman, P. S.; Rathmell, J. C.; Riley, J. L.; Thompson, C. B., Cytokine stimulation of aerobic glycolysis in hematopoietic cells exceeds proliferative demand. *FASEB J* 2004, 18, (11), 1303-5.
113. Elstrom, R. L.; Bauer, D. E.; Buzzai, M.; Karnauskas, R.; Harris, M. H.; Plas, D. R.; Zhuang, H.; Cinalli, R. M.; Alavi, A.; Rudin, C. M.; Thompson, C. B., Akt stimulates aerobic glycolysis in cancer cells. *Cancer Res* 2004, 64, (11), 3892-9.
114. Roos, S.; Jansson, N.; Palmberg, I.; Saljo, K.; Powell, T. L.; Jansson, T., Mammalian target of rapamycin in the human placenta regulates leucine transport and is down-regulated in restricted fetal growth. *J Physiol* 2007, 582, (Pt 1), 449-59.

115. Gingras, A. C.; Raught, B.; Sonenberg, N., Regulation of translation initiation by FRAP/mTOR. *Genes Dev* 2001, 15, (7), 807-26.
116. Ohgaki, H., Genetic pathways to glioblastomas. *Neuropathology* 2005, 25, (1), 1-7.
117. Presneau, N.; Shalaby, A.; Idowu, B.; Gikas, P.; Cannon, S. R.; Gout, I.; Diss, T.; Tirabosco, R.; Flanagan, A. M., Potential therapeutic targets for chordoma: PI3K/AKT/TSC1/TSC2/mTOR pathway. *Br J Cancer* 2009, 100, (9), 1406-14.
118. Pore, N.; Jiang, Z.; Shu, H. K.; Bernhard, E.; Kao, G. D.; Maity, A., Akt1 activation can augment hypoxia-inducible factor-1alpha expression by increasing protein translation through a mammalian target of rapamycin-independent pathway. *Mol Cancer Res* 2006, 4, (7), 471-9.
119. Jiang, B. H.; Jiang, G.; Zheng, J. Z.; Lu, Z.; Hunter, T.; Vogt, P. K., Phosphatidylinositol 3-kinase signaling controls levels of hypoxia-inducible factor 1. *Cell Growth Differ* 2001, 12, (7), 363-9.
120. Majumder, P. K.; Febbo, P. G.; Bikoff, R.; Berger, R.; Xue, Q.; McMahon, L. M.; Manola, J.; Brugarolas, J.; McDonnell, T. J.; Golub, T. R.; Loda, M.; Lane, H. A.; Sellers, W. R., mTOR inhibition reverses Akt-dependent prostate intraepithelial neoplasia through regulation of apoptotic and HIF-1-dependent pathways. *Nat Med* 2004, 10, (6), 594-601.
121. Soucek, T.; Cumming, R.; Dargusch, R.; Maher, P.; Schubert, D., The regulation of glucose metabolism by HIF-1 mediates a neuroprotective response to amyloid beta peptide. *Neuron* 2003, 39, (1), 43-56.
122. Song, I. S.; Wang, A. G.; Yoon, S. Y.; Kim, J. M.; Kim, J. H.; Lee, D. S.; Kim, N. S., Regulation of glucose metabolism-related genes and VEGF by HIF-1alpha and HIF-1beta, but not HIF-2alpha, in gastric cancer. *Exp Mol Med* 2009, 41, (1), 51-8.
123. Dang, C. V., Rethinking the Warburg effect with Myc micromanaging glutamine metabolism. *Cancer Res* 2010, 70, (3), 859-62.
124. Dang, C. V.; Le, A.; Gao, P., MYC-induced cancer cell energy metabolism and therapeutic opportunities. *Clin Cancer Res* 2009, 15, (21), 6479-83.
125. Gao, P.; Tchernyshyov, I.; Chang, T. C.; Lee, Y. S.; Kita, K.; Ochi, T.; Zeller, K. I.; De Marzo, A. M.; Van Eyk, J. E.; Mendell, J. T.; Dang, C. V., c-Myc suppression of miR-23a/b enhances mitochondrial glutaminase expression and glutamine metabolism. *Nature* 2009, 458, (7239), 762-5.
126. Myllyharju, J.; Kivirikko, K. I., Collagens and collagen-related diseases. *Ann Med* 2001, 33, (1), 7-21.
127. Franklin, T. J., Therapeutic approaches to organ fibrosis. *Int J Biochem Cell Biol* 1997, 29, (1), 79-89.
128. Brodsky, B.; Shah, N. K., Protein motifs. 8. The triple-helix motif in proteins. *FASEB J* 1995, 9, (15), 1537-46.
129. Krane, S. M., The importance of proline residues in the structure, stability and susceptibility to proteolytic degradation of collagens. *Amino Acids* 2008, 35, (4), 703-10.
130. Heikkinen, J.; Risteli, M.; Wang, C.; Latvala, J.; Rossi, M.; Valtavaara, M.; Myllyla, R., Lysyl hydroxylase 3 is a multifunctional protein possessing collagen glucosyltransferase activity. *J Biol Chem* 2000, 275, (46), 36158-63.

131. Tsukada, Y.; Fang, J.; Erdjument-Bromage, H.; Warren, M. E.; Borchers, C. H.; Tempst, P.; Zhang, Y., Histone demethylation by a family of JmjC domain-containing proteins. *Nature* 2006, 439, (7078), 811-6.
132. He, J.; Kallin, E. M.; Tsukada, Y.; Zhang, Y., The H3K36 demethylase Jhdm1b/Kdm2b regulates cell proliferation and senescence through p15(Ink4b). *Nat Struct Mol Biol* 2008, 15, (11), 1169-75.
133. Klose, R. J.; Zhang, Y., Regulation of histone methylation by demethylimination and demethylation. *Nat Rev Mol Cell Biol* 2007, 8, (4), 307-18.
134. Zeng, J.; Ge, Z.; Wang, L.; Li, Q.; Wang, N.; Bjorkholm, M.; Jia, J.; Xu, D., The histone demethylase RBP2 Is overexpressed in gastric cancer and its inhibition triggers senescence of cancer cells. *Gastroenterology* 2010, 138, (3), 981-92.
135. Yamane, K.; Tateishi, K.; Klose, R. J.; Fang, J.; Fabrizio, L. A.; Erdjument-Bromage, H.; Taylor-Papadimitriou, J.; Tempst, P.; Zhang, Y., PLU-1 is an H3K4 demethylase involved in transcriptional repression and breast cancer cell proliferation. *Mol Cell* 2007, 25, (6), 801-12.
136. Xiang, Y.; Zhu, Z.; Han, G.; Ye, X.; Xu, B.; Peng, Z.; Ma, Y.; Yu, Y.; Lin, H.; Chen, A. P.; Chen, C. D., JARID1B is a histone H3 lysine 4 demethylase up-regulated in prostate cancer. *Proc Natl Acad Sci U S A* 2007, 104, (49), 19226-31.
137. Shin, S.; Janknecht, R., Activation of androgen receptor by histone demethylases JMJD2A and JMJD2D. *Biochem Biophys Res Commun* 2007, 359, (3), 742-6.
138. Cloos, P. A.; Christensen, J.; Agger, K.; Maiolica, A.; Rappsilber, J.; Antal, T.; Hansen, K. H.; Helin, K., The putative oncogene GASC1 demethylates tri- and dimethylated lysine 9 on histone H3. *Nature* 2006, 442, (7100), 307-11.
139. King, O. N.; Li, X. S.; Sakurai, M.; Kawamura, A.; Rose, N. R.; Ng, S. S.; Quinn, A. M.; Rai, G.; Mott, B. T.; Beswick, P.; Klose, R. J.; Oppermann, U.; Jadhav, A.; Heightman, T. D.; Maloney, D. J.; Schofield, C. J.; Simeonov, A., Quantitative high-throughput screening identifies 8-hydroxyquinolines as cell-active histone demethylase inhibitors. *PLoS One* 2010, 5, (11), e15535.
140. Myllyharju, J., HIF prolyl 4-hydroxylases and their potential as drug targets. *Curr Pharm Des* 2009, 15, (33), 3878-85.
141. Chan, D. A.; Sutphin, P. D.; Yen, S. E.; Giaccia, A. J., Coordinate regulation of the oxygen-dependent degradation domains of hypoxia-inducible factor 1 alpha. *Mol Cell Biol* 2005, 25, (15), 6415-26.
142. Tian, Y.-M.; Yeoh, K. K.; Lee, M. K.; Eriksson, T.; Kessler, B. M.; Kramer, H. B.; Edelmann, M. J.; Willam, C.; Pugh, C. W.; Schofield, C. J.; Ratcliffe, P. J., Differential Sensitivity of Hypoxia Inducible Factor Hydroxylation Sites to Hypoxia and Hydroxylase Inhibitors. *Journal of Biological Chemistry* 2011, 286, (15), 13041-13051.
143. Lee, S. H.; Jeong Hee, M.; Eun Ah, C.; Ryu, S. E.; Myung Kyu, L., Monoclonal antibody-based screening assay for factor inhibiting hypoxia-inducible factor inhibitors. *J Biomol Screen* 2008, 13, (6), 494-503.
144. Chan, D. A.; Sutphin, P. D.; Denko, N. C.; Giaccia, A. J., Role of prolyl hydroxylation in oncogenically stabilized hypoxia-inducible factor-1alpha. *J Biol Chem* 2002, 277, (42), 40112-7.

145. Nardinocchi, L.; Pantisano, V.; Puca, R.; Porru, M.; Aiello, A.; Grasselli, A.; Leonetti, C.; Safran, M.; Rechavi, G.; Givol, D.; Farsetti, A.; D'Orazi, G., Zinc downregulates HIF-1alpha and inhibits its activity in tumor cells in vitro and in vivo. *PLoS One* 2010, 5, (12), e15048.
146. Sowter, H. M.; Raval, R. R.; Moore, J. W.; Ratcliffe, P. J.; Harris, A. L., Predominant role of hypoxia-inducible transcription factor (Hif)-1alpha versus Hif-2alpha in regulation of the transcriptional response to hypoxia. *Cancer Res* 2003, 63, (19), 6130-4.
147. Banerji, B.; Conejo-Garcia, A.; McNeill, L. A.; McDonough, M. A.; Buck, M. R.; Hewitson, K. S.; Oldham, N. J.; Schofield, C. J., The inhibition of factor inhibiting hypoxia-inducible factor (FIH) by beta-oxocarboxylic acids. *Chem Commun (Camb)* 2005, (43), 5438-40.
148. Kang, G. S.; Li, Q.; Chen, H.; Costa, M., Effect of metal ions on HIF-1alpha and Fe homeostasis in human A549 cells. *Mutat Res* 2006, 610, (1-2), 48-55.
149. Tschank, G.; Raghunath, M.; Gunzler, V.; Hanauske-Abel, H. M., Pyridinedicarboxylates, the first mechanism-derived inhibitors for prolyl 4-hydroxylase, selectively suppress cellular hydroxyprolyl biosynthesis. Decrease in interstitial collagen and Clq secretion in cell culture. *Biochem J* 1987, 248, (3), 625-33.
150. Leung, I. K.; Krojer, T. J.; Kochan, G. T.; Henry, L.; von Delft, F.; Claridge, T. D.; Oppermann, U.; McDonough, M. A.; Schofield, C. J., Structural and mechanistic studies on gamma-butyrobetaine hydroxylase. *Chem Biol* 2010, 17, (12), 1316-24.
151. Clement, B.; Chesne, C.; Satie, A. P.; Guillouzo, A., Effects of the prolyl 4-hydroxylase proinhibitor HOE 077 on human and rat hepatocytes in primary culture. *J Hepatol* 1991, 13 Suppl 3, S41-7.
152. Matsumura, Y.; Sakaida, I.; Uchida, K.; Kimura, T.; Ishihara, T.; Okita, K., Prolyl 4-hydroxylase inhibitor (HOE 077) inhibits pig serum-induced rat liver fibrosis by preventing stellate cell activation. *J Hepatol* 1997, 27, (1), 185-92.
153. Ito, Y.; Ahmad, A.; Kewley, E.; Mason, R. J., Hypoxia Inducible Factor Regulates Surfactant Protein Expression in Alveolar Type II Cells in vitro. *Am J Respir Cell Mol Biol* 2011.
154. Cummins, E. P.; Seeballuck, F.; Keely, S. J.; Mangan, N. E.; Callanan, J. J.; Fallon, P. G.; Taylor, C. T., The hydroxylase inhibitor dimethyloxalylglycine is protective in a murine model of colitis. *Gastroenterology* 2008, 134, (1), 156-65.
155. Takeda, K.; Ichiki, T.; Narabayashi, E.; Inanaga, K.; Miyazaki, R.; Hashimoto, T.; Matsuura, H.; Ikeda, J.; Miyata, T.; Sunagawa, K., Inhibition of prolyl hydroxylase domain-containing protein suppressed lipopolysaccharide-induced TNF-alpha expression. *Arterioscler Thromb Vasc Biol* 2009, 29, (12), 2132-7.
156. Kivirikko, K. I.; Myllyharju, J., Prolyl 4-hydroxylases and their protein disulfide isomerase subunit. *Matrix Biol* 1998, 16, (7), 357-68.
157. McNeill, L. A.; Flashman, E.; Buck, M. R.; Hewitson, K. S.; Clifton, I. J.; Jeschke, G.; Claridge, T. D.; Ehrismann, D.; Oldham, N. J.; Schofield, C. J., Hypoxia-inducible factor prolyl hydroxylase 2 has a high affinity for ferrous iron and 2-oxoglutarate. *Mol Biosyst* 2005, 1, (4), 321-4.

158. Yuan, Y.; Hilliard, G.; Ferguson, T.; Millhorn, D. E., Cobalt inhibits the interaction between hypoxia-inducible factor-alpha and von Hippel-Lindau protein by direct binding to hypoxia-inducible factor-alpha. *J Biol Chem* 2003, 278, (18), 15911-6.
159. Salnikow, K.; Donald, S. P.; Bruick, R. K.; Zhitkovich, A.; Phang, J. M.; Kasprzak, K. S., Depletion of intracellular ascorbate by the carcinogenic metals nickel and cobalt results in the induction of hypoxic stress. *J Biol Chem* 2004, 279, (39), 40337-44.
160. Bruegge, K.; Jelkmann, W.; Metzen, E., Hydroxylation of hypoxia-inducible transcription factors and chemical compounds targeting the HIF-alpha hydroxylases. *Curr Med Chem* 2007, 14, (17), 1853-62.
161. McDonough, M. A.; McNeill, L. A.; Tilliet, M.; Papamicael, C. A.; Chen, Q. Y.; Banerji, B.; Hewitson, K. S.; Schofield, C. J., Selective inhibition of factor inhibiting hypoxia-inducible factor. *J Am Chem Soc* 2005, 127, (21), 7680-1.
162. Warshakoon, N. C.; Wu, S.; Boyer, A.; Kawamoto, R.; Sheville, J.; Renock, S.; Xu, K.; Pokross, M.; Zhou, S.; Winter, C.; Walter, R.; Mekel, M.; Evdokimov, A. G., Structure-based design, synthesis, and SAR evaluation of a new series of 8-hydroxyquinolines as HIF-1alpha prolyl hydroxylase inhibitors. *Bioorg Med Chem Lett* 2006, 16, (21), 5517-22.
163. Kawamura, A.; Tumber, A.; Rose, N. R.; King, O. N.; Daniel, M.; Oppermann, U.; Heightman, T. D.; Schofield, C., Development of homogeneous luminescence assays for histone demethylase catalysis and binding. *Anal Biochem* 2010, 404, (1), 86-93.
164. Ullman, E. F.; Kirakossian, H.; Singh, S.; Wu, Z. P.; Irvin, B. R.; Pease, J. S.; Switchenko, A. C.; Irvine, J. D.; Dafforn, A.; Skold, C. N.; et al., Luminescent oxygen channeling immunoassay: measurement of particle binding kinetics by chemiluminescence. *Proc Natl Acad Sci U S A* 1994, 91, (12), 5426-30.
165. Stubbs, C. J.; Loenarz, C.; Mecinovic, J.; Yeoh, K. K.; Hindley, N.; Lienard, B. M.; Sobott, F.; Schofield, C. J.; Flashman, E., Application of a proteolysis/mass spectrometry method for investigating the effects of inhibitors on hydroxylase structure. *J Med Chem* 2009, 52, (9), 2799-805.
166. Rose, N. R.; Ng, S. S.; Mecinovic, J.; Lienard, B. M.; Bello, S. H.; Sun, Z.; McDonough, M. A.; Oppermann, U.; Schofield, C. J., Inhibitor scaffolds for 2-oxoglutarate-dependent histone lysine demethylases. *J Med Chem* 2008, 51, (22), 7053-6.
167. Coleman, M. L.; McDonough, M. A.; Hewitson, K. S.; Coles, C.; Mecinovic, J.; Edelmann, M.; Cook, K. M.; Cockman, M. E.; Lancaster, D. E.; Kessler, B. M.; Oldham, N. J.; Ratcliffe, P. J.; Schofield, C. J., Asparaginyl hydroxylation of the Notch ankyrin repeat domain by factor inhibiting hypoxia-inducible factor. *J Biol Chem* 2007, 282, (33), 24027-38.
168. Wilkins, S. E.; Hyvarinen, J.; Chicher, J.; Gorman, J. J.; Peet, D. J.; Bilton, R. L.; Koivunen, P., Differences in hydroxylation and binding of Notch and HIF-1alpha demonstrate substrate selectivity for factor inhibiting HIF-1 (FIH-1). *Int J Biochem Cell Biol* 2009, 41, (7), 1563-71.

169. Cockman, M. E.; Webb, J. D.; Kramer, H. B.; Kessler, B. M.; Ratcliffe, P. J., Proteomics-based identification of novel factor inhibiting hypoxia-inducible factor (FIH) substrates indicates widespread asparaginyl hydroxylation of ankyrin repeat domain-containing proteins. *Mol Cell Proteomics* 2009, 8, (3), 535-46.
170. Cockman, M. E.; Lancaster, D. E.; Stolze, I. P.; Hewitson, K. S.; McDonough, M. A.; Coleman, M. L.; Coles, C. H.; Yu, X.; Hay, R. T.; Ley, S. C.; Pugh, C. W.; Oldham, N. J.; Masson, N.; Schofield, C. J.; Ratcliffe, P. J., Posttranslational hydroxylation of ankyrin repeats in IkappaB proteins by the hypoxia-inducible factor (HIF) asparaginyl hydroxylase, factor inhibiting HIF (FIH). *Proc Natl Acad Sci U S A* 2006, 103, (40), 14767-72.
171. Yang, M.; Ge, W.; Chowdhury, R.; Claridge, T. D.; Kramer, H. B.; Schmierer, B.; McDonough, M. A.; Gong, L.; Kessler, B. M.; Ratcliffe, P. J.; Coleman, M. L.; Schofield, C. J., Asparagine and aspartate hydroxylation of the cytoskeletal ankyrin family is catalyzed by factor-inhibiting hypoxia-inducible factor. *J Biol Chem* 2011, 286, (9), 7648-60.
172. GlaxoSmithKline Prolyl hydroxylase antagonists. 2007.
173. GlaxoSmithKline Prolyl hydroxylase inhibitors. 2007.
174. GlaxoSmithKline Prolyl hydroxylase inhibitors. 2010.
175. Amgen Azaquinolone based compounds exhibiting prolyl hydroxylase inhibitory activity, compositions, and uses thereof. 2008.
176. Amgen Quinolones and azaquinolones that inhibit prolyl hydroxylase. 2008.
177. Amgen Diazaquinolones that inhibit prolyl hydroxylase activity. 2008.
178. Tegley, C. M.; Viswanadhan, V. N.; Biswas, K.; Frohn, M. J.; Peterkin, T. A.; Chang, C.; Burli, R. W.; Dao, J. H.; Veith, H.; Rogers, N.; Yoder, S. C.; Biddlecome, G.; Tagari, P.; Allen, J. R.; Hungate, R. W., Discovery of novel hydroxy-thiazoles as HIF-alpha prolyl hydroxylase inhibitors: SAR, synthesis, and modeling evaluation. *Bioorg Med Chem Lett* 2008, 18, (14), 3925-8.
179. Stiehl, D. P.; Wirthner, R.; Koditz, J.; Spielmann, P.; Camenisch, G.; Wenger, R. H., Increased prolyl 4-hydroxylase domain proteins compensate for decreased oxygen levels. Evidence for an autoregulatory oxygen-sensing system. *J Biol Chem* 2006, 281, (33), 23482-91.
180. Kaelin, W. G., Proline hydroxylation and gene expression. *Annu Rev Biochem* 2005, 74, 115-28.
181. Gothie, E.; Richard, D. E.; Berra, E.; Pages, G.; Pouyssegur, J., Identification of alternative spliced variants of human hypoxia-inducible factor-1alpha. *J Biol Chem* 2000, 275, (10), 6922-7.
182. Ruas, J. L.; Berchner-Pfannschmidt, U.; Malik, S.; Gradin, K.; Fandrey, J.; Roeder, R. G.; Pereira, T.; Poellinger, L., Complex regulation of the transactivation function of hypoxia-inducible factor-1 alpha by direct interaction with two distinct domains of the CREB-binding protein/p300. *J Biol Chem* 2010, 285, (4), 2601-9.
183. Stolze, I. P.; Tian, Y. M.; Appelhoff, R. J.; Turley, H.; Wykoff, C. C.; Gleadle, J. M.; Ratcliffe, P. J., Genetic analysis of the role of the asparaginyl hydroxylase factor inhibiting hypoxia-inducible factor (FIH) in regulating hypoxia-inducible factor (HIF) transcriptional target genes [corrected]. *J Biol Chem* 2004, 279, (41), 42719-25.

184. Chowdhury, R.; Yeoh, K. K.; Tian, Y. M.; Hillringhaus, L.; Bagg, E. A.; Rose, N. R.; Leung, I. K.; Li, X. S.; Woon, E. C.; Yang, M.; McDonough, M. A.; King, O. N.; Clifton, I. J.; Klose, R. J.; Claridge, T. D.; Ratcliffe, P. J.; Schofield, C. J.; Kawamura, A., The oncometabolite 2-hydroxyglutarate inhibits histone lysine demethylases. *EMBO Rep* 2011, 12, (5), 463-9.
185. Ayoub, N.; Noma, K.; Isaac, S.; Kahan, T.; Grewal, S. I.; Cohen, A., A novel jmjC domain protein modulates heterochromatization in fission yeast. *Mol Cell Biol* 2003, 23, (12), 4356-70.
186. Perez-Perri, J. I.; Acevedo, J. M.; Wappner, P., Epigenetics: new questions on the response to hypoxia. *Int J Mol Sci* 2011, 12, (7), 4705-21.
187. Lim, S.; Metzger, E.; Schule, R.; Kirfel, J.; Buettner, R., Epigenetic regulation of cancer growth by histone demethylases. *Int J Cancer* 2010, 127, (9), 1991-8.
188. Varier, R. A.; Timmers, H. T., Histone lysine methylation and demethylation pathways in cancer. *Biochim Biophys Acta* 2011, 1815, (1), 75-89.
189. Ellis, L.; Atadja, P. W.; Johnstone, R. W., Epigenetics in cancer: targeting chromatin modifications. *Mol Cancer Ther* 2009, 8, (6), 1409-20.
190. Loenarz, C.; Schofield, C. J., Expanding chemical biology of 2-oxoglutarate oxygenases. *Nat Chem Biol* 2008, 4, (3), 152-6.
191. Simmons, J. M.; Muller, T. A.; Hausinger, R. P., Fe(II)/alpha-ketoglutarate hydroxylases involved in nucleobase, nucleoside, nucleotide, and chromatin metabolism. *Dalton Trans* 2008, (38), 5132-42.
192. Xu, W.; Yang, H.; Liu, Y.; Yang, Y.; Wang, P.; Kim, S. H.; Ito, S.; Yang, C.; Xiao, M. T.; Liu, L. X.; Jiang, W. Q.; Liu, J.; Zhang, J. Y.; Wang, B.; Frye, S.; Zhang, Y.; Xu, Y. H.; Lei, Q. Y.; Guan, K. L.; Zhao, S. M.; Xiong, Y., Oncometabolite 2-hydroxyglutarate is a competitive inhibitor of alpha-ketoglutarate-dependent dioxygenases. *Cancer Cell* 2011, 19, (1), 17-30.
193. Kaelin, W. G., Jr.; Thompson, C. B., Q&A: Cancer: clues from cell metabolism. *Nature* 2010, 465, (7298), 562-4.
194. Flashman, E.; Davies, S. L.; Yeoh, K. K.; Schofield, C. J., Investigating the dependence of the hypoxia-inducible factor hydroxylases (factor inhibiting HIF and prolyl hydroxylase domain 2) on ascorbate and other reducing agents. *Biochem J* 2010, 427, (1), 135-42.
195. Couture, J. F.; Collazo, E.; Ortiz-Tello, P. A.; Brunzelle, J. S.; Trievel, R. C., Specificity and mechanism of JMJD2A, a trimethyllysine-specific histone demethylase. *Nat Struct Mol Biol* 2007, 14, (8), 689-95.
196. Elkins, J. M.; Hewitson, K. S.; McNeill, L. A.; Seibel, J. F.; Schlemminger, I.; Pugh, C. W.; Ratcliffe, P. J.; Schofield, C. J., Structure of factor-inhibiting hypoxia-inducible factor (HIF) reveals mechanism of oxidative modification of HIF-1 alpha. *J Biol Chem* 2003, 278, (3), 1802-6.
197. Chen, Z.; Zang, J.; Whetstine, J.; Hong, X.; Davrazou, F.; Kutateladze, T. G.; Simpson, M.; Mao, Q.; Pan, C. H.; Dai, S.; Hagman, J.; Hansen, K.; Shi, Y.; Zhang, G., Structural insights into histone demethylation by JMJD2 family members. *Cell* 2006, 125, (4), 691-702.

198. Ng, S. S.; Kavanagh, K. L.; McDonough, M. A.; Butler, D.; Pilka, E. S.; Lienard, B. M.; Bray, J. E.; Savitsky, P.; Gileadi, O.; von Delft, F.; Rose, N. R.; Offer, J.; Scheinost, J. C.; Borowski, T.; Sundstrom, M.; Schofield, C. J.; Oppermann, U., Crystal structures of histone demethylase JMJD2A reveal basis for substrate specificity. *Nature* 2007, 448, (7149), 87-91.
199. Dalgliesh, G. L.; Furge, K.; Greenman, C.; Chen, L.; Bignell, G.; Butler, A.; Davies, H.; Edkins, S.; Hardy, C.; Latimer, C.; Teague, J.; Andrews, J.; Barthorpe, S.; Beare, D.; Buck, G.; Campbell, P. J.; Forbes, S.; Jia, M.; Jones, D.; Knott, H.; Kok, C. Y.; Lau, K. W.; Leroy, C.; Lin, M. L.; McBride, D. J.; Maddison, M.; Maguire, S.; McLay, K.; Menzies, A.; Mironenko, T.; Mulderrig, L.; Mudie, L.; O'Meara, S.; Pleasance, E.; Rajasingham, A.; Shepherd, R.; Smith, R.; Stebbings, L.; Stephens, P.; Tang, G.; Tarpey, P. S.; Turrell, K.; Dykema, K. J.; Khoo, S. K.; Petillo, D.; Wondergem, B.; Anema, J.; Kahnoski, R. J.; Teh, B. T.; Stratton, M. R.; Futreal, P. A., Systematic sequencing of renal carcinoma reveals inactivation of histone modifying genes. *Nature* 2010, 463, (7279), 360-3.
200. van Haaften, G.; Dalgliesh, G. L.; Davies, H.; Chen, L.; Bignell, G.; Greenman, C.; Edkins, S.; Hardy, C.; O'Meara, S.; Teague, J.; Butler, A.; Hinton, J.; Latimer, C.; Andrews, J.; Barthorpe, S.; Beare, D.; Buck, G.; Campbell, P. J.; Cole, J.; Forbes, S.; Jia, M.; Jones, D.; Kok, C. Y.; Leroy, C.; Lin, M. L.; McBride, D. J.; Maddison, M.; Maquire, S.; McLay, K.; Menzies, A.; Mironenko, T.; Mulderrig, L.; Mudie, L.; Pleasance, E.; Shepherd, R.; Smith, R.; Stebbings, L.; Stephens, P.; Tang, G.; Tarpey, P. S.; Turner, R.; Turrell, K.; Varian, J.; West, S.; Widaa, S.; Wray, P.; Collins, V. P.; Ichimura, K.; Law, S.; Wong, J.; Yuen, S. T.; Leung, S. Y.; Tonon, G.; DePinho, R. A.; Tai, Y. T.; Anderson, K. C.; Kahnoski, R. J.; Massie, A.; Khoo, S. K.; Teh, B. T.; Stratton, M. R.; Futreal, P. A., Somatic mutations of the histone H3K27 demethylase gene UTX in human cancer. *Nat Genet* 2009, 41, (5), 521-3.
201. Frescas, D.; Guardavaccaro, D.; Bassermann, F.; Koyama-Nasu, R.; Pagano, M., JHDM1B/FBXL10 is a nucleolar protein that represses transcription of ribosomal RNA genes. *Nature* 2007, 450, (7167), 309-13.
202. Steenweg, M. E.; Jakobs, C.; Errami, A.; van Dooren, S. J.; Adeva Bartolome, M. T.; Aerssens, P.; Augoustides-Savvapoulou, P.; Baric, I.; Baumann, M.; Bonafe, L.; Chabrol, B.; Clarke, J. T.; Clayton, P.; Coker, M.; Cooper, S.; Falik-Zaccai, T.; Gorman, M.; Hahn, A.; Hasanoglu, A.; King, M. D.; de Klerk, H. B.; Korman, S. H.; Lee, C.; Meldgaard Lund, A.; Mejaski-Bosnjak, V.; Pascual-Castroviejo, I.; Raadhyaksha, A.; Rootwelt, T.; Roubertie, A.; Ruiz-Falco, M. L.; Scalais, E.; Schimmel, U.; Seijo-Martinez, M.; Suri, M.; Sykut-Cegielska, J.; Trefz, F. K.; Uziel, G.; Valayannopoulos, V.; Vianey-Saban, C.; Vlaho, S.; Vodopiutz, J.; Wajner, M.; Walter, J.; Walter-Derbort, C.; Yapici, Z.; Zafeiriou, D. I.; Spreeuwenberg, M. D.; Celli, J.; den Dunnen, J. T.; van der Knaap, M. S.; Salomons, G. S., An overview of L-2-hydroxyglutarate dehydrogenase gene (L2HGDH) variants: a genotype-phenotype study. *Hum Mutat* 2010, 31, (4), 380-90.

203. Topcu, M.; Jobard, F.; Halliez, S.; Coskun, T.; Yalcinkayal, C.; Gerceker, F. O.; Wanders, R. J.; Prud'homme, J. F.; Lathrop, M.; Ozguc, M.; Fischer, J., L-2-Hydroxyglutaric aciduria: identification of a mutant gene C14orf160, localized on chromosome 14q22.1. *Hum Mol Genet* 2004, 13, (22), 2803-11.
204. Nyhan, W. L.; Shelton, G. D.; Jakobs, C.; Holmes, B.; Bowe, C.; Curry, C. J.; Vance, C.; Duran, M.; Sweetman, L., D-2-hydroxyglutaric aciduria. *J Child Neurol* 1995, 10, (2), 137-42.
205. Struys, E. A., D-2-Hydroxyglutaric aciduria: unravelling the biochemical pathway and the genetic defect. *J Inherit Metab Dis* 2006, 29, (1), 21-9.
206. Hsu, P. P.; Sabatini, D. M., Cancer cell metabolism: Warburg and beyond. *Cell* 2008, 134, (5), 703-7.
207. Lu, H.; Dalgard, C. L.; Mohyeldin, A.; McFate, T.; Tait, A. S.; Verma, A., Reversible inactivation of HIF-1 prolyl hydroxylases allows cell metabolism to control basal HIF-1. *J Biol Chem* 2005, 280, (51), 41928-39.
208. Thirstrup, K.; Christensen, S.; Moller, H. A.; Ritzen, A.; Bergstrom, A. L.; Sager, T. N.; Jensen, H. S., Endogenous 2-oxoglutarate levels impact potencies of competitive HIF prolyl hydroxylase inhibitors. *Pharmacol Res* 2011.
209. Kim, K. B.; Yang, J. Y.; Kwack, S. J.; Park, K. L.; Kim, H. S.; Ryu do, H.; Kim, Y. J.; Hwang, G. S.; Lee, B. M., Toxicometabolomics of urinary biomarkers for human gastric cancer in a mouse model. *J Toxicol Environ Health A* 2010, 73, (21-22), 1420-30.
210. Patton, M. A.; Krywawych, S.; Winter, R. M.; Brenton, D. P.; Baraitser, M., DOOR syndrome (deafness, onycho-osteodystrophy, and mental retardation): elevated plasma and urinary 2-oxoglutarate in three unrelated patients. *Am J Med Genet* 1987, 26, (1), 207-15.
211. Surendran, S.; Michals-Matalon, K.; Krywawych, S.; Qazi, Q. H.; Tuchman, R.; Rady, P. L.; Tyring, S. K.; Matalon, R., DOOR syndrome: deficiency of E1 component of the 2-oxoglutarate dehydrogenase complex. *Am J Med Genet* 2002, 113, (4), 371-4.
212. Siess, E. A.; Brocks, D. G.; Lattke, H. K.; Wieland, O. H., Effect of glucagon on metabolite compartmentation in isolated rat liver cells during gluconeogenesis from lactate. *Biochem J* 1977, 166, (2), 225-35.
213. Haussinger, D.; Sies, H., Effect of phenylephrine on glutamate and glutamine metabolism in isolated perfused rat liver. *Biochem J* 1984, 221, (3), 651-8.
214. Dubus, A.; Lloyd, M. D.; Lee, H. J.; Schofield, C. J.; Baldwin, J. E.; Frere, J. M., Probing the penicillin sidechain selectivity of recombinant deacetoxycephalosporin C synthase. *Cell Mol Life Sci* 2001, 58, (5-6), 835-43.
215. Holme, E., A kinetic study of thymine 7-hydroxylase from neurospora crassa. *Biochemistry* 1975, 14, (22), 4999-5003.
216. Welford, R. W.; Schlemminger, I.; McNeill, L. A.; Hewitson, K. S.; Schofield, C. J., The selectivity and inhibition of AlkB. *J Biol Chem* 2003, 278, (12), 10157-61.
217. Nytko, K. J.; Maeda, N.; Schlafli, P.; Spielmann, P.; Wenger, R. H.; Stiehl, D. P., Vitamin C is dispensable for oxygen sensing in vivo. *Blood* 2011, 117, (20), 5485-93.

218. Willenborg, M.; Panten, U.; Rustenbeck, I., Triggering and amplification of insulin secretion by dimethyl alpha-ketoglutarate, a membrane permeable alpha-ketoglutarate analogue. *Eur J Pharmacol* 2009, 607, (1-3), 41-6.
219. Fernandez-Pascual, S.; Mukala-Nsengu-Tshibangu, A.; Martin Del Rio, R.; Tamarit-Rodriguez, J., Conversion into GABA (gamma-aminobutyric acid) may reduce the capacity of L-glutamine as an insulin secretagogue. *Biochem J* 2004, 379, (Pt 3), 721-9.
220. Odegaard, M. L.; Joseph, J. W.; Jensen, M. V.; Lu, D.; Ilkayeva, O.; Ronnebaum, S. M.; Becker, T. C.; Newgard, C. B., The mitochondrial 2-oxoglutarate carrier is part of a metabolic pathway that mediates glucose- and glutamine-stimulated insulin secretion. *J Biol Chem* 2010, 285, (22), 16530-7.
221. Lauzier, M. C.; Robitaille, G. A.; Chan, D. A.; Giaccia, A. J.; Richard, D. E., (2R)-[(4-Biphenylylsulfonyl)amino]-N-hydroxy-3-phenylpropionamide (BiPS), a matrix metalloprotease inhibitor, is a novel and potent activator of hypoxia-inducible factors. *Mol Pharmacol* 2008, 74, (1), 282-8.
222. Mecinovic, J.; Loenarz, C.; Chowdhury, R.; Schofield, C. J., 2-Oxoglutarate analogue inhibitors of prolyl hydroxylase domain 2. *Bioorg Med Chem Lett* 2009, 19, (21), 6192-5.
223. Maxwell, P. H.; Wiesener, M. S.; Chang, G.-W.; Clifford, S. C.; Vaux, E. C.; Cockman, M. E.; Wykoff, C. C.; Pugh, C. W.; Maher, E. R.; Ratcliffe, P. J., The tumour suppressor protein VHL targets hypoxia-inducible factors for oxygen-dependent proteolysis. *Nature* 1999, 399, (6733), 271-275.
224. Marxsen, J. H.; Stengel, P.; Doege, K.; Heikkinen, P.; Jokilehto, T.; Wagner, T.; Jelkmann, W.; Jaakkola, P.; Metzen, E., Hypoxia-inducible factor-1 (HIF-1) promotes its degradation by induction of HIF-alpha-prolyl-4-hydroxylases. *Biochem J* 2004, 381, (Pt 3), 761-7.
225. Knowles, H. J.; Raval, R. R.; Harris, A. L.; Ratcliffe, P. J., Effect of ascorbate on the activity of hypoxia-inducible factor in cancer cells. *Cancer Res* 2003, 63, (8), 1764-8.
226. Tuckerman, J. R.; Zhao, Y.; Hewitson, K. S.; Tian, Y. M.; Pugh, C. W.; Ratcliffe, P. J.; Mole, D. R., Determination and comparison of specific activity of the HIF-prolyl hydroxylases. *FEBS Lett* 2004, 576, (1-2), 145-50.
227. Huang, H. M.; Zhang, H.; Xu, H.; Gibson, G. E., Inhibition of the alpha-ketoglutarate dehydrogenase complex alters mitochondrial function and cellular calcium regulation. *Biochim Biophys Acta* 2003, 1637, (1), 119-26.
228. Hewitson, K. S.; Granatino, N.; Welford, R. W.; McDonough, M. A.; Schofield, C. J., Oxidation by 2-oxoglutarate oxygenases: non-haem iron systems in catalysis and signalling. *Philos Transact A Math Phys Eng Sci* 2005, 363, (1829), 807-28; discussion 1035-40.
229. Titheradge, M. A.; Picking, R. A.; Haynes, R. C., Jr., Physiological concentrations of 2-oxoglutarate regulate the activity of phosphoenolpyruvate carboxykinase in liver. *Biochem J* 1992, 285 (Pt 3), 767-71.
230. Spinella, F.; Rosano, L.; Del Duca, M.; Di Castro, V.; Nicotra, M. R.; Natali, P. G.; Bagnato, A., Endothelin-1 inhibits prolyl hydroxylase domain 2 to activate hypoxia-inducible factor-1alpha in melanoma cells. *PLoS One* 2010, 5, (6), e11241.

231. Laughner, E.; Taghavi, P.; Chiles, K.; Mahon, P. C.; Semenza, G. L., HER2 (neu) signaling increases the rate of hypoxia-inducible factor 1alpha (HIF-1alpha) synthesis: novel mechanism for HIF-1-mediated vascular endothelial growth factor expression. *Mol Cell Biol* 2001, 21, (12), 3995-4004.
232. Treins, C.; Giorgetti-Peraldi, S.; Murdaca, J.; Semenza, G. L.; Van Obberghen, E., Insulin stimulates hypoxia-inducible factor 1 through a phosphatidylinositol 3-kinase/target of rapamycin-dependent signaling pathway. *J Biol Chem* 2002, 277, (31), 27975-81.
233. Wang, H.; Shimizu, E.; Tang, Y. P.; Cho, M.; Kyin, M.; Zuo, W.; Robinson, D. A.; Alaimo, P. J.; Zhang, C.; Morimoto, H.; Zhuo, M.; Feng, R.; Shokat, K. M.; Tsien, J. Z., Inducible protein knockout reveals temporal requirement of CaMKII reactivation for memory consolidation in the brain. *Proc Natl Acad Sci U S A* 2003, 100, (7), 4287-92.
234. Chen, X.; Ye, H.; Kuruvilla, R.; Ramanan, N.; Scangos, K. W.; Zhang, C.; Johnson, N. M.; England, P. M.; Shokat, K. M.; Ginty, D. D., A chemical-genetic approach to studying neurotrophin signaling. *Neuron* 2005, 46, (1), 13-21.
235. Burkard, M. E.; Randall, C. L.; Larochelle, S.; Zhang, C.; Shokat, K. M.; Fisher, R. P.; Jallepalli, P. V., Chemical genetics reveals the requirement for Polo-like kinase 1 activity in positioning RhoA and triggering cytokinesis in human cells. *Proc Natl Acad Sci U S A* 2007, 104, (11), 4383-8.
236. Kim, J. S.; Lilley, B. N.; Zhang, C.; Shokat, K. M.; Sanes, J. R.; Zhen, M., A chemical-genetic strategy reveals distinct temporal requirements for SAD-1 kinase in neuronal polarization and synapse formation. *Neural Dev* 2008, 3, 23.
237. Okuzumi, T.; Ducker, G. S.; Zhang, C.; Aizenstein, B.; Hoffman, R.; Shokat, K. M., Synthesis and evaluation of indazole based analog sensitive Akt inhibitors. *Mol Biosyst* 2010, 6, (8), 1389-402.
238. Sliedrecht, T.; Zhang, C.; Shokat, K. M.; Kops, G. J., Chemical genetic inhibition of Mps1 in stable human cell lines reveals novel aspects of Mps1 function in mitosis. *PLoS One* 2010, 5, (4), e10251.
239. Hanke, J. H.; Gardner, J. P.; Dow, R. L.; Changelian, P. S.; Brissette, W. H.; Weringer, E. J.; Pollok, B. A.; Connelly, P. A., Discovery of a novel, potent, and Src family-selective tyrosine kinase inhibitor. Study of Lck- and FynT-dependent T cell activation. *J Biol Chem* 1996, 271, (2), 695-701.
240. Liu, Y.; Shah, K.; Yang, F.; Witucki, L.; Shokat, K. M., Engineering Src family protein kinases with unnatural nucleotide specificity. *Chem Biol* 1998, 5, (2), 91-101.
241. Bishop, A. C.; Kung, C.-y.; Shah, K.; Witucki, L.; Shokat, K. M.; Liu, Y., Generation of Monospecific Nanomolar Tyrosine Kinase Inhibitors via a Chemical Genetic Approach. *Journal of the American Chemical Society* 1999, 121, (4), 627-631.
242. Bishop, A. C.; Shah, K.; Liu, Y.; Witucki, L.; Kung, C.; Shokat, K. M., Design of allele-specific inhibitors to probe protein kinase signaling. *Curr Biol* 1998, 8, (5), 257-66.

243. Bishop, A. C.; Ubersax, J. A.; Petsch, D. T.; Matheos, D. P.; Gray, N. S.; Blethrow, J.; Shimizu, E.; Tsien, J. Z.; Schultz, P. G.; Rose, M. D.; Wood, J. L.; Morgan, D. O.; Shokat, K. M., A chemical switch for inhibitor-sensitive alleles of any protein kinase. *Nature* 2000, 407, (6802), 395-401.
244. Whitney, J. A., Reference systems for kinase drug discovery: chemical genetic approaches to cell-based assays. *Assay Drug Dev Technol* 2004, 2, (4), 417-29.
245. Kawasumi, M.; Nghiem, P., Chemical genetics: elucidating biological systems with small-molecule compounds. *J Invest Dermatol* 2007, 127, (7), 1577-84.
246. Jing, Q.; Zhao, J.; Zhao, B.; Zhang, S.; Miao, J., [Applications of chemical genetics in biomedical research]. *Sheng Wu Yi Xue Gong Cheng Xue Za Zhi* 2009, 26, (2), 448-51.
247. Chen, T.; Ozel, D.; Qiao, Y.; Harbinski, F.; Chen, L.; Denoyelle, S.; He, X.; Zvereva, N.; Supko, J. G.; Chorev, M.; Halperin, J. A.; Aktas, B. H., Chemical genetics identify eIF2alpha kinase heme-regulated inhibitor as an anticancer target. *Nat Chem Biol* 2011.
248. Sachinidis, A.; Sotiriadou, I.; Seelig, B.; Berkessel, A.; Hescheler, J., A chemical genetics approach for specific differentiation of stem cells to somatic cells: a new promising therapeutical approach. *Comb Chem High Throughput Screen* 2008, 11, (1), 70-82.
249. Balla, A.; Tuymetova, G.; Toth, B.; Szentpetery, Z.; Zhao, X.; Knight, Z. A.; Shokat, K.; Steinbach, P. J.; Balla, T., Design of drug-resistant alleles of type-III phosphatidylinositol 4-kinases using mutagenesis and molecular modeling. *Biochemistry* 2008, 47, (6), 1599-607.
250. Jungbauer, A.; Hahn, R., Ion-exchange chromatography. *Methods Enzymol* 2009, 463, 349-71.
251. Barth, H. G.; Jackson, C.; Boyes, B. E., Size Exclusion Chromatography. *Analytical Chemistry* 1994, 66, (12), 595R-620R.
252. Baader, E.; Tschank, G.; Baringhaus, K. H.; Burghard, H.; Gunzler, V., Inhibition of prolyl 4-hydroxylase by oxalyl amino acid derivatives in vitro, in isolated microsomes and in embryonic chicken tissues. *Biochem J* 1994, 300 (Pt 2), 525-30.
253. Cunliffe, C. J.; Franklin, T. J.; Hales, N. J.; Hill, G. B., Novel inhibitors of prolyl 4-hydroxylase. 3. Inhibition by the substrate analogue N-oxaloglycine and its derivatives. *J Med Chem* 1992, 35, (14), 2652-8.
254. Leung, I. K.; Flashman, E.; Yeoh, K. K.; Schofield, C. J.; Claridge, T. D., Using NMR solvent water relaxation to investigate metalloenzyme-ligand binding interactions. *J Med Chem* 2010, 53, (2), 867-75.
255. Henkel, J.; Du, H.; Yang, P.; Qyang, Y.; Kansra, S.; Ko, M.; Kim, H. W.; Marcus, S., Bob1, a Gim5/MM-1/Pfd5 homolog, interacts with the MAP kinase kinase Byr1 to regulate sexual differentiation in the fission yeast, Schizosaccharomyces pombe. *Differentiation* 2001, 67, (4-5), 98-106.
256. Gregan, J.; Zhang, C.; Rumpf, C.; Cipak, L.; Li, Z.; Uluocak, P.; Nasmyth, K.; Shokat, K. M., Construction of conditional analog-sensitive kinase alleles in the fission yeast Schizosaccharomyces pombe. *Nat Protoc* 2007, 2, (11), 2996-3000.

257. Adam, J.; Hatipoglu, E.; O'Flaherty, L.; Ternette, N.; Sahgal, N.; Lockstone, H.; Baban, D.; Nye, E.; Stamp, G. W.; Wolhuter, K.; Stevens, M.; Fischer, R.; Carmeliet, P.; Maxwell, P. H.; Pugh, C. W.; Frizzell, N.; Soga, T.; Kessler, B. M.; El-Bahrawy, M.; Ratcliffe, P. J.; Pollard, P. J., Renal cyst formation in Fh1-deficient mice is independent of the Hif/Phd pathway: roles for fumarate in KEAP1 succination and Nrf2 signaling. *Cancer Cell* 2011, 20, (4), 524-37.
258. McDonough, M. A.; Loenarz, C.; Chowdhury, R.; Clifton, I. J.; Schofield, C. J., Structural studies on human 2-oxoglutarate dependent oxygenases. *Curr Opin Struct Biol* 2010, 20, (6), 659-72.
259. Mecinovic, J.; Chowdhury, R.; Flashman, E.; Schofield, C. J., Use of mass spectrometry to probe the nucleophilicity of cysteinyl residues of prolyl hydroxylase domain 2. *Anal Biochem* 2009, 393, (2), 215-21.
260. Mecinovic, J. Enzymatic and Non-Enzymatic Iron Catalysis: Mechanistic and Inhibition Studies. University of Oxford, 2009.
261. Bernhardt, P. V.; Chin, P.; Richardson, D. R., Unprecedented oxidation of a biologically active aroylhydrazone chelator catalysed by iron(III): serendipitous identification of diacylhydrazine ligands with high iron chelation efficacy. *J Biol Inorg Chem* 2001, 6, (8), 801-9.
262. Li, D.; Wang, S.; Xu, H.; Yang, Y.; Zeng, S.; Zhao, J.; Wang, D.; Dou, J., Supramolecular architectures based on di-, tri- and tetrameric complexes with N,N′-diacylhydrazide ligands. *Inorganica Chimica Acta* 2011, 365, (1), 85-95.
263. Liu, S.-X.; Lin, S.; Lin, B.-Z.; Lin, C.-C.; Huang, J.-Q., [30]Metallacrown-10 Compounds: [Mn(C14H9N2O3)(CH3OH)]10·5 CH2Cl2·16 CH3OH·H2O and [Fe(C14H9N2O3)(CH3OH)]10·3 CH2Cl2·12.5 CH3OH·5 H2O. *Angewandte Chemie International Edition* 2001, 40, (6), 1084-1087.
264. Bernhardt, P. V.; Chin, P.; Sharpe, P. C.; Wang, J. Y.; Richardson, D. R., Novel diaroylhydrazine ligands as iron chelators: coordination chemistry and biological activity. *J Biol Inorg Chem* 2005, 10, (7), 761-77.
265. Christensen, J. B., A Simple Method for Synthesis of Active Esters of Isonicotinic and Picolinic Acids. *Molecules* 2001, 6, (1), 47-51.
266. Loenarz, C.; Mecinovic, J.; Chowdhury, R.; McNeill, L. A.; Flashman, E.; Schofield, C. J., Evidence for a stereoelectronic effect in human oxygen sensing. *Angew Chem Int Ed Engl* 2009, 48, (10), 1784-7.
267. Jones, G.; Willett, P.; Glen, R. C.; Leach, A. R.; Taylor, R., Development and validation of a genetic algorithm for flexible docking. *J Mol Biol* 1997, 267, (3), 727-48.
268. Verdonk, M. L.; Cole, J. C.; Hartshorn, M. J.; Murray, C. W.; Taylor, R. D., Improved protein-ligand docking using GOLD. *Proteins* 2003, 52, (4), 609-23.
269. Katz, B. A.; Clark, J. M.; Finer-Moore, J. S.; Jenkins, T. E.; Johnson, C. R.; Ross, M. J.; Luong, C.; Moore, W. R.; Stroud, R. M., Design of potent selective zinc-mediated serine protease inhibitors. *Nature* 1998, 391, (6667), 608-12.
270. Semenza, G. L., HIF-1, O(2), and the 3 PHDs: how animal cells signal hypoxia to the nucleus. *Cell* 2001, 107, (1), 1-3.
271. Ryle, M. J.; Hausinger, R. P., Non-heme iron oxygenases. *Curr Opin Chem Biol* 2002, 6, (2), 193-201.

272. Monga, V.; Nayyar, A.; Vaitilingam, B.; Palde, P. B.; Jhamb, S. S.; Kaur, S.; Singh, P. P.; Jain, R., Ring-substituted quinolines. Part 2: Synthesis and antimycobacterial activities of ring-substituted quinolinecarbohydrazide and ring-substituted quinolinecarboxamide analogues. *Bioorg Med Chem* 2004, 12, (24), 6465-72.
273. Dodd, R. H.; Ouannes, C.; de Carvalho, L. P.; Valin, A.; Venault, P.; Chapouthier, G.; Rossier, J.; Potier, P., 3-Amino-beta-carboline derivatives and the benzodiazepine receptor. Synthesis of a selective antagonist of the sedative action of diazepam. *J Med Chem* 1985, 28, (6), 824-8.
274. Jack, D. B., One hundred years of aspirin. *The Lancet* 1997, 350, (9075), 437-439.
275. Weissmann, G., Aspirin. *Sci Am* 1991, 264, (1), 84-90.
276. Lienard, B. M. New Approaches to the Inhibition of Mettalo Enzymes. University of Oxford, 2006.
277. Lip, G. Y. H., The role of aspirin for stroke prevention in atrial fibrillation. *Nat Rev Cardiol* 2011, advance online publication.
278. Hennekens, C. H., Update on aspirin in the treatment and prevention of cardiovascular disease. *Am J Manag Care* 2002, 8, (22 Suppl), S691-700.
279. de Gaetano, G., Low-dose aspirin and vitamin E in people at cardiovascular risk: a randomised trial in general practice. Collaborative Group of the Primary Prevention Project. *Lancet* 2001, 357, (9250), 89-95.
280. Maloney, A.; Workman, P., HSP90 as a new therapeutic target for cancer therapy: the story unfolds. *Expert Opin Biol Ther* 2002, 2, (1), 3-24.
281. Wood, A.; Baxter, G.; Thies, F.; Kyle, J.; Duthie, G., A systematic review of salicylates in foods: estimated daily intake of a Scottish population. *Mol Nutr Food Res* 2011, 55 Suppl 1, S7-S14.
282. Swain, A. R.; Dutton, S. P.; Truswell, A. S., Salicylates in foods. *J Am Diet Assoc* 1985, 85, (8), 950-60.
283. Jacobs, E. J.; Rodriguez, C.; Mondul, A. M.; Connell, C. J.; Henley, S. J.; Calle, E. E.; Thun, M. J., A large cohort study of aspirin and other nonsteroidal anti-inflammatory drugs and prostate cancer incidence. *J Natl Cancer Inst* 2005, 97, (13), 975-80.
284. Fuchs, C. S., The role of aspirin in prevention and management of colorectal cancer. *Clin Adv Hematol Oncol* 2011, 9, (4), 330-2.
285. Flossmann, E.; Rothwell, P. M., Effect of aspirin on long-term risk of colorectal cancer: consistent evidence from randomised and observational studies. *Lancet* 2007, 369, (9573), 1603-13.
286. DuBois, R. N., Aspirin and breast cancer prevention: the estrogen connection. *JAMA* 2004, 291, (20), 2488-9.
287. Tait, C. R., Aspirin and breast cancer prevention--a link to ER status. *Breast Cancer Res* 2004, 6, (5), 211-2.
288. Cook, N. R.; Lee, I. M.; Gaziano, J. M.; Gordon, D.; Ridker, P. M.; Manson, J. E.; Hennekens, C. H.; Buring, J. E., Low-dose aspirin in the primary prevention of cancer: the Women's Health Study: a randomized controlled trial. *JAMA* 2005, 294, (1), 47-55.

289. Chan, A. T.; Manson, J. E.; Feskanich, D.; Stampfer, M. J.; Colditz, G. A.; Fuchs, C. S., Long-term aspirin use and mortality in women. *Arch Intern Med* 2007, 167, (6), 562-72.
290. Zhang, S. M.; Cook, N. R.; Manson, J. E.; Lee, I. M.; Buring, J. E., Low-dose aspirin and breast cancer risk: results by tumour characteristics from a randomised trial. *Br J Cancer* 2008, 98, (5), 989-91.
291. Collet, J. P.; Sharpe, C.; Belzile, E.; Boivin, J. F.; Hanley, J.; Abenhaim, L., Colorectal cancer prevention by non-steroidal anti-inflammatory drugs: effects of dosage and timing. *Br J Cancer* 1999, 81, (1), 62-8.
292. Baron, J. A., Epidemiology of non-steroidal anti-inflammatory drugs and cancer. *Prog Exp Tumor Res* 2003, 37, 1-24.
293. Ruffin, M. T. t.; Krishnan, K.; Rock, C. L.; Normolle, D.; Vaerten, M. A.; Peters-Golden, M.; Crowell, J.; Kelloff, G.; Boland, C. R.; Brenner, D. E., Suppression of human colorectal mucosal prostaglandins: determining the lowest effective aspirin dose. *J Natl Cancer Inst* 1997, 89, (15), 1152-60.
294. Terry, M. B.; Gammon, M. D.; Zhang, F. F.; Tawfik, H.; Teitelbaum, S. L.; Britton, J. A.; Subbaramaiah, K.; Dannenberg, A. J.; Neugut, A. I., Association of frequency and duration of aspirin use and hormone receptor status with breast cancer risk. *JAMA* 2004, 291, (20), 2433-40.
295. Rothwell, P. M.; Fowkes, F. G.; Belch, J. F.; Ogawa, H.; Warlow, C. P.; Meade, T. W., Effect of daily aspirin on long-term risk of death due to cancer: analysis of individual patient data from randomised trials. *Lancet* 2011, 377, (9759), 31-41.
296. Elwood, P. C.; Gallagher, A. M.; Duthie, G. G.; Mur, L. A.; Morgan, G., Aspirin, salicylates, and cancer. *Lancet* 2009, 373, (9671), 1301-9.
297. Smith, W. L.; DeWitt, D. L.; Garavito, R. M., Cyclooxygenases: structural, cellular, and molecular biology. *Annu Rev Biochem* 2000, 69, 145-82.
298. Vane, J. R., Inhibition of prostaglandin synthesis as a mechanism of action for aspirin-like drugs. *Nat New Biol* 1971, 231, (25), 232-5.
299. Wang, D.; Dubois, R. N., Prostaglandins and cancer. *Gut* 2006, 55, (1), 115-22.
300. Herschman, H. R., Prostaglandin synthase 2. *Biochim Biophys Acta* 1996, 1299, (1), 125-40.
301. Morita, I.; Schindler, M.; Regier, M. K.; Otto, J. C.; Hori, T.; DeWitt, D. L.; Smith, W. L., Different intracellular locations for prostaglandin endoperoxide H synthase-1 and -2. *J Biol Chem* 1995, 270, (18), 10902-8.
302. Turnberg, L. A.; Rees, W. D., Aspirin, ulcer, and intestinal bleeding: what do the data show? *Gastroenterology* 1982, 83, (3), 726-7.
303. Chell, S.; Kaidi, A.; Williams, A. C.; Paraskeva, C., Mediators of PGE2 synthesis and signalling downstream of COX-2 represent potential targets for the prevention/treatment of colorectal cancer. *Biochim Biophys Acta* 2006, 1766, (1), 104-19.
304. Gonzalez, E. R.; Kannewurf, B. S., Atherosclerosis: a unifying disorder with diverse manifestations. *Am J Health Syst Pharm* 1998, 55, (19 Suppl 1), S4-7.
305. Mitchell, J. A.; Akarasereenont, P.; Thiemermann, C.; Flower, R. J.; Vane, J. R., Selectivity of nonsteroidal antiinflammatory drugs as inhibitors of constitutive and inducible cyclooxygenase. *Proc Natl Acad Sci U S A* 1993, 90, (24), 11693-7.

306. Furst, D. E., Are there differences among nonsteroidal antiinflammatory drugs? Comparing acetylated salicylates, nonacetylated salicylates, and nonacetylated nonsteroidal antiinflammatory drugs. *Arthritis Rheum* 1994, 37, (1), 1-9.
307. Wu, K. K., Aspirin and salicylate: An old remedy with a new twist. *Circulation* 2000, 102, (17), 2022-3.
308. Xu, X. M.; Sansores-Garcia, L.; Chen, X. M.; Matijevic-Aleksic, N.; Du, M.; Wu, K. K., Suppression of inducible cyclooxygenase 2 gene transcription by aspirin and sodium salicylate. *Proc Natl Acad Sci U S A* 1999, 96, (9), 5292-7.
309. Paterson, J. R.; Lawrence, J. R., Salicylic acid: a link between aspirin, diet and the prevention of colorectal cancer. *QJM* 2001, 94, (8), 445-8.
310. Weissmann, G., NSAIDS: aspirin and aspirin-like drugs. In *Cecil Textbook of Medicine*, Goldman, L.; Bennett, J. C., Eds. W.B. Saunders: Philadelphia, 2000; pp 114-118.
311. Featherstone, C., Aspirin for bowel cancer: an old friend finds a new role. *Lancet* 1997, 350, (9075), 418.
312. Janne, P. A.; Mayer, R. J., Chemoprevention of colorectal cancer. *N Engl J Med* 2000, 342, (26), 1960-8.
313. Shureiqi, I.; Xu, X.; Chen, D.; Lotan, R.; Morris, J. S.; Fischer, S. M.; Lippman, S. M., Nonsteroidal anti-inflammatory drugs induce apoptosis in esophageal cancer cells by restoring 15-lipoxygenase-1 expression. *Cancer Res* 2001, 61, (12), 4879-84.
314. Zhang, Z.; DuBois, R. N., Par-4, a proapoptotic gene, is regulated by NSAIDs in human colon carcinoma cells. *Gastroenterology* 2000, 118, (6), 1012-7.
315. Schwenger, P.; Bellosta, P.; Vietor, I.; Basilico, C.; Skolnik, E. Y.; Vilcek, J., Sodium salicylate induces apoptosis via p38 mitogen-activated protein kinase but inhibits tumor necrosis factor-induced c-Jun N-terminal kinase/stress-activated protein kinase activation. *Proc Natl Acad Sci U S A* 1997, 94, (7), 2869-73.
316. Mahdi, J. G.; Alkarrawi, M. A.; Mahdi, A. J.; Bowen, I. D.; Humam, D., Calcium salicylate-mediated apoptosis in human HT-1080 fibrosarcoma cells. *Cell Prolif* 2006, 39, (4), 249-60.
317. Pierce, J. W.; Read, M. A.; Ding, H.; Luscinskas, F. W.; Collins, T., Salicylates inhibit I kappa B-alpha phosphorylation, endothelial-leukocyte adhesion molecule expression, and neutrophil transmigration. *J Immunol* 1996, 156, (10), 3961-9.
318. Yin, M. J.; Yamamoto, Y.; Gaynor, R. B., The anti-inflammatory agents aspirin and salicylate inhibit the activity of I(kappa)B kinase-beta. *Nature* 1998, 396, (6706), 77-80.
319. Din, F. V.; Dunlop, M. G.; Stark, L. A., Evidence for colorectal cancer cell specificity of aspirin effects on NF kappa B signalling and apoptosis. *Br J Cancer* 2004, 91, (2), 381-8.
320. Stark, L. A.; Din, F. V.; Zwacka, R. M.; Dunlop, M. G., Aspirin-induced activation of the NF-kappaB signaling pathway: a novel mechanism for aspirin-mediated apoptosis in colon cancer cells. *FASEB J* 2001, 15, (7), 1273-5.
321. Levy, G., Comparative pharmacokinetics of aspirin and acetaminophen. *Arch Intern Med* 1981, 141, (3 Spec No), 279-81.

322. Patel, D. K.; Hesse, A.; Ogunbona, A.; Notarianni, L. J.; Bennett, P. N., Metabolism of aspirin after therapeutic and toxic doses. *Hum Exp Toxicol* 1990, 9, (3), 131-6.
323. Levy, G., Pharmacokinetics of salicylate elimination in man. *J Pharm Sci* 1965, 54, (7), 959-67.
324. Grootveld, M.; Halliwell, B., Aromatic hydroxylation as a potential measure of hydroxyl-radical formation in vivo. Identification of hydroxylated derivatives of salicylate in human body fluids. *Biochem J* 1986, 237, (2), 499-504.
325. Tishler, S. L.; Goldman, P., Properties and reactions of salicyl-coenzyme A. *Biochem Pharmacol* 1970, 19, (1), 143-50.
326. Forman, W. B.; Davidson, E. D.; Webster, L. T., Jr., Enzymatic conversion of salicylate to salicylurate. *Mol Pharmacol* 1971, 7, (3), 247-59.
327. Haynes, D. R.; Wright, P. F.; Gadd, S. J.; Whitehouse, M. W.; Vernon-Roberts, B., Is aspirin a prodrug for antioxidant and cytokine-modulating oxymetabolites? *Agents Actions* 1993, 39, (1-2), 49-58.
328. Wilson, J. T.; Howell, R. L.; Holladay, M. W.; Brilis, G. M.; Chrastil, J.; Watson, J. T.; Taber, D. F., Gentisuric acid: metabolic formation in animals and identification as a metabolite of aspirin in man. *Clin Pharmacol Ther* 1978, 23, (6), 635-43.
329. DeBlassio, J. L.; deLong, M. A.; Glufke, U.; Kulathila, R.; Merkler, K. A.; Vederas, J. C.; Merkler, D. J., Amidation of salicyluric acid and gentisuric acid: a possible role for peptidylglycine alpha-amidating monooxygenase in the metabolism of aspirin. *Arch Biochem Biophys* 2000, 383, (1), 46-55.
330. Hutt, A. J.; Caldwell, J.; Smith, R. L., The metabolism of aspirin in man: a population study. *Xenobiotica* 1986, 16, (3), 239-49.
331. Chrastil, J.; Wilson, J. T., Quantitative estimation of salicylic acid and its metabolites by thin-layer densitometry. *J Chromatogr* 1978, 152, (1), 183-9.
332. Ohsako, M.; Matsumoto, Y.; Goto, S., Transport of aspirin and its metabolites through human erythrocyte membrane. *Biol Pharm Bull* 1993, 16, (2), 154-7.
333. Bochner, F.; Graham, G. G.; Cham, B. E.; Imhoff, D. M.; Haavisto, T. M., Salicylate metabolite kinetics after several salicylates. *Clin Pharmacol Ther* 1981, 30, (2), 266-75.
334. Abdallah, H. Y.; Mayersohn, M.; Conrad, K. A., The influence of age on salicylate pharmacokinetics in humans. *J Clin Pharmacol* 1991, 31, (4), 380-7.
335. McLaughlin, J. K.; Lipworth, L., Epidemiologic aspects of renal cell cancer. *Semin Oncol* 2000, 27, (2), 115-23.
336. Yagoda, A., Phase II cytotoxic chemotherapy trials in renal cell carcinoma: 1983-1988. *Prog Clin Biol Res* 1990, 350, 227-41.
337. Yao, M.; Yoshida, M.; Kishida, T.; Nakaigawa, N.; Baba, M.; Kobayashi, K.; Miura, T.; Moriyama, M.; Nagashima, Y.; Nakatani, Y.; Kubota, Y.; Kondo, K., VHL tumor suppressor gene alterations associated with good prognosis in sporadic clear-cell renal carcinoma. *J Natl Cancer Inst* 2002, 94, (20), 1569-75.
338. Cockman, M. E.; Masson, N.; Mole, D. R.; Jaakkola, P.; Chang, G. W.; Clifford, S. C.; Maher, E. R.; Pugh, C. W.; Ratcliffe, P. J.; Maxwell, P. H., Hypoxia inducible factor-alpha binding and ubiquitylation by the von Hippel-Lindau tumor suppressor protein. *J Biol Chem* 2000, 275, (33), 25733-41.

339. Thelen, P.; Hemmerlein, B.; Kugler, A.; Seiler, T.; Ozisik, R.; Kallerhoff, M.; Ringert, R. H., Quantification by competitive quantitative RT-PCR of VEGF121 and VEGF165 in renal cell carcinoma. *Anticancer Res* 1999, 19, (2C), 1563-5.
340. Krieg, M.; Haas, R.; Brauch, H.; Acker, T.; Flamme, I.; Plate, K. H., Up-regulation of hypoxia-inducible factors HIF-1alpha and HIF-2alpha under normoxic conditions in renal carcinoma cells by von Hippel-Lindau tumor suppressor gene loss of function. *Oncogene* 2000, 19, (48), 5435-43.
341. Talks, K. L.; Turley, H.; Gatter, K. C.; Maxwell, P. H.; Pugh, C. W.; Ratcliffe, P. J.; Harris, A. L., The expression and distribution of the hypoxia-inducible factors HIF-1alpha and HIF-2alpha in normal human tissues, cancers, and tumor-associated macrophages. *Am J Pathol* 2000, 157, (2), 411-21.
342. Hewitson, K. S.; Schofield, C. J., The HIF pathway as a therapeutic target. *Drug Discov Today* 2004, 9, (16), 704-11.
343. Shinojima, T.; Oya, M.; Takayanagi, A.; Mizuno, R.; Shimizu, N.; Murai, M., Renal cancer cells lacking hypoxia inducible factor (HIF)-1alpha expression maintain vascular endothelial growth factor expression through HIF-2alpha. *Carcinogenesis* 2007, 28, (3), 529-36.
344. Kaelin, W. G., Jr., The von Hippel-Lindau tumor suppressor gene and kidney cancer. *Clin Cancer Res* 2004, 10, (18 Pt 2), 6290S-5S.
345. Onnis, B.; Rapisarda, A.; Melillo, G., Development of HIF-1 inhibitors for cancer therapy. *J Cell Mol Med* 2009, 13, (9A), 2780-6.
346. Raval, R. R.; Lau, K. W.; Tran, M. G.; Sowter, H. M.; Mandriota, S. J.; Li, J. L.; Pugh, C. W.; Maxwell, P. H.; Harris, A. L.; Ratcliffe, P. J., Contrasting properties of hypoxia-inducible factor 1 (HIF-1) and HIF-2 in von Hippel-Lindau-associated renal cell carcinoma. *Mol Cell Biol* 2005, 25, (13), 5675-86.
347. Csermely, P.; Schnaider, T.; Soti, C.; Prohaszka, Z.; Nardai, G., The 90-kDa molecular chaperone family: structure, function, and clinical applications. A comprehensive review. *Pharmacol Ther* 1998, 79, (2), 129-68.
348. Liu, Y. V.; Baek, J. H.; Zhang, H.; Diez, R.; Cole, R. N.; Semenza, G. L., RACK1 competes with HSP90 for binding to HIF-1alpha and is required for O(2)-independent and HSP90 inhibitor-induced degradation of HIF-1alpha. *Mol Cell* 2007, 25, (2), 207-17.
349. van de Sluis, B.; Groot, A. J.; Vermeulen, J.; van der Wall, E.; van Diest, P. J.; Wijmenga, C.; Klomp, L. W.; Vooijs, M., COMMD1 Promotes pVHL and O2-Independent Proteolysis of HIF-1alpha via HSP90/70. *PLoS One* 2009, 4, (10), e7332.
350. Isaacs, J. S.; Jung, Y. J.; Mimnaugh, E. G.; Martinez, A.; Cuttitta, F.; Neckers, L. M., Hsp90 regulates a von Hippel Lindau-independent hypoxia-inducible factor-1 alpha-degradative pathway. *J Biol Chem* 2002, 277, (33), 29936-44.
351. Pearl, L. H.; Prodromou, C., Structure and mechanism of the Hsp90 molecular chaperone machinery. *Annu Rev Biochem* 2006, 75, 271-94.
352. Vilenchik, M.; Solit, D.; Basso, A.; Huezo, H.; Lucas, B.; He, H.; Rosen, N.; Spampinato, C.; Modrich, P.; Chiosis, G., Targeting wide-range oncogenic transformation via PU24FCl, a specific inhibitor of tumor Hsp90. *Chem Biol* 2004, 11, (6), 787-97.

353. Schulte, T. W.; Akinaga, S.; Soga, S.; Sullivan, W.; Stensgard, B.; Toft, D.; Neckers, L. M., Antibiotic radicicol binds to the N-terminal domain of Hsp90 and shares important biologic activities with geldanamycin. *Cell Stress Chaperones* 1998, 3, (2), 100-8.
354. Wu, C. Z.; Moon, A. N.; Choi, O.; Kang, S. Y.; Lee, J. J.; Lee, D.; Hwang, B. Y.; Kim, Y. H.; Lee, H. S.; Hong, Y. S., 6-Alkylsalicylic acid analogues inhibit in vitro ATPase activity of heat shock protein 90. *Arch Pharm Res* 2010, 33, (12), 1997-2001.
355. Zubriene, A.; Matuliene, J.; Baranauskiene, L.; Jachno, J.; Torresan, J.; Michailoviene, V.; Cimmperman, P.; Matulis, D., Measurement of nanomolar dissociation constants by titration calorimetry and thermal shift assay - radicicol binding to Hsp90 and ethoxzolamide binding to CAII. *Int J Mol Sci* 2009, 10, (6), 2662-80.
356. Murray, C. W.; Carr, M. G.; Callaghan, O.; Chessari, G.; Congreve, M.; Cowan, S.; Coyle, J. E.; Downham, R.; Figueroa, E.; Frederickson, M.; Graham, B.; McMenamin, R.; O'Brien, M. A.; Patel, S.; Phillips, T. R.; Williams, G.; Woodhead, A. J.; Woolford, A. J., Fragment-based drug discovery applied to Hsp90. Discovery of two lead series with high ligand efficiency. *J Med Chem* 2010, 53, (16), 5942-55.
357. Kitamura, Y.; Kanda, Y.; Nakasima, T. Hsp90 Family Protein Inhibitors. US 7781485B2, 2010.
358. Petrikaitė, V., Matulis, D., Thermodynamics of Natural and Synthetic Inhibitor Binding to Human Hsp90. In *Application of Thermodynamics to Biological and Materials Science*, Tadashi, M., Ed. InTech: 2011; pp 77-92.
359. Dalvit, C.; Fogliatto, G.; Stewart, A.; Veronesi, M.; Stockman, B., WaterLOGSY as a method for primary NMR screening: practical aspects and range of applicability. *J Biomol NMR* 2001, 21, (4), 349-59.
360. Zurawska, A.; Urbanski, J.; Matuliene, J.; Baraniak, J.; Klejman, M. P.; Filipek, S.; Matulis, D.; Bieganowski, P., Mutations that increase both Hsp90 ATPase activity in vitro and Hsp90 drug resistance in vivo. *Biochim Biophys Acta* 2010, 1803, (5), 575-83.
361. Jones, M. K.; Szabo, I. L.; Kawanaka, H.; Husain, S. S.; Tarnawski, A. S., von Hippel Lindau tumor suppressor and HIF-1alpha: new targets of NSAIDs inhibition of hypoxia-induced angiogenesis. *FASEB J* 2002, 16, (2), 264-6.
362. Yang, Z. F.; Poon, R. T.; To, J.; Ho, D. W.; Fan, S. T., The potential role of hypoxia inducible factor 1alpha in tumor progression after hypoxia and chemotherapy in hepatocellular carcinoma. *Cancer Res* 2004, 64, (15), 5496-503.
363. Kisselev, A. F.; Goldberg, A. L., Proteasome inhibitors: from research tools to drug candidates. *Chem Biol* 2001, 8, (8), 739-58.
364. Navas, T. A.; Nguyen, A. N.; Hideshima, T.; Reddy, M.; Ma, J. Y.; Haghnazari, E.; Henson, M.; Stebbins, E. G.; Kerr, I.; O'Young, G.; Kapoun, A. M.; Chakravarty, S.; Mavunkel, B.; Perumattam, J.; Luedtke, G.; Dugar, S.; Medicherla, S.; Protter, A. A.; Schreiner, G. F.; Anderson, K. C.; Higgins, L. S., Inhibition of p38alpha MAPK enhances proteasome inhibitor-induced apoptosis of myeloma cells by modulating Hsp27, Bcl-X(L), Mcl-1 and p53 levels in vitro and inhibits tumor growth in vivo. *Leukemia* 2006, 20, (6), 1017-27.

365. Rock, K. L.; Gramm, C.; Rothstein, L.; Clark, K.; Stein, R.; Dick, L.; Hwang, D.; Goldberg, A. L., Inhibitors of the proteasome block the degradation of most cell proteins and the generation of peptides presented on MHC class I molecules. *Cell* 1994, 78, (5), 761-71.
366. Soulere, L.; Viode, C.; Perie, J.; Hoffmann, P., Selective inhibition of Fe- versus Cu/Zn-superoxide dismutases by 2,3-dihydroxybenzoic acid derivatives. *Chem Pharm Bull (Tokyo)* 2002, 50, (5), 578-82.
367. Klabunde, T.; Eicken, C.; Sacchettini, J. C.; Krebs, B., Crystal structure of a plant catechol oxidase containing a dicopper center. *Nat Struct Biol* 1998, 5, (12), 1084-90.
368. Solomon, E. I.; Sundaram, U. M.; Machonkin, T. E., Multicopper Oxidases and Oxygenases. *Chem Rev* 1996, 96, (7), 2563-2606.
369. Matoba, Y.; Kumagai, T.; Yamamoto, A.; Yoshitsu, H.; Sugiyama, M., Crystallographic evidence that the dinuclear copper center of tyrosinase is flexible during catalysis. *J Biol Chem* 2006, 281, (13), 8981-90.
370. Mer, V. K. L.; Rideal, E. K., THE INFLUENCE OF HYDROGEN CONCENTRATION ON THE AUTO-OXIDATION OF HYDROQUINONE. A NOTE ON THE STABILITY OF THE QUINHYDRONE ELECTRODE. *Journal of the American Chemical Society* 1924, 46, (1), 223-231.
371. Martin Jr, J. P.; Batkoff, B., Homogentisic acid autoxidation and oxygen radical generation: implications for the etiology of alkaptonuric arthritis. *Free Radical Biology and Medicine* 1987, 3, (4), 241-250.
372. Kietzmann, T.; Gorlach, A., Reactive oxygen species in the control of hypoxia-inducible factor-mediated gene expression. *Semin Cell Dev Biol* 2005, 16, (4-5), 474-86.
373. LaVoie, M. J.; Hastings, T. G., Dopamine quinone formation and protein modification associated with the striatal neurotoxicity of methamphetamine: evidence against a role for extracellular dopamine. *J Neurosci* 1999, 19, (4), 1484-91.
374. Belisario, M. A.; Pecce, R.; Maturo, M.; De Rosa, S., Arylation of sulfhydryl groups in vitro by the naturally occurring sesquiterpenoid benzoquinone avarone. *Toxicology* 1994, 86, (1-2), 89-108.
375. Llovet, J. M.; Bruix, J., Systematic review of randomized trials for unresectable hepatocellular carcinoma: Chemoembolization improves survival. *Hepatology* 2003, 37, (2), 429-42.
376. Harris, A. L., Hypoxia--a key regulatory factor in tumour growth. *Nat Rev Cancer* 2002, 2, (1), 38-47.
377. Sangro, B.; Rios, R.; Bilbao, I.; Beloqui, O.; Herrero, J. I.; Quiroga, J.; Prieto, J., Efficacy and toxicity of intra-arterial cisplatin and etoposide for advanced hepatocellular carcinoma. *Oncology* 2002, 62, (4), 293-8.
378. Comerford, K. M.; Wallace, T. J.; Karhausen, J.; Louis, N. A.; Montalto, M. C.; Colgan, S. P., Hypoxia-inducible factor-1-dependent regulation of the multidrug resistance (MDR1) gene. *Cancer Res* 2002, 62, (12), 3387-94.
379. Hu, C. J.; Wang, L. Y.; Chodosh, L. A.; Keith, B.; Simon, M. C., Differential roles of hypoxia-inducible factor 1alpha (HIF-1alpha) and HIF-2alpha in hypoxic gene regulation. *Mol Cell Biol* 2003, 23, (24), 9361-74.

380. Semenza, G. L., Hydroxylation of HIF-1: oxygen sensing at the molecular level. *Physiology (Bethesda)* 2004, 19, 176-82.
381. Zatyka, M.; da Silva, N. F.; Clifford, S. C.; Morris, M. R.; Wiesener, M. S.; Eckardt, K. U.; Houlston, R. S.; Richards, F. M.; Latif, F.; Maher, E. R., Identification of cyclin D1 and other novel targets for the von Hippel-Lindau tumor suppressor gene by expression array analysis and investigation of cyclin D1 genotype as a modifier in von Hippel-Lindau disease. *Cancer Res* 2002, 62, (13), 3803-11.
382. Papandreou, I.; Cairns, R. A.; Fontana, L.; Lim, A. L.; Denko, N. C., HIF-1 mediates adaptation to hypoxia by actively downregulating mitochondrial oxygen consumption. *Cell Metab* 2006, 3, (3), 187-97.
383. Pollard, P. J.; El-Bahrawy, M.; Poulsom, R.; Elia, G.; Killick, P.; Kelly, G.; Hunt, T.; Jeffery, R.; Seedhar, P.; Barwell, J.; Latif, F.; Gleeson, M. J.; Hodgson, S. V.; Stamp, G. W.; Tomlinson, I. P.; Maher, E. R., Expression of HIF-1alpha, HIF-2alpha (EPAS1), and their target genes in paraganglioma and pheochromocytoma with VHL and SDH mutations. *J Clin Endocrinol Metab* 2006, 91, (11), 4593-8.
384. Lou, J. J.; Chua, Y. L.; Chew, E. H.; Gao, J.; Bushell, M.; Hagen, T., Inhibition of hypoxia-inducible factor-1alpha (HIF-1alpha) protein synthesis by DNA damage inducing agents. *PLoS One* 2010, 5, (5), e10522.
385. Sato, S.; Fujita, N.; Tsuruo, T., Modulation of Akt kinase activity by binding to Hsp90. *Proc Natl Acad Sci U S A* 2000, 97, (20), 10832-7.
386. Basso, A. D.; Solit, D. B.; Chiosis, G.; Giri, B.; Tsichlis, P.; Rosen, N., Akt forms an intracellular complex with heat shock protein 90 (Hsp90) and Cdc37 and is destabilized by inhibitors of Hsp90 function. *J Biol Chem* 2002, 277, (42), 39858-66.
387. Gould, C. M.; Kannan, N.; Taylor, S. S.; Newton, A. C., The chaperones Hsp90 and Cdc37 mediate the maturation and stabilization of protein kinase C through a conserved PXXP motif in the C-terminal tail. *J Biol Chem* 2009, 284, (8), 4921-35.
388. Brajenovic, M.; Joberty, G.; Kuster, B.; Bouwmeester, T.; Drewes, G., Comprehensive proteomic analysis of human Par protein complexes reveals an interconnected protein network. *J Biol Chem* 2004, 279, (13), 12804-11.
389. Crevecoeur, J.; Merville, M. P.; Piette, J.; Gloire, G., Geldanamycin inhibits tyrosine phosphorylation-dependent NF-kappaB activation. *Biochem Pharmacol* 2008, 75, (11), 2183-91.
390. Kaelin, W. G., Jr., Treatment of kidney cancer: insights provided by the VHL tumor-suppressor protein. *Cancer* 2009, 115, (10 Suppl), 2262-72.
391. Thomas, G. V.; Tran, C.; Mellinghoff, I. K.; Welsbie, D. S.; Chan, E.; Fueger, B.; Czernin, J.; Sawyers, C. L., Hypoxia-inducible factor determines sensitivity to inhibitors of mTOR in kidney cancer. *Nat Med* 2006, 12, (1), 122-7.
392. Le Tourneau, C.; Faivre, S.; Serova, M.; Raymond, E., mTORC1 inhibitors: is temsirolimus in renal cancer telling us how they really work? *Br J Cancer* 2008, 99, (8), 1197-203.
393. Wysocki, P. J., mTOR in renal cell cancer: modulator of tumor biology and therapeutic target. *Expert Rev Mol Diagn* 2009, 9, (3), 231-41.

394. Figueroa, Y. G.; Chan, A. K.; Ibrahim, R.; Tang, Y.; Burow, M. E.; Alam, J.; Scandurro, A. B.; Beckman, B. S., NF-kappaB plays a key role in hypoxia-inducible factor-1-regulated erythropoietin gene expression. *Exp Hematol* 2002, 30, (12), 1419-27.
395. Gorlach, A.; Bonello, S., The cross-talk between NF-kappaB and HIF-1: further evidence for a significant liaison. *Biochem J* 2008, 412, (3), e17-9.
396. Kopp, E.; Ghosh, S., Inhibition of NF-kappa B by sodium salicylate and aspirin. *Science* 1994, 265, (5174), 956-9.
397. Gao, Z.; Zuberi, A.; Quon, M. J.; Dong, Z.; Ye, J., Aspirin inhibits serine phosphorylation of insulin receptor substrate 1 in tumor necrosis factor-treated cells through targeting multiple serine kinases. *J Biol Chem* 2003, 278, (27), 24944-50.
398. Meteoglu, I.; Erdogdu, I. H.; Meydan, N.; Erkus, M.; Barutca, S., NF-KappaB expression correlates with apoptosis and angiogenesis in clear cell renal cell carcinoma tissues. *J Exp Clin Cancer Res* 2008, 27, 53.
399. Hudes, G. R., Targeting mTOR in renal cell carcinoma. *Cancer* 2009, 115, (10 Suppl), 2313-20.
400. Engers, R.; Mrzyk, S.; Springer, E.; Fabbro, D.; Weissgerber, G.; Gernharz, C. D.; Gabbert, H. E., Protein kinase C in human renal cell carcinomas: role in invasion and differential isoenzyme expression. *Br J Cancer* 2000, 82, (5), 1063-9.
401. Liou, J. S.; Chen, J. S.; Faller, D. V., Characterization of p21Ras-mediated apoptosis induced by protein kinase C inhibition and application to human tumor cell lines. *J Cell Physiol* 2004, 198, (2), 277-94.
402. Siebenlist, U.; Franzoso, G.; Brown, K., Structure, regulation and function of NF-kappa B. *Annu Rev Cell Biol* 1994, 10, 405-55.
403. Wiesener, M. S.; Turley, H.; Allen, W. E.; Willam, C.; Eckardt, K. U.; Talks, K. L.; Wood, S. M.; Gatter, K. C.; Harris, A. L.; Pugh, C. W.; Ratcliffe, P. J.; Maxwell, P. H., Induction of endothelial PAS domain protein-1 by hypoxia: characterization and comparison with hypoxia-inducible factor-1alpha. *Blood* 1998, 92, (7), 2260-8.
404. Akimoto, K.; Mizuno, K.; Osada, S.; Hirai, S.; Tanuma, S.; Suzuki, K.; Ohno, S., A new member of the third class in the protein kinase C family, PKC lambda, expressed dominantly in an undifferentiated mouse embryonal carcinoma cell line and also in many tissues and cells. *J Biol Chem* 1994, 269, (17), 12677-83.

Appendix

	FIH	PHD2	JMJD2A	JMJD2C	FBXL11
Enzyme (μM)	1	0.5	2	1	2
2OG (μM) (K_m^{app}, μM)	100 (143*)	60 (55*)	10 (6)	10 (4)	10 (6)
Substrate (μM) (K_m^{app}, μM)	100 (395*)	50 (22*)	100 (45)	100 (48)	200 (60)
Fe(II) (μM)	10	10	10	10	10
Ascorbate (μM)	100	100	100	100	100
Buffer (mM)	50 (Hepes-Na, pH 7.5)	50 (Hepes-Na, pH 7.5)	50 (Hepes-Na, pH 7.5)	50 (Hepes-Na, pH 7.5)	50 (Hepes-Na, pH 7.5)
Tween-20 (%)	-	-	0.01	0.01	0.01
FDH (U)	-	-	0.025	0.025	0.025
NAD (μM)	-	-	500	500	500
Final reaction volume (μl)	20	20	25	25	25
Assay method	MALDI	MALDI	FDH	FDH	FDH

Appendix 1: *In vitro* assay conditions used for assessing inhibition of 2OG oxygenases by *R*- and *S*-2HG. Substrates used in the assays for JMJD2A/JMJD2C, FBXL11, PHD2, and FIH were histone H3 fragment substrate H3(7-14)K9me$_3$, H3(30-41)K36me$_2$, HIF-1αCODD (residues 556-574), and HIF-1αCAD (residues 786-826) respectively. FDH = formaldehyde dehydrogenase. No inhibition was observed by FDH itself with *R*- and *S*-2HG. *Data from (Ehrismann *et al., 2007*)